IMPERIAL COLLEGE OF SCIENCE, TECHNOLOGY AND MEDICINE

University of London

EXTRACTION OF VALID MODAL PROPERTIES FROM MEASURED DATA IN STRUCTURAL VIBRATIONS

by

Nuno Manuel Mendes Maia

A thesis submitted to the University of London for the degree of Doctor of Philosophy and for the Diploma of Imperial College.

Department of Mechanical Engineering
Imperial College, London SW7, U. K.

December 1988

To my wife, Maria José

ABSTRACT

Current experimental modal analysis methods for identifying structures are usually based either on very simple and flexible techniques, or on very sophisticated computational ones. The former, implemented in interactive computer programs, allow for a complete intervention of the user. The latter tend to be used as black boxes, where the user does not have any control of the identification process. The overall objective of the present work is to combine the advantages of both approaches, developing automatic means of performing experimental modal analysis. Here, the intervention of the user is reduced to a minimum, while some "intelligence" is incorporated in the computer programs so that "decisions" can be taken automatically and results produced with an indication of the quality or reliability of the analysis.

A survey and classification of the different modal analysis methods is made; however, the focus of this thesis is placed on frequency-domain methods. Some of these methods are examined in detail, including both single-degree-of-freedom and multi-degree-of-freedom approaches using single and global frequency-response analysis concepts.

The theory behind each of these various analysis methods is presented in depth, together with the development of computer programs, theoretical and experimental examples and discussion, in order to evaluate the capabilities of those methods. The problem of identifying properties of structures that possess close modes is treated in particular detail, as this is a difficult situation to handle and yet a very common one in many structures.

It is essential to obtain a good model for the behaviour of the structure in order to pursue various applications of experimental modal analysis, namely: updating of finite element models, structural modification,

subsystem-coupling and calculation of real modes from complex modes, to name a few. This last topic is particularly important for the validation of finite element models and for this reason, a number of different methods to calculate real modes from complex modes are presented and discussed in this thesis.

ACKNOWLEDGEMENTS

The author would like to express his gratitude to Prof. D. J. Ewins, for his untiring supervision, advice and dedication, which have mostly contributed to the success of this thesis.

Other members of the staff are also acknowledged, namely Mr. D. Robb, Dr. M. Imregun and Dr. J. He, for their helpful guidance in the conducting of experimental work and computing.

Sincere thanks are also due to all collegues, for the many interesting and fruitful discussions and suggestions to the present work.

Prof. Lallement and Dr. Fillod, from the Université de Franche-Comté, Besançon, France, are very much acknowledged for their useful clarifications on one of the methods discussed in this work.

The author is grateful to Prof. Júlio M. M. Silva, from the Instituto Superior Técnico, Lisbon, Portugal, for his constant support during the course of the present work, and to the Reitoria da Universidade Técnica de Lisboa for their scholarship equivalence.

The Overseas Research Students (ORS) Awards Scheme is also acknowledged for the finantial equivalence to a "home student" during the first three months of the present research.

The author is also indebted to the Calouste Gulbenkian Foundation for the finantial support provided throughout the whole period of this work.

Finally, a word of thanks to my wife, for sharing all the good and bad moments. Without her dedication and encouragement, this thesis could not have been brought to completion.

CONTENTS

ABSTRACT 3

ACKNOWLEDGEMENTS 5

NOTATION 13

CHAPTER 1 - INTRODUCTION 22

1-1 General considerations *22*

1-2 Testing a structure *24*

1-2-1 Measurement procedures *24*

1-2-2 Types of excitation signals *24*

1-2-3 Structural behaviour assumptions *26*

1-3 Classification of modal analysis identification methods *27*

1-4 General objectives of the work *30*

1-5 Preview of the thesis *32*

CHAPTER 2 - A DESCRIPTION OF MODAL ANALYSIS IDENTIFICATION METHODS 34

2-1 Introduction *34*

2-2 Time domain methods *35*

2-2-1 Indirect or Modal methods *35*

The Complex Exponential method (CE) *35*

The Least-Squares Complex Exponential method (LSCE) *40*

The Polyreference Complex Exponential method (PRCE) *42*

The Ibrahim Time Domain method (ITD) *51*

The Single-Station Time Domain method

(SSTD) *56*
The Eigensystem Realization Algorithm (ERA) *56*
2-2-2 Direct methods *67*
The Autoregressive Moving-average method (ARMA) *67*
The Direct System Parameter Identification method (DSPI) *71*
2-3 Frequency Domain methods *77*
2-3-1 Indirect SDOF methods *78*
The Peak Amplitude method *79*
The Quadrature Response and Maximum Quadrature Component methods *79*
The Kennedy-Pancu (or Maximum Frequency Spacing) method *80*
The Circle-Fitting method *81*
The Inverse method *82*
The "Bendent" (or Dobson) method *82*
Other methods *82*
2-3-2 Indirect MDOF methods *83*
The Gaukroger-Skingle -Heron method (GSH) *84*
The Ewins-Gleeson method *87*
The Frequency Domain Prony method (FDPM) *89*
The Complex Exponential Frequency Domain method (CEFD) *92*
The Eigensystem Realization Algorithm in the frequency domain (ERA-FD) *97*
The Rational Fraction Polynomial method (RFP) *98*
The Global Rational Fraction Polynomial method (GRFP) *99*
The Global method *99*

The Polyreference Frequency Domain method (PRFD) *100*
Other methods *103*
2-3-3 Direct methods *104*
The Spectral method *104*
The Simultaneous Frequency Domain method (SFD) *105*
The Identification of Structural System Parameters method (ISSPA) *111*
The Multi-Matrix method *115*
2-4 Tuned-sinusoidal methods *123*
2-5 Conclusions *128*

CHAPTER 3 - SDOF MODAL ANALYSIS METHODS - CAPABILITIES AND LIMITATIONS WHEN DEALING WITH CLOSE MODES 129

3-1 Introduction *129*
3-2 Indicators of close modes *130*
3-2-1 Interference criteria *131*
Comments on expressions (3-4) and (3-5) *133*
Examples *135*
Discussion *141*
3-2-2 The circle centres *142*
3-2-3 The inverse of receptance *145*
Real modes case *145*
Complex modes case *147*
Discussion *155*
3-3 Identification in the presence of close modes *156*
3-3-1 Circle-fitting and Inverse methods - which one to use ? *158*
Examples *159*

Discussion *164*
3-3-2 The "Bendent" method *164*
3-4 Conclusions *171*

CHAPTER 4 - AN INVESTIGATION OF SOME *SISO* MDOF METHODS 173

4-1 Introduction *173*
4-2 The Rational Fraction Polynomial method (RFP) *175*
4-2-1 Theory *176*
Calculation of orthogonal polynomials φ and θ *182*
Calculation of the modal parameters *188*
4-2-2 Computer program description *191*
4-2-3 Numerical Examples *195*
Theoretical case - evaluation of the method *195*
Experimental case *200*
4-3 A new approach for the identification of lightly damped structures *202*
4-3-1 Theory *203*
4-3-2 Considerations on the choice of data points *210*
4-3-3 Comparison with previous work *215*
4-3-4 Computer program description *216*
Criteria for the "best" modal constants *216*
Flow-chart description *217*
Discussion *221*
4-3-5 Examples *222*
Theoretical cases *222*
Experimental case *228*
4-4 Conclusions *230*
4-4-1 Conclusions on the RFP method *230*
4-4-2 Conclusions on the new approach for lightly damped structures *231*

CHAPTER 5 - AN INVESTIGATION OF SOME *SIMO* AND *MIMO* METHODS 233

5-1 Introduction *233*

5-2 The Global Rational Fraction Polynomial method (GRFP) *234*

5-2-1 Theory *235*

Calculation of the global properties *235*

Calculation of the local properties *237*

5-2-2 Computer program description *240*

5-2-3 Numerical examples *243*

Theoretical case - Evaluation of the method *243*

Experimental cases *246*

Discussion *246*

5-2-4 Improvement of the algorithm *247*

Theoretical evaluation *248*

Experimental cases *249*

Discussion *261*

5-2-5 Alternative way to calculate the global parameters *262*

5-3 The Global method *264*

5-3-1 Introduction *264*

5-3-2 Theory *264*

Basic developments *264*

Specific developments concerning the Global method *272*

Use of the Singular Value Decomposition *277*

Note on the use of differences of forced response *282*

Calculation of the eigenvectors *284*

5-3-3 Computer program description *287*

New developments to the Global method *287*

5-3-4 Examples *289*
Theoretical case - evaluation of the method for two close modes *289*
Experimental cases *292*
5-4 The Spectral method *299*
5-4-1 Introduction *299*
5-4-2 Theory *300*
Klosterman's approach *302*
Alternative approach *307*
5-4-3 Computer program description *309*
5-4-4 Examples *309*
Theoretical cases *309*
Experimental cases *314*
Comparison with the GRFP and Global methods *317*
5-4-5 Discussion *321*
5-5 Conclusions *322*
5-5-1 Conclusions on the GRFP method *322*
5-5-2 Conclusions on the Global method *323*
5-5-3 Conclusions on the Spectral method *325*

CHAPTER 6 - REAL MODES vs. COMPLEX MODES 326

6-1 Introduction *326*
6-2 Theory *327*
6-2-1 Niedbal's method *327*
6-2-2 Asher's method *330*
6-3 Numerical examples *332*
6-3-1 Example 1 *333*
Discussion *336*
6-3-2 Example 2 *339*
Discussion *343*

6-4 Conclusions *343*

CHAPTER 7 - CONCLUSIONS **344**

7-1 General conclusions *344*
7-2 New contributions of the present research *346*
7-3 Suggestions for future work *349*

APPENDIX A - Derivation of Eq. (4-10) **351**
APPENDIX B - Orthogonal Functions **353**
APPENDIX C - Method of partial fractions **355**
APPENDIX D - The Singular Value Decomposition technique (SVD) **357**

REFERENCES **368**

NOTATION

The list of symbols described below represents the standard notation used in this thesis. However, the notation used in the description of the methods presented in Chapter 2 should be read as a "local" one, although an effort has been made to keep that notation as consistent as possible with the rest of the work.

a	-	ratio between two natural frequencies;
a_k	-	coefficients of the numerator polynomial of $\alpha(j\omega)$ (real);
a_r	-	element of $[\ a_r\ ]$ for each mode r (complex);
${}_rA_{ik}$, A_r'	-	residue of mode r, corresponding to $\alpha_{ik}(j\omega)$ and its simplified notation, respectively (complex);
A_r	-	constant related to the modal constant, for each mode r (real);
$\{a\}$	-	vector of coefficients a_k (real);
$\{A\}$	-	vector formed by R_K, R_M and ${}_rA_{ik}$ (complex);
$[\ a_r\ ]$	-	state space diagonal matrix, from the orthogonal properties of [A] (complex);
$[A]$	-	state space system matrix (real, symmetric);
$[A_S]$	-	system matrix (complex);
b_k	-	coefficients of the denominator polynomial of $\alpha(j\omega)$ (real);
b_r	-	element $[\ b_r\ ]$, for each mode r (complex);
B_r	-	constant related to the modal constant, for each mode r (real);
$\{b\}$	-	vector of coefficients b_k (real);
$[\ b_r\ ]$	-	state space diagonal matrix, from the orthogonal properties of [B] (complex);
$[B]$	-	state space system matrix (real, symmetric);
c	-	shift in the reference number of a frequency data point;
c_k	-	coefficients of the numerator of the orthogonal polynomials (real);

c_I, c_R - origin intercepts of $Im(1/\alpha_r)$ and $Re(1/\alpha_r)$, respectively (real);

C_r - modal constant for mode r (real);

$\{c\}$ - vectors of coefficients c_k (real);

$[C]$ - viscous damping matrix (real);

d_k - coefficients of the denominator of the orthogonal polynomials (real);

d_I, d_R - origin intercepts of t_I, t_R, respectively (real);

D_k, D_k^+ - coefficients defined in Eqs. (4-33) and (4-35 b), respectively (real);

$\{d\}$ - vectors of coefficients d_k (real);

e_i , e_i' - error function and modified error function, at frequency ω_i (complex);

$\{E\}$, $\{E\}_i$ - error vector and error vector corresponding to the ith set of data points (complex);

$\bar{F}_k$ - element of $\{\bar{F}\}$, at the input coordinate k;

$\{F\}$ - vector defined in Eq. (4-14) (real);

$\{f(t)\}$, $\{F(t)\}$ - vector space vector of applied forces (complex);

$\{F'(t)\}$ - state space vector of applied forces (complex);

$\{\bar{F}\}$ - vector of input force amplitudes (complex);

g_i - value of the denominator of either Eq. (5-9) or Eq. (4-65) for each frequency data point (complex);

$1/g_i$ - inverse of g_i - acts as weighting function - Eqs.(4-64) and (5-23) - (complex);

$\{G\}$, $\{G'\}$ - vectors defined in Eqs. (4-14) and (4-38), respectively (real);

$\{g(j\omega)\}$ - auxiliar vector, defined in Eq. (5-75) (complex);

$\{\Delta g(j\omega_i)\}$ - difference of vectors $\{g(j\omega)\}$ between two data points;

$[\ 1/g\ ]$ - diagonal matrix formed by $1/g_i$ elements (complex);

$[\Delta g]$ - matrix formed by $\{\Delta g(j\omega_i)\}$ elements;

$h_{ik}(t)$, $h(t)$ - impulse response function corresponding to $\alpha_{ik}(j\omega)$ and its simplified notation, respectively (real);

$\{h_i(t)\}$ - vector formed by $h_{ik}(t)$ elements (real);

$[H]$ - hysteretic damping matrix (real);

$[H(t)]$ - impulse response function matrix (real);

Im - coefficient of the imaginary part of a complex quantity;

$[I]$ - identity matrix;

$[I]'$ - modified identity matrix (Eq. (5-117));

j - imaginary unit ($=\sqrt{-1}$); also an index;

J - squared error;

k_r' - modal stiffness of mode r (complex);

$[k']$, $[\bar{k}]$ - diagonal stiffness matrices of the damped (complex) and undamped (real) system, respectively;

$[K]$ - stiffness matrix of the system (real);

$[\bar{K}']$, $[\bar{K}]$ - stiffness matrix after transformation by the real modal matrix (complex) and its real part, respectively;

$[K']$ - stiffness matrix of the system which includes [H] (complex);

L - number of measured frequency points taken into the analysis;

m - degree of the orthogonal polynomial $\gamma(\omega)$;

M - degree of polynomial;

m_I, m_R - origin intercepts of $\mathrm{Im}(1/\alpha_r)$ and $\mathrm{Re}(1/\alpha_r)$, respectively;

m_r - modal mass of mode r (complex);

$[m]$, $[\bar{m}]$ - diagonal mass matrices of the damped (complex) and undamped system (real);

$[M]$ - mass matrix of the system (real);

$[\bar{M}]$ - mass matrices after transformation by the real modal matrix (real);

N - number of degrees-of-freedom of the system;

n_I, n_R - slopes of $\mathrm{Im}(1/\alpha_r)$ and $\mathrm{Re}(1/\alpha_r)$, respectively;

NR - number of runs;

N_0 - number of measured degrees-of-freedom of the system;

p - number of measured response locationss;

p' - number of pairs of data points;

$\bar{p}_r$ - amplitude of $p_r(t)$ - modal participation factor (complex);

$p_r(t)$ - state space pricipal coordinate of mode r (complex);

$\{p(t)\}$ - state space vector of the pricipal coordinates (complex);

$[P]$ - matrix defined in Eq. (4-8) (complex);

q - number of force input locations;

q_i - weighting function for each frequency ω_i;

q_α - variable defined in Eq. (5-171) (complex);

$\{q_u\}, \{p_u\}$ - real general and principal coordinates of the undamped system;

$[Q]$ - matrix defined in Eq. (4-81);

r - subscript for mode counter;

Re - real part of a complex quantity;

R_K, R_M - constants associated with $R_1(j\omega)$ - Eq. (5-135) (complex);

$R_1(j\omega), R_2(j\omega)$ - residuals corresponding to $\alpha_{ik}(j\omega)$ and $\dot{\alpha}_{ik}(j\omega)$, respectively (complex);

$\{R_1(j\omega)\}, \{R_2(j\omega)\}$ - vectors formed by $R_1(j\omega)$ and $R_2(j\omega)$ elements, respectively;

$\{R\}$ - vector in the relation between $\{d\}$ and $\{b\}$ - (Eq. 4-40 b) (real);

s - Laplace variable;

s_r - eigenvalue of a system with viscous damping (complex);

s_I, s_R - origin intercepts of c_I, c_R, respectively;

$[\ s_r\ ]$ - diagonal matrix of eigenvalues s_r;

t - time variable;

$t_{i,k}$ - variable defined in Eq. (5-11) (complex);

t_I, t_R - slopes of $\mathrm{Im}(1/\alpha_r)$ and $\mathrm{Re}(1/\alpha_r)$, respectively;

$[T]$ - matrix defined in Eq. (4-8) (complex);

$[T_{ac}], [T_{bd}]$ - matrices relating $\{c\}$ to $\{a\}$ and $\{d\}$ to $\{b\}$, respectively (real);

$[T_G]$ - matrix formed by $t_{i,k}$ elements (complex);

$[T_S]$ - matrix defined in Eq. (5-138) (complex);

$[T_1]$ - transformation matrix (complex);

$[T_2]$ - transformation matrix (real);

$[T']$ - matrix relating $\{a\}$ with $\mathrm{Re}\{\tilde{\alpha}\}$ - Eq. (4-71) (real);

Δt - time interval;

u_k - coefficient defined in Eq. (4-33 a) (real);

u_I, u_R - slopes of t_I, t_R, respectively (real);

$\{u(t)\}$ - state space vector formed by $\{y(t)\}$, $\{\dot{y}(t)\}$ (complex);

$\{\bar{u}(t)\}$ - vector of the amplitudes of $\{u(t)\}$ (complex);

$[U]$ - orthogonal (or unitary) matrix of left singular vectors, in the SVD technique (real or complex);

$[U_G]$ - matrix defined in Eq. (5-5 a) (real);

$[U_G]_k$ - $[U_G]$ for each FRF k;

$[U_T]$ - matrix formed by matrices $[U_G]$ (real);

$[U]_\alpha$ - $[U]$ corresponding to $[\Delta\tilde{\alpha}]^T$;

$[U]_{\dot{\alpha}}$ - $[U]$ corresponding to $[\Delta\dot{\tilde{\alpha}}]^T$;

v_I, v_R - slopes of c_I, c_R, respectively (real);

v_k, v_k^+ - coefficients defined in Eqs. (4- 33 b) and (4-35 a), respectively (real);

$\{V_G\}$ - vector defined in Eq. (5-5 b) (real);

$\{V_T\}$ - vector formed by vectors $\{V_G\}$ (real);

$[V]$ - orthogonal (or unitary) matrix of right singular vectors, in the SVD technique (real or complex);

$[V]_\alpha$ - $[V]$ corresponding to $[\Delta\tilde{\alpha}]^T$;

$[V]_{\dot{\alpha}}$ - $[V]$ corresponding to $[\Delta\dot{\tilde{\alpha}}]^T$;

$\{W\}$ - vector defined in Eqs. (4-8) and (4-19) in terms of orthogonal polynomials (complex);

$x_i(t_j)$ - free response at point i and time input t_j (real);

$[X]$, $[X']$ - matrices defined in Eqs. (4-14) and (4-38), respectively (real);

$\{y(t)\}$ - vector space displacement response vector (complex);

$\{\bar{y}\}$ - vector of the amplitudes of $\{y(t)\}$ (complex);

$[Y]$ - matrix defined in Eq. (4-14) (real);

$z_{i,k}$ - variable defined in Eq. (5-20) (complex);

z_r - element of $\{z_r\}$;

$\{z_r\}$ - eigenvector (complex);

$[z]$ - auxiliar matrix defined in Eq. (5-94) (complex);

$[Z]$ - matrix defined in Eq. (4-14) (real);

$[Z_G]$ - matrix formed by $z_{i,k}$ elements (complex);

$\{0\}$, $[0]$ - null vector and matrix, respectively;

α_1, α_2 - amplitude of receptance at natural frequencies 1 and 2, respectively;

$\alpha_{ik}(j\omega)$, $\alpha(j\omega)$ - receptance - response at point i due to a force at point k - and its simplified form, respectively (complex);

$\{\alpha_k(j\omega)\}$, $\{\alpha(j\omega)\}$ - vector, formed by $\alpha_{ik}(j\omega)$ elements, for the same input reference k and its simplified form, respectively (complex);

$\{\tilde{\alpha}\}$ - vector formed by $\tilde{\alpha}(j\omega_i)$ elements (complex);

$\{\Delta\alpha(j\omega_i)\}$, $\{\Delta\dot{\alpha}(j\omega_i)\}$ - difference receptance and mobility vectors between two data points, respectively (complex);

$[\alpha]$ - receptance matrix (complex);

$[\alpha_T]$, $[\alpha_T]'$ - matrices defined in Eqs. (5-164) and (5-184), respectively (complex);

$[\alpha]_{\omega_i}$ - $[\alpha]$ evaluated at frequency ω_i;

$[\tilde{\alpha}]$ - diagonal matrix formed by $\tilde{\alpha}(j\omega_i)$ (complex);

$[\Delta\alpha]$, $[\Delta\dot{\alpha}]$ - matrices formed by $\{\Delta\alpha(j\omega_i)\}$ and $\{\Delta\dot{\alpha}(j\omega_i)\}$ elements, respectively (complex);

$[\Delta\tilde{\alpha}]'$, $[\Delta\dot{\tilde{\alpha}}]'$ - recalculated $[\Delta\tilde{\alpha}]$ and $[\Delta\dot{\tilde{\alpha}}]$, respectively;

γ - ratio between two damping factors;

γ_r, γ_T - variables defined in Eqs. (5-158) and (5-164), respectively (complex);

$\gamma_k(\omega)$ - common designation for $\varphi_k(\omega)$ and $\theta_k(\omega)$;

$\{\Gamma\}$, $[\Gamma]$ - force location vector and matrix, respectively (real);

δ - ratio between two modal constants;

Δ - function of frequency, defined in Eq. (3-26);

δ_0 - tolerance for the modal constants;

ϕ_r - phase angle of modal constant for mode r;

${}_r\phi_i$, ${}_r\phi_k$ - elements of $\{\phi_r\}$, at the response coordinate i and input coordinate k, respectively;

$\{\phi_r\}$, $\{\phi_r'\}$ - vector space and state space normalized eigenvectors of mode r, respectively (complex);

$\{\phi_u\}$ - undamped mode of the system;

$\{\phi_k\}^T$ - row vector, formed by ${}_r\phi_k$ elements (complex);

$[\Phi]$, $[\Phi_u]$ - complex modal matrix, formed by ${}_r\phi_k$ elements, and real modal matrix, respectively;

$\varphi_{i,j}$ - complex orthogonal polynomial of order j, evaluated at frequency ω_i, associated with the numerator of $\alpha(j\omega)$;

$\varphi^-_{i,j}$, $\varphi^+_{i,j}$ - $\varphi_{i,j}$ defined for negative and positive frequencies, respectively;

$\varphi_k(\omega)$ - $\varphi_{i,j}$ as a continuous function of ω;

$[\vartheta]$ - matrix of orthogonal polynomials $\varphi_{i,j}$ (complex);

$[\vartheta^+]$ - matrix whose elements are $\varphi^+_{i,j}$;

λ_r - eigenvalue of mode r for a system with hysteretic damping (complex);

$[\lambda_u]$ - diagonal matrix of real eigenvalues;

$[\lambda']$ - matrix of the identified complex eigenvalues;

${}_r\psi_i$ - unscaled eigenvector element i of mode r (complex);

$\{\psi_r\}$, $[\Psi]$ - vector space unscaled eigenvector of mode r and corresponding modal matrix (complex);

$\{\psi_r'\}$, $[\Psi']$ - state space unscaled eigenvector of mode r and corresponding modal matrix, respectively (complex);

ν - threshold value for interference criteria;

θ - phase angle between response displacement and input force;

$\theta_{i,j}$ - complex orthogonal polynomial of order j, evaluated at frequency ω_i, associated with the denominator of $\alpha(j\omega)$;

$\theta^{-}_{i,j}$, $\theta^{+}_{i,j}$ - $\theta_{i,j}$ defined for negative and positive frequencies, respectively;

$\theta_k(\omega)$ - $\theta_{i,j}$ as a continuous function of ω;

$[\Theta]$ - matrix of orthogonal polynomials $\theta_{i,j}$ (complex);

σ - damping coefficient;

σ_i - singular values - elements of $[\Sigma]$ (real);

$[\Sigma]$ - singular value matrix (real);

$[\Sigma]_\alpha$, $[\Sigma]_{\dot{\alpha}}$ - $[\Sigma]$ corresponding to $[\Delta\tilde{\alpha}]^T$ and $[\Delta\dot{\tilde{\alpha}}]^T$, respectively;

$[\Sigma]_\alpha'$, $[\Sigma]_{\dot{\alpha}}'$ - $[\Sigma]_\alpha$ and $[\Sigma]_{\dot{\alpha}}$ after putting to zero the small singular values;

ξ_r - viscous damping factor of mode r;

ω - circular frequency;

ω_r' - damped natural frequency;

ω_r - natural frequency of mode r;

Ω_i - frequency value at data point i;

$[\Omega]$, $[\Omega_T]$ - matrices defined in Eqs. (4-58) and (5-183), respectively (real).

Operators

Σ - summation;

Π - product;

$| \, |$ - modulus;

$\| \, \|$ - Euclidean norm;

$\dot{(\,)}$, $\ddot{(\,)}$ - first and second time derivatives;

$\{\,\}^T$, $[\,]^T$ - transpose;

$\{\,\}^*$, $[\,]^*$ - complex conjugate;

$\{\,\}^H$, $[\,]^H$ - hermitian transpose (complex conjugate + transpose);

$[\,]^{-1}$ - standard inverse;

$[\,]^+$ - pseudo-inverse.

Symbols

$(\tilde{\ })$	-	experimentally measured quantity;
$[\ \ddots]$	-	diagonal matrix.

Abbreviations

ARMA	-	autoregressive moving-average;
CE	-	complex exponential;
CEFD	-	complex exponential frequency domain;
DOF	-	degree-of-freedom;
DSPI	-	direct system parameter identification;
EMA	-	experimental modal analysis;
ERA	-	eigensystem realization algorithm;
ERA-FD	-	eigensystem realization algorithm in the frequency domain;
FDPM	-	frequency domain Prony method;
FEM	-	finite element method;
FFT	-	fast Fourier transform;
FRF	-	frequency response function;
GHS	-	Gaukroger-Heron-Skingle;
GRFP	-	global rational fraction polynomial;
IRF	-	impulse response function;
ISSPA	-	identification of structural system parameters;
ITD	-	Ibrahim time domain;
LSCE	-	least-squares complex exponential;
MAC	-	modal assurance criterium;
MCF	-	modal confidence factor;
MDOF	-	multi degree-of-freedom;
MIMO	-	multi input multi output;
PRCE	-	polyreference complex exponential;
PRFD	-	polyreference frquency domain;
RFP	-	rational fraction polynomial;
SDOF	-	single dgree-of-freedom;
SFD	-	simultaneous frequency domain;
SIMO	-	single input multi output;
SISO	-	single input single output;
SSTD	-	single-station time domain;
SVD	-	singular value decomposition.

CHAPTER 1

INTRODUCTION

1-1 General considerations

In current engineering practice, it is of major concern to be able to incorporate vibration studies at the level of design as well as at the prototype stage. The former involves prediction of the frequencies and vibration levels at which the structure may experience high values of stress, leading to failure or at least malfunction. This prediction is based on the establishment of mathematical models which can be formulated on analytical and/or numerical calculations. Due to the high complexity of almost all engineering structures and machines, analytical solutions are usually impossible to obtain and, therefore, numerical methods represent the major percentage of all the calculations that have to be pursued. The numerical methods widely used are the finite difference method, especially in fluid mechanics, and the finite element method, in structural mechanics. The construction of a prototype or the actual structure does not mean the end of the uncertainties for the engineer. He is well aware that the

theoretical concepts involved in the calculations have incorporated several assumptions and simplifications that may not (and in general do not) reflect the actual behaviour of the real structure. Experimental procedures start, then, to play their role by evaluating the extent to which the theoretical predictions compare to the experimental results. Some aspects of the behaviour of the structure may not have been foreseen at all and are only made clear by experimental tests. Provided sufficient care is given to the experimental procedures, the results thus obtained are those that should be understood as the most correct. These should be used in two ways: (i) to make direct modifications to the structure and start an iteration process based on modification-testing and, (ii) to provide information to correct the theoretical models so that future structures can be more rigorously designed. This last aspect is very important, especially if we think that it is not always possible to test completely an already built structure, due to many limitations, one of which is the cost inherent in experimental work.

To summarize, one must say that the theoretical and the experimental procedures have a complementary role for the complete description and understanding of the dynamic behaviour of a structure and that one cannot be substituted for the other. In the present work, we shall be dealing with the experimental side of the problem of evaluating the dynamic characteristics of mechanical structures, by the use of experimental modal analysis.

Experimental modal analysis is a vast area of study that comprises three stages: (i) the testing of the stucture to obtain the relevant raw measured data, (ii) the analysis of these data by the use of numerical techniques and (iii) the post-processing of the results obtained. The overall objective is to obtain a mathematical model of the structure that matches as closely as possible the experimental results obtained in the tests. The post-processing stage encompasses the use of the results to update previous theoretical predictions, optimization via structural modification, subsystem coupling,

calculation of real modes from complex modes, etc.

1-2 Testing a structure

1-2-1 Measurement procedures

The measurement procedures must be established with great care in order to acquire reliable response data for subsequent analysis. The structure must be well positioned, either for a free-free test case - with soft suspension - or for a grounded test, well mounted on a foundation block that must be isolated from neighbouring machines. Depending on the type of structure and on the kind of desired measurement, the size of the shakers or impact hammers, the transducers (for force and response), charge amplifiers and other devices must be chosen accordingly. Of paramount importance is also the correct calibration of the transducers, and this must be checked again after the completion of the measurements. Spectral or sine-sweep analysers must be used according to the required type of measurement. Also depending on the type of desired analysis, a judicious choice of the excitation and response locations must be made. A careful set up of all the instrumentation, including alignment of the shaker and location of the transducers, must be made.

Another very important aspect is the signal processing, i. e., the choice of the type of excitation signal, filters, type of windows to use, number of averages to take into account, etc. After the measurement has been completed, some checks must be made, for instance on the coherence (whenever applicable), input auto-spectrum and signal-to-noise ratio.

1-2-2 Types of excitation signals

The type of excitation signal depends on the objectives of the study. We can

have, for instance, excitation due to ambient phenomena, like wind, seismic activity or traffic. Usually, this kind of excitation is very difficult or impossible to measure and the analysis of the acquired data only provides limited information. Another form of excitation is the transient type such as can result from a load that is suddenly released or from an impact, usually using a hammer. The use of a hammer is, nowadays, a very popular means of exciting a structure, due to the possibility of having easy access to many points of the structure and also because a lot of data can be acquired very rapidly. Another advantage is that in this case there is minimal attachement between the excitation device and the structure, thus reducing unwanted interactions. The time response to the impulse will contain information of all the modes of vibration of the structure, provided enough energy has been put into the impact, for the frequency range one is interested in. The use of two-channel Fast-Fourier-Transform (FFT) analysers enables the time signals of the input and of the output (usually measured with an accelerometer) to be transformed into the frequency domain, from where the relation between the two signals can be calculated, giving the so-called frequency-response-function (FRF) containing information about the dynamic properties of the structure.

However, noisier results are to be expected using this excitation than those obtained using, for instance, random excitation. Besides the hammer, we can use an electro-magnetic shaker which, driven by a signal generator, can excite the structure with a different number of excitation signals. The most common is random excitation. A random input implies a random output and again using an FFT analyser the FRF can be estimated. The random signal provides an input with a spectrum in all the frequency range of interest, but an averaging procedure is necessary to eliminate noise, due to the fact that the signal is constantly varying and although it is not periodic, each separate sample is assumed periodic by the analyser. The use of a "window", i. e., multiplication by a function that dies out in the

begining and at the end of the sample period, is usually essential. Tests using random excitation are generally very fast. The main disadvantage is that statistical testing makes non-linear structures appear to be linear. Alternative but similar excitations applied via a shaker are pseudo-random, which is a periodic signal,but with a random amplitude and phase within each period, and burst-random, which is a random signal that starts shortly after the starting of the acquisition and ends well before the completion of the data acquisition. Another form of signal is the "chirp", which is a fast sine sweep. It is quicker than the previously mentioned signals.

The noise is also reduced.

Step-sine excitation does not require an FFT analyser, but another type, to perform a sweep over the frequency range of interest and to calculate the FRF. Although slower than random excitation, sine-wave excitation is very good for analysing narrow frequency bands and for characterizing non-linearities. A disadvantage is that it may excite quite strongly the structure at a resonance frequency, causing damage to it.

Practical considerations on measurement procedures and signal processing can be found in Refs. [1] to [6], as well as in the Technical Review series of Brüel & Kjær. Refs. [7] and [8] (for example) constitute more fundamental and classical text books on this subject. In all these references the interested reader can find many more articles and text books dealing with this matter.

1-2-3 Structural behaviour assumptions

In experimental modal analysis the structure usually is assumed to exhibit a linear behaviour, meaning that the response to a combination of forces applied simultaneously is the summation of the individual responses corresponding to each force applied individually. This is, in general, quite

a reasonable assumption to make, even if in practice the structure exhibits a slightly non-linear behaviour. For higher degrees of non-linearity, though, appropriate techniques must be used.

Another assumption is that the structure is time invariant, i. e., its dynamic properties do not vary with time. A common example of time variance concerns the dependence on temperature. A structure may be composed of materials that can be sensitive to changes of temperature and, implicitly, dependent on time. This can be quite a critical factor in some modern structures, often composed of non-metallic elements, and gives credit to the increasing tendency of creating rapid data acquisition systems that are able to obtain a large amount of data in a minimum time. In our study we shall consider that these two assumptions (linearity and time-invariance) hold.

In Section 1-3, a general classification of the various methods of analysis (identification) of the measured data is given; the analysis of those data constitutes the second stage of experimental modal analysis cited above and is the focus of our attention in this work. One of the possible applications of the post-processing of the results (third stage) is the calculation of real modes from the identified complex modes (as afore-mentioned) and methods of analysis for this purpose will be presented in Chapter 6.

1-3 Classification of modal analysis identification methods

During the last two decades or so, many researchers have devoted their efforts to the development of techniques that aim to produce a reliable identification of the dynamic properties of structures. Those efforts have been fruitful due largely to the introduction of the Fast-Fourier-Transform (FFT) (Ref. [9]) and to the development in recent years of very powerful multi-channel spectrum analysers, dedicated desktop computers

and instrumentation in general, that permit the acquisition and treatment of large quantities of data. In this way, it was possible to evolve from very simple techniques (e. g., Refs. [10] to [13]) where analyses were based on data from single input excitation and single output response to highly sophisticated ones (e. g., Refs. [14], [15]) where data from multi-input excitation and multi-output responses are treated simultaneously. The turning point in this evolution was made in 1971 by Klosterman (Ref. [16]), introducing on-line testing controlled by mini-computers.

The current trend of experimental modal analysis (EMA) seems to be a progressive abandonment of interactive analysis programs and a development of completly automated systems of acquisition and analysis of data, to accompany the developments in other areas of structural design, like the Finite Element Method (FEM) and the Computer-Aided Design (CAD). A perspective of the evolution and future of EMA is given in Ref. [17].

Nowadays, the number of technical publications on EMA is such (to have an idea, see Ref. [18]) that the task of classifying the available methods of analysis (itself only part of EMA's vast field of study) represents a great effort. Previous surveys, Refs. [19] to [29], are a good starting point for our investigation.

The major grouping concerns the domain in which the data are treated numerically. There are time-domain and frequency-domain methods. Tuned-sinusoidal methods are a special category and will be considered separately. Early methods used to work in the frequency domain, but problems associated with frequency resolution, leakage and high modal densities led workers to start looking at time domain methods as a promising alternative. The calculation of the impulse-response-function (IRF) corresponding to an FRF involves the calculation of the inverse FFT,

a standard feature in spectral analysers. In this case, however, leakage can still be a problem, and to avoid this some methods use the force and response histories directly. In general, time domain models tend to provide the best results when a large frequency range or large number of modes exist in the data, whereas frequency domain models tend to provide the best results when the frequency range of interest is limited and the number of modes is relatively small. However, time domain methods have a major disadvantage in that they can only estimate modes inside the frequency range of analysis, and take no account on the residual effects of modes that lie outside that range. This is why, recently, people have returned to frequency domain techniques, which can improve the accuracy of the results by accounting for residual terms or by increasing the order of the model. The eventual application of the resulting models has a major influence on the importance (or otherwise) of these residual effects.

Time domain and frequency domain methods can be divided into indirect (or modal) and direct methods. The former designation (indirect) means that the identification of the FRF(s) is based on the modal model, i. e., on the modal parameters (natural frequencies, damping ratios, modal constants and their phases) which are the quantities in the characteristic solutions of the dynamic equations of equilibrium. The latter designation (direct) means that the identification is directly based on the spatial model, i. e., on the general matrix equation of dynamic equilibrium, the primitive equation from which all the methods are derived. In some of the methods in this last category, the system matrices of the referred equation can be evaluated and the corresponding eigenproblem solved in order to calculate the modal parameters.

A further division concerns the number of modes which can be analysed. In this respect, we can have single-degree-of-freedom (SDOF) and multi-degree-of-freedom (MDOF) analyses. In the time domain we have only MDOF analysis, while in the frequency domain we can have SDOF or

MDOF analyses with the indirect methods. Direct methods only apply to MDOF analysis.

When we have tested a structure in order to collect the measured data, we usually have at our disposal a set of FRFs. These FRFs are the result of exciting the structure at each selected point and measuring the response at several locations across that structure. Some modal analysis methods can be applied only to a single FRF at a time. These are called single FRF or single-input-single-output (SISO) methods. Other methods allow for several FRFs to be analysed simultaneously, with responses taken at various points on the structure, but using one excitation point. These are called global or single-input-multi-output (SIMO) methods. The philosophy behind this category of methods is that the natural frequencies and damping ratios do not vary (theoretically) from FRF to FRF (they are global properties of a structure) and, thus, it should be possible to obtain a consistent and unique set of those properties by processing several FRFs at the same time. This procedure would automatically average out small variations in those modal properties that will necessarily occur when analysing one FRF at a time and it would, in principle, be preferable to a simple or weighted average of the results from several single analyses. Finally, there are methods that can process all the available FRFs simultaneously, from various excitation and response locations. These methods are usually called polyreference or multi-input-multi-output (MIMO) methods. Fig. 1-1 shows a diagram with the various possible categories of methods.

1-4 General objectives of the work

The main objectives of the present work are:

(i) to give a general classification for the modal analysis identification

methods, together with a detailed interpretation of the most significant and most widely used ones, as a general review containing such an information is not currently available;

(ii) to explore, in a critical sense, some of the most used frequency domain methods, providing means of improving them and paying special attention to the common problem of the recognition and identification of close modes;

(iii) to explain and justify, whenever possible, either theoretical procedures or physical interpretations that have not been clarified so far, therefore contributing to the future development of modal analysis technology;

(iv) to develop more automatic and "intelligent" procedures which, when incorporated into the computer programs, can provide answers with inherent indications of their quality, so that the intervention and judgement of the user is minimized or even eliminated. In other words, to extract valid modal properties from measured data.

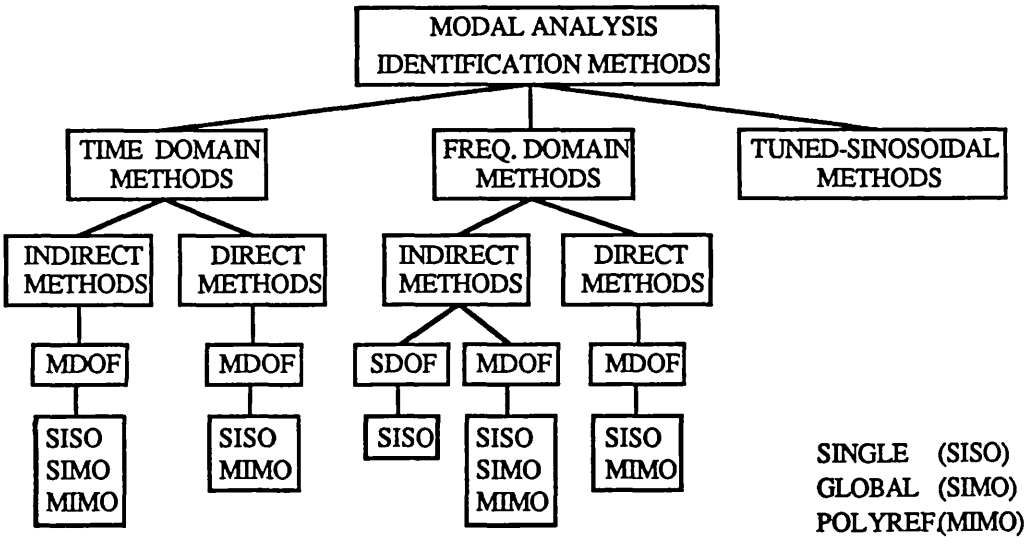

Fig. 1-1 Classification of modal analysis methods

1-5 Preview of the thesis

In Chapter 2, a description of the most widely used methods of modal identification is given. In this exposition, we have tried to follow a certain chronological order, usually accompanied by a logical (?) growth in the complication and sophistication of the algorithms used. The emphasis of this thesis is on frequency domain methods. This choice is due to several reasons:

(i) more facility in the incorporation of residual terms in the theoretical formulation;

(ii) to avoid the calculation of the IRF via an inverse FFT;

(iii) current trend in modal analysis research;

(iv) more tradition, previous experience and available software, and personal preference.

In Chapter 3, a discussion of SDOF methods is provided, seeking to understand the limitations of this kind of method, namely in what concerns the recognition and identification of close modes. Improvements on this matter are proposed. This kind of method can provide a useful physical understanding of the implications of the existence of close modes and is shown to be quite useful and appropriate for a large range of applications.

In Chapter 4, the Rational Fraction Polynomial method is developed in its *SISO* version and described in full detail. A new automatic procedure to establish the existence of one or two close modes is proposed and theoretical and practical examples are given. A new approach to the identification of lightly damped structures based on the Rational Fraction Polynomial method is made, and a discussion on the effects of the choice of the data points to be used is carried out. The "best" results are found by an automatic procedure. This approach is shown to be closely related to the

Ewins-Gleeson method, described in the following chapter.

In Chapter 5, a *SIMO* version of the Rational Fraction Polynomial method is described and alternative formulations to calculate the modal parameters are proposed. Special attention is again given to the case of two close modes. A method called Global is also described in detail and an improvement is given in order to obtain results with indications of their quality. Another method, the Spectral method is also discussed, some improvements are tried and a comparison with the other two methods presented.

Another important related field of investigation is the calculation of real modes of vibration based on measured complex modes. This is also a very important matter in the assessment of the validity of theoretical calculations, usually using the finite element method. In Chapter 6 two of the many existing methods for this type of calculations are compared and some examples are given.

Finally, in Chapter 7, conclusions and contributions of the current work are presented together with suggestions for future research.

CHAPTER 2

A DESCRIPTION OF MODAL ANALYSIS IDENTIFICATION METHODS

2-1 Introduction

Based on the classification given in Fig. 1-1, a wide range of modal analysis identification methods are described in the present chapter. The most relevant methods in the time and frequency domains are presented and a historical note on the tuned-sinusoidal methods is also given. The objective of this chapter is to provide the interested reader with a comprehensive review of the various methods of identification, usually distributed over a large number of publications and with a wide diversity in the notation used. We have tried to keep the notation as consistent as possible. Moreover, it is hoped that the review will be useful to those interested in investigating one or more methods, to decide on which ones to study and to understand more readily the similarities and differences amongst the several approaches. For the thesis, the given description helps essentially to frame the methods on which focus is put in subsequent chapters of this work.

2-2 Time domain methods

2-2-1 Indirect or Modal methods

In this category, the most widely known methods are the Complex Exponential (CE), the Least-Squares Complex Exponential (LSCE), the Polyreference Complex Exponential (PRCE), the Ibrahim Time Domain (ITD), the Single-Station Time Domain (SSTD), and the Eigensystem Realization Algorithm (ERA). We shall describe each of these, providing an explanation of the theory and the most relevant references, and seeking to highlight the common features and the differences between them. In Fig. 2-1, a diagram of the classification of time domain methods is shown.

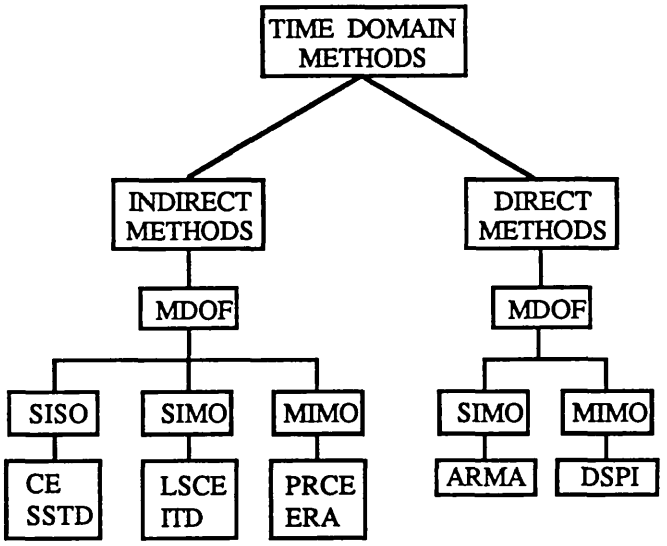

Fig. 2-1 Classification of Time domain methods.

The Complex Exponential method (CE)

In the frequency domain, the FRF in terms of receptance α_{ik} (displacement

at point i due to a force at point k) for a linear, viscously damped system with N degrees-of-freedom (DOF) can be given by (e. g., Ref. [1]):

$$\alpha_{ik}(j\omega) = \sum_{r=1}^{N} \left[\frac{{}_rA_{ik}}{\omega_r\xi_r + j(\omega - \omega_r\sqrt{(1-\xi_r^2)})} + \frac{{}_rA_{ik}^*}{\omega_r\xi_r + j(\omega + \omega_r\sqrt{(1-\xi_r^2)})} \right] \quad (2\text{-}1)$$

where ω_r is the natural frequency, ξ_r is the viscous damping factor and ${}_rA_{ik}$ is the residue corresponding to each mode **r**; * denotes complex conjugate. Another way of writing Eq. (2-1) is

$$\alpha_{ik}(j\omega) = \sum_{r=1}^{2N} \frac{{}_rA_{ik}}{\omega_r\xi_r + j(\omega - \omega_r')} \quad (2\text{-}2)$$

where

$$\begin{aligned} \omega_r' &= \omega_r \sqrt{(1-\xi_r^2)} \\ \omega_{r+N}' &= -\omega_r' \\ {}_{r+N}A_{ik} &= {}_rA_{ik}^* \end{aligned} \quad (2\text{-}3)$$

The **CE** method (Refs. [30], [31], [27]) works with the corresponding impulse-response-function (IRF), obtained from (2-2) by an inverse Fourier transform :

$$h_{ik}(t) = \sum_{r=1}^{2N} {}_rA_{ik}\, e^{s_r t} \quad (2\text{-}4)$$

or, simply

$$h(t) = \sum_{r=1}^{2N} A_r' e^{s_r t} \quad (2\text{-}5)$$

where $s_r = -\omega_r\xi_r + j\omega_r'$ and the properties (2-3) hold. Considering the time response **h(t)** (real-valued) at a series of **L** equally spaced time

intervals Δt, we have

$$\begin{aligned} h_0 &= h(0) = \sum_{r=1}^{2N} A_r' \\ h_1 &= h(\Delta t) = \sum_{r=1}^{2N} A_r' e^{s_r(\Delta t)} \\ &\vdots \\ h_L &= h(L\Delta t) = \sum_{r=1}^{2N} A_r' e^{s_r(L\Delta t)} \end{aligned} \tag{2-6}$$

or, simply

$$\begin{aligned} h_0 &= \sum_{r=1}^{2N} A_r' \\ h_1 &= \sum_{r=1}^{2N} A_r' V_r \\ &\vdots \\ h_L &= \sum_{r=1}^{2N} A_r' V_r^L \end{aligned} \tag{2-7}$$

with

$$V_r = e^{s_r \Delta t} \tag{2-8}$$

It must be noted that in Eq. (2-7) the values of $\mathbf{A_r'}$ and $\mathbf{V_r}$ are not known. How can these values be calculated ? The solution is an ingenious technique devised in 1795 by Prony (Ref. [32]) and known as Prony's method. Because the roots $\mathbf{s_r}$ for a sub-critically damped system always occur in complex conjugate pairs, so do the modified variables $\mathbf{V_r}$. Thus, there always exists a polynomial in $\mathbf{V_r}$ of order $\mathbf{L}$ with real coefficients β (called the autoregressive coefficients) such that Eq. (2-9) is verified:

$$\beta_0 + \beta_1 V_r + \beta_2 V_r^2 + \ldots + \beta_L V_r^L = 0 \tag{2-9}$$

In order to calculate the coefficients β to evaluate V_r, it is necessary just to multiply both sides of Eq. (2-7) by β_0 to β_L and to sum the result. This gives:

$$\sum_{i=0}^{L} \beta_i h_i = \sum_{i=0}^{L} [\beta_i \sum_{r=1}^{2N} A_r' V_r^i] \tag{2-10}$$

or

$$\sum_{i=0}^{L} \beta_i h_i = \sum_{r=1}^{2N} [A_r' \sum_{i=0}^{L} \beta_i V_r^i] \tag{2-11}$$

In this way, the inner summation in Eq. (2-11) is exactly the polynomial of Eq. (2-9). As this polynomial vanishes for each value of V_r, the right-hand-side of Eq. (2-11) becomes null for each root of that polynomial, becoming

$$\sum_{i=0}^{L} \beta_i h_i = 0 \quad \text{, for each } V_r \tag{2-12}$$

From Eq. (2-12) it will be possible to calculate the coefficients β_i which will yield the solution of the polynomial (2-9) for its roots, V_r. To calculate β_i, we proceed as follows: **L** will be taken equal to **2N** for convenience and so we shall need **2N** sets of data points h_i, each one shifted one time interval and β_{2N} will be set to **1**. The result will be:

$$\begin{bmatrix} h_0 & h_1 & h_2 & \ldots & h_{2N-1} \\ h_1 & h_2 & h_3 & \ldots & h_{2N} \\ \cdot & \cdot & \cdot & & \cdot \\ \cdot & \cdot & \cdot & & \cdot \\ \cdot & \cdot & \cdot & & \cdot \\ h_{2N-1} & h_{2N} & h_{2N+1} & \ldots & h_{4N-2} \end{bmatrix} \begin{Bmatrix} \beta_0 \\ \beta_1 \\ \cdot \\ \cdot \\ \beta_{2N-1} \end{Bmatrix} = - \begin{Bmatrix} h_{2N} \\ h_{2N+1} \\ \cdot \\ \cdot \\ h_{4N-1} \end{Bmatrix} \tag{2-13}$$

or

$$\underset{(2Nx2N)}{[h]} \quad \underset{(2Nx1)}{\{\beta\}} = \underset{(2Nx1)}{\{h'\}} \tag{2-14}$$

knowing the coefficients β_i, we can use a polynomial solver (or, even better, an eigensolver) to calculate the roots V_r. Using Eq. (2-8) and its corresponding complex conjugate value, we can determine the natural frequencies and damping factors. With the values of V_r, we can use Eq. (2-7) to calculate the residues and consequently the modal constants and phase angles. The residues A_r' are easy to calculate if we write Eq. (2-7) as:

$$\begin{bmatrix} 1 & 1 & \cdots & 1 \\ V_1 & V_2 & \cdots & V_{2N} \\ V_1^2 & V_2^2 & \cdots & V_{2N}^2 \\ \vdots & \vdots & & \vdots \\ V_1^{2N-1} & V_2^{2N-1} & \cdots & V_{2N}^{2N-1} \end{bmatrix} \begin{Bmatrix} A_1' \\ A_2' \\ A_3' \\ \vdots \\ A_{2N}' \end{Bmatrix} = - \begin{Bmatrix} h_0 \\ h_1 \\ h_2 \\ \vdots \\ h_{2N-1} \end{Bmatrix} \tag{2-15}$$

where, for convenience (to have a square matrix), we have only taken the first **2N-1** values of h_i. In fact, we need use only **N-1** values, as V_r and A_r' appear in complex conjugate pairs.

The **CE** method is an MDOF indirect method that falls in the category of *SISO* methods, as it is designed to analyse a single IRF at a time. It is a simple method that does not require initial estimates for the modal parameters and the only unknown is the number of modes that must be considered in the analysis. An overspecified number of modes is usually given and we shall have to distinguish later between genuine and computational modes. Another way of determining the correct number of

modes is to repeat the analysis several times, decreasing each time the specified number of modes. A plot of the error between the original and regenerated curves for each number of modes will give an indication of the correct order of the model. A drop on this error graph corresponding to the correct number of modes is expected to be visible. An alternative to the calculation of the effective number of modes is the calculation of the rank of the coefficient matrix used to calculate the eigenvalues. Another way could be the use of different sets of data and analyse the consistency (or the variation) of the solutions for the modal parameters. Both these kind of techniques will be discussed in Chapters 4 and 5, applied to frequency domain methods. One of the biggest disadvantages of the **CE** method appears to be its sensitivity to noise (Ref. [27]).

The Least-Squares Complex Exponential method (LSCE)

The **LSCE**, introduced in 1979 (Ref. [27]), is the extension of the **CE** to a global procedure. It is therefore a *SIMO* method, processing simultaneously several IRFs obtained by exciting a structure at one single point and measuring the responses at several locations. With such a procedure, a consistent set of global parameters (natural frequencies and damping factors) are obtained, thus overcoming the variations obtained in the results for those parameters when applying the **CE** method on different IRFs.

The extension from the **CE** to the **LSCE** method is quite straightforward. Referring to Eq. (2-14), it can be seen that the coefficients β that provide the solution of the characteristic polynomial (2-9) are global quantities, i. e., they must be the same for every IRF used. Therefore, if we write Eq. (2-14) for **p** IRFs, we obtain

$$\begin{bmatrix} [h]_1 \\ [h]_2 \\ \cdot \\ \cdot \\ \cdot \\ [h]_p \end{bmatrix} \{\beta\} = \begin{Bmatrix} \{h'\}_1 \\ \{h'\}_2 \\ \cdot \\ \cdot \\ \cdot \\ \{h'\}_p \end{Bmatrix} \tag{2-16}$$

or

$$\underset{(2Npx2N)}{[h_G]} \underset{(2Nx1)}{\{\beta\}} = \underset{(2Npx1)}{\{h_G'\}} \tag{2-17}$$

The least-squares solution can be found via the pseudo-inverse technique:

$$\{\beta\} = ([h_G]^T [h_G])^{-1} [h_G]^T \{h_G'\} \tag{2-18}$$

We can see that a solution of this type could already have been applied in the **CE** method for Eq. (2-13). Considering more than **2N** sets of points would already have been an improvement in the averaging out of noise disturbances in the data. Therefore, in Eq. (2-17) we can also have more than **2N** sets of data points. Knowing the coefficients $\{\beta\}$, we obtain the values of $\mathbf{V_r}$ as before (solving Eq. (2-9)) and then, for each IRF, we can calculate the residues $\mathbf{A_r'}$ using again Eq. (2-15) and, consequently, the modal constants and phase angles. For these later calculations, a frequency domain algorithm could alternatively be used.

The problems associated with the estimation of the correct number of modes still remain, as for the **CE** method. The calculation of the rank of matrix $[\mathbf{h_G}]$ in Eq. (2-17) can be used as an indication of that quantity (Ref. [27]).

The Polyreference Complex Exponential method (PRCE)

The **PRCE** method, developed in 1982 by Vold *et al.* (Refs. [33], [34]), constitutes the extention of the **LSCE** method to a *MIMO* version, i. e., including information not only from several output locations, but also from several input reference points on the structure. Apart from being a more general and automatic way of analysing dynamically a structure, this overcomes the problem that sometimes occurs when using a *SIMO* method, where one mode of vibration may not be excited because the excitation may be located close to a node of the structure.

In the explanation that follows, we shall try to keep a similar notation as used in the previous two methods, and a similar philosophy, to show as clearly as possible how the **PRCE** is an extension of the **LSCE** method. In this effort, we shall follow closely the development given by Deblauwe and Allemang (Ref. [35]).

As we saw in Eq. (2-4), the IRF at a point **i** due to an input at point **k** is given by

$$h_{ik}(t) = \sum_{r=1}^{2N} {}_rA_{ik}\, e^{s_r t} \tag{2-4}$$

Considering **q** input reference points, we have

$$\begin{aligned} h_{i1}(t) &= \sum_{r=1}^{2N} {}_rA_{i1}\, e^{s_r t} \\ h_{i2}(t) &= \sum_{r=1}^{2N} {}_rA_{i2}\, e^{s_r t} \\ &\vdots \qquad\qquad \vdots \\ h_{iq}(t) &= \sum_{r=1}^{2N} {}_rA_{iq}\, e^{s_r t} \end{aligned} \tag{2-19}$$

But, for each mode **r**, the residues ${}_rA_{ik}$ are related through a scaling factor

Q_r to the eigenvector elements ${}_r\psi_i$ and ${}_r\psi_k$ of the system by the relationship:

$$ {}_rA_{ik} = Q_r \, {}_r\psi_i \, {}_r\psi_k \tag{2-20} $$

So, if the first residue is given by

$$ {}_rA_{i1} = Q_r \, {}_r\psi_i \, {}_r\psi_1 \tag{2-21} $$

we can write for the residue at point **k**,

$$ {}_rA_{ik} = {}_rW_{k1} \, {}_rA_{i1} \tag{2-22} $$

where ${}_rW_{k1}$ is a weighting factor or a modal participation factor, given by:

$$ {}_rW_{k1} = \frac{{}_r\psi_k}{{}_r\psi_1} \tag{2-23} $$

In this way, Eq. (2-19) will be

$$ \begin{aligned} h_{i1}(t) &= \sum_{r=1}^{2N} {}_rA_{i1} \, e^{s_r t} \\ h_{i2}(t) &= \sum_{r=1}^{2N} {}_rW_{21} \, {}_rA_{i1} \, e^{s_r t} \\ &\vdots \qquad\qquad \vdots \\ h_{iq}(t) &= \sum_{r=1}^{2N} {}_rW_{q1} \, {}_rA_{i1} \, e^{s_r t} \end{aligned} \tag{2-24} $$

In matrix form, we can write Eq. (2-24) as

$$ \underset{(q\times 1)}{\begin{Bmatrix} h_{i1}(t) \\ h_{i2}(t) \\ \vdots \\ h_{iq}(t) \end{Bmatrix}} = \underset{(q\times 2N)}{\begin{bmatrix} 1 & 1 & \cdots & 1 \\ {}_1W_{21} & {}_2W_{21} & \cdots & {}_{2N}W_{21} \\ \vdots & \vdots & & \vdots \\ {}_1W_{q1} & {}_2W_{q1} & \cdots & {}_{2N}W_{q1} \end{bmatrix}} \underset{(2N\times 2N)}{\begin{bmatrix} e^{s_1 t} & & & 0 \\ & e^{s_2 t} & & \\ & & \ddots & \\ 0 & & & e^{s_{2N} t} \end{bmatrix}} \underset{(2N\times 1)}{\begin{Bmatrix} {}_1A_{i1} \\ {}_2A_{i1} \\ \vdots \\ {}_{2N}A_{i1} \end{Bmatrix}} \tag{2-25} $$

or simply

$$\underset{(qx1)}{\{h_i(t)\}} = \underset{(qx2N)}{[W]} \underset{(2Nx2N)}{\begin{bmatrix} e^{s_1 t} & & 0 \\ & e^{s_2 t} & \\ & & \ddots \\ 0 & & e^{s_{2N} t} \end{bmatrix}} \underset{(2Nx1)}{\{A_{i1}\}} \tag{2-26}$$

where [W] is the modal participation matrix. Considering L+1 time intervals,

$$\begin{aligned} \{h_i(0)\} &= [W]\{A_{i1}\} \\ \{h_i(\Delta t)\} &= [W][\Lambda]\{A_{i1}\} \\ &\vdots \\ \{h_i(L\Delta t)\} &= [W][\Lambda]^L\{A_{i1}\} \end{aligned} \tag{2-27}$$

where

$$[\Lambda] = \begin{bmatrix} e^{s_1 \Delta t} & & 0 \\ & e^{s_2 \Delta t} & \\ & & \ddots \\ 0 & & e^{s_{2N} \Delta t} \end{bmatrix} \tag{2-28}$$

It must be remembered that in Eqs. (2-27) the elements of {h(t)} are the only known quantities. As for the CE method (Eq. (2-9)), the 2N eigenvalues can now be seen as solutions of a matrix polynomial, given by:

$$[\beta_0] + [\beta_1][W][\Lambda] + [\beta_2][W][\Lambda]^2 + \ldots + [\beta_L][W][\Lambda]^L = [0] \tag{2-29}$$

where $[\beta_0]$, ..., $[\beta_L]$ are real, square coefficient matrices of order q (the number of input references). How big must the order of the matrix polynomial (L) be in order to obtain the 2N eigenvalue solutions? The

number of eigenvalues of a matrix polynomial is equal to the order of the polynomial times the dimension of the matrix coefficients, i. e., in this case,

$$2N = Lq \tag{2-30}$$

This means that in order to calculate at least **2N** eigenvalues we must have

$$Lq \geq 2N \tag{2-31}$$

hence,

$$L \geq 2N/q \tag{2-32}$$

If **Lq > 2N**, then there will be computational modes. As before, we shall multiply each side of Eqs. (2-27) by $[\beta_0]$, ..., $[\beta_L]$:

$$\begin{aligned}
[\beta_0]\,\{h_i(0)\} &= [\beta_0]\,[W]\,\{A_{i1}\} \\
[\beta_1]\,\{h_i(\Delta t)\} &= [\beta_1]\,[W]\,[\Gamma\,V\,\lrcorner]\,\{A_{i1}\} \\
[\beta_2]\,\{h_i(2\Delta t)\} &= [\beta_2]\,[W]\,[\Gamma\,V\,\lrcorner]^2\,\{A_{i1}\} \\
&\;\;\vdots \qquad\qquad\qquad\quad \vdots \\
[\beta_L]\,\{h_i(L\Delta t)\} &= [\beta_L]\,[W]\,[\Gamma\,V\,\lrcorner]^L\,\{A_{i1}\}
\end{aligned} \tag{2-33}$$

Summing each side of Eqs. (2-33), we obtain:

$$\sum_{k=0}^{L} [\beta_k]\,\{h_i(k\Delta t)\} = \sum_{k=0}^{L} [\beta_k]\,[W]\,[\Gamma\,V\,\lrcorner]^k\,\{A_{i1}\} \tag{2-34}$$

From Eq. (2-29), we see that the right-hand-side of Eq. (2-34) is zero, and thus,

$$\sum_{k=0}^{L} [\beta_k]\,\{h_i(k\Delta t)\} = \{0\} \tag{2-35}$$

Assuming $[\beta_L]$ to be the unit matrix [**I**], we have

$$\sum_{k=0}^{L-1} [\beta_k] \{h_i(k\Delta t)\} = - \{h_i(L\Delta t)\} \tag{2-36}$$

We can consider now several sets of time data points (N_t sets of L points each: $N_t \geq L$), each set shifted by one interval Δt:

$$\begin{aligned}
&[\beta_0] \{h_i(0)\} + \ldots \quad \ldots + [\beta_{L-1}] \{h_i((L-1)\Delta t)\} = - \{h_i(L\Delta t)\} \\
&[\beta_0] \{h_i(\Delta t)\} + \ldots \quad \ldots + [\beta_{L-1}] \{h_i(L\Delta t)\} = - \{h_i((L+1)\Delta t)\} \\
&\quad \vdots \qquad\qquad\qquad \vdots \qquad\qquad\qquad \vdots \\
&[\beta_0] \{h_i((N_t-1)\Delta t)\} + \ldots + [\beta_{L-1}] \{h_i((L+N_t-2)\Delta t)\} = - \{h_i((L+N_t-1)\Delta t)\}
\end{aligned} \tag{2-37}$$

or

$$[[\beta_0] \; [\beta_1] \ldots [\beta_{L-1}]] \begin{bmatrix} \{h_i(0)\} & \{h_i(\Delta t)\} & \ldots \{h_i((N_t-1)\Delta t)\} \\ \{h_i(\Delta t)\} & \{h_i(2\Delta t)\} & \ldots \{h_i(N_t\Delta t)\} \\ \vdots & \vdots & \vdots \\ \{h_i((L-1)\Delta t)\} & \{h_i(L\Delta t)\} & \ldots \{h_i((L+N_t-2)\Delta t)\} \end{bmatrix} =$$

$$- [\{h_i(L\Delta t)\} \; \{h_i((L+1)\Delta t)\} \ldots \{h_i((L+N_t-1)\Delta t)\}] \tag{2-38}$$

or

$$\underset{(qxLq)}{[B_T]} \; \underset{(LqxN_t)}{[h_i]} = \underset{(qxN_t)}{[h_i']} \tag{2-39}$$

Considering now Eq. (2-39) for each response location, with **i = 1, ..., p,**

$$
\begin{aligned}
[B_T]\ [h_1] &= [h_1'] \\
[B_T]\ [h_2] &= [h_2'] \\
&\ \ \vdots \qquad\ \ \vdots \\
[B_T]\ [h_p] &= [h_p']
\end{aligned}
\tag{2-40}
$$

or

$$
\underset{(qxLq)}{[B_T]}\ \underset{(LqxN_tp)}{[[h_1]\ [h_2] \ldots [h_p]]} = \underset{(qxN_tp)}{[[h_1']\ [h_2'] \ldots [h_p']]} \tag{2-41}
$$

or, in a short form,

$$
[B_T]\ [h_T] = [h_T'] \tag{2-42}
$$

from which

$$
\underset{(qxLq)}{[B_T]} = \underset{(qxLq)}{[h_T']}\ \underset{(LqxLq)}{[h_T]^T\ ([h_T]\ [h_T]^T)^{-1}} \tag{2-43}
$$

We should note that in Eq. (2-41) we must have $\mathbf{N_t p \geq Lq}$ in order that in Eq. (2-43) the resulting matrices are of full rank. Knowing the coefficient matrix **[B]**, we can return to Eq. (2-29), and must now solve it for the eigenvalues [` **V** ·] . Rewriting Eq. (2-29) as

$$
\sum_{k=0}^{L} [\beta_k]\ [W]\ [\grave{\ } V \cdot]^k = [0] \tag{2-44}
$$

we can post-multiply each side of this equation by a unit vector of dimensions **2Nx1**, composed of zeros except for unity at the position corresponding to the eigenvalue to be calculated:

$$\sum_{k=0}^{L} [\beta_k] [W] [V]^k \begin{Bmatrix} 1 \\ 0 \\ \vdots \\ 0 \end{Bmatrix} = \sum_{k=0}^{L} [\beta_k] (e^{s_1 \Delta t})^k \{W_1\} = \{0\}$$

$$\sum_{k=0}^{L} [\beta_k] [W] [V]^k \begin{Bmatrix} 0 \\ 1 \\ \vdots \\ 0 \end{Bmatrix} = \sum_{k=0}^{L} [\beta_k] (e^{s_2 \Delta t})^k \{W_2\} = \{0\} \quad (2\text{-}45)$$

$$\vdots \qquad\qquad \vdots \qquad\qquad \vdots$$

$$\sum_{k=0}^{L} [\beta_k] [W] [V]^k \begin{Bmatrix} 0 \\ 0 \\ \vdots \\ 1 \end{Bmatrix} = \sum_{k=0}^{L} [\beta_k] (e^{s_{2N} \Delta t})^k \{W_{2N}\} = \{0\}$$

where $\{W_1\}, ..., \{W_{2N}\}$ are the columns of the modal participation matrix. For each eigenvalue **r**, and using the definition of Eq. (2-8),

$$\left[\sum_{k=0}^{L} [\beta_k] V_r^k \right] \{W_r\} = \{0\} \qquad r = 1, ..., 2N \quad (2\text{-}46)$$

$\{W_r\}$ is a non-zero vector, independent of the summation in **k**. Each one of the **2N** possible equations (2-46) represents the same eigenvalue problem, providing **Lq** solutions. Expanding Eq. (2-46) and remembering that $[\beta_L] = [\mathbf{I}]$, it follows that

$$[[\beta_0] + [\beta_1] V_r + [\beta_2] V_r^2 + ... + [\beta_{L-1}] V_r^{L-1}] \{W_r\} = - V_r^L \{W_r\} \quad (2\text{-}47)$$

If one defines

$$
\begin{aligned}
\{z_0\} &= \{W_r\} \\
\{z_1\} &= V_r\{W_r\} &&= V_r\{z_0\} \\
\{z_2\} &= V_r^2\{W_r\} &&= V_r\{z_1\} \\
&\vdots &&\vdots \\
\{z_{L-1}\} &= V_r^{L-1}\{W_r\} &&= V_r\{z_{L-2}\} \\
\{z_L\} &= V_r^{L}\{W_r\} &&= V_r\{z_{L-1}\}
\end{aligned}
\tag{2-48}
$$

then,

$$
[\beta_0]\{z_0\} + [\beta_1]\{z_1\} + \ldots + [\beta_{L-1}]\{z_{L-1}\} = -V_r\{z_{L-1}\} \tag{2-49}
$$

or

$$
\begin{bmatrix}
-[\beta_{L-1}] & -[\beta_{L-2}] & \ldots & -[\beta_1] & -[\beta_0] \\
[I] & [0] & \ldots & [0] & [0] \\
\vdots & \vdots & & \vdots & \vdots \\
[0] & [0] & \ldots & [I] & [0]
\end{bmatrix}
\begin{Bmatrix}
\{z_{L-1}\} \\ \{z_{L-2}\} \\ \vdots \\ \{z_0\}
\end{Bmatrix}
= V_r
\begin{Bmatrix}
\{z_{L-1}\} \\ \{z_{L-2}\} \\ \vdots \\ \{z_0\}
\end{Bmatrix}
\tag{2-50}
$$

(LqxLq) (Lqx1) (Lqx1)

Eq. (2-50) is known as the companion matrix equation of the eigenproblem of Eq. (2-47). This represents a standard eigenvalue problem of the type $[[A] - \lambda[I]]\{x\} = \{0\}$. Knowing the **Lq** eigenvalues V_r, it is easy to calculate the natural frequencies and damping factors, using Eq. (2-8). We can also calculate the **Lq** eigenvectors of Eq. (2-50) for each value of V_r. The corresponding values of $\{z_0\}$ are the values of $\{W_r\}$ in Eq. (2-47)

(see Eq. (2-48)). Therefore, we also know at this stage the modal participation matrix [W] and we now have to calculate the residues. Returning to Eq. (2-27),

$$\{h_i(k\Delta t)\} = [W]\,[\,V\,]^k\,\{A_{i1}\} \qquad k = 0, 1, ..., L \tag{2-51}$$

where

$$\{h_i(k\Delta t)\} = \begin{Bmatrix} h_{i1}(k\Delta t) \\ h_{i2}(k\Delta t) \\ \vdots \\ h_{iq}(k\Delta t) \end{Bmatrix} \tag{2-52}$$

and [V] is given by Eq. (2-28). While in the **CE** or **LSCE** methods each residue vector was calculated based upon one location of the input, now there is information from several inputs for each time interval (Eq. (2-52)). Varying **k** in Eq. (2-51), we obtain:

$$\begin{Bmatrix} \{h_i(0)\} \\ \{h_i(\Delta t)\} \\ \vdots \\ \{h_i(L\Delta t)\} \end{Bmatrix} = \begin{bmatrix} [W]\,[\,V\,]^0 \\ [W]\,[\,V\,]^1 \\ \vdots \\ [W]\,[\,V\,]^L \end{bmatrix} \{A_{i1}\} \tag{2-53}$$

or

$$\underset{((L+1)qx1)}{\{H_i\}} = \underset{((L+1)qx2N)}{[W_V]}\ \underset{(2Nx1)}{\{A_{i1}\}} \tag{2-54}$$

from which

$$\{A_{il}\} = (\{H_i\}^H [W_V])^{-1} \{H_i\}^H \{H_i\} \qquad (2\text{-}55)$$

where the superscript ^{H} denotes hermitian transpose. This calculation will be repeated for all the response locations, i. e., $i = 1, ..., p$. Knowing all the $\{A_{il}\}$, Eq. (2-22) can be used to calculate all the residues. In summary, the necessary steps to use the present method are as follows: first, to take all the time records of the IRFs to enter in Eq. (2-38) and solve for the coefficients **[B]** using Eq. (2-43); second, to calculate the eigenvalues and eigenvectors of Eq. (2-50) in order to find the natural frequencies and damping factors, and build the matrices **[W]** and [` **V** ·]; and finally, to calculate the residues by making use of Eqs. (2-55) and (2-22).

Besides the fact of providing a more accurate modal representation of the test structure, this method can determine multiple roots or closely spaced modes of a structure, as claimed by its authors. The time required for the analysis is reduced and the accuracy in the results increased. The major disadvantages seem to be the sensitivity to nonlinearities and to any lack of reciprocity in the frequency response matrix. It has also shown some difficulties in analysing satisfactorily structures with more than **5%** of equivalent viscous damping (Ref. [36]). The problems associated with the judgement of genuine and computational modes remain. Finally, it requires a considerable computer capacity.

The Ibrahim Time Domain method (ITD)

This method was introduced by Ibrahim in the 1970's (Refs. [37], [38]). The formulation of the method included state vectors, where displacement and velocity responses were needed and were calculated by integration of the free acceleration response. Further improvements were given by the

same author in 1977 (Ref. [39]), where only free acceleration responses were used. This is a *SIMO* method that uses free decay responses instead of IRFs, as in the previously described methods (the IRFs may benefit from the fact that they are inverse FFTs of FRFs that could already have been averaged, reducing the noise). For a system with **N** DOF, the free response of the structure at a point **i** and for the instant of time t_j is expressed as a summation of the individual responses of each mode:

$$x_i(t_j) = \sum_{r=1}^{2N} {}_r\psi_i \, e^{s_r t_j} \tag{2-56}$$

where ${}_r\psi_i$ is the ith component of the eigenvector $\{\psi_r\}$ (complex, in general). Considering **q** response locations and **L** time instants, we can write:

$$\begin{bmatrix} x_1(t_1) & x_1(t_2) & \dots & x_1(t_L) \\ x_2(t_1) & x_2(t_2) & \dots & x_2(t_L) \\ \cdot & \cdot & & \cdot \\ \cdot & \cdot & & \cdot \\ \cdot & \cdot & & \cdot \\ x_q(t_1) & x_q(t_2) & \dots & x_q(t_L) \end{bmatrix} = \begin{bmatrix} {}_1\psi_1 & {}_2\psi_1 & \cdots & {}_{2N}\psi_1 \\ {}_1\psi_2 & {}_2\psi_2 & \cdots & {}_{2N}\psi_2 \\ \cdot & \cdot & & \cdot \\ \cdot & \cdot & & \cdot \\ \cdot & \cdot & & \cdot \\ {}_1\psi_q & {}_2\psi_q & \cdots & {}_{2N}\psi_q \end{bmatrix} \begin{bmatrix} e^{s_1 t_1} & e^{s_1 t_2} & e^{s_1 t_L} \\ e^{s_2 t_1} & e^{s_2 t_2} & e^{s_2 t_L} \\ \cdot & \cdot & \cdot \\ \cdot & \cdot & \cdot \\ \cdot & \cdot & \cdot \\ e^{s_{2N} t_1} & e^{s_{2N} t_2} & e^{s_{2N} t_L} \end{bmatrix} \tag{2-57}$$

or

$$\underset{(qxL)}{[X]} = \underset{(qx2N)}{[\Psi]} \; \underset{(2NxL)}{[\Lambda]} \tag{2-58}$$

where it is reasonable to admit

$$L \geq q \geq 2N \tag{2-59}$$

If we consider a second set of **L** data points, shifted one interval Δt with

respect to the first one, we have

$$x_i(t_j + \Delta t) = \sum_{r=1}^{2N} {}_r\psi_i \, e^{s_r(t_j + \Delta t)} \tag{2-60}$$

or

$$x_i(t_j + \Delta t) = \sum_{r=1}^{2N} ({}_r\psi_i \, e^{s_r \Delta t}) \, e^{s_r t_j} \tag{2-61}$$

Defining

$$\hat{x}_i(t_j) = x_i(t_j + \Delta t) \tag{2-62 a}$$

and

$${}_r\hat{\psi}_i = {}_r\psi_i \, e^{s_r \Delta t} \tag{2-62 b}$$

we obtain

$$\hat{x}_i(t_j) = \sum_{r=1}^{2N} {}_r\hat{\psi}_i \, e^{s_r t_j} \tag{2-63}$$

and therefore, we can write a similar expression to Eq. (2-58):

$$\underset{(qxL)}{[\hat{X}]} = \underset{(qx2N)}{[\hat{\Psi}]} \; \underset{(2NxL)}{[\Lambda]} \tag{2-64}$$

We now define a square matrix $[\mathbf{A_S}]$ of order $\mathbf{q}$ (usually called the "system matrix" and, in general, complex), as

$$\underset{(qxq)}{[A_S]} = \underset{(qx2N)}{[\Psi]} \; \underset{(qx2N)}{[\hat{\Psi}]} \tag{2-65}$$

Pre-multiplying Eq. (2-58) by $[\mathbf{A_S}]$, we obtain

$$[A_S]\ [X] = [A_S]\ [\Psi]\ [\Lambda] \qquad (2\text{-}66)$$
(qxq) (qxL) (qxq) (qx2N) (2NxL)

Substituting Eq. (2-65) in Eq. (2-66), we have

$$[A_S]\ [X] = [\hat{\Psi}]\ [\Lambda] \qquad (2\text{-}67)$$
(qxq) (qxL) (qx2N) (2NxL)

Substituting Eq. (2-64) in Eq. (2-67), we obtain

$$[A_S]\ [X] = [\hat{X}] \qquad (2\text{-}68)$$
(qxq) (qxL) (qxL)

From this equation it is possible to calculate $[A_S]$, as $[X]$ and $[\hat{X}]$ are known matrices. This can be done, via the pseudo-inverse technique, either by post-multiplying Eq. (2-68) by $[\hat{X}]^T$ or by $[X]^T$. In the first case, we obtain

$$[A_S] = ([\hat{X}]\ [\hat{X}]^T)\ ([X]\ [\hat{X}]^T)^{-1} \qquad (2\text{-}69)$$

In the second case, we obtain

$$[A_S] = ([\hat{X}]\ [X]^T)\ ([X]\ [X]^T)^{-1} \qquad (2\text{-}70)$$

Which of these two expressions should be used ? A combination of both Eqs. (2-69) and (2-70), known as Double Least-Squares (DLS), seems to be preferable, as it leads to better estimates of the damping factors (Ref. [40]). Thus, we use

$$[A_S] = \frac{1}{2}\{([\hat{X}]\ [\hat{X}]^T)\ ([X]\ [\hat{X}]^T)^{-1} + ([\hat{X}]\ [X]^T)\ ([X]\ [X]^T)^{-1}\} \qquad (2\text{-}71)$$

From Eq. (2-62 b), each eigenvector $\{\hat{\psi}_r\}$ can be written as

$$\{\hat{\psi}_r\} = \{\psi_r\}\ e^{s_r \Delta t} \qquad (2\text{-}72)$$

and from Eq. (2-65), we can write

$$[A_S]\{\psi_r\} = \{\psi_r\} e^{s_r \Delta t} \tag{2-73}$$

or

$$[[A_S] - e^{s_r \Delta t}[I]]\{\psi_r\} = \{0\} \tag{2-74}$$

which is a standard eigenvalue problem. Since $[A_S]$ is of order q, there will be q eigenvalues and eigenvectors and if $q>2N$, there will be computational modes. From the eigenvalues, it will be easy to calculate the natural frequencies and damping factors. As noted by Ewins (Ref. [1]), the eigenvectors cannot be mass-normalized, as we have only recorded free-response data. This fact may or may not constitute a disadvantage, depending on the purpose of the study.

As mentioned before, we shall obtain, generally, computational modes. One way of distinguishing these modes from the genuine ones can be established by means of the relationship (2-72). If we repeat the calculations taking a different time interval shift, it is possible, for each mode, to assess its authenticity by means of a Modal Confidence Factor (MCF) (Ref. [41]); this factor compares the expected value of $\{\hat{\psi}_r\}$ (from the calculated $\{\psi_r\}$) for one time interval with the calculated value of $\{\hat{\psi}_r\}$ for the following time interval. Thus, the philosophy of this method provides a very useful and automatic check on the calculated modes of vibration.

An extensive evaluation of the **ITD** method is provided in Ref. [42]. Among the advantages of this method are the need for little interaction, effective calculation of closely spaced modes and the possibility of verification of the quality of the results, via the MCF. The main disadvantage seems to be the tendency to give nonconservative damping

estimates with noisy data.

A variation of the **ITD** method, the Sparse Time Domain algorithm (STD), has been proposed (Ref. [43]), making use of a sparse upper Hessenberg matrix. The main advantages here are the reduction in computer storage and time, and higher identification accuracy.

The Single-Station Time Domain method (SSTD)

This method was presented in 1980 by Zaghlool (Ref. [44]), and it is a *SISO* version of the **ITD** method. Matrices **[X]** and $\hat{\mathbf{X}}$ in Eqs. (2-58) and (2-64) are formed by shifting several times the response from one single station. It will not be developed here, but the corresponding version in the frequency domain will be explained in Section 2-3-2. The similarities between the two domains are immediately obvious.

The Eigensystem Realization Algorithm (ERA)

This method is due to the work of Juang and Pappa (e. g., Ref. [45]). It is a *MIMO* method and its derivation is based upon concepts associated with control theory and, therefore, it differs from the usual developments found in EMA literature. We shall try to give a concise but hopefully clear explanation of the philosophy and main steps taken in this technique. Some alterations to the notation usually given by the authors of this method (following mainly Ref. [46]) will be made, in order to retain as much coherence as possible with the general notation used in this and other chapters of the thesis.

Let the dynamic equations of equilibrium for an N DOF viscously damped system be expressed as

$$[M]\{\ddot{y}(t)\} + [C]\{\dot{y}(t)\} + [K]\{y(t)\} = \{f(y(t),t)\} \tag{2-75}$$

Defining a state vector of dimensions **2Nx1**, we have

$$\{u(t)\} = \begin{Bmatrix} \{y(t)\} \\ \{\dot{y}(t)\} \end{Bmatrix} \tag{2-76}$$

(2Nx1)

Defining also

$$[A'] = \begin{bmatrix} [0] & [I] \\ -[M]^{-1}[K] & -[M]^{-1}[C] \end{bmatrix} \tag{2-77}$$

(2Nx2N)

$$\{f(x,t)\} = [F]\{\delta(t)\} \tag{2-78}$$

(Nx1) (Nxq) (qx1)

$$[B'] = \begin{bmatrix} [0] \\ [M]^{-1}[F] \end{bmatrix} \tag{2-79}$$

(2Nxq)

where $\{\delta(t)\}$ is the input vector at **q** locations and **[F]** is a matrix of input coefficients, we can write Eq. (2-75) in the state space, as:

$$\{\dot{u}(t)\} = [A']\{u(t)\} + [B']\{\delta(t)\} \tag{2-80}$$

(2Nx1) (2Nx2N) (2Nx1) (2Nxq) (qx1)

It will be possible to relate **{u(t)}** to the measured responses at **p** physical coordinates **{x(t)}** through a transformation matrix **[R]**:

$$\{x(t)\} = [R]\{u(t)\} \tag{2-81}$$

(px1) (px2N) (2Nx1)

The solution of Eq. (2-80) to an input $\{\delta(t)\}$ is given by

$$\{u(t)\} = e^{[A'](t-t_0)}\{u(t_0)\} + \int_{t_0}^{t} e^{[A'](t-\tau)}[B']\{\delta(\tau)\}d\tau \qquad (2\text{-}82)$$

for any time t after an initial time t_0 ($t \geq t_0$). To give a discrete representation of Eq. (2-82) we shall consider several equally spaced time intervals, $0, \Delta t, \ldots, k\Delta t$. We can consider then $t = (k+1)\Delta t$ and $t_0 = k\Delta t$:

$$\{u((k+1)\Delta t)\} = e^{[A']\Delta t}\{u(k\Delta t)\} + \int_{k\Delta t}^{(k+1)\Delta t} e^{[A']((k+1)\Delta t-\tau)}[B']\{\delta(\tau)\}d\tau \qquad (2\text{-}83)$$

Assuming the input $\{\delta(\tau)\}$ is constant during the time interval $k\Delta t \leq \tau \leq (k+1)\Delta t$, given by $\{\delta(k\Delta t)\}$, and making the change of variable $\tau' = (k+1)\Delta t - \tau$, we obtain:

$$\{u((k+1)\Delta t)\} = e^{[A']\Delta t}\{u(k\Delta t)\} - \int_{0}^{\Delta t} e^{[A']\tau'} d\tau' [B']\{\delta(k\Delta t)\} \qquad (2\text{-}84)$$

Defining

$$[A] = e^{[A']\Delta t} \qquad (2\text{-}85)$$

$$[B] = -\int_{0}^{\Delta t} e^{[A']\tau'} d\tau' [B'] \qquad (2\text{-}86)$$

$$\{u(k+1)\} = \{u((k+1)\Delta t)\} \qquad (2\text{-}87)$$

$$\{\delta(k)\} = \{\delta(k\Delta t)\} \qquad (2\text{-}88)$$

we can write Eq. (2-84) as

$$\{u(k+1)\} = [A]\{u(k)\} + [B]\{\delta(k)\} \quad \text{for } k = 0, 1, 2 \ldots \qquad (2\text{-}89)$$

Eq. (2-81) becomes, then

$$\{x(k)\} = [R]\,\{u(k)\} \tag{2-90}$$

Let us consider the response to an impulse at $\mathbf{k = 0}$ and at one of the first of the input variables. Like this, $\{\delta(0)\} = \{1, 0, ...0\}^T$ and $\{\delta(k)\} = \{0\}$ for $\mathbf{k > 0}$. Substituting in Eq. (2-89),

$$\{u(1)\} = [A]\,\{u(0)\} + \{B\} \tag{2-91}$$

and hence,

$$\{x(1)\} = [R]\,\{u(1)\} \tag{2-92}$$

Substituting Eq. (2-91) in Eq. (2-92), we obtain

$$\{x(1)\} = [R]\,[A]\,\{u(0)\} + [R]\,\{B\} \tag{2-93}$$

Considering, for simplicity, $\{\mathbf{u(0)}\} = \{\mathbf{0}\}$, we have

$$\{u(1)\} = \{B\} \tag{2-94}$$

$$\underset{(px1)}{\{x(1)\}} = \underset{(px2N)}{[R]}\ \underset{(2Nx1)}{\{B\}} \tag{2-95}$$

For the other time intervals, $\{\delta(\mathbf{k})\} = \{\mathbf{0}\}$ and we have

$$\{u(2)\} = [A]\,\{u(1)\} \tag{2-96}$$

and so,

$$\{x(2)\} = [R]\,[A]\,\{B\} \tag{2-97}$$

Likewise,

$$\{x(3)\} = [R]\,\{u(3)\} = [R]\,[A]\,\{u(2)\} = [R]\,[A]^2\,\{B\} \tag{2-98}$$

and, in general,

$$\underset{(px1)}{\{x(k)\}} = \underset{(px2N)}{[R]} \quad \underset{(2Nx2N)}{[A]^{k-1}} \underset{(2Nx1)}{\{B\}} \tag{2-99}$$

If we consider the impulse at all the **q** input locations, we obtain

$$\underset{(pxq)}{[X(k)]} = \underset{(px2N)}{[R]} \quad \underset{(2Nx2N)}{[A]^{k-1}} \underset{(2Nxq)}{[B]} \tag{2-100}$$

Matrices **[X(k)]** are usually called the Markov parameters. These are used to form the generalized Hankel matrices, given by:

$$\underset{(prxqs)}{[H(k-1)]} = \begin{bmatrix} [X(k)] & [X(k+1)] & \dots [X(k+j)] \\ [X(k+1)] & [X(k+2)] & \dots [X(k+j+1)] \\ \vdots & \vdots & \vdots \\ [X(k+i)] & [X(k+i+1)] & \dots [X(k+i+j)] \end{bmatrix} \tag{2-101}$$

where **i = 1, ..., r-1** and **j = 1, ..., s-1**, with **r** and **s** as integers. If there is an initial state response measurement, we must simply replace **[H(k-1)]** by **[H(k)]**. In Eq. (2-101), **k** will be greater or equal to **1**. Substituting Eq. (2-100) in Eq. (2-101), we obtain

$$[H(k)] = [Q] [A]^k [W] \qquad k \geq 0 \tag{2-102}$$

where

$$\underset{(prx2N)}{[Q]} = \begin{bmatrix} [R] \\ [R] [A] \\ \vdots \\ [R] [A]^{r-1} \end{bmatrix} \tag{2-103}$$

$$\underset{(2Nxqs)}{[W]} = \begin{bmatrix} [B] & [A] [B] & \dots [A]^{s-1} [B] \end{bmatrix}$$

[Q] and [W] are called the observability and controllability matrices, respectively. It must be remembered that **[H(k)]** is a known matrix of the responses. One of the advantages of this formulation is that in **[H(k)]** we may include only good responses, i. e., responses with low levels of noise. The objective is to reconstruct Eq. (2-100) from the experimental data. This process is known as realization and implies the determination of matrices **[R]**, **[A]** and **[B]**. There are an infinite number of sets of these three matrices satisfying Eq. (2-100), i. e., there are an infinite number of realizations. The objective is to obtain a minimum realization, i. e., the realization corresponding to the minimum order of the state space formulation that can still represent the dynamic behaviour of the structure.

In the first place, we shall look for a matrix **[H]'** such that

$$\underset{(2Nxqs)}{[W]}\ \underset{(qsxpr)}{[H]'}\ \underset{(prx2N)}{[Q]} = \underset{(2Nx2N)}{[I]} \tag{2-104}$$

Let us pre-multiply and post-multiply Eq. (2-104) by **[Q]** and **[W]**, respectively:

$$[Q][W][H]'[Q][W] = [Q][W] \tag{2-105}$$

But, from Eq (2-102), we see that

$$[Q][W] = [H(0)] \tag{2-106}$$

Thus,

$$[H(0)][H]'[H(0)] = [H(0)] \tag{2-107}$$

Therefore, **[H]'** is the pseudo-inverse of **[H(0)]**:

$$[H]' = [H(0)]^{+} \tag{2-108}$$

We can calculate the pseudo-inverse of **[H(0)]** via the Singular Value

Decomposition (see Appendix D):

$$[H(0)] = [U]\ [\Sigma]\ [V]^T \qquad (2\text{-}109)$$
(prxqs) (prxpr) (prxps) (psxqs)

Matrix **[H(0)]** will have **2N** non-zero singular values (rank = 2N), equivalent to the order of the space state system. **[H(0)]** can therefore be recomputed using only the first **2N** columns of **[U]** and **[V]**:

$$[H(0)] = [U_{2N}]\ [\Sigma_{2N}]\ [V_{2N}]^T \qquad (2\text{-}110)$$
(prxqs) (prx2N) (2Nx2N) (2Nxqs)

with

$$[U_{2N}]^T [U_{2N}] = [V_{2N}]^T [V_{2N}] = [I] \qquad (2\text{-}111)$$

Matrix **[H]'** (= $[H(0)]^+$) is therefore given by

$$[H]' = [V_{2N}]\ [\Sigma_{2N}]^{-1}\ [U_{2N}]^T \qquad (2\text{-}112)$$

To obtain the realization we are looking for, we shall start from Eq. (2-100), which can be written for $\mathbf{k \geq 0}$ as

$$[X(k+1)] = [R]\ [A]^k\ [B] \qquad (2\text{-}113)$$

and use the identity

$$[X(k+1)] = [E_p]^T\ [H(k)]\ [E_q] \qquad (2\text{-}114)$$
(pxq) (pxpr) (prxqs) (qsxq)

where

$$[E_p]^T = [\,[I]\ [0] \ldots [0]\,] \qquad (2\text{-}115\ a)$$
(pxpr) (pxp) (pxp) (pxp)

$$[E_q]_{(qxq)} = \begin{bmatrix} [I] \\ [0] \\ \vdots \\ [0] \end{bmatrix} \qquad (2\text{-}115\ b)$$

[I] being the identity matrix. Substituting Eq. (2-102) in Eq. (2-114), we obtain:

$$[X(k+1)] = [E_p]^T [Q] [A]^k [W] [E_q] \qquad (2\text{-}116)$$

Introducing Eq. (2-104) in Eq. (2-116), we obtain

$$[X(k+1)] = [E_p]^T [Q] [[W] [H]'[Q]] [A]^k [[W] [H]'[Q]] [W] [E_q] \qquad (2\text{-}117)$$

Substituting Eq. (2-106) in Eq. (2-117),

$$[X(k+1)] = [E_p]^T [H(0)] [H]' [[Q] [A]^k [W]] [H]' [H(0)] [E_q] \qquad (2\text{-}118)$$

Using Eq. (2-112),

$$[X(k+1)] = [E_p]^T [H(0)] [[V_{2N}] [\Sigma_{2N}]^{-1} [U_{2N}]^T][[Q] [A]^k [W]] [[V_{2N}] [\Sigma_{2N}]^{-1} [U_{2N}]^T] [H(0)] [E_q] \qquad (2\text{-}119)$$

Using Eq. (2-110), it follows

$$[X(k+1)] = [E_p]^T [[U_{2N}] [\Sigma_{2N}] [V_{2N}]^T] [[V_{2N}] [\Sigma_{2N}]^{-1} [U_{2N}]^T][[Q] [A]^k [W]][[V_{2N}] [\Sigma_{2N}]^{-1} [U_{2N}]^T][[U_{2N}] [\Sigma_{2N}] [V_{2N}]^T] [E_q] \qquad (2\text{-}120)$$

Due to Eq. (2-111), it is possible to write

$$[X(k+1)] = [E_p]^T [U_{2N}] [\Sigma_{2N}] [\Sigma_{2N}]^{-1} [U_{2N}]^T [[Q] [A]^k [W]] [V_{2N}]$$
$$[\Sigma_{2N}]^{-1} [\Sigma_{2N}] [V_{2N}]^T [E_q] \quad (2\text{-}121)$$

or,

$$[X(k+1)] = [[E_p]^T [U_{2N}] [\Sigma_{2N}]^{1/2}][[\Sigma_{2N}]^{-1/2} [U_{2N}]^T [[Q] [A]^k [W]]$$
$$[V_{2N}] [\Sigma_{2N}]^{-1/2}][[\Sigma_{2N}]^{1/2} [V_{2N}]^T [E_q]] \quad (2\text{-}122)$$

From Eq. (2-122), some similarities with Eq. (2-113) (that we wish to recover) are already apparent. Some modifications, though, need to be made in Eq. (2-122), in the second block of matrices. Writing this block for **k=1**, we have

$$[\Sigma_{2N}]^{-1/2} [U_{2N}]^T [[Q] [A] [W]] [V_{2N}] [\Sigma_{2N}]^{-1/2} \quad (2\text{-}123)$$

For **k=2**, we have

$$[\Sigma_{2N}]^{-1/2} [U_{2N}]^T [[Q] [A]^2 [W]] [V_{2N}] [\Sigma_{2N}]^{-1/2} \quad (2\text{-}124)$$

Trying to relate expressions (2-123) and (2-124), let us multiply expression (2-123) by itself:

$$[\Sigma_{2N}]^{-1/2} [U_{2N}]^T [[Q] [A] [W]] [V_{2N}] [\Sigma_{2N}]^{-1/2} [\Sigma_{2N}]^{-1/2} [U_{2N}]^T [[Q] [A]$$
$$[W]] [V_{2N}] [\Sigma_{2N}]^{-1/2} \quad (2\text{-}125)$$

Due to Eq. (2-112), we obtain

$$[\Sigma_{2N}]^{-1/2} [U_{2N}]^T [[Q] [A] [W]] [H]' [[Q] [A] [W]] [V_{2N}] [\Sigma_{2N}]^{-1/2} \quad (2\text{-}126)$$

and due to Eq. (2-104), we can write

$$[\Sigma_{2N}]^{-1/2}\,[U_{2N}]^T\,[Q]\,[A]\,[A]\,[W]\,[V_{2N}]\,[\Sigma_{2N}]^{-1/2} \tag{2-127}$$

which is exactly expression (2-124). Therefore,

$$([\Sigma_{2N}]^{-1/2}\,[U_{2N}]^T\,[[Q]\,[A]\,[W]]\,[V_{2N}]\,[\Sigma_{2N}]^{-1/2})^2 =$$

$$[\Sigma_{2N}]^{-1/2}\,[U_{2N}]^T\,[[Q]\,[A]^2\,[W]]\,[V_{2N}]\,[\Sigma_{2N}]^{-1/2} \tag{2-128}$$

or, using Eq. (2-102), and generalizing for any **k**,

$$([\Sigma_{2N}]^{-1/2}\,[U_{2N}]^T\,[H(1)]\,[V_{2N}]\,[\Sigma_{2N}]^{-1/2})^k =$$

$$[\Sigma_{2N}]^{-1/2}\,[U_{2N}]^T\,[H(k)]\,[V_{2N}]\,[\Sigma_{2N}]^{-1/2} \tag{2-129}$$

Returning to Eq. (2-122), we can write it as

$$[X(k+1)] = [[E_p]^T\,[U_{2N}]\,[\Sigma_{2N}]^{1/2}][[\Sigma_{2N}]^{-1/2}\,[U_{2N}]^T\,[H(1)]\,[V_{2N}]$$
$$[\Sigma_{2N}]^{-1/2}]^k\,[[\Sigma_{2N}]^{1/2}\,[V_{2N}]^T\,[E_q]] \tag{2-130}$$

Comparing Eq. (2-130) with Eq. (2-113), we see that the desired realization has been achieved, where

$$[R] = [[E_p]^T\,[U_{2N}]\,[\Sigma_{2N}]^{1/2}]$$
$$[A] = [[\Sigma_{2N}]^{-1/2}\,[U_{2N}]^T\,[H(1)]\,[V_{2N}]\,[\Sigma_{2N}]^{-1/2}] \tag{2-131}$$
$$[B] = [[\Sigma_{2N}]^{1/2}\,[V_{2N}]^T\,[E_q]]$$

In order to determine the modal parameters of the system, we must solve an eigenproblem based on the "realized" matrix **[A]**, of the form

$$[A]\,\{\psi_u\} = \lambda\,\{\psi_u\} \tag{2-132}$$

To obtain the modeshapes in terms of the physical coordinates of the system, we must use the transformation given by (see Eq. (2-90)):

$$\underset{(px1)}{\{\psi_x\}} = \underset{(px2N)}{[R]} \underset{(2Nx1)}{\{\psi_u\}} \qquad (2\text{-}133)$$

The modal parameters are easily calculated from the eigenproblem results. In summary, the necessary steps to perform an analysis with the ERA are as follows:

(1) choice of the measured data to construct matrix **[H(0)]**;

(2) calculation of the SVD of **[H(0)]**, to calculate $[U_{2N}]$, $[V_{2N}]$ and $[\Sigma_{2N}]$ and to recalculate **[H(0)]** based on the value of the rank found (order of the system);

(3) construction of matrix **[H(1)]** and calculation of the "realized" matrices **[R]**, **[A]** and **[B]** (Eq.(2-131)); and

(4) calculation of the eigenvalues and eigenvectors of matrix **[A]** and the eigenvectors corresponding to the physical coordinates (Eqs. (2-132) and (2-133)) and calculation of the modal parameters.

This method (like the ITD), also provides checks on the calculated modes, to distinguish between genuine and computational modes, as the results from the SVD, in some cases, may not be correct due to noise or nonlinearities. The first check is known as the Modal Amplitude Coherence and is defined as the coherence between each modal amplitude history and an ideal one, formed by extrapolating the initial value of the history to other points, using the identified eigenvalue. Another check is the Modal Phase Collinearity, for lightly damped structures, where real mode behaviour is expected. This indicator measures the strength of the linear functional relationship between the real and imaginary parts of the modeshape, for each mode. Model reduction is then possible, by truncating the modes with low accuracy indicators. The final model can be assessed by comparing the initial free responses with the ones calculated by

Eq. (2-130).

An investigation on the effects of noise on the identified modal parameters using the **ERA** is given in Ref. [47]. In Ref. [46], the **ERA** is shown to be a more general formulation for modal analysis identification, as some other methods can be understood as particular cases of a unified approach. In the same reference, an extensive bibliography on System-Realization Theory can be found.

2-2-2 Direct methods

According to the classification given in the beginning Section 2-2-1, we have in this category essentially two methods, the Autoregressive Moving-average method (ARMA) and the Direct System Parameter Identification method (DSPI).

The Autoregressive Moving-average method (ARMA)

This is a *SISO* method that is mainly based on the works of Gersch (Refs. [48] to [57]). Once again, this is a method that comes from the control theory. Here, we shall try to give the basic ideas and the interested reader in invited to study the mentioned references, where the theory is explained in detail and different variations of the algorithm are given. Calls to other references and fundamental texts can be found in those works. Let us consider the behaviour of a linear system with a single input **f(t)** and a single output **y(t)** as described by the following linear differential equation of constant coefficients:

$$a_n \frac{d^n y(t)}{dt^n} + a_{n-1} \frac{d^{n-1} y(t)}{dt^{n-1}} + \ldots + a_1 \frac{dy(t)}{dt} + a_0 y(t) = b_m \frac{d^m f(t)}{dt^m} + \ldots$$

$$+ b_1 \frac{df(t)}{dt} + b_0 f(t) \qquad (2\text{-}134)$$

If we calculate the Laplace transform of Eq. (2-134) and consider the initial conditions as zero, we obtain

$$(a_n s^n + ... + a_1 s + a_0)\, Y(s) = (b_m s^m + ... + b_1 s + b_0)\, F(s) \qquad (2\text{-}135)$$

where **s** is the Laplace variable. The transfer function, defined as **H(s) = Y(s)/F(s)**, will be

$$H(s) = \frac{b_m s^m + ... + b_1 s + b_0}{a_n s^n + ... + a_1 s + a_0} \qquad (2\text{-}136)$$

In the frequency domain, putting **s=jω**, we obtain the frequency response function

$$H(j\omega) = \frac{b_m (j\omega)^m + ... + b_1 (j\omega) + b_0}{a_n (j\omega)^n + ... + a_1 (j\omega) + a_0} \qquad (2\text{-}137)$$

It is also possible (and appropriate) to establish a linear difference equation corresponding to Eq. (2-134), when we have equally spaced time samples, as the following time series:

$$\alpha_n y(t\text{-}n) + \alpha_{n-1} y(t\text{-}n+1) + ... + \alpha_1 y(t\text{-}1) + \alpha_0 y(t) = \beta_m f(t\text{-}m) + ...$$

$$+ \beta_1 f(t\text{-}1) + \beta_0 f(t) \qquad (2\text{-}138)$$

or

$$\sum_{k=0}^{n} \alpha_k y(t\text{-}k) = \sum_{k=0}^{m} \beta_k f(t\text{-}k) \qquad (2\text{-}139)$$

where α_k and β_k are known as the autoregressive and moving-average

parameters, respectively; α_0 and β_0 are taken as **1**. This model assumes that the output **y(t)** is contaminated with a zero mean sequence of additive noise and that the time series input set **f(t)** is a zero mean uncorrelated history. The input and output histories are supposed to be known, and α_k and β_k unknown.

If the sampled time interval is Δt, then by introducing the **z** transform, where $z=e^{s\Delta t}$, we can write Eq. (2-138) as

$$(\alpha_n z^{-n} + \alpha_{n-1} z^{-n+1} + \ldots + \alpha_1 z^{-1} + \alpha_0)\, Y(z) = (\beta_m z^{-m} + \ldots + \beta_1 z^{-1} + \beta_0)\, F(z) \tag{2-140}$$

Because Eq. (2-140) is the equivalent sampled representation of Eq. (2-134), the transfer function in terms of the **z** variable will be:

$$H(z) = \frac{Y(z)}{F(z)} = \frac{\sum_{k=0}^{m} \beta_k z^{-k}}{\sum_{k=0}^{n} \alpha_k z^{-k}} \tag{2-141}$$

where the roots (poles) of the denominator polynomial are related to the natural frequencies and damping factors of the system. For a system with **N** DOF, those roots will be given by the solution of the characteristic polynomial:

$$\sum_{k=0}^{2N} \alpha_k u^{2N-k} = 0 \tag{2-142}$$

where α_k are the same as in Eq. (2-141). The problem now arises as how to compute the autoregressive parameters α_k. To do this. Eq. (2-139) is written for an **N** DOF system as

$$\alpha_0\, y(t) + \sum_{k=1}^{2N} \alpha_k\, y(t-k) = \sum_{k=0}^{2N-1} \beta_k\, f(t-k) \tag{2-143}$$

and, because $\alpha_0=1$, we can write the current observation $y(t)$ as the sum of its own past (the autoregressive part) plus a linear combination of uncorrelated terms (the moving-average):

$$y(t) = -\sum_{k=1}^{2N} \alpha_k\, y(t-k) + \sum_{k=0}^{2N-1} \beta_k\, f(t-k) \tag{2-144}$$

and, more realistically, by considering a prediction error $e(t)$,

$$y(t) = \{-y(t-1) \ldots -y(t-2N)\ \ f(t) \ldots f(t-2N+1)\} \begin{Bmatrix} \alpha_1 \\ \vdots \\ \alpha_{2N} \\ \beta_0 \\ \vdots \\ \beta_{2N-1} \end{Bmatrix} + e(t) \tag{2-145}$$

Collecting terms for $t=2N+1, 2N+2, \ldots, 2N+L$, we have

$$\underset{(Lx1)}{\begin{Bmatrix} y(2N+1) \\ y(2N+2) \\ \vdots \\ y(2N+L) \end{Bmatrix}} = \underset{(Lx4N)}{\begin{bmatrix} -y(2N) & \ldots & -y(1) & f(2N+1) & \ldots & f(2) \\ -y(2N+1) & \ldots & -y(2) & f(2N+2) & \ldots & f(3) \\ \vdots & & \vdots & \vdots & & \vdots \\ -y(2N+L-1) & \ldots & -y(L) & f(2N+L) & \ldots & f(L+1) \end{bmatrix}} \underset{(4Nx1)}{\begin{Bmatrix} \alpha_1 \\ \vdots \\ \alpha_{2N} \\ \beta_0 \\ \vdots \\ \beta_{2N-1} \end{Bmatrix}} + \underset{(Lx1)}{\begin{Bmatrix} e(2N+1) \\ e(2N+2) \\ \vdots \\ e(2N+L) \end{Bmatrix}} \tag{2-146}$$

or simply,

$$\{y\} = [X]\,\{\theta\} + \{e\} \tag{2-147}$$

from which

$$\{e\} = \{y\} - [X]\{\theta\} \tag{2-148}$$

Minimizing the squared error $\{e\}^T\{e\}$, $\{\theta\}$ will be given by

$$\{\theta\} = ([X]^T[X])^{-1}[X]^T\{y\} \tag{2-149}$$

Knowing $\{\theta\}$ and therefore the **2N** values of α_k, we can return to Eq. (2-142), and write it as

$$\sum_{k=0}^{2N} \alpha_k u^{2N-k} = \prod_{k=1}^{N} (u-u_k)(u-u_k^*) = 0 \tag{2-150}$$

where

$$u_k = e^{s_r \Delta t}$$
$$u_k^* = e^{s_r^* \Delta t} \tag{2-151}$$

are the roots (poles) of the polynomial, from which it is possible to calculate the natural frequencies and damping factors. Knowing the **2N** values of β_k, it is also possible to calculate the residues, using Eq. (2-141). This method can also provide statistical confidence factors (coefficients of variation). This method seems not to be very widely used by modal analysts, as very few articles mention it.

The Direct System Parameter Identification method (DSPI)

This method is due to the work of Leuridan (Refs. [58], [14]), and is based on the same kind of approach given above for the **ARMA** method. The basic ideas behind this method are as follows: let us consider the dynamic

equilibrium equation for N_0 DOF, where N_0 is part of the N expected number of DOF of the structure, as

$$[M]\{\ddot{y}(t)\} + [C]\{\dot{y}(t)\} + [K]\{y(t)\} = [\Gamma]\{f(t)\} \qquad (2\text{-}152)$$

where **[M]**, **[C]** and **[K]** are $N_0 x N_0$ real matrices, **{f}** (qx1) is the input vector at **q** locations, and **[Γ]** is an $N_0 x q$ matrix whose elements e_{ij} are **1** when the input location **j** corresponds to the response location **i** and zero elsewhere. Alternatively, Eq. (2-152) can be written as

$$\{\ddot{y}(t)\} + [C]'\{\dot{y}(t)\} + [K]'\{y(t)\} = [\Gamma]'\{f(t)\} \qquad (2\text{-}153)$$

with

$$\underset{(N_0xN_0)}{[C]'} = \underset{(N_0xN_0)}{[M]^{-1}}\ \underset{(N_0xN_0)}{[C]}$$

$$\underset{(N_0xN_0)}{[K]'} = \underset{(N_0xN_0)}{[M]^{-1}}\ \underset{(N_0xN_0)}{[K]} \qquad (2\text{-}154)$$

$$\underset{(N_0xq)}{[\Gamma]'} = \underset{(N_0xN_0)}{[M]^{-1}}\ \underset{(N_0xq)}{[\Gamma]}$$

As for Eq. (2-145), we can write now Eq. (2-153) as an autoregressive moving-average model:

$$\{y(t)\} = [A_1]\{y(t-1)\} + \ldots + [A_p]\{y(t-p)\} + [B_0]\{f(t)\} + [B_1]\{f(t-1)\} + \ldots + [B_{p-1}]\{f(t-p+1)\} + \{e(t)\} \qquad (2\text{-}155)$$

where the coefficient matrices **[A]** and **[B]** are of dimensions $N_0 x N_0$ and $N_0 x q$, respectively, and **p** is chosen so that $pN_0 \geq 2N$. Considering **m** sets

of inputs and responses, we have

$$[y(t)] = [A_1][y(t-1)] + \ldots + [A_p][y(t-p)] + [B_0][f(t)] + \ldots + [B_{p-1}][f(t-p+1)] + [e(t)] \quad (2\text{-}156)$$

where

$$[y(t)] = [\{y(t)\}_1 \ldots \{y(t)\}_m]$$

$(N_0 x m)$

$$[f(t)] = [\{f(t)\}_1 \ldots \{f(t)\}_m] \quad (2\text{-}157)$$

$(q x m)$

$$[e(t)] = [\{e(t)\}_1 \ldots \{e(t)\}_m]$$

$(N_0 x m)$

Eq. (2-156) can still be written as

$$[y(t)] = [[A_1][A_2] \ldots [A_p]\ [B_0][B_1] \ldots [B_{p-1}]] \begin{bmatrix} [y(t-1)] \\ [y(t-2)] \\ \vdots \\ [y(t-p)] \\ [f(t)] \\ [f(t-1)] \\ \vdots \\ [f(t-p+1)] \end{bmatrix} + [e(t)] \quad (2\text{-}158)$$

Considering all the **L** sampled time intervals, **t=p+1, ..., p+L,**

$$[[y(p+1)] \ldots [y(p+L)]] =$$

$$(N_0 x L m)$$

$$[[A_1] \ldots [A_p]\ [B_0] \ldots [B_{p-1}]] \begin{bmatrix} [y(p)] & \ldots & [y(p+L-1)] \\ \vdots & & \vdots \\ [y(1)] & \ldots & [y(L)] \\ [f(p+1)] & \ldots & [f(p+L)] \\ \vdots & & \vdots \\ [f(2)] & \ldots & [f(L+1)] \end{bmatrix} + [[e(p+1)] \ldots [e(p+L)]] \quad (2\text{-}159)$$

$$(N_0 x (N_0 p+qp)) \qquad ((N_0 p+qp) x L m) \qquad (N_0 x L m)$$

In a compact form, we can write

$$[y] = [\theta]\,[X] + [e] \quad (2\text{-}160)$$

The minimization of $[\mathbf{e}]^T\,[\mathbf{e}]$ leads to

$$[\theta] = [y]\,[X]^T\,([X]\,[X]^T)^{-1} \quad (2\text{-}161)$$

Considering impulse response functions instead of free decay responses, and using the **z** transform, with $\mathbf{z}=\mathbf{e}^{s\Delta t}$, we shall have a similar expression to Eq. (2-141) for the transfer function **H(z)**:

$$[[\,I\,] - [A_1]\,z^{-1} - \ldots - [A_p]\,z^{-p}]\,[H(z)] = (\Delta t)^{-1}\,[[B_0] + [B_1]\,z^{-1} + \ldots + [B_{p-1}]\,z^{-p+1}] \quad (2\text{-}162)$$

or,

$$[[\,I\,]\,z^p - [A_1]\,z^{p-1} - \ldots - [A_p]]\,[H(z)] = (\Delta t)^{-1}\,[[B_0]\,z^p + [B_1]\,z^{p-1} + \ldots + [B_{p-1}]\,z] \quad (2\text{-}163)$$

where matrices $[A_1]$, ..., $[A_p]$ and $[B_0]$, ..., $[B_{p-1}]$ are already known. This equation can be written as

$$[z\,[I] - [A]]\,[I(z)]\,[H(z)] = [B(z)] \tag{2-164}$$

with

$$[A] = \underset{(N_0 p x N_0 p)}{\begin{bmatrix} [A_1] & [A_2] & \dots & [A_p] \\ [I] & [0] & \dots & [0] \\ [0] & [I] & \dots & [0] \\ \vdots & \vdots & & \vdots \\ [0] & [0] & \dots & [I]\ [0] \end{bmatrix}} \qquad [I(z)] = \underset{(N_0 p x N_0)}{\begin{bmatrix} z^{p-1}[I] \\ \vdots \\ [I] \end{bmatrix}} \tag{2-165}$$

$$[B(z)] = (\Delta t)^{-1} \underset{(N_0 p x q)}{\begin{bmatrix} z^p [B_0] + \dots + z\,[B_{p-1}] \\ [0] \\ \vdots \\ [0] \end{bmatrix}}$$

The $N_0 p$ eigenvalues and eigenvectors are obtained by the solution of

$$\underset{(N_0 p x N_0 p)}{[z\,[I] - [A]]}\ \underset{(N_0 p x 1)}{\{\tilde{\psi}\}} = \underset{(N_0 p x 1)}{\{0\}} \tag{2-166}$$

with

$$\underset{(N_0 p x 1)}{\{\tilde{\psi}\}} = \underset{(N_0 p x N_0)}{[I(z)]}\ \underset{(N_0 p x 1)}{\{\psi\}} \tag{2-167}$$

From the eigenvalues of matrix [A], the natural frequencies and damping factors are easily calculated. $\{\psi\}$ are the eigenvectors we are looking for.

From Eqs. (2-165) and (2-167), and for all the N_0p eigenvectors $[\tilde{\Psi}]$,

$$\underset{(N_0p \times N_0p)}{[\tilde{\Psi}]} = \begin{bmatrix} [\Psi]\,[\,z_r\,]^{2N-1} \\ \vdots \\ [\Psi] \end{bmatrix} \tag{2-168}$$

where $[\,z_r\,] = [\,e^{s_r \Delta t}\,]$. The last block of matrix $[\tilde{\Psi}]$ in Eq. (2-168) is precisely $[\Psi]$. It is known that the impulse response function matrix **[H(t)]** can be given by

$$\underset{(N_0p \times q)}{[H(t)]} = \underset{(N_0 \times N_0p)}{[\Psi]}\ \underset{(N_0p \times N_0p)}{[\,e^{\Lambda t}\,]}\ \underset{(N_0p \times q)}{[W]^T} \tag{2-169}$$

where **[W]** is the matrix of participation factors, as defined in Eqs. (2-25) and (2-26). This is the matrix that remains to be calculated to complete the method. In the **z** domain, Eq. (2-169) can be written as

$$\underset{(N_0p \times q)}{[H(z)]} = \underset{(N_0 \times N_0p)}{[\Psi]}\ \underset{(N_0p \times N_0p)}{[[\,I\,] - z^{-1}\,[\,z_r\,]]^{-1}}\ \underset{(N_0p \times q)}{[W]^T} \tag{2-170}$$

Pre-multiplying Eq. (2-164) by $[\tilde{\Psi}]^{-1}$, we obtain

$$[\tilde{\Psi}]^{-1}\,[z\,[\,I\,] - [A]]\,[I(z)]\,[H(z)] = [\tilde{\Psi}]^{-1}\,[B(z)] \tag{2-171}$$

Substituting Eq. (2-170) in Eq. (2-171), it follows that

$$[\tilde{\Psi}]^{-1}\,[z\,[\,I\,] - [A]]\,[I(z)]\,[\Psi]\,[[\,I\,] - z^{-1}\,[\,z_r\,]]^{-1}\,[W]^T = [\tilde{\Psi}]^{-1}\,[B(z)] \tag{2-172}$$

From Eq. (2-166), we can write

$$[A]\,[\tilde{\Psi}] = [\tilde{\Psi}]\,[\,z_r\,] \tag{2-173}$$

or

$$[A] = [\tilde{\Psi}] [\lceil z_r \rfloor] [\tilde{\Psi}]^{-1} \tag{2-174}$$

Substituting Eq. (2-174) in Eq. (2-172), we obtain

$$[z [I] - [\lceil z_r \rfloor]] [\tilde{\Psi}]^{-1} [I(z)] [\Psi] [[I] - z^{-1} [\lceil z_r \rfloor]]^{-1} [W]^T = [\tilde{\Psi}]^{-1} [B(z)] \tag{2-175}$$

where everything is known except the modal participation matrix **[W]**. By taking limits on both sides of Eq. (2-175) when $\mathbf{z} \rightarrow \mathbf{z_r}$ (see Ref. [14]), and assuming that the **2N** modes have already been sorted out from the $\mathbf{N_0 p}$ modes, we obtain

$$\{W^T\}_r = z_r \{[\tilde{\Psi}]^{-1} \{B(z_r)\}\}_r \qquad \text{for } r = 1, ..., 2N \tag{2-176}$$

The model of expression (2-169) is therefore complete. The residue matrix for each mode **r** is given by

$$\underset{(N_0 x q)}{[A]_r} = \underset{(N_0 x 1)}{\{\psi\}_r} \underset{(1 x q)}{\{W^T\}_r} \tag{2-177}$$

Knowing the residues, it is easy to evaluate the modal constants and phase angles.

This method is said to give very good results, even for almost repeated modes. In Ref. [14] it is shown that this method can be seen as a generalization of other methods, like the **CE**, **PRCE** and **ITD**.

2-3 Frequency domain methods

Frequency domain methods will be presented in this section. Simple and very well known methods will be explained briefly; more advanced methods will be explained in greater detail. Some of the methods will be

the subject of detailed discussion later in this thesis and therefore will not be presented in detail in this chapter. Fig. 2-2 presents a diagram of the classification of the several methods that will be discussed here and in the following chapters.

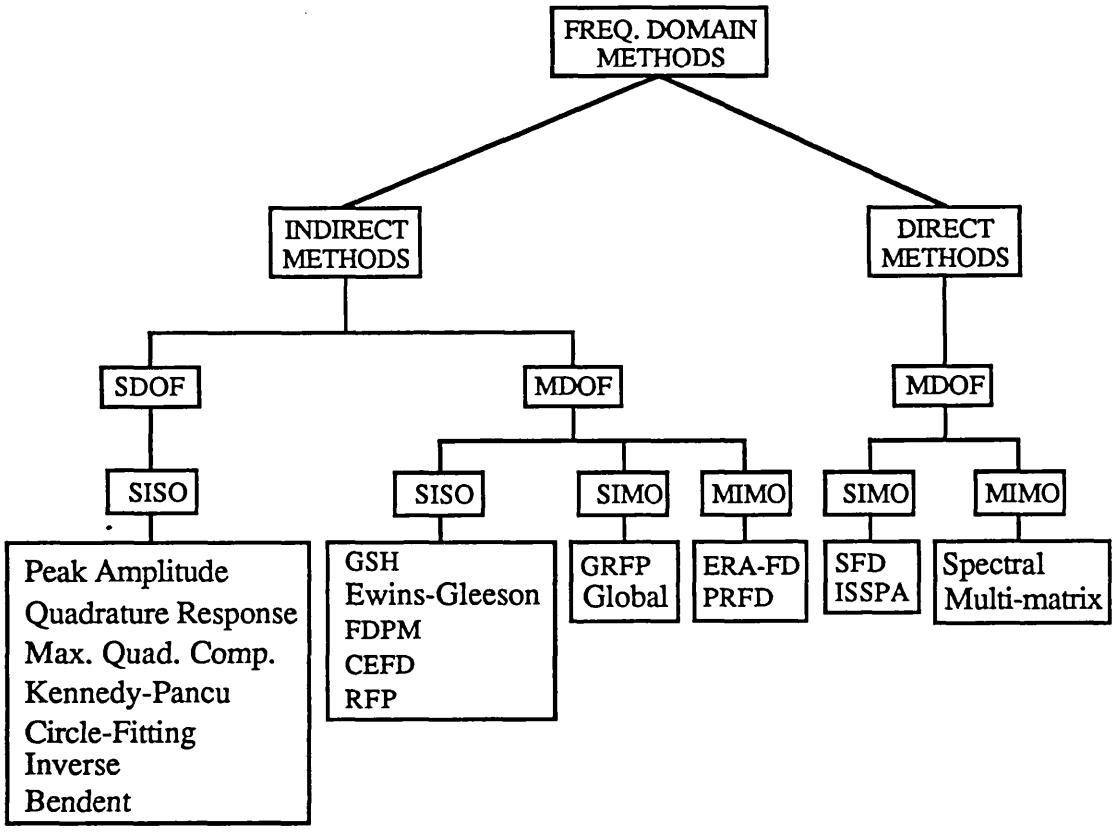

Fig. 2-2 Classification of Frequency domain methods.

2-3-1 Indirect SDOF methods

In this category, we shall discuss the Peak Amplitude, the Quadrature Response, the Maximum Quadrature Component, the Kennedy-Pancu, the Circle-Fitting, the Inverse and the "Bendent" methods. All these are *SISO* methods.

The Peak Amplitude method

This is the simplest known method for identifying the modal parameters of a structure (see Ref. [10]). The natural frequencies are simply taken from the observation of the peaks on the graphs of the magnitude of the response. The damping ratios are calculated from the sharpness of the peaks and the modeshapes are calculated from the ratios of the peak amplitudes at various points in the structure. In order to take into account the amplitude of the excitation force, the use of receptance represented an improvement to this method (Ref. [59]). This method assumes that the modes are real and, albeit being quite "crude", it may provide reasonable results if the modes are well separated and if the damping is not very high. A critical comparison between this and the **Kennedy-Pancu** method is given in Ref. [59], where some alternatives are suggested for the calculation of the damping ratios.

The Quadrature Response and Maximum Quadrature Component methods

These methods (Ref. [60]) differ from the **Peak Amplitude** method in the location of the natural frequencies of the structure. The **Quadrature Response** locates the natural frequencies at the points where the in-phase component of the response (the real part) is zero. This corresponds to a **90** degree phase difference between the forcing function and the response. The **Maximum Quadrature Component** considers that the natural frequencies occur at the points where the quadrature component of the response (the imaginary part) has a maximum (or minimum). This component is **90** degrees out-of-phase with the forcing function.

The Kennedy-Pancu (or Maximum Frequency Spacing) method

This method, first introduced by Kennedy and Pancu (Ref. [12]) uses the Argand plane to display the real and the imaginary parts of the receptance. Around each natural frequency the curve approaches a circle and the natural frequency is located at the point where the rate of change of arc length with frequency attains a maximum. The model assumed for the damping is the hysteretic one and the damping factor is evaluated from a simplified half-power-points calculation and the modeshapes are calculated from the ratios of the diameters of the circles, fitted around each natural frequency for the various output responses. Here, it is still assumed that the modes are real and that the damping is small. Some problems concerning the existence of close modes were already encountered by these authors.

Pendered (Ref. [60]) made a critical comparison between this and the previous methods cited above, concluding that the **Kennedy-Pancu** method was the one that could resolve more accurately two close modes and that the **Quadrature Response Method** was the worst one, concerning this aspect. Woodcock (Ref. [61]) extended this method to systems with viscous, non-proportional damping and without the restriction of small amounts of damping. Klosterman (Ref. [16]) continued the investigation on the **Kennedy-Pancu** method, establishing more efficient techniques for the determination of the modal parameters for systems with general non-proportional damping, using either the viscous or the hysteretic model. In 1973, Marples (Ref. [62]) gave a new formula for the calculation of the hysteretic damping factor. A systematic use of this formula (Ref. [63]) around the resonance region allows for the calculation of the mean value for the damping factor and can also give an indication of the presence of nonlinearities and other potential problem areas.

The Circle-Fitting method

Basically, after the cited work of Klosterman, the **Kennedy-Pancu** method became known as the **Circle-Fitting** method, easy to implement in small computers. A comprehensive study of the **Circle-Fitting** method has been presented by Ewins (Ref. [1]). Although well established, this method has recently been still the object of some refinements (Refs. [64], [65]). Because it surely is the best known method used in EMA, we shall not present it in detail here. Despite being well known, it is often disregarded and said to only work well for widely separated modes and lightly damped structures. This is probably because in some modal analysis packages and analysers the versions used are the very basic ones, that coincide nearly with the **Kennedy-Pancu** method. It is our opinion (and experience) that the **Circle-Fitting** method works very well for the majority of situations and even for highly complicated structures. Some works based on the application of this method have demonstrated its robustness. (Refs. [66], [67], [68]).

One of the most important improvements associated with the **Circle-Fitting** method is the possibility to subtract the effect of modes already analysed before analysing the one we are interested in (Ref. [69]). This leads to an iteration process that will be mentioned in Chapter 3. Some efforts to obtain consistent sets of natural frequencies and damping factors have been tried. The objective is to avoid variations on the estimates of those parameters when several FRFs are analysed individually. The simplest way of all is to average all the estimates obtained for each FRF. This was applied with success by Talapatra (Ref. [70]). A weighted average of the natural frequencies and damping factors was also proposed and applied successfully by Kirshenboim (Ref. [71]). The weighting factors are given by the RMS errors obtained in the circle-fitting procedure divided by the diameter, for each mode. The initial estimates of the modal

constants are then corrected, using the averaged values. An intermediate option is to use this last technique for correcting the modal constants, but using simple averages instead of weighted ones. This alternative was used in Ref. [67].

The Inverse method

The Inverse method was presented by Dobson (Ref. [72]) and relies on the fact that the imaginary and real parts of the inverse of the receptance (dynamic stiffness) are straight lines in the frequency and frequency squared, respectively. Because it is based on the assumption that the modes are real and relies on well spaced natural frequencies, we can say that it represents the "inverse" of the **Kennedy-Pancu** method. More details are given in Chapter 3. In that chapter it is also proposed an extension of the method that works for complex modes.

The "Bendent" (or Dobson) method

Also developed by Dobson (Ref. [73]), this method is an extension of the inverse method, considering complex modes and also automatically compensating for the effects of neighbouring modes. It will also be developed in more detail in the next chapter.

Other methods

The method proposed by Goyder (Ref. [74]) is a variation of the **GSH** method that we shall present in the next section, applied for the SDOF case. It considers hysteretic damping instead, and the extraction of the modal parameters for each mode is also based on the minimization of an error

function in a least-squares sense, but where the linearization of the error is made through a weighting function instead of by truncation of the Taylor's expansion. This method was also formulated for the case of one force input and several response locations, i. e., a global formulation but for one mode at a time. It is therefore a *SIMO* method. As the **GSH** method, it also requires initial estimates and as the process progresses from mode to mode, the ones already identified are subtracted from the initial FRFs, in order to take out the influence of the residual terms. This process is repeated until covergence is attained. Because this method is a particular case of an MDOF method, applied to analyse one DOF at a time, it is not considered as a true SDOF method. SDOF methods are usually designed specifically for one DOF and therefore have particular characteristics. Otherwise, all MDOF methods could be considered as SDOF ones. The same applies, for instance, to the sometimes called SDOF polynomial, which is the **RFP** method applied for one DOF (e. g., Ref. [75]). In Ref. [75], the author applies the SDOF polynomial to several FRFs, each at a time, and calculates average values for the modal parameters in a similar way as in Ref. [71]. The approach assumes, however, real modes.

2-3-2 Indirect MDOF methods

Indirect MDOF methods include the Gaukroger-Skingle-Heron (GSH), the Ewins-Gleeson, the Frequency-Domain Prony (FDPM), the Complex Exponential Frequency Domain (CEFD), the Eigensystem Realization Algorithm in the frequency domain (ERA-FD), the Rational Fraction Polynomial (RFP), the Global Rational Fraction Polynomial (GRFP), the Global method and the Polyreference Frequency Domain (PRFD).

The Gaukroger-Skingle-Heron method (GSH)

Presented in 1973 (Ref. [76]), this method is based on a least-squares fit of the receptance, considering several modes at a time, for one input and one output locations (SISO). The model assumes viscous damping, and is an attempt to circumvent possible difficulties associated with the graphical techniques used in the **Circle-Fitting** method. It is, however, interactive, leaving the possibility for the user to take decisions. As the procedure needs initial estimates for the modal parameters, **Circle-Fitting** is suggested at a first stage of the analysis.

The method begins by considering the receptance response of an **N** DOF system as:

$$\alpha(j\omega) = \alpha_0 + \left[\sum_{r=1}^{N} \frac{A_r + j\omega\, B_r}{\omega_r^2 - \omega^2 + j\, 2\omega\omega_r\xi_r}\right] e^{j\phi} \qquad (2\text{-}178)$$

where α_0 is a complex constant and ϕ is a rotation angle that seek to reflect the influence of out-of-range modes. Let **e** be an error function between the theoretical values $\alpha(j\omega)$ and the measured values $\tilde{\alpha}(j\omega)$, for all the measured points **L**:

$$e = \sum_{i=1}^{L} (\tilde{\alpha}(j\omega_i) - \alpha(j\omega_i))^* \, (\tilde{\alpha}(j\omega_i) - \alpha(j\omega_i)) \qquad (2\text{-}179)$$

Simplifying the notation by writing α_i and $\tilde{\alpha}_i$ for $\alpha(j\omega_i)$ and $\tilde{\alpha}(j\omega_i)$, respectively, we obtain

$$e = \sum_{i=1}^{L} (\tilde{\alpha}_i^* - \alpha_i^*)\, (\tilde{\alpha}_i - \alpha_i) \qquad (2\text{-}180)$$

We shall seek the minimization of this error, by taking derivatives with respect to the variables and equaling to zero. It is shown in Ref. [76] that the following relationship holds:

$$B_N = -\sum_{r=1}^{N-1} B_r \tag{2-181}$$

and, therefore, there will be **4N+2** unknowns to be calculated and we shall need **4N+2** equations. As $\alpha_0 = \mathbf{Re}(\alpha_0)+\mathbf{jIm}(\alpha_0)$, we make

$$\begin{array}{llll} k_1 = \mathrm{Re}\,(\alpha_0) & k_2 = \mathrm{Im}\,(\alpha_0) & k_3 = \phi & \\ k_4 = \omega_1^2 & k_5 = 2\omega_1\xi_1 & k_6 = A_1 & k_7 = B_1 \\ \vdots & \vdots & \vdots & \\ k_{4N} = \omega_N^2 & k_{4N+1} = 2\omega_N\xi_N & k_{4N+2} = A_N & \end{array} \tag{2-182}$$

The **4N+2** equations will then be:

$$\frac{\partial e}{\partial k_j} = -\sum_{i=1}^{L} \left[(\tilde{\alpha}_i^* - \alpha_i^*)\frac{\partial \alpha_i}{\partial k_j} + (\tilde{\alpha}_i - \alpha_i)\frac{\partial \alpha_i^*}{\partial k_j}\right] = 0 \tag{2-183}$$

$$\text{for } j = 1, 2, \ldots, 4N+2$$

These equations are nonlinear and an iterative procedure is sought. Writing each of Eqs. (2-183) as a general function $\mathbf{f_j}$ of the variables $\mathbf{k_j}$, we have

$$\frac{\partial e}{\partial k_j} = f_j(k_1, k_2, \ldots, k_{4N+2}) = 0 \qquad \text{for } j = 1, 2, \ldots, 4N+2 \tag{2-184}$$

Now, if we call $\mathbf{k'_j}$ to the initial estimates of $\mathbf{k_j}$, we shall look for the variations $\delta\mathbf{k_j}$ so that the following equation is verified:

$$f_j(k'_1 + \delta k_1, k'_2 + \delta k_2, \ldots, k'_{4N+2} + \delta k_{4N+2}) = 0 \tag{2-185}$$

Doing an expansion using Taylor's theorem, Eq. (2-185) can be written as

$$f_j(k'_1 + \delta k_1, ..., k'_{4N+2} + \delta k_{4N+2}) = f_j(k'_1, ..., k'_{4N+2}) +$$

$$\sum_{i=1}^{4N+2} \frac{\partial f_j(k'_1, ..., k'_{4N+2})}{\partial k_i} \delta k_i + \text{higher order terms in } \delta k_i \qquad (2\text{-}186)$$

$$j = 1, 2, ..., 4N+2$$

The problem is now linearized by neglecting the higher order terms. Applying Eq. (2-185), we obtain

$$f_j(k'_1, ..., k'_{4N+2}) + \sum_{i=1}^{4N+2} \frac{\partial f_j(k'_1, ..., k'_{4N+2})}{\partial k_i} \delta k_i = 0 \qquad (2\text{-}187)$$

$$j = 1, 2, ..., 4N+2$$

For each set of new estimates $\mathbf{k}'_j$, we can write

$$\frac{\partial e}{\partial k_j} = f_j(k'_1, k'_2 ..., k'_{4N+2}) \neq 0 \qquad j = 1, 2, ..., 4N+2 \qquad (2\text{-}188)$$

and substituting in Eq. (2-187), we obtain

$$\frac{\partial e}{\partial k_j} + \sum_{i=1}^{4N+2} \frac{\partial^2 e}{\partial k_j \partial k_i} \delta k_i = 0 \qquad j = 1, 2, ..., 4N+2 \qquad (2\text{-}189)$$

Expanding Eq. (2-189) in matrix form, we have

$$\begin{bmatrix} \frac{\partial^2 e}{\partial k_1^2} & \frac{\partial^2 e}{\partial k_1 \partial k_2} & \cdots & \frac{\partial^2 e}{\partial k_1 \partial k_{4N+2}} \\ & \frac{\partial^2 e}{\partial k_2^2} & \cdots & \frac{\partial^2 e}{\partial k_2 \partial k_{4N+2}} \\ & & \ddots & \vdots \\ \text{Sym.} & & & \frac{\partial^2 e}{\partial k_{4N+2}^2} \end{bmatrix} \begin{Bmatrix} \delta k_1 \\ \delta k_2 \\ \vdots \\ \delta k_{4N+2} \end{Bmatrix} = - \begin{Bmatrix} \frac{\partial e}{\partial k_1} \\ \frac{\partial e}{\partial k_2} \\ \vdots \\ \frac{\partial e}{\partial k_{4N+2}} \end{Bmatrix} \qquad (2\text{-}190)$$

This equation can be solved for the variations δk_j, and new estimates are taken as the previous ones plus δk_j, until convergence is achieved. From Eq. (2-183), the second derivatives in Eq. (2-190) are given by:

$$\frac{\partial^2 e}{\partial k_j \partial k_i} = -\sum_{i=1}^{L} \left[(\tilde{\alpha}_i^* - \alpha_i^*) \frac{\partial^2 \alpha_i}{\partial k_j \partial k_i} - \frac{\partial \alpha_i^*}{\partial k_i} \frac{\partial \alpha_i}{\partial k_j} + (\tilde{\alpha}_i - \alpha_i) \frac{\partial^2 \alpha_i^*}{\partial k_j \partial k_i} - \frac{\partial \alpha_i^*}{\partial k_j} \frac{\partial \alpha_i}{\partial k_i} \right] \quad (2\text{-}191)$$

If the data are not too noisy, $(\tilde{\alpha}_i^* - \alpha_i^*)$ and $(\tilde{\alpha}_i - \alpha_i)$ will be small and so an approximation for Eq. (2-191) may be used:

$$\frac{\partial^2 e}{\partial k_j \partial k_i} \approx \sum_{i=1}^{L} \left(\frac{\partial \alpha_i^*}{\partial k_i} \frac{\partial \alpha_i}{\partial k_j} + \frac{\partial \alpha_i^*}{\partial k_j} \frac{\partial \alpha_i}{\partial k_i} \right) \quad (2\text{-}192)$$

Good initial estimates must be provided, in order that the process converges. It was found that initial zero values for α_0 and ϕ were satisfactory. Initial estimates for the natural frequencies and damping factors can be provided by a quick circle-fitting analysis. Then, $\mathbf{A}_r$ and $\mathbf{B}_r$ can be obtained by a non-iterative least-squares analysis. All the modal parameters will then be known and the iterative process will begin. Our experience with this method showed that, although the identifications were quite satisfactory, the whole process and in particular the iterative part was, generally, very slow.

The Ewins-Gleeson method

Introduced in 1982 (Ref. [77]), this *SISO* method is dedicated to the identification of lightly damped structures, assuming the hysteretic model. In the referred article, the problem is presented in terms of inertance, but

we shall derive it here for an FRF in terms of receptance.

Because the system is assumed to be lightly damped, the modes are taken as real, i. e., with phase angles of **0** or **180** degrees. The mathematical model is, therefore,

$$\alpha(j\omega) = \sum_{r=1}^{N} \frac{C_r}{\omega_r^2 - \omega^2 + j\omega_r^2\eta_r} \tag{2-193}$$

In a first stage, it is considered that there is no damping. Hence,

$$\mathrm{Re}(\alpha(j\omega)) = \sum_{r=1}^{N} \frac{C_r}{\omega_r^2 - \omega^2} \tag{2-194}$$

If, in addition, we take the natural frequencies as the frequencies corresponding to the peaks in the FRF receptance curve (which are supposed, in such a structure, to be well separated and sharp and, thus, well visible), we only have as unknowns the modal constants C_r.

To calculate the **N** unknowns C_r , we need **N** equations. Thus, we take **N** frequencies Ω_1, Ω_2, ..., Ω_N and the corresponding real part of the measured receptances, that we shall write, shortly, as $\mathbf{Re}(\tilde{\alpha}_1)$, $\mathbf{Re}(\tilde{\alpha}_2)$, ..., $\mathbf{Re}(\tilde{\alpha}_N)$. Thus, The modal constants are given by:

$$\begin{Bmatrix} C_1 \\ C_2 \\ \vdots \\ C_N \end{Bmatrix} = \begin{bmatrix} \frac{1}{\omega_1^2 - \Omega_1^2} & \frac{1}{\omega_2^2 - \Omega_1^2} & \frac{1}{\omega_N^2 - \Omega_1^2} \\ \frac{1}{\omega_1^2 - \Omega_2^2} & \frac{1}{\omega_2^2 - \Omega_2^2} & \frac{1}{\omega_N^2 - \Omega_2^2} \\ \vdots & \vdots & \vdots \\ \frac{1}{\omega_1^2 - \Omega_N^2} & \frac{1}{\omega_2^2 - \Omega_N^2} & \frac{1}{\omega_N^2 - \Omega_N^2} \end{bmatrix}^{-1} \begin{Bmatrix} \mathrm{Re}(\tilde{\alpha}_1) \\ \mathrm{Re}(\tilde{\alpha}_2) \\ \vdots \\ \mathrm{Re}(\tilde{\alpha}_N) \end{Bmatrix} \tag{2-195}$$

or

$$\{C\} = [R]\, Re\{\tilde{\alpha}\} \qquad (2\text{-}196)$$

(Nx1) (NxN) (Nx1)

The sign of each C_r tells us whether a response is in-phase or out-of-phase. In a second stage, the damping factors are calculated from the peak amplitudes. From Eq. (2-193), at each resonance, we have

$$|\tilde{\alpha}(j\omega_r)| \approx \frac{|C_r|}{\omega_r^2 \eta_r} \qquad (2\text{-}197)$$

from which,

$$\eta_r \approx \frac{|C_r|}{|\tilde{\alpha}(j\omega_r)|\,\omega_r^2} \qquad (2\text{-}198)$$

The effects of residual modes can be introduced later and details are given in Ref. [77]. An alternative to this is to consider **N+2** points and calculate **N+2** modal constants. The matrix **[R]** in Eq. (2-196) would be of order **N+2**.

This method works very well if in fact the structure is lightly damped. The method is extremely simple and fast, and very easy to incorporate in small computers (in fact, even in common calculators). The disadvantage is that it is sensitive to the points chosen from the FRF, mainly with noisy measurements. Some experience is required to make the proper choice of points. To avoid this drawback, a new approach is proposed in Chapter 4, where a comparison with the method now presented is made.

The Frequency Domain Prony method (FDPM)

This is also a *SISO* method and it corresponds to the complex exponential

method in the time domain. It was introduced in 1980 (Ref. [78]).

For an **N** DOF system with viscous damping, it is possible to write the receptance FRF as the ratio of two polynomials in $j\omega$ (see Section 4-2-1):

$$\alpha(j\omega) = \frac{\sum_{k=0}^{2N-1} a_k (j\omega)^k}{\sum_{k=0}^{2N} b_k (j\omega)^k} \tag{2-199}$$

In factorized form, it is possible to write $\alpha(j\omega)$ as

$$\alpha(j\omega) = \frac{\prod_{k=1}^{2N-1} (j\omega - z_k)}{\prod_{k=1}^{2N} (j\omega - p_k)} \tag{2-200}$$

where $\mathbf{z_k}$ are the zeros and $\mathbf{p_k}$ the poles of the numerator and denominator polynomials, respectively. From Eq. (2-199), and making $\mathbf{b_{2N}=1}$, it is possible to write:

$$\sum_{k=0}^{2N-1} (j\omega)^k [\, b_k \alpha(j\omega) - a_k \,] = - (j\omega)^{2N} \alpha(j\omega) \tag{2-201}$$

Separating into real and imaginary parts, we obtain:

$$\sum_{k=1}^{N} (-1)^k \omega^{2k-2} [\, -b_{2k-2} \mathrm{Re}(\alpha(j\omega)) + \omega b_{2k-1} \mathrm{Im}(\alpha(j\omega)) + a_{2k-2}] = (-1)^{N+1} \omega^{2N} \mathrm{Re}(\alpha(j\omega))$$

$$\sum_{k=1}^{N} (-1)^{k+1} \omega^{2k-2} [b_{2k-2} \mathrm{Im}(\alpha(j\omega)) + \omega b_{2k-1} \mathrm{Re}(\alpha(j\omega)) - \omega a_{2k-1}] = (-1)^{N+1} \omega^{2N} \mathrm{Im}(\alpha(j\omega)) \tag{2-202}$$

Eqs. (2-202) have **4N** unknowns (coefficients a_k and b_k). They can be obtained by considering at least **2N** data points (because each one has real and imaginary information), by solving the resulting linear system of equations. After finding those coefficients, it is possible to solve the denominator polynomial of Eq. (2-199) to calculate the poles and consequently the natural frequencies and damping factors. The residues and the modal constants and phase angles will be calculated afterwards, as explained in Section 4-2-1 for the **RFP** method. If we simply wish to regenerate the original FRF, then the coefficients $\mathbf{a_k}$ and $\mathbf{b_k}$ can be substituted directly in Eq. (2-199). We shall explain next an alternative procedure.

Let us suppose now that only the magnitude of the FRF is available from the measurements. The complex conjugate of Eq. (2-200) will be:

$$\alpha^*(j\omega) = \frac{\prod_{k=1}^{2N-1} (-j\omega - z_k^*)}{\prod_{k=1}^{2N} (-j\omega - p_k^*)} = \frac{\prod_{k=1}^{2N-1} (j\omega + z_k^*)}{\prod_{k=1}^{2N} (j\omega + p_k^*)} \tag{2-203}$$

Multiplying Eqs. (2-203) and (2-200), we obtain

$$|\alpha(j\omega)|^2 = \frac{\prod_{k=1}^{2N-1} [(j\omega + z_k^*)(j\omega - z_k)]}{\prod_{k=1}^{2N} [(j\omega + p_k^*)(j\omega - p_k)]} \tag{2-204}$$

which can be written in a similar form to Eq. (2-199):

$$|\alpha(j\omega)|^2 = \frac{\sum_{k=0}^{2N-1} a'_k (j\omega)^{2k}}{\sum_{k=0}^{2N} b'_k (j\omega)^{2k}} \tag{2-205}$$

By considering now $\mathbf{b'_{2N}=1}$, we obtain a similar expression to Eq. (2-201):

$$\sum_{k=0}^{2N-1} (j\omega)^{2k} \left[b'_k |\alpha(j\omega)|^2 - a'_k\right] = - (j\omega)^{2N} |\alpha(j\omega)|^2 \qquad (2\text{-}206)$$

or

$$\sum_{k=0}^{2N-1} (-1)^k \omega^{2k} \left[b'_k |\alpha(j\omega)|^2 - a'_k\right] = (-1)^{N+1} \omega^{2N} |\alpha(j\omega)|^2 \qquad (2\text{-}207)$$

which corresponds to Eqs. (2-202). We have again **4N** unknowns (a'_k and b'_k) and this time we need at least **4N** data points to solve the linear system of equations. With $\mathbf{a'_k}$ and $\mathbf{b'_k}$, we can reconstitute $|\alpha(j\omega)|^2$ using Eq. (2-205) and by solving the denominator polynomial we can calculate the poles. It should be noted that in this case we have **4N** poles, instead of **2N** in the previous case. The **2N** poles in excess are reflections of the other ones, with respect to the imaginary axis, i. e., they will have positive real parts, while the ones we are interested in have negative real parts. This fact allows for the sorting of the poles we want. The calculation of the natural frequencies and damping factors is therefore possible. For calculation of the residues, that would lead us to the modal constants and phase angles, a degree of ambiguity is expected, as we only have measured the magnitude of the FRF. Thus, this alternative procedure is not convenient for the calculation of those parameters. Comparison of this method with the **CE** method showed a reasonable agreement (Ref. [78]).

The Complex Exponential Frequency Domain method (CEFD)

This method, due to Schmerr (Ref. [79]), is the corresponding frequency domain version of the **SSTD**, which in turn is, as mentioned previously,

the **ITD** method for the particular case of only one output measurement (perhaps it should more appropriately be called SSFD). The **CEFD** is therefore, like the **SSTD**, a *SISO* method. From Eq. (2-4), and considering only one input and output locations, the IRF is given by:

$$h(t) = \sum_{r=1}^{2N} A_r' e^{s_r t} \tag{2-208}$$

Applying a Fourier transform, the FRF will be

$$\alpha(j\omega) = \sum_{r=1}^{2N} \frac{A_r'}{j\omega - s_r} \tag{2-209}$$

Considering a series of **N** shifted responses from the same IRF,

$$h_k(t) = h(t+kT) \qquad k = 1, 2, ..., N \tag{2-210}$$

where **T** is an arbitrary time lag, the corresponding FRF will be

$$\alpha_k(j\omega) = \sum_{r=1}^{2N} \frac{A_r' e^{s_r kT}}{j\omega - s_r} \qquad k = 1, 2, ..., N \tag{2-211}$$

Expanding Eq. (2-211) for all **k** values, we obtain

$$\begin{aligned}
\alpha_1(j\omega) &= \frac{A_1' e^{s_1 T}}{j\omega - s_1} + \frac{A_2' e^{s_2 T}}{j\omega - s_2} + ... + \frac{A_{2N}' e^{s_{2N} T}}{j\omega - s_{2N}} \\
\alpha_2(j\omega) &= \frac{A_1' e^{s_1 2T}}{j\omega - s_1} + \frac{A_2' e^{s_2 2T}}{j\omega - s_2} + ... + \frac{A_{2N}' e^{s_{2N} 2T}}{j\omega - s_{2N}} \\
&\vdots \qquad\qquad \vdots \\
\alpha_N(j\omega) &= \frac{A_1' e^{s_1 NT}}{j\omega - s_1} + \frac{A_2' e^{s_2 NT}}{j\omega - s_2} + ... + \frac{A_{2N}' e^{s_{2N} NT}}{j\omega - s_{2N}}
\end{aligned} \tag{2-212}$$

or

$$\underset{(Nx1)}{\{\alpha(j\omega)\}} = \underset{(Nx2N)}{\begin{bmatrix} A_1' e^{s_1 T} & A_2' e^{s_2 T} & \dots & A_{2N}' e^{s_{2N} T} \\ A_1' e^{s_1 2T} & A_2' e^{s_2 2T} & \dots & A_{2N}' e^{s_{2N} 2T} \\ \vdots & \vdots & & \vdots \\ A_1' e^{s_1 NT} & A_2' e^{s_2 NT} & \dots & A_{2N}' e^{s_{2N} NT} \end{bmatrix}} \underset{(2Nx1)}{\begin{Bmatrix} \frac{1}{j\omega - s_1} \\ \frac{1}{j\omega - s_2} \\ \vdots \\ \frac{1}{j\omega - s_{2N}} \end{Bmatrix}} \tag{2-213}$$

If each shifted sample contains **L** frequency points, then

$$[\{\alpha(j\omega_1)\}\ \{\alpha(j\omega_2)\}\ \dots\ \{\alpha(j\omega_L)\}] =$$

$$\begin{bmatrix} A_1' e^{s_1 T} & A_2' e^{s_2 T} & \dots & A_{2N}' e^{s_{2N} T} \\ A_1' e^{s_1 2T} & A_2' e^{s_2 2T} & \dots & A_{2N}' e^{s_{2N} 2T} \\ \vdots & \vdots & & \vdots \\ A_1' e^{s_1 NT} & A_2' e^{s_2 NT} & \dots & A_{2N}' e^{s_{2N} NT} \end{bmatrix} \begin{bmatrix} \frac{1}{j\omega_1 - s_1} & \frac{1}{j\omega_2 - s_1} & \dots & \frac{1}{j\omega_L - s_1} \\ \frac{1}{j\omega_1 - s_2} & \frac{1}{j\omega_2 - s_2} & \dots & \frac{1}{j\omega_L - s_2} \\ \vdots & \vdots & & \vdots \\ \frac{1}{j\omega_1 - s_{2N}} & \frac{1}{j\omega_2 - s_{2N}} & \dots & \frac{1}{j\omega_L - s_{2N}} \end{bmatrix} \tag{2-214}$$

or

$$\underset{(NxL)}{[\alpha]} = \underset{(Nx2N)}{[A_T]}\ \underset{(2NxL)}{[\Lambda]} \tag{2-215}$$

If we repeat this whole procedure taking the responses shifted one interval

of time Δt, Eqs. (2-211) will become:

$$\alpha_k'(j\omega) = \sum_{r=1}^{2N} \frac{A_r' e^{s_r kT} e^{s_r \Delta t}}{j\omega - s_r} \qquad k = 1, 2, ..., N \tag{2-216}$$

and if we shift **2** time intervals, we obtain

$$\alpha_k''(j\omega) = \sum_{r=1}^{2N} \frac{A_r' e^{s_r kT} e^{s_r 2\Delta t}}{j\omega - s_r} \qquad k = 1, 2, ..., N \tag{2-217}$$

For the series of **N** shifted responses and for the **L** frequency points, we obtain the following matrix corresponding to Eq. (2-216):

$$\underset{(NxL)}{[\alpha']} = \underset{(Nx2N)}{[A_T]} \begin{bmatrix} e^{s_1\Delta t} & & 0 \\ & e^{s_2\Delta t} & \\ 0 & & \ddots \\ & & & e^{s_{2N}\Delta t} \end{bmatrix}_{(2Nx2N)} \underset{(2NxL)}{[\Lambda]} \tag{2-218}$$

or

$$[\alpha'] = [A_T'] [\Lambda] \tag{2-219}$$

Similarly, for Eq. (2-217),

$$[\alpha''] = [A_T] \begin{bmatrix} e^{s_1 2\Delta t} & & 0 \\ & e^{s_2 2\Delta t} & \\ 0 & & \ddots \\ & & & e^{s_{2N} 2\Delta t} \end{bmatrix} [\Lambda] \tag{2-220}$$

or

$$[\alpha''] = [A_T''] [\Lambda] \tag{2-221}$$

Combining Eqs. (2-215) and (2-219), we can write

$$\underset{(2NxL)}{\begin{bmatrix}[\alpha] \\ [\alpha']\end{bmatrix}} = \underset{(2Nx2N)}{\begin{bmatrix}[A_T] \\ [A_T']\end{bmatrix}} \underset{(2NxL)}{[\Lambda]} \qquad (2\text{-}222)$$

or

$$\underset{(2Nx2N)}{[\alpha_A]} = \underset{(2Nx2N)}{[A_A]} \underset{(2Nx2N)}{[\Lambda]} \qquad (2\text{-}223)$$

where, to simplify the exposition, we have assumed **L=2N**. Combining Eqs. (2-219) and (2-221), we obtain

$$\underset{(2NxL)}{\begin{bmatrix}[\alpha'] \\ [\alpha'']\end{bmatrix}} = \underset{(2Nx2N)}{\begin{bmatrix}[A_T'] \\ [A_T'']\end{bmatrix}} \underset{(2NxL)}{[\Lambda]} \qquad (2\text{-}224)$$

or

$$\underset{(2Nx2N)}{[\hat{\alpha}_A]} = \underset{(2Nx2N)}{[\hat{A}_A]} \underset{(2Nx2N)}{[\Lambda]} \qquad (2\text{-}225)$$

From Eq. (2-223), we can write

$$[A_A]^{-1}[\alpha_A] = [\Lambda] \qquad (2\text{-}226)$$

Substituting Eq. (2-226) in Eq. (2-225), we obtain

$$[\hat{\alpha}_A] = [\hat{A}_A][A_A]^{-1}[\alpha_A] \qquad (2\text{-}227)$$

Post-multiplying by $[\alpha_A]^{-1}$, it follows that

$$[A_S] = [\hat{\alpha}_A]\,[\alpha_A]^{-1} = [\hat{A}_A]\,[A_A]^{-1} \qquad (2\text{-}228)$$

where $[A_S]$ is known as the system matrix. Post-multiplying Eq. (2-228) by $[A_A]$, we obtain

$$[A_S]\,[A_A] = [\hat{A}_A] \qquad (2\text{-}229)$$

But each column **r** of $[\hat{A}_A]$ is related to the corresponding one of matrix $[A_A]$ by

$$\{\hat{A}_A\}_r = \{A_A\}_r\, e^{s_r \Delta t} \qquad r = 1, 2, ..., 2N \qquad (2\text{-}230)$$

Thus, we have the following eigenproblem to solve:

$$[[A_S] - e^{s_r \Delta t}[I]]\,\{A_A\}_r = \{0\} \qquad (2\text{-}231)$$

from which the modal parameters can be calculated. The calculation of mass-normalized modeshapes is not a problem in this case. A *SIMO* version of this method could also be developed and this would be the equivalent to the **ITD** method. Even as a *SISO* method, we can easily establish a parallel with the **ITD** method. No experimental examples were given in Ref. [79] and thus, no comments on the performance of this method for real cases are possible. We have no information of other articles about this method.

The Eigensystem Realization Algorithm in the frequency domain (ERA-FD)

A new version of the **ERA** in the frequency domain was presented recently (Ref. [80]). The procedure follows the same steps as for the time domain version and the mathematical development is entirely similar. Therefore,

we do not think it is worthwhile to develop it here. The frequency domain version can also provide checks to distinguish between genuine and computational modes. It features a reduced computational time and storage, being appropriate for small computers and the examples tried revealed its good performance, both on theoretical and experimental cases.

The Rational Fraction Polynomial method (RFP)

This is a *SISO* method that first appeared in 1982 (Ref. [81]). Like the **GHS** method, it is based on the minimization of an error function, using the least-squares technique. The main differences with respect to the **GHS** method are:

(i) the formulation of the FRF is expressed in rational fraction form, instead of the partial fraction form;

(ii) the error function to be minimized is established in such a way that the resulting system of equations is linear, without requiring initial estimates for the modal parameters.

Because the resulting linear system of equations involves matrices that are ill-conditioned, the rational fraction form of the FRF is expressed in terms of orthogonal Forsythe polynomials. For this reason, this method is also known as the Rational Fraction Orthogonal Polynomial method (RFOP). A variation of this method, the Complex Orthogonal Polynomial Functions method (COPF), was described (Ref. [82]), but the theory was not presented. Another variation was proposed (Ref. [83]), using Chebyshev polynomials instead of the Forsythe ones, with the main objective of obtaining a faster algorithm. The **RFP** method will be developed in detail in Chapter 4.

The Global Rational Fraction Polynomial method (GRFP)

This method is an extension of the **RFP** method to analyse globally a set of FRFs, using one single input reference. It is, therefore, a *SIMO* method. This extension of the **RFP**, already mentioned in Ref. [81], was developed further in Refs. [84] and [85]. The **GRFP** method will also be developed in detail, in Chapter 5.

An extension of the **GRFP** method to incorporate multiple input locations, i. e., its *MIMO* version is developed in Ref. [86]. This development follows exactly the same steps as explained in Chapters 4 and 5 for the **RFP** and **GRFP** methods, with the corresponding extensions to incorporate the additional information from several inputs. It will not be presented here, as we believe that a good understanding of the developments of the **RFP** and **GRFP** methods will allow an easy comprehension of that *MIMO* version.

The Global method

The **Global** method (Refs. [87], [88]) is a *SIMO* method, and the approach used differs completely from the **GRFP**. It is based on the construction of matrices of differences of receptances and mobilities, in order to avoid the effects of neighbouring modes. In those matrices, the number of FRFs is overspecified with respect to the expected number of modes existing in the selected frequency range. Application of the SVD technique enables the determination of the genuine number of existing modes. A detailed explanation of this method is given in Chapter 5. A variation of the method, allowing the structure to be excited simultaneously by several input forces (with the condition that the input force vectors are linearly independent), is proposed in Ref. [89], with the objective of having a better excitation of all the modes that are to be identified.

The Polyreference Frequency Domain method (PRFD)

This is a *MIMO* method, due to the works of Zhang *et al.* (Refs. [90], [91], [92]). Considering **p** response locations and **q** input references, the impulse response matrix in terms of receptance, for an **N** DOF system, can be given by (see Eq. (2-169):

$$\underset{(pxq)}{[H(t)]} = \underset{(px2N)}{[\Psi]} \underset{(2Nx2N)}{[\,e^{s_r t}\,]} \underset{(2Nxq)}{[W]^T} \tag{2-232}$$

where $[\Psi]$ is the modeshape matrix and **[W]** is the modal participation matrix, as defined in Eqs. (2-25) and (2-26). The corresponding Laplace transform of Eq. (2-232), is

$$[H(s)] = [\Psi]\,[s[\,I\,] - [\,s_r\,]]^{-1}\,[W]^T \tag{2-233}$$

Defining

$$\underset{(2Nxq)}{[G(s)]} = \underset{(2Nx2N)}{[s[\,I\,] - [\,s_r\,]]^{-1}} \underset{(2Nxq)}{[W]^T} \tag{2-234}$$

we can write

$$\underset{(pxq)}{[H(s)]} = \underset{(px2N)}{[\Psi]} \underset{(2Nxq)}{[G(s)]} \tag{2-235}$$

Applying the Laplace transform to the first time derivative of Eq. (2-232), i. e., to the impulse response matrix in terms of mobility, we obtain

$$[H(s)]_M = \mathbf{L}\,[\dot{H}(t)] = s[H(s)] - [H(t)]_{t=0} \tag{2-236}$$

where the subscript ^{M} denotes mobility. From Eq. (2-232) for **t=0**,

$$[H(s)]_M = s[H(s)] - [\Psi]\,[W]^T \tag{2-237}$$

But it is also true that

$$[H(s)]_M = [\Psi] [\ s_r \,] [G(s)] \tag{2-238}$$

Thus,

$$s[H(s)] - [\Psi] [W]^T = [\Psi] [\ s_r \,] [G(s)] \tag{2-239}$$

Combining Eqs. (2-235) and (2-239), we have

$$\begin{bmatrix} [H(s)] \\ s[H(s)] \end{bmatrix} - \begin{bmatrix} [0] \\ [\Psi] [W]^T \end{bmatrix} = \begin{bmatrix} [\Psi] \\ [\Psi] [\ s_r \,] \end{bmatrix} [G(s)] \tag{2-240}$$

From Eq. (2-235), we can extract the value of [G(s)]:

$$[G(s)] = ([\Psi]^T [\Psi])^{-1} [\Psi]^T [H(s)] \tag{2-241}$$

Substituting into Eq. (2-238), we obtain

$$[H(s)]_M = [\Psi] [\ s_r \,] ([\Psi]^T [\Psi])^{-1} [\Psi]^T [H(s)] \tag{2-242}$$

or

$$\underset{(pxq)}{[H(s)]_M} = \underset{(pxp)}{[A_S]} \underset{(pxq)}{[H(s)]} \tag{2-243}$$

where

$$[A_S] = [\Psi] [\ s_r \,] ([\Psi]^T [\Psi])^{-1} [\Psi]^T \tag{2-244}$$

is called the system matrix. Post-multiplying Eq. (2-244) by [Ψ], we obtain

$$[A_S] [\Psi] = [\Psi] [\ s_r \,] \tag{2-245}$$

which represents an eigenproblem that will give us the modeshapes [Ψ] and the natural frequencies and damping factors from [s_r]. The problem is now how to evaluate the system matrix $[A_S]$. Eq. (2-245) can be written as

$$\left[-[A_S] \; [I]\right] \begin{bmatrix} [\Psi] \\ [\Psi]\,[\,s_r\,] \end{bmatrix} = [0] \tag{2-246}$$

Post-multiplying both sides by **[G(s)]**, we obtain

$$\left[-[A_S] \; [I]\right] \begin{bmatrix} [\Psi] \\ [\Psi]\,[\,s_r\,] \end{bmatrix} [G(s)] = [0] \tag{2-247}$$

Substituting Eq. (2-240) in Eq. (2-247), we obtain

$$\left[-[A_S] \; [I]\right] \begin{bmatrix} [H(s)] \\ s[H(s)] - [\Psi]\,[W]^T \end{bmatrix} = [0] \tag{2-248}$$

or

$$-[A_S]\,[H(s)] + s[H(s)] - [\Psi]\,[W]^T = [0] \tag{2-249}$$

from which

$$\underset{(px(p+q))}{[[A_S] \; [\Psi]\,[W]^T]} \underset{((p+q)xq)}{\begin{bmatrix} [H(s)] \\ [I] \end{bmatrix}} = \underset{(pxq)}{s[H(s)]} \tag{2-250}$$

Passing to the frequency domain by putting $s=j\omega$ and considering **L** measured frequencies, we obtain

$$\underset{(px(p+q))}{[[A_S] \; [\Psi]\,[W]^T]} \underset{((p+q)xLq)}{\begin{bmatrix} [H(j\omega_1)] \; ... \; [H(j\omega_L)] \\ [I] \quad ... \quad [I] \end{bmatrix}} = \underset{(pxLq)}{[[H(j\omega_1)] \; ... \; [H(j\omega_L)]]}\; x$$

$$\begin{bmatrix} j\omega_1[I] & & 0 \\ & \ddots & \\ 0 & & j\omega_L[I] \end{bmatrix}_{(LqxLq)} \tag{2-251}$$

from which it is easy to extract $[A_S]$ and $[\Psi]\,[W]^T$. After solving the eigenproblem (2-245), $[\Psi]$ will be known and therefore we shall know $[W]^T$, completing the mathematical model. The residues can be calculated as in Eq. (2-177), from where it is easy to calculate the modal constants and phase angles. The correct number of modes can be calculated by an SVD, in a similar way as explained for the **Multi-Matrix** method, later in this chapter. The **PRFD** method has given evidence of good performance when dealing with close modes; it appears also to be less sensitive to computational modes when compared to time domain methods and allows for the use of unequal frequency steps. A more general version of this method, including also information in terms of inertance, is presented in Ref. [93].

Other methods

An enormous number of methods can nowadays be found, the majority of them being just slight variations of the best known ones. We shall refer briefly to some of those methods. One of them is the Constrained Global Nonlinear (CGN) (Ref. [94]). In this *SIMO* method, the curve-fitting is reduced to a minimization problem with constraint equations, related to the orthogonal properties of the modeshapes. An objective function is then constructed, where the constraint equations are incorporated in the form of Lagrange multipliers. All the modal parameters are derived from the minimization procedure, and therefore in this method there is not the usual two stage calculation (e. g., like in the RFP), where the natural frequencies

and damping factors are calculated first and the modeshapes in a second stage. The procedure is, however, restricted to real modes.

Recently, in Ref. [95], an improvement to the **GRFP** method was introduced with the objective of determining the correct number of modes present in a given frequency range. The analysis is repeated with an increasing number of assumed modes and a statistical parameter is introduced with the property that it stabilizes when the correct number of modes is achieved; further increments of the number of modes will not alter the value of that parameter. This parameter is a direct function of the computed least-squares error of the fit.

In Ref. [96], the **GRFP** method is extended to a *MIMO* version, making use of a matrix autoregressive moving-average model in the Laplace domain, with the advantages of being appropriate for high modal density cases. A complex mode indicator function (CMIF) is a plot of eigenvalues as a function of the frequency and it is used to determine the number of modes.

2-3-3 Direct methods

In this category, we include four methods: the Spectral method, the Simultaneous Frequency Domain method (SFD), the Identification of Structural System Parameters method (ISSPA) and the Multi-Matrix method.

The Spectral method

The **Spectral** method, introduced by Klosterman (Ref. [16]) with the objective of identifying close modes, is probably the simplest of all the *MIMO* direct frequency domain methods, where the matrices of the

governing differential equation of the system are evaluated from the measured FRF receptances, considering only two frequency points. The theoretical background, discussion and an attempt to improve it are given in Chapter 5.

The Simultaneous Frequency Domain method (SFD)

The **SFD** method (Refs. [97], [98]) is a *SIMO* method where the aim is to form the matrices of the system based on responses at several locations on the structure. From a knowledge of those matrices, the eigenvalues and eigenvectors are calculated. Because in the frequency range of interest there will be **N** modes, only **N** DOF from the **p** measured ones will be effective in the characterization of the response of the system. These **N** DOF form what is called the "independent" set of DOF. In this way, the **p-N** measured responses will form a set of "dependent" DOF. These designations are, in our opinion, somewhat unfortunate, as a DOF is - by definition - an independent coordinate that reflects the behaviour of the system, but we shall still use it for the sake of being close to the terminology given by the authors of the method. The independent set will have the subscript $_1$ and the dependent one, the subscript $_2$. Writing the dynamic equation of the system for the **N** DOF, we have

$$[M] \{\ddot{y}_1\} + [C] \{\dot{y}_1\} + [K] \{y_1\} = \{\Gamma\} F \qquad (2\text{-}252)$$

where **F** is the single applied force and $\{\Gamma\}$ is the force location vector, formed by zeros except for the input location coordinate, where it is **1**. Pre-multiplying Eq. (2-252) by $[M]^{-1}$, we obtain

$$\{\ddot{y}_1\} + [M]^{-1} [C] \{\dot{y}_1\} + [M]^{-1} [K] \{y_1\} = [M]^{-1} \{\Gamma\} F \qquad (2\text{-}253)$$

or

$$\{\ddot{y}_1\} + [C]'\{\dot{y}_1\} + [K]'\{y_1\} = \{\Gamma\}'F \tag{2-254}$$

For sinusoidal excitation, we have

$$-\omega^2\{\bar{y}_1\} + j\omega[C]'\{\bar{y}_1\} + [K]'\{\bar{y}_1\} = \{\Gamma\}'F \tag{2-255}$$

where $\{\bar{y}_1\}$ is the complex amplitude of $\{y_1\}$. It may be assumed that the dependent set of responses will be related to the independent one by a linear transformation:

$$\underset{((p-N)x1)}{\{\bar{y}_2\}} = \underset{((p-N)xN)}{[T]} \underset{(Nx1)}{\{\bar{y}_1\}} \tag{2-256}$$

where [T] will, in general, be complex. We can write Eq. (2-255) as

$$j\omega[C]'\{\bar{y}_1\} + [K]'\{\bar{y}_1\} - \{\Gamma\}'F = \omega^2\{\bar{y}_1\} \tag{2-257}$$

Writing Eq. (2-257) for L frequencies, we obtain:

$$\begin{aligned}
j\omega_1[C]'\{\bar{y}_1\}_1 + [K]'\{\bar{y}_1\}_1 - \{\Gamma\}'F &= \omega_1^2\{\bar{y}_1\}_1 \\
j\omega_2[C]'\{\bar{y}_1\}_2 + [K]'\{\bar{y}_1\}_2 - \{\Gamma\}'F &= \omega_2^2\{\bar{y}_1\}_2 \\
&\vdots \qquad\qquad \vdots \\
j\omega_L[C]'\{\bar{y}_1\}_L + [K]'\{\bar{y}_1\}_L - \{\Gamma\}'F &= \omega_L^2\{\bar{y}_1\}_L
\end{aligned} \tag{2-258}$$

or

$$\underset{(NxN)}{[C]'}\underset{(NxL)}{[\{\bar{y}_1\}_1\ \{\bar{y}_1\}_2 \cdots \{\bar{y}_1\}_L]}\underset{(LxL)}{\begin{bmatrix} j\omega_1 & & 0 \\ & j\omega_2 & \\ & & \ddots \\ 0 & & j\omega_L \end{bmatrix}} + \underset{(NxN)}{[K]'}\underset{(NxL)}{[\{\bar{y}_1\}_1\ \{\bar{y}_1\}_2 \cdots \{\bar{y}_1\}_L]} -$$

$$\underset{(Nx1)}{\{\Gamma\}'F}\ \underset{(1xL)}{\{1\ \ 1\ \ ...\ 1\}} = \underset{(NxL)}{[\{\bar{y}_1\}_1\ \{\bar{y}_1\}_2 ... \{\bar{y}_1\}_L]} \underset{(LxL)}{\begin{bmatrix} \omega_1^2 & & 0 \\ & \omega_2^2 & \\ & & \ddots \\ 0 & & \omega_L^2 \end{bmatrix}} \tag{2-259}$$

or

$$j[C]'[Y_1][\Omega] + [K]'[Y_1] - \{\Gamma\}'F\{v\} = [Y_1][\Omega]^2 \tag{2-260}$$

with

$$[\Omega] = \begin{bmatrix} \omega_1 & & 0 \\ & \omega_2 & \\ & & \ddots \\ 0 & & \omega_L \end{bmatrix}$$

$$\{v\} = \{1\ \ 1\ \ ...\ 1\} \tag{2-261}$$

Because $[\mathbf{Y}_1]$ is a complex matrix, Eq. (2-260) can be written in terms of its real and imaginary parts:

$$j[C]'(\mathrm{Re}[Y_1] + j\mathrm{Im}[Y_1])[\Omega] + [K]'(\mathrm{Re}[Y_1] + j\mathrm{Im}[Y_1]) -$$

$$\{\Gamma\}'F\{v\} = (\mathrm{Re}[Y_1] + j\mathrm{Im}[Y_1])[\Omega]^2 \tag{2-262}$$

Separating the real and imaginary parts, we obtain:

$$-[C]'\mathrm{Im}[Y_1][\Omega] + [K]'\mathrm{Re}[Y_1] - \{\Gamma\}'F\{v\} = \mathrm{Re}[Y_1][\Omega]^2$$

$$[C]'\mathrm{Re}[Y_1][\Omega] + [K]'\mathrm{Im}[Y_1] = \mathrm{Im}[Y_1][\Omega]^2 \tag{2-263}$$

or

$$\underset{(Nx(2N+1))}{[[C]' \quad [K]' \quad \{\Gamma\}'F]} \begin{bmatrix} -Im[Y_1]\,[\Omega] & Re[Y_1]\,[\Omega] \\ Re[Y_1] & Im[Y_1] \\ -\{v\} & \{0\} \end{bmatrix}_{((2N+1)x2L)} =$$

$$\underset{(Nx2L)}{[Re[Y_1]\,[\Omega]^2 \quad Im[Y_1]\,[\Omega]^2]} \tag{2-264}$$

or simply

$$[X]\,[A] = [B] \tag{2-265}$$

From Eq. (2-265), we can calculate **[X]** by a pseudo-inverse:

$$[X] = [B]\,[A]^T([A]\,[A]^T)^{-1} \tag{2-266}$$

Thus, matrices **[C]'**, **[K]'** and the vector **{Γ}'F** are now known. The homogeneous solution, in state space formulation, of Eq. (2-254), can be written as (see Cap. 5):

$$\underset{(2Nx2N)}{\begin{bmatrix} [C]' & [I] \\ [I] & [0] \end{bmatrix}} \underset{(2Nx1)}{\begin{Bmatrix} \dot{y}_1 \\ \ddot{y}_1 \end{Bmatrix}} + \underset{(2Nx2N)}{\begin{bmatrix} [K]' & [0] \\ [0] & -[I] \end{bmatrix}} \underset{(2Nx1)}{\begin{Bmatrix} y_1 \\ \dot{y}_1 \end{Bmatrix}} = \underset{(2Nx1)}{\begin{Bmatrix} \{0\} \\ \{0\} \end{Bmatrix}} \tag{2-267}$$

From this equation, the complex modeshape matrix $[\Phi_1]$ of dimensions **Nx2N** and the **2N** eigenvalues s_r can be calculated, enabling the modal parameters to be evaluated. The solution for $\{\bar{y}_1\}$ can be written as

$$\underset{(Nx1)}{\{\bar{y}_1\}} = \underset{(Nx2N)}{[\Phi_1]}\,\underset{(2Nx2N)}{[j\omega[I] - [s_r]]^{-1}}\,\underset{(2NxN)}{[\Phi_1]^T}\,\underset{(Nx1)}{\{\Gamma\}'F} \tag{2-268}$$

Substituting Eq. (2-256) in Eq. (2-268), we obtain:

$$\{\bar{y}_2\} = [T]\,[\Phi_1]\,[j\omega\,[I] - [s_r]]^{-1}\,[\Phi_1]^T\,\{\Gamma\}'\,F \tag{2-269}$$

or

$$\{\bar{y}_2\} = [\Phi_2]\,[j\omega\,[I] - [s_r]]^{-1}\,[\Phi_1]^T\,\{\Gamma\}'\,F \tag{2-270}$$

where

$$\underset{((p-N)x2N)}{[\Phi_2]} = \underset{((p-N)xN)}{[T]}\ \ \underset{(Nx2N)}{[\Phi_1]} \tag{2-271}$$

From this equation we see that the same linear relationship between $\{\bar{y}_1\}$ and $\{\bar{y}_2\}$ applies for the modeshapes $[\Phi_1]$ and $[\Phi_2]$. In order to calculate the modeshapes corresponding to the set of "dependent" DOF, we only have to evaluate **[T]** from Eq. (2-256):

$$\underset{((p-N)xL)}{[Y_2]} = \underset{((p-N)xN)}{[T]}\ \ \underset{(NxL)}{[Y_1]} \tag{2-272}$$

from which

$$[T] = [Y_2]\,[Y_1]^T\,([Y_1]\,[Y_1]^T)^{-1} \tag{2-273}$$

and the complete modeshapes for all measured coordinates will be known. We may also seek the conservative homogeneous solution of Eq. (2-254) in order to calculate the real modes of the structure:

$$[[K]' - \omega^2[I]]\,\{y_1\} = \{0\} \tag{2-274}$$

The real modeshape matrix will be $[\Phi_1]_R$, of dimensions **NxN** and there will be **N** eigenvalues s_r, from which the modal parameters can be

evaluated. The proportional viscous damping factors can be calculated by using:

$$[\Phi_1]_R^T [C]' [\Phi_1]_R = [\ 2\xi_r\omega_r\ ] \tag{2-275}$$

A similar relationship as in Eq. (2-271), between the "independent" and "dependent" sets of real modeshapes exists:

$$\underset{((p-N)xN)}{[\Phi_2]_R} = \underset{((p-N)xN)}{[T]'} \ \underset{(NxN)}{[\Phi_1]_R} \tag{2-276}$$

with the difference that now, matrix **[T]'** must be real. This can be imposed in Eq. (2-272), writting

$$Re[Y_2] + j\, Im[Y_2] = [T]' (Re[Y_1] + j\, Im[Y_1]) \tag{2-277}$$

from which

$$\begin{aligned} Re[Y_2] &= [T]' Re[Y_1] \\ Im[Y_2] &= [T]' Im[Y_1] \end{aligned} \tag{2-278}$$

or

$$\underset{((p-N)x2L)}{[Re[Y_2] \quad Im[Y_2]]} = \underset{((p-N)xN)}{[T]'} \ \underset{(Nx2L)}{[Re[Y_1] \quad Im[Y_1]]} \tag{2-279}$$

Writing Eq. (2-279) as

$$[Y_2]' = [T]' [Y_1]' \tag{2-280}$$

we obtain

$$[T]' = [Y_2]' [Y_1]'^T ([Y_1]' [Y_1]'^T)^{-1} \tag{2-281}$$

which, substituted in Eq. (2-276), enables the calculation of the complete set of real modeshapes.

The possibility of this method to evaluate the system matrices and therefore the complex and/or real modeshapes is a great advantage. The main problems are related to the correct choice of the "independent" set of measured coordinates, as a different choice may lead to different answers. A repeated analysis could be beneficial. In order to determine the correct number of modes to consider in the "independent" set of coordinates, a first view of the FRFs on the Argand plane can be pursued. Usually, the number of modes taken are the visible ones plus two, to take into account residual effects. Better results were found when several narrow frequency bands were selected around regions of resonant peaks.

An improved selection method for the number of modes to analyse is given in Ref. [98]. This method has been applied very successfully in complex spacecraft structures. Craig and Blair (Ref. [99]) have extended this method, in order to permit multiple exciter testing. The theoretical development is entirely similar to the one just given above.

The Identification of Structural System Parameters method (ISSPA)

Presented in 1978 (Ref. [100]), this *SIMO* direct method is based on the identification of the system matrices to solve an eigenproblem. Let us begin by considering the differential equation of equilibrium for a SDOF system:

$$m\ddot{y} + c\dot{y} + ky = f \qquad (2\text{-}282)$$

This method considers the more general case where there is also a moving base exciting the system, like in Fig. (2-3).

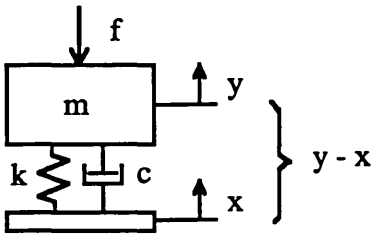

Fig. 2-3 Moving base SDOF system.

For this case, Eq. (2-282) becomes:

$$m\ddot{y} + c(\dot{y} - \dot{x}) + k(y - x) = f \tag{2-283}$$

Defining the relative displacement between the mass and the base, as

$$y_r = y - x \tag{2-284}$$

we have, in terms of y_r, the following equation:

$$m(\ddot{y}_r + \ddot{x}) + c\dot{y}_r + ky_r = f \tag{2-285}$$

or

$$m\ddot{y}_r + c\dot{y}_r + ky_r = -m\ddot{x} + f \tag{2-286}$$

For an MDOF system, it will be

$$[M]\{\ddot{y}_r\} + [C]\{\dot{y}_r\} + [K]\{y_r\} = -[M]\{\ddot{x}\} + \{F\} \tag{2-287}$$

For harmonic base and force excitation, we can write

$$[-\omega^2[M] + j\omega[C] + [K]]\{\bar{y}_r\} = -\omega^2[M]\{x\} + \{F\} \tag{2-288}$$

or, pre-multiplying by $[M]^{-1}$,

$$[-\omega^2[I] + j\omega[C]' + [K]']\{\bar{y}_r\} = -\omega^2\{x\} + [M]^{-1}\{F\} \tag{2-289}$$

where $\{\bar{y}_r\}$ is the complex amplitude of $\{y_r\}$. Eq. (2-289) can still be written as

$$[-\omega^2 [I] + j\omega [C]' + [K]'] \{\bar{y}_r\} = \omega^2 \{F\}' \tag{2-290}$$

where

$$\{F\}' = -\{x\} + \omega^{-2} [M]^{-1} \{F\} \tag{2-291}$$

At this stage, $\{F\}'$ and $\{\bar{y}_r\}$ are supposed to be known for each FRF. Supposing an **N** DOF system, the matrices in Eq. (2-290) have dimensions **NxN** and the vectors, **Nx1**. From Eq. (2-291), we see that for pure excitation of the base it is not necessary to know **[M]**, but for an applied force, **[M]** must be known, which usually is introduced from a theoretical evaluation via a finite element analysis. Considering **L** measured frequency points, we have, from Eq. (2-290),

$$\begin{aligned}
&-\omega_1^2 \{\bar{y}_r\}_1 + j\omega_1 [C]' \{\bar{y}_r\}_1 + [K]' \{\bar{y}_r\}_1 = \omega_1^2 \{F\}' \\
&-\omega_2^2 \{\bar{y}_r\}_2 + j\omega_2 [C]' \{\bar{y}_r\}_2 + [K]' \{\bar{y}_r\}_2 = \omega_2^2 \{F\}' \\
&\qquad\vdots \qquad\qquad\qquad\qquad\qquad\qquad \vdots \\
&-\omega_L^2 \{\bar{y}_r\}_L + j\omega_L [C]' \{\bar{y}_r\}_L + [K]' \{\bar{y}_r\}_L = \omega_L^2 \{F\}'
\end{aligned} \tag{2-292}$$

or

$$\underset{(NxL)}{[\{\bar{y}_r\}_1 \{\bar{y}_r\}_2 \ldots \{\bar{y}_r\}_L]} \underset{(LxL)}{\begin{bmatrix} -\omega_1^2 & & 0 \\ & -\omega_2^2 & \\ & & \ddots \\ 0 & & -\omega_L^2 \end{bmatrix}} + j \underset{(NxN)}{[C]'} \underset{(NxL)}{[\{\bar{y}_r\}_1 \{\bar{y}_r\}_2 \ldots \{\bar{y}_r\}_L]} x$$

$$\begin{bmatrix} \omega_1 & & 0 \\ & \omega_2 & \\ 0 & & \omega_L \end{bmatrix}_{(LxL)} + [K]' \underset{(NxN)}{} [(\bar{y}_r)_1 \ (\bar{y}_r)_2 \ldots (\bar{y}_r)_L] = \underset{(NxL)}{[\{F\}' \ \{F\}' \ \ldots \ \{F\}']} \ x$$

$$\begin{bmatrix} \omega_1^2 & & 0 \\ & \omega_2^2 & \\ 0 & & \omega_L^2 \end{bmatrix}_{(LxL)} \qquad (2\text{-}293)$$

or

$$-[Y_r]\,[\Omega]^2 + j\,[C]'\,[Y_r]\,[\Omega] + [K]'\,[Y_r] = [F]''\,[\Omega]^2 \qquad (2\text{-}294)$$

with

$$[\Omega] = \begin{bmatrix} \omega_1 & & 0 \\ & \omega_2 & \\ 0 & & \omega_L \end{bmatrix} \qquad (2\text{-}295)$$

Writing $[Y_r]$ as

$$[Y_r] = \mathrm{Re}[Y_r] + j\,\mathrm{Im}[Y_r] \qquad (2\text{-}296)$$

Eq. (2-294) can be separated into its real and imaginary parts:

$$\begin{aligned} -\mathrm{Re}[Y_r]\,[\Omega]^2 - [C]'\,\mathrm{Im}[Y_r]\,[\Omega] + [K]'\,\mathrm{Re}[Y_r] &= [F]''\,[\Omega]^2 \\ -\mathrm{Im}[Y_r]\,[\Omega]^2 + [C]'\,\mathrm{Re}[Y_r]\,[\Omega] + [K]'\,\mathrm{Im}[Y_r] &= [0] \end{aligned} \qquad (2\text{-}297)$$

where **[C]'** and **[K]'** are the unknowns to be calculated. Their calculation gives:

$$[C]' = \left[\mathrm{Im}[Y_r]\,[\Omega]^2\,\mathrm{Im}[Y_r]^+ - [\mathrm{Re}[Y_r] + [F]'']\,[\Omega]^2\,\mathrm{Re}[Y_r]^+\right] \times$$
$$[\mathrm{Im}[Y_r]\,[\Omega]\,\mathrm{Re}[Y_r]^+ + \mathrm{Re}[Y_r]\,[\Omega]\,\mathrm{Im}[Y_r]^+]^{-1}$$
$$[K]' = [\mathrm{Im}[Y_r]\,[\Omega] - [C]'\,\mathrm{Re}[Y_r]\,]\,[\Omega]\,\mathrm{Im}[Y_r]^+ \qquad (2\text{-}298)$$

where $\mathbf{Re}\,[Y_r]^+$ and $\mathbf{Im}\,[Y_r]^+$ are the pseudo-inverses of $\mathbf{Re}\,[Y_r]$ and $\mathbf{Im}\,[Y_r]$, respectively, and are given by:

$$\mathrm{Re}[Y_r]^+ = \mathrm{Re}[Y_r]^T\,(\mathrm{Re}[Y_r]\,\mathrm{Re}[Y_r]^T)^{-1}$$
$$\mathrm{Im}[Y_r]^+ = \mathrm{Im}[Y_r]^T\,(\mathrm{Im}[Y_r]\,\mathrm{Im}[Y_r]^T)^{-1} \qquad (2\text{-}299)$$

Knowing **[C]'** and **[K]'**, the eigenvalues and eigenvectors can be calculated. The general solution can be found by solving an equation similar to Eq. (2-267) and the solution corresponding to real modes is found by solving an equation like Eq. (2-274) in the **SFD** method.

In the **ISSPA** method we need to measure the input forces and to know the mass matrix of the system This may not be very easy to introduce and therefore this method is probably more suitable for base excitation tests, usually with a shaker table. Although not referred to here, the SVD technique is usually employed in this method to determine the effective number of DOF of the system under study. For more details, see Refs. [100] and [101].

The Multi-Matrix method

This is a *MIMO* direct method (Refs. [102], [15], [14]) where a general matrix input-output polynomial is estimated using frequency responses from several input and output locations. Residual terms rather than

additional modes are used to describe the contribution of out-of-range modes. By a principal response analysis, the effective number of modes is determined and the governing system matrices are identified, from which the modal parameters can be evaluated. Using harmonic excitation, the dynamic equilibrium equation is

$$\underset{(pxp)}{[(j\omega)^2\,[M] + (j\omega)\,[C] + [K]]}\ \underset{(px1)}{\{y\}} = \underset{(pxq)\ (qx1)}{[\Gamma]\ \{f\}} \qquad (2\text{-}300)$$

where $\{y\}$ is the response at p coordinates, $\{f\}$ the input force at q references and $[\Gamma]$ is a transformation matrix relating the coordinate location q with p. The effective number of modes in the frequency range of interest is N ($N<q$). The N responses $\{y\}'$ must be related to the p responses $\{y\}$ by a linear transformation $[T]$:

$$\underset{(Nx1)}{\{y\}'} = \underset{(Nxp)\ (px1)}{[T]\ \{y\}} \qquad (2\text{-}301)$$

The effective number of modes can be calculated using a pincipal response analysis, i. e., via an SVD analysis. Considering measurements at L frequency points in the frequency range of interest, we can write

$$\underset{(pxL)}{[Y]} = [\mathrm{Re}\{y\}_1\,\mathrm{Im}\{y\}_1\,\mathrm{Re}\{y\}_2\,\mathrm{Im}\{y\}_2\ \ldots\mathrm{Re}\{y\}_L\,\mathrm{Im}\{y\}_L] \qquad (2\text{-}302)$$

and Eqs. (2-301) becomes

$$\underset{(NxL)}{[Y]'} = \underset{(Nxp)\ (pxL)}{[T]\ [Y]} \qquad (2\text{-}303)$$

where the composition of $[Y]'$ is similar to Eq. (2-302).We can also apply an SVD to the product $[Y]\,[Y]^T$, giving (see Appendix D)

$$\underset{(pxp)}{[Y]}\,\underset{}{[Y]^H} = \underset{(pxN)}{[U]}\,\underset{(NxN)}{[\Sigma]^2}\,\underset{(Nxp)}{[U]^H} \tag{2-304}$$

where $[\Sigma]$ is the matrix of the singular values and $[U]$ is a unitary matrix. This decomposition will have N non-zero singular values, corresponding to the number of modes. Matrix $[U]^H$ can then be used as the transformation matrix $[T]$. Because $[U]$ is unitary, we can write

$$\underset{(pxL)}{[Y]} = \underset{(pxN)}{[U]}\,\underset{(NxL)}{[Y]'} \tag{2-305}$$

and, for each measured frequency,

$$\underset{(px1)}{\{y\}} = \underset{(pxN)}{[U]}\,\underset{(Nx1)}{\{y\}'} \tag{2-306}$$

Substituting in Eq. (2-300), we obtain

$$\underset{(pxN)}{\left[(j\omega)^2 [M] [U] + (j\omega) [C] [U] + [K] [U]\right]}\,\underset{(Nx1)}{\{y\}'} = \underset{(pxq)}{[\Gamma]}\,\underset{(qx1)}{\{f\}} \tag{2-307}$$

For convenience, we shall pre-multiply Eq. (2-307) by $[K]^{-1}$, giving

$$\underset{(pxN)}{\left[(j\omega)^2 [K]^{-1} [M] [U] + (j\omega) [K]^{-1} [C] [U] + [U]\right]}\,\underset{(Nx1)}{\{y\}'} = \underset{(px1)}{[K]^{-1} [\Gamma] \{f\}} \tag{2-308}$$

Pre-multiplying Eq. (2-308) by $[U]^H$, we obtain

$$\underset{(NxN)}{\left[(j\omega)^2 [U]^H [K]^{-1} [M] [U] + (j\omega) [U]^H [K]^{-1} [C] [U] + [I]\right]}\,\underset{(Nx1)}{\{y\}'} =$$

$$\underset{(Nx1)}{[U]^H [K]^{-1} [\Gamma] \{f\}} \tag{2-309}$$

or

$$[(j\omega)^2 [D]_2 + (j\omega) [D]_1 + [I]] \{y\}' = [P]_0 \{f\}$$

(NxN) (Nx1) (Nxq) (qx1) (2-310)

When more than **2N** complex conjugate modes are contributing to the response (say, **2N'**), it is convenient to use a more general matrix equation of order **m** to model the forced system responses. The order **m** will be selected such that **mxN** is larger than **2N'** (Ref. [15]). Thus, we shall have, more generally,

$$[(j\omega)^m [D]_m + ...+ (j\omega) [D]_1 + [I]] \{y\}' = [(j\omega)^{m-1} [P]_{m-1} + ...$$

$$+ (j\omega) [P]_1 + [P]_0] \{f\} \quad (2\text{-}311)$$

where **m** must be even. This equation can be considered as an autoregressive moving-average frequency domain model for $\{y\}'$. The effect of out-ofrange modes is accounted for by using residual terms. The substraction of this effect must leave us with the correct response in the frequency range of interest. Considering here only upper residual terms, $[R]_u$, Eq. (2-311) must then be modified to

$$[(j\omega)^m [D]_m + ...+ (j\omega) [D]_1 + [I]] [\{y\}' - [R]_u \{f\}] =$$

$$[(j\omega)^{m-1} [P]_{m-1} + ...+ (j\omega) [P]_1 + [P]_0] \{f\} \quad (2\text{-}312)$$

Developing Eq. (2-312),

$$[(j\omega)^m [D]_m + ...+ (j\omega) [D]_1 + [I]] \{y\}' =$$

$$[(j\omega)^m [D]_m [R]_u + ...+ (j\omega) [D]_1 [R]_u + [R]_u + (j\omega)^{m-1} [P]_{m-1} + ...$$

$$+ (j\omega) [P]_1 + [P]_0] \{f\} \quad (2\text{-}313)$$

or

$$[(j\omega)^m [D]_m + ...+ (j\omega) [D]_1 + [I]] \{y\}' =$$

$$[(j\omega)^m [D]_m [R]_u + (j\omega)^{m-1} ([D]_{m-1} [R]_u + [P]_{m-1}) + ...$$

$$+ (j\omega) ([D]_1 [R]_u + [P]_1) + [R]_u + [P]_0] \{f\} \quad (2\text{-}314)$$

or

$$[(j\omega)^m [D]_m + ...+ (j\omega) [D]_1 + [I]] \{y\}' =$$

$$[(j\omega)^m [P']_m + (j\omega)^{m-1} [P']_{m-1} + ...+ (j\omega) [P']_1 + [P']_0] \{f\} \quad (2\text{-}315)$$

where

$$\begin{aligned} [P']_m &= [D]_m [R]_u \\ [P']_{m-1} &= [D]_{m-1} [R]_u + [P]_{m-1} \\ [P']_0 &= [R]_u + [P]_0 \end{aligned} \quad (2\text{-}316)$$

Eq. (2-315) can still be written as

$$[(j\omega)^m [D]_m + ...+ (j\omega) [D]_1] \{y\}' - [(j\omega)^m [P']_m + ...$$

$$+ (j\omega) [P']_1 + [P']_0] \{f\} = - \{y\}' \quad (2\text{-}317)$$

For all the **L** measured frequencies, we have

$$\underset{(Nx(Nm+q(m+1)))}{[[D]_m \ ... \ [D]_1 \ [P']_m \ ... \ [P']_0]} \underset{((Nm+q(m+1))xL)}{\begin{bmatrix} (j\omega_1)^m \{y\}_1' & (j\omega_2)^m \{y\}_2' & ... & (j\omega_L)^m \{y\}_L' \\ \vdots & \vdots & & \vdots \\ (j\omega_1) \{y\}_1' & (j\omega_2) \{y\}_2' & ... & (j\omega_L) \{y\}_L' \\ \hline -(j\omega_1)^m \{f\}_1 & -(j\omega_2)^m \{f\}_2 & ... & -(j\omega_L)^m \{f\}_L \\ \vdots & \vdots & & \vdots \\ -\{f\}_1 & -\{f\}_2 & ... & -\{f\}_L \end{bmatrix}} =$$

$$\underset{(NxL)}{[-\{y\}_1' -\{y\}_2' \ ...-\{y\}_L']} \tag{2-318}$$

This equation can be solved by a weighted least-squares procedure for the matrices **[D]** and **[P']**. Now, the modal parameters must be solved. If the receptance matrix is given by

$$\underset{(Nxq)}{[\alpha(j\omega)]} = \sum_{r=1}^{2N} \underset{(Nxq)}{\frac{[A]_r}{j\omega - s_r}} + \underset{(Nxq)}{[R]_u} \tag{2-319}$$

where $[A]_r$ is the **Nxq** residue matrix for mode **r**. It is clear from Eq. (2-315) that $[\alpha(j\omega)]$ also satisfies

$$[(j\omega)^m [D]_m + ...+ (j\omega) [D]_1 + [\,I\,]]\ [\alpha(j\omega)] =$$

$$[(j\omega)^m [P']_m + \ ...+ \ [P']_0] \tag{2-320}$$

Matrix $[R]_u$ can be calculated from the first of Eqs. (2-316) and matrices **[P]** can be calculated from the other Eqs. (2-316). Therefore, according to Eq. (2-312), Eq. (2-320) can be written as

$$[(j\omega)^m [D]_m + ...+ (j\omega) [D]_1 + [\,I\,]][[\alpha(j\omega)] - [R]_u] =$$

$$[(j\omega)^{m-1} [P]_{m-1} + \ ...+ \ [P]_0] \tag{2-321}$$

This equation can be written in companion matrix form as

$$[-(j\omega) [D]' + [\,I\,]][\alpha(j\omega)]' = [P(j\omega)]'' \tag{2-322}$$

where

$$[D]' = \underset{(NmxNm)}{\begin{bmatrix} -[D]_1 & -[D]_2 & \cdots & -[D]_m \\ [I] & [0] & \cdots & [0] \\ [0] & [I] & \cdots & [0] \\ \vdots & \vdots & & \vdots \\ [0] & [0] & \cdots [I] & [0] \end{bmatrix}} \qquad (2\text{-}323\ a)$$

$$[\alpha(j\omega)]' = \underset{(Nmxq)}{\begin{bmatrix} [\alpha(j\omega)] - [R]_u \\ (j\omega)[[\alpha(j\omega)] - [R]_u] \\ \vdots \\ (j\omega)^{m-1}[[\alpha(j\omega)] - [R]_u] \end{bmatrix}} \qquad (2\text{-}323\ b)$$

$$[P(j\omega)]'' = \underset{(Nmxq)}{\begin{bmatrix} (j\omega)^{m-1}[P]_{m-1} + \cdots + (j\omega)[P]_1 + [P]_0 \\ [0] \\ \vdots \\ [0] \end{bmatrix}} \qquad (2\text{-}323\ c)$$

If $[\ s_r\ ]^{-1}$ are the eigenvalues of **[D]'** and $[\Psi]'$ the eigenvectors, we can write

$$\underset{(NmxNm)}{[\Psi]'} \ \underset{(NmxNm)}{[\ s_r\ ]^{-1}} = \underset{(NmxNm)}{[D]'} \ \underset{(NmxNm)}{[\Psi]'} \qquad (2\text{-}324)$$

where

$$[\Psi]' = \underset{(NmxNm)}{\begin{bmatrix} [\Psi] \\ [\Psi][\ s_r\ ] \\ \vdots \\ [\Psi][\ s_r\ ]^{m-1} \end{bmatrix}} \qquad (2\text{-}325)$$

Once the eigenvalues are known, the natural frequencies and damping factors can be calculated. We have still to calculate the residues $[A]_r$ in order to calculate the modeshapes. From Eq. (2-324), we can write

$$[D]^{-1} = [\Psi]' [\lceil s_r \rfloor]^{-1} [\Psi]^{-1} \tag{2-326}$$

Substituting Eq. (2-326) in Eq. (2-322), we obtain

$$[-(j\omega)[\Psi]' [\lceil s_r \rfloor]^{-1} [\Psi]^{-1} + [I]] [\alpha(j\omega)]' = [P(j\omega)]'' \tag{2-327}$$

Pre-multiplying by $-[\lceil s_r \rfloor] [\Psi]'^{-1}$, we obtain

$$[(j\omega)[\Psi]^{-1} - [\lceil s_r \rfloor] [\Psi]^{-1}] [\alpha(j\omega)]' = -[\lceil s_r \rfloor] [\Psi]^{-1} [P(j\omega)]'' \tag{2-328}$$

or

$$[(j\omega)[I] - [\lceil s_r \rfloor]] [\Psi]^{-1} [\alpha(j\omega)]' = -[\lceil s_r \rfloor] [\Psi]^{-1} [P(j\omega)]'' \tag{2-329}$$

Assuming now **Nxm=2N'**, Eq. (2-319) can also be written as

$$\underset{(Nxq)}{[\alpha(j\omega)] - [R]_u} = \underset{(NxNm)}{[\Psi]} \underset{(NmxNm)}{[(j\omega)[I] - [\lceil s_r \rfloor]]^{-1}} \underset{(Nmxq)}{[W]^T} \tag{2-330}$$

where **[W]** is the modal participation matrix, as defined in Eqs. (2-25) and (2-26). It is shown in Ref. [15] that each row of $[W]^T$ is given by the corresponding row of the right-hand-side of Eq. (2-329), at the pole s_r. The residue matrix for each mode **r** is given by

$$\underset{(Nxq)}{[A]_r} = \underset{(Nx1)}{\{\Psi\}_r} \underset{(1xq)}{\{W\}_r^T} \tag{2-331}$$

from which the modal constants and phase angles can be evaluated.

This method has the ability of handling a large amount of data, being stable and robust, and has proven to be able to deal with closely spaced modes and highly modal damping and/or high modal density. In Ref. [102] a favorable comparison with the **PRCE** method is carried out. The main disadvantages of the **Multi-matrix** method are the considerable computational requirements and complexity for an easy computer implementation. It is, however, one of the most significant contributions in the direction of a more automatic processing and analysis of large amounts of data.

2-4 Tuned-sinusoidal methods

These methods are a special class of modal identification methods in general. They are essentially based upon the experimental "isolation" or tuning of real modes of vibration, by means of the excitation of the structure at each natural frequency by a set of exciters appropriately distributed in space and time. The *a priori* need of approximatly locating the natural frequencies of the stucture to be analysed, implies that another identification method must be used in advance. This justifies Ibrahim's comment (Ref. [25]) that this category of methods cannot be considered as genuine identification methods. Nevertheless, these methods constitute one of the oldest approaches to the study of the dynamic properties of structures and are still widely used nowadays in the aeronautical industry.

Lewis and Wrisley (Ref. [103]) were the first to recognize that real modes of vibration - i. e., those of the undamped structure - could be found if applied forces by several exciters could balance the dissipative forces in the structure and that this could happen if the measured displacements were in quadrature with those applied forces. In such conditions, the dynamic equations of equilibrium are reduced to their homogeneous solution at the undamped natural frequencies of the structure. Moreover, those authors

state that the magnitude of the applied forces at the natural frequencies must be proportional to the product of the mass of the structure on which they act and to the amplitude of that mass in the mode being excited. Once a mode is tuned, it is a simple matter to determine the modal parameters - the excitation frequency is the natural frequency and the measured motion is the modeshape. Damping can be evaluated by cutting the excitation and measuring the rate of decay of the response. The correctness of the tuning could be assessed by the absence of beating (due to the presence of another mode) in the free decay response.

In 1958, Asher (Ref. [104]) provided a mathematical description to calculate the natural frequencies, by zeroing the determinant of the real part of the FRF matrix, and to calculate the force distribution among the several shakers that must be applied to tune the desired mode. Since then, this procedure has become known as the **Asher**'s method, although, also in 1958, Trail-Nash (Ref. [105]) had published a similar procedure, where it was shown that the number of exciters to be used was a function of the effective number of DOF of the structure, and suggested the **Kennedy-Pancu** method for the localization of the natural frequencies.

A description of the basic theory of **Asher**'s method is given in Chapter 6, when we apply it to solve the problem of calculating the real modes of a structure from a knowledge of its measured complex modes. Because subsequent work related to this type of methods are - in general - variations and improvements to **Asher**'s method, we shall only present in this section a brief historical note on the evolution of that method.

The necessity for considerable data acquisition capacity for practical applications justified that only in the seventies these methods have started to be more widely used. In 1974, Craig and Su (Ref. [106]) carried out a study on the number and localization of exciters on a structure, in order to

properly tune the real modes of vibration. Considering that the number of measured responses, **p**, is always greater than the number of exciters, **q**, it is not usually possible to have all the **p** responses in quadrature with the forces. Those authors introduced the concept of Modal Purity as a criterion to decide whether or not the measurements obtained at the **p** locations represented a true mode of vibration. This criterion establishes a tolerance for the phase angle of the response with respect to the force and if the phase deviates from **90** or **270** degrees by the amount of the given tolerance, then the test is rejected, meaning that either more exciters are necessary or that their position on the stucture must be altered. As already mentioned, the natural frequencies are calculated in **Asher**'s method by putting the determinant of the real part of the measured FRF matrix to zero, where each element is obtained by exciting the structure at one point and measuring at another point. Craig and Su, in the same work, proposed a method for the localization of the exciters, by taking several sets of FRFs for different exciter locations and so forming different FRF matrices. Each of these matrices gave results for the natural frequencies and an analysis of their repeatability provided the most desirable locations for the shakers. The influence of varying the number of shakers was also investigated and numerical cases with close modes analysed with success. It was also found that the force distribution necessary to tune a mode does not agree with the conditions given by Lewis and Wrisley.

In 1975, Smith et al. (Ref. [107]) presented a computerized system for the automatic acquisition, processing and analysis of structural dynamic data.

In 1976, Ibáñez (Ref. [108]) proposed an extension of **Asher**'s method that consisted basically of considering more responses than exciters, with the advantage of reducing the occurence of spurious resonant frequencies that sometimes happens in the standard method.

In 1978, Hallauer and Stafford (Ref. [109]) presented a detailed revision and discussion of **Asher**'s method, showing its strengths and weaknesses. Systems with non-proportional damping and close modes are discussed, and numerical techniques are presented. Problems associated with the incompleteness of the FRF matrix are also discussed. Numerical simulations are given, where the normal modes calculated by theory are compared with the normal modes regenerated after calculating the force distribution.

Following this work, Gold and Hallauer, in 1979 (Ref. [110]), proposed an analytical application of **Asher**'s method, calculating the modeshapes after evaluating the force distribution vector. However, the calculation of the FRF matrix was not given directly from the measurements, but was generated after having identified it using a least-squares curve-fitting method. This procedure sought to avoid the storage of large amounts of acquired data, storing instead the identified modal parameters. Numerical simulations worked well, but experimental cases failed due to the poor quality of the measured data.

Also in 1979, Ensminger and Turner (Ref. [111]) proposed a variation of **Asher**'s method, again with prior curve-fitting of the measured FRFs, called the **Minimum Coincident Response** method. The real part of the FRF matrix could be rectangular and by minimizing (by a least-squares technique) the sum of the squares of the in-phase (real) displacements subjected to a normalization constraint on the quadrature (imaginary) response, it was possible to calculate the force vector as a function of the frequency and also the error (again, a function of the frequency). Plotting the error function for each measured frequency, the natural frequencies are obtained from the minima on the graph. For these natural frequencies, the force distributions can be calculated and the real modeshapes too. This plot showed to be more efficient in the detection of close natural

frequencies than the plot of the determinant of the real part of the FRF matrix, because it is visually clearer. This approach also replaces the multi-shaker test by an analytical simulation. However, in 1981, Craig and Chung (Ref. [112]) concluded essentially that **Asher**'s method has greater capability for identifying close modes than the **Minimum Coincident Response** method.

In 1983, Rades (Ref. [113]) proposed the use of the SVD technique to localize the natural frequencies of the structure when the FRF matrix is rectangular, i. e. when there are more responses than exciters. A matrix is formed by the product of the transpose of the real part of the FRF matrix by itself and the plots of the singular values of such a matrix with the frequency shows minima at the natural frequencies. It was shown that those plots give clearer indications of the localization of the natural frequencies than the usual plots of the determinant of the real part of the FRF matrix.

An automatic procedure, the force appropriation for modal evaluation (FAME) was proposed by Ibañez and Blakely in 1984 (Ref. [114]), being essentially the automatic implementation of the extended **Asher**'s method developed in Ref. [108].

In 1984, Hunt et al. (Ref. [115]) presented an automatic method based on the perturbations of the exciting frequencies and force ratios to minimize the ratio of coincident response to quadrature response.

An overall review on this type of method can be found in Ref. [116]. The pratical implementation of these types of procedure to actually test a structure is very expensive and time consuming, as it requires a lot of equipment and because of the difficulty of the tuning process. As Ibrahim notes (Ref. [25]), it can be very dangerous to have a structure in resonance for several minutes, as damage or failure may occur. It is our opinion that nowadays, with the advanced computer technology and graphic

visualization, there is no reason why these methods could not be entirely simulated instead of actually testing real structures, experimental data being acquired as usual for the identification using other EMA methods.

2-5 Conclusions

From all the methods described in this chapter, we can note that in many cases the similarities among them are very clear, namely between the time and frequency domains. This is not very surprising, as all of them start from the same basic dynamic equations of equilibrium. If a "best" method exists, it is surely still to be discovered as, from the information we have collected, some methods work better for some applications than others. At the present time, the "best" method depends on the available resources, on the available timing, on the objectives of the study, on the personal experience of the user, gained when applying a particular method, etc. Although, in general, more experience exists on frequency domain methods, where more feeling about the vibration phenomena is possible due to an easier visualization, some time domain methods are also very popular and quite reliable. In this thesis, we shall dedicate special attention to frequency domain methods, for the reasons already stated in Section 1-5.

CHAPTER 3

SDOF MODAL ANALYSIS METHODS - CAPABILITIES AND LIMITATIONS WHEN DEALING WITH CLOSE MODES

3-1 Introduction

In the identification of the dynamic properties of structures via experimental modal analysis, single-degree-of-freedom methods continue to play an important role due, mainly, to two factors: simplicity of use and ready physical interpretation of the results. These two factors allow the user to have complete control of the identification process and a deeper understanding of the dynamic behaviour of a structure. The price to pay is in terms of time consumption, and therefore it may become an expensive choice for typical large-scale industrial modal tests. It is very important, however, to have a clear understanding of the capabilities and, probably even more important than this, of the limitations of this type of method. In general, from our experience, it can be said that the only limitation is encountered when the structure under consideration exhibits close modes which, on its own, may constitute a severe restriction. Apart from this, all

methods (and not only SDOF ones) give satisfactory results, although some may be more appropriate for some cases than others. In fact, it can be stated that the existence of close modes is often the major problem that one has to face in the modal identification of a structure (assuming that it is linear).

In this chapter, we shall explore the possibilities and limitations of SDOF methods when applied to close modes. Two major questions arise: first, how can we recognize the existence of two close modes, and second, how should we analyse them to obtain a satisfactory modal identification?

3-2 Indicators of close modes

A survey of modal analysis literature concerning methods of identification, reveals that in the great majority of them the problem of close modes is considered. Either it is stated "provided the system does not exhibit close modes ..." or examples contemplating their existence are presented to demonstrate the capabilities of a particular method. It can be said that the consideration of close modes is the ultimate test for any method. But, in fact, what can be considered as close or separate modes ? We shall discuss this problem considering the most common case of two close modes.

Intuitively, the concept of close modes is associated with the proximity of the values of the natural frequencies. In fact, it is inadequate to discuss the problem only in these terms. It seems more correct to say that two modes are close if their mutual influence is such that the results from an analysis of each mode separately are afflicted by large errors or, in other words, if the usual assumption (that the contribution of the modes other than the one under consideration is constant) is no longer true. If the errors obtained in the modal parameters are due to the presence of a close mode, it makes sense to admit that all four modal parameters of this neighbouring mode

are interfering on the mode under consideration, and not only its natural frequency.

3-2-1 Interference criteria

A number of studies have already been published on this matter (e. g., Refs. [60], [117], [62], [64]). In this section the interference criteria between two modes given in Ref. [64] are reviewed and the main conclusions presented. However, the numerical study and examples presented here constitute new material that is believed to provide a better understanding of the phenomenon of two close modes and to justify the frontiers of what can or cannot be considered as close modes. A further contribution given in this section is the implementation of the resulting interference criterion in a modal analysis computer program.

Let us consider the response of a 2 DOF system, and suppose the magnitude of the receptance , $|\alpha(j\omega)|$, as given in Fig. 3-1.

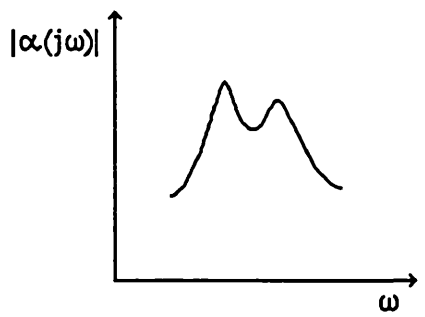

Fig. 3-1 Receptance magnitude of a 2 DOF system.

Let us indicate the separate contribution of each mode, $|\alpha_1(j\omega)|$ and $|\alpha_2(j\omega)|$ - which will be denoted by α_1 and α_2 for simplicity - as in Fig. 3-2, where ω_1 is the natural frequency of mode 1 and ω_{11} and ω_{21}

are the frequencies of the half-power points; one of the criteria states that there is no interference of mode **2** on mode **1** if the variation of the amplitude of α_2 in the frequency range ω_{11} to ω_{21} is small compared with the amplitude value of α_1 at its natural frequency, i. e.,

$$\frac{\Delta\alpha_2}{\alpha_1} \leq \nu \tag{3-1}$$

where ν is a small quantity, to be defined later in the text. Likewise, there will be no interference of mode **1** on mode **2** if

$$\frac{\Delta\alpha_1}{\alpha_2} \leq \nu \tag{3-2}$$

around the frequency range of the half-power points of mode **2**.

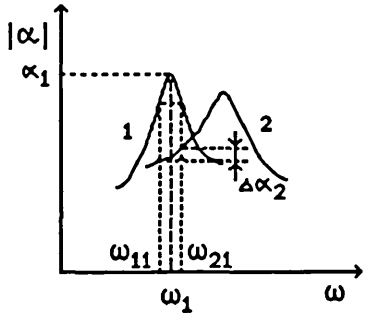

Fig. 3-2 Separate contribution of modes **1** and **2**.

Taking the expression of the receptance for a **1** DOF system with hysteretic damping, we have

$$\alpha_r(j\omega) = \frac{C_r e^{j\phi_r}}{\omega_r^2 - \omega^2 + j\eta_r\omega_r^2} \tag{3-3}$$

According to Ref. [64], expressions (3-1) and (3-2) become, respectively:

$$\delta a^2 \left\{ \frac{1}{\sqrt{\left(\frac{1 - a^2}{\eta_1} - a^2\right)^2 + \gamma^2}} - \frac{1}{\sqrt{\left(\frac{1 - a^2}{\eta_1} + a^2\right)^2 + \gamma^2}} \right\} \leq \nu \quad (3\text{-}4)$$

(condition of non-interference of mode 2 on mode 1)

$$\frac{1}{\delta a^2} \left\{ \frac{1}{\sqrt{\left(\frac{1 - (1/a)^2}{\eta_2} - (1/a)^2\right)^2 + (1/\gamma)^2}} - \frac{1}{\sqrt{\left(\frac{1 - (1/a)^2}{\eta_2} + (1/a)^2\right)^2 + (1/\gamma)^2}} \right\} \leq \nu \quad (3\text{-}5)$$

(condition of non-interference of mode 1 on mode 2)

where

$$a = \frac{\omega_1}{\omega_2}, \quad \gamma = \frac{\eta_2}{\eta_1}, \quad \delta = \frac{C_2}{C_1}$$

Also in Ref. [64], it was shown that the errors obtained in the identification of the modal parameters were small if ν was inferior to **0.5 %**.

Comments on expressions (3-4) and (3-5)

It should be noted that, in practice, expressions (3-4) and (3-5) can only be applied using the estimated values of the modal parameters, i. e., after having identified once each mode. As indicated in Ref. [62] and confirmed in Ref [64], the use of the estimated values instead of the theoretical ones does not modify the results significantly. Studying expressions (3-4) and (3-5), we can see that, in fact, several parameters other than the frequency spacing contribute to the interference phenomenon. Thus, besides the

frequency ratio, **a**, there is the damping ratio, γ, the modal constant ratio, δ, and a combined factor involving the frequency ratio and the damping of the mode under consideration, $(1-a^2)/\eta$.

In addition, attention is called to the fact that the existence of interference of mode **2** on mode **1** does not necessarily mean that there is interference of mode **1** on mode **2** (or vice-versa). For example, observing Fig. 3-2, it can be understood that even if the frequency spacing is small, the ratio of the damping factors and/or modal constants can be such that one mode suffers a big interference while the other is almost unaffected. In Fig. 3-2, it is obvious that mode **1** is "stronger" (possibly due to a light damping factor) than mode **2** and therefore is bound to influence mode **2** much more than this one does on mode **1**.

This indicator of the mutual influence between two close modes has been implemented in a modal analysis computer program, with an automatic warning that a more careful analysis must be carried on whenever the value of ν exceeds **0.5 %**.

It should be noticed that expression (3-4) (or (3-5)) has only considered the variation in magnitude of the FRF and not the variation in phase. Due to this restriction, it is not possible from this expression to conclude anything about the relative importance of different situations of close modes, i.e., two different cases of frequency spacing may lie in the interference range, but it is not possible to tell if one is worse or better than the other. In fact, in the limiting case of **a=1**, the left-hand-sides of expressions (3-4) and (3-5) give a zero value, implying that there would be no interference! The reason why the variation in phase of the FRF has not been applied is beause it was not possible to establish a correlation between the values obtained for the interference factor and the errors obtained in the identification of the modal parameters, whereas with expression (3-4) it has been possible to establish a threshold value of **0.5 %** for ν, making this criterion a very

useful indicator of the quality of the results of the modal parameters. Provided that $\nu \leq 0.5\ \%$, we can be sure that the modal parameters need no more correction due to interference from neighbouring modes.

Examples

Let us suppose $\delta = \gamma = 1$. We are looking for the minimum frequency spacing we must have when varying the damping factor, so that $\nu \leq 0.5\ \%$. The results are shown in Table 3-1.

η	a
0.05	0.708
0.03	0.791
0.01	0.913
0.005	0.953
0.001	0.990

Table 3-1 Minimum values of **a**, so that $\nu \leq 0.5\ \%$.

We can conclude from Table 3-1 that, if ω_1 is set as **100 Hz**, no correction is necessary provided the values of ω_2 are as given in Table 3-2. For example, when $\eta = 0.01$ (and considering $\delta = \gamma = 1$), the SDOF analysis will always have to be refined if the frequency ratio **a** is higher than **0.913** or, for $\omega_1 = 100$ **Hz**, if ω_2 is equal to or smaller than **109.5 Hz**.

η	a	ω_1	ω_2
0.05	0.708	100	141.2
0.03	0.791	100	126.4
0.01	0.913	100	109.5
0.005	0.953	100	104.9
0.001	0.990	100	101.0

Table 3-2 Minimum values of ω_2 if $\omega_1 = 100$ **Hz**, so that $\nu \leq 0.5\ \%$.

As mentioned previously, when the factor **a** approaches **1**, expression (3-4) tends to zero, so we could be misled by the resulting value of ν if the frequency ratio is close to **1**. It will be shown that, for ν = **0.5 %**, this does not constitute a problem, because the expression is only less than **0.5 %** if the frequency ratio is practically equal to **1**. So, for the values of δ, γ and η as before, we obtain (Table 3-3):

η	a_{max}	ω_1	$\omega_{2\,min}$
0.05	0.999830	100	100.01700
0.03	0.999900	100	100.01000
0.01	0.999964	100	100.00360
0.005	0.999983	100	100.00170
0.001	0.999996	100	100.00036

Table 3-3 The criterion only fails if $\omega_2 \leq \omega_{2\,min}$ ($\delta = \gamma = 1$)

The results shown in Table 3-3 mean that problems would only arise if ω_1 and ω_2 were closer than the values presented. This is not a big restriction for formula (3-4), as a_{max} is almost equal to **1**.

The effect of δ and γ being different from **1** will now be investigated. Taking the value of δ ($= C_2/C_1$) greater than **1** is the same as decreasing the value of ν (see expression (3-4)), and so, the net effect will be to decrease the values of **a** in Table 3-2, meaning that there will be no interference of mode **2** on mode **1** for a wider spacing of the natural frequencies. This makes sense because if $C_2 > C_1$, the peak of mode **2** will be higher than the peak of mode **1**. A value of δ less than **1** will have the opposite effect. It is also expected that the variation of the factor $\gamma = \eta_2/\eta_1$ will be in the opposite sense to that of factor δ, because $\eta_2 > \eta_1$ means a smaller peak in mode **2** by comparison with mode **1**. Increasing or decreasing both δ and γ

should make the results invariant, if their relative incidence is identical. The variation noticed in this case will show which of them is dominant. The cases to be analysed are shown in Table 3-4 and the results in Table 3-5.

Case	δ	γ
1	1.25	1
2	1	0.8
3	1.25	1.25

Table 3-4 Example data.

Case	δ	γ	η	a
1	1.25	1	0.05	0.688
			0.03	0.774
			0.01	0.904
			0.005	0.948
			0.001	0.989
2	1	0.8	0.05	0.707
			0.03	0.790
			0.01	0.912
			0.005	0.953
			0.001	0.990
3	1.25	1.25	0.05	0.688
			0.03	0.774
			0.01	0.904
			0.005	0.948
			0.001	0.989

Table 3-5 Minimum values of **a**, so that $v \leq 0.5$ %, for different values of δ and γ.

Comparing these results with the ones in Table 3-1 we confirm what was expected for case no. **1**, but it can be seen from case no. **2** that the influence of γ is very small and, in fact, in case no. **3**, the results are, to three decimal places, the same as for case no. **1**. Therefore, the factors that contribute most to the interference between two modes are δ, **a** and $(1\text{-}a^2)/\eta$. For case no. **1**, the values of a_{max} may also be calculated (as in Table 3-3 for

$\delta = \gamma = 1$), so that expression (3-4) is verified. Results for the case when $\omega_1 = 100$ Hz are presented in Table 3-6.

δ	γ	η	a	ω_1	ω_2	a_{max}	ω_1	$\omega_{2\,min}$
		0.05	0.688	100	145.3	0.999858	100	100.01420
		0.03	0.774	100	129.2	0.999915	100	100.00850
1.25	1	0.01	0.904	100	110.6	0.999971	100	100.00290
		0.005	0.948	100	105.5	0.999985	100	100.00150
		0.001	0.989	100	101.1	0.999997	100	100.00029

Table 3-6 Results for case no. **1**.

With these values, it is concluded that the effect of a neighbouring mode starts to be significant whenever ω_2 is smaller than the value presented in Table 3-6. In such cases, expression (3-4) always gives that indication, as its value is higher than **0.5 %**, provided that ω_2 is not smaller than the corresponding value of $\omega_{2\,min}$.

Although, as said before, the criterion concerning the change in phase does not provide a correlation with the errors in the identified modal parameters, it can be used as a comparative tool for the degree of interference. This criterion will be explained briefly: usually, it is considered that the effect of neighbouring modes can be represented by a constant complex vector. The other criterion that has been considered analyses the influence of a variation of this vector in magnitude, but keeping the same direction, while in the region within the half-power-point frequencies of the mode under consideration. The other criterion considers that this complex vector can also modify its direction in that same region, and it states that if the length of the arc corresponding to the angle swept by the vector (response of mode 2) is small compared with the diameter of the circle of mode **1**, there is no interference of mode **2** in mode **1**. Fig. 3-3 gives a representation of both criteria.

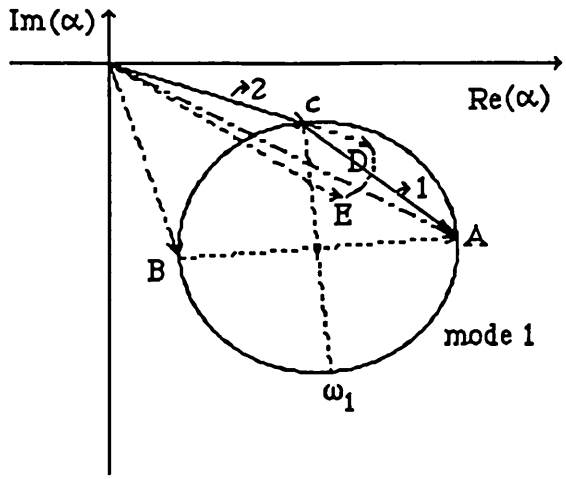

Fig. 3-3 Representation of the interference criteria.

In Fig. 3-3, **A** and **B** represent the half-power-points of mode **1**. Vector **1** represents the response of mode **1** and vector **2** the response of mode **2**. The first criterion compares the change in magnitude of vector **2** - from **C** to **D** - with the magnitude of vector **1** at the resonance frequency ω_1. The second criterion compares the arc **DE** described by vector **2** with the diameter **AB**. To draw a conclusion about the level of interference we must consider both criteria together as, in general, vector **2** will vary in both magnitude and phase.

From the previous numerical study it was shown that the magnitude criterion tends to zero as the ratio of natural frequencies (a) approaches **1**. If the phase criterion is also considered, it can be seen that it increases when **a** approaches **1**, meaning that when the two natural frequencies come very close, the effect of one mode on the other is governed by the variation in phase and not in magnitude.

Expressions (3-6) and (3-7) give, for this criterion, the conditions for non-interference of mode **2** on mode **1** and mode **1** on mode **2**, respectively:

$$\frac{2\delta a^4\gamma}{\left[\left(\frac{1-a^2}{\eta_1}\right)^2+\gamma^2-a^4\right]\sqrt{\left(\frac{1-a^2}{\eta_1}\right)^2+\gamma^2}} \leq \nu \qquad (3\text{-}6)$$

$$\frac{2}{\delta a^4\gamma\left[\left(\frac{1-(1/a)^2}{\eta_2}\right)^2+(1/\gamma)^2-(1/a)^4\right]\sqrt{\left(\frac{1-(1/a)^2}{\eta_2}\right)^2+(1/\gamma)^2}} \leq \nu \qquad (3\text{-}7)$$

In Table 3-7 the results of ν for expression (3-6) are presented, considering various values for η_1, γ and a.

		γ		
a	η_1	1	1.25	1.5
0.990	0.05	9.0240	2.4076	1.2826
	0.01	0.2157	0.2240	0.2203
	0.001	0.0002	0.0003	0.0004
0.992	0.05	13.8536	2.6976	1.3696
	0.01	0.4004	0.3814	0.3474
	0.001	0.0005	0.0006	0.0007
0.994	0.05	23.4308	2.9798	1.4485
	0.01	0.8605	0.6991	0.5643
	0.001	0.0011	0.0014	0.0017
0.996	0.05	46.9439	3.2329	1.5155
	0.01	2.3542	1.3642	0.9128
	0.001	0.0038	0.0047	0.0056
0.998	0.05	137.6947	3.4324	1.5670
	0.01	10.9891	2.5883	1.3524
	0.001	0.0302	0.0358	0.0405
0.999	0.05	355.9152	3.5047	1.5859
	0.01	44.4411	3.2435	1.5260
	0.001	0.2228	0.2315	0.2277

Table 3-7 Study of the influence of the phase criterion (results of ν for different values of a, η_1 and γ).

The effect of δ is only a multiplicative one. From these results it is concluded that the interference increases as **a** increases and for each value of **a**, it increases with the increase of η_1. On the other hand, for each **a**, the interference decreases with the increasing of the damping ratio η_2/η_1 (γ), except for low values of η_1, but the variations are very small meaning that the factor γ is not very important in this case.

Discussion

This study of the interference between two modes shows that the magnitude criterion is useful as it enables us to know if it is necessary a more careful identification of the two modes. This is possible because a limit for the value of ν could be established by relating it with the errors obtained in the modal parameters: anything beyond **0.5 %** needs correction. The phase criterion does not give this indication, but allows a comparison between different cases, and it can be concluded that more interference exists whenever **a**, η_1 and δ increase and γ decreases. So, the worst possible situation when there are two modes is to have high values for **a** (maximum equals 1), η_1 and δ and a small value for γ. From Table 3-7, the worst case corresponds to $\mathbf{a = 0.999}$, $\eta_1 = \mathbf{0.05}$ and $\gamma = \mathbf{1}$.

If it is considered that the modal constants and the damping factors are aproximately the same for both modes ($\delta \approx 1$, $\gamma \approx 1$), the interference values of mode **2** in mode **1** and of mode **1** in mode **2** are very similar. This is found many times in practical situations and in this case, it is always true that the closer the natural frequencies are, the more interference exists between the modes. So, the usual connection between the existence of close modes and the proximity of natural frequencies pre-supposes that $\delta \approx \mathbf{1}$

and $\gamma \approx 1$.

It is important to notice that these criteria suppose that the existence of two modes has previously been recognized. They are not indicators of their existence, but of the necessity of correction of the analysis.

3-2-2 The circle centres

A possible indicator of the existence of close modes can be found from the analysis of the Nyquist plot in the vicinity of these modes. Let us consider first of what happens when there is only one mode and theoretical data, and a circle is fitted around the resonance (Fig. 3-4). In this case, the least-squares **Circle-fitting** procedure would give exact values for the coordinates of the centre, x_0, y_0 and the radius r_0, no matter how many or which points have been taken into account to do the circle-fit. Instead, if some noise is added to the theoretical data, and if several circles are fitted considering different sets of data points (4 at least, as a least-squares method is used), different answers for the values x_0, y_0 and r_0 are obtained and if the centres of the circles are plotted, a small "cloud" around the true value of the centre (Fig. 3-5) will be observed.

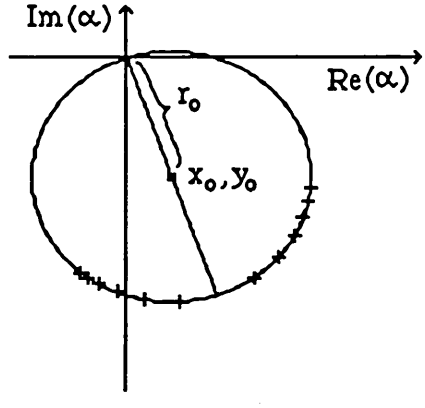

Fig. 3-4 Nyquist plot and **Circle-fitting** of a **1** DOF system.

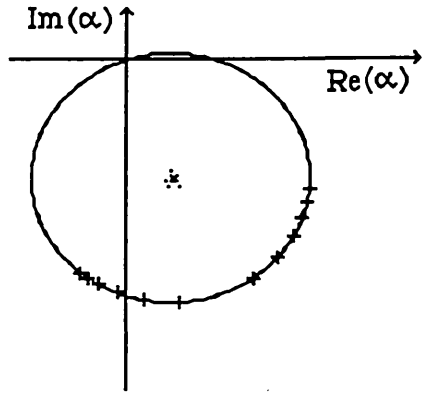

Fig. 3-5 Plot of the circle centres for a **1** DOF system (theo. data + noise).

The least-squares fit considering all the points together will supply a kind of average of all the possible values for the centre. If this idea is extended to the analysis of two close modes, when successive sets of **4** points along the frequency range encompassing the two modes are considered, it is expected that two distinct "clouds" will be seen, one around each centre (Fig. 3-6).

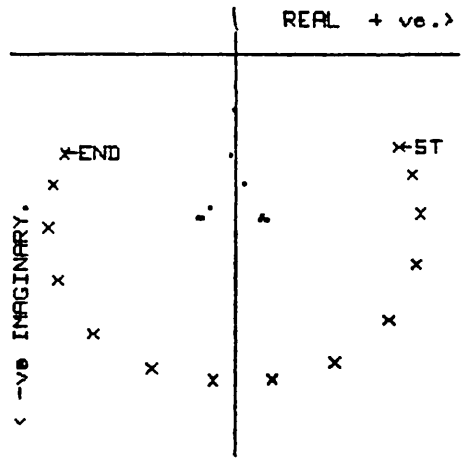

Fig. 3-6 Plot of the circle centres for a **2** DOF system (theo. data).

This could be a good and simple indicator of the existence of two close modes and moreover an indicator of the range of frequency that should be used around each mode, keeping only the ranges where the centres hold

together. This indicator works quite well with noiseless theoretical data (Fig 3-7).

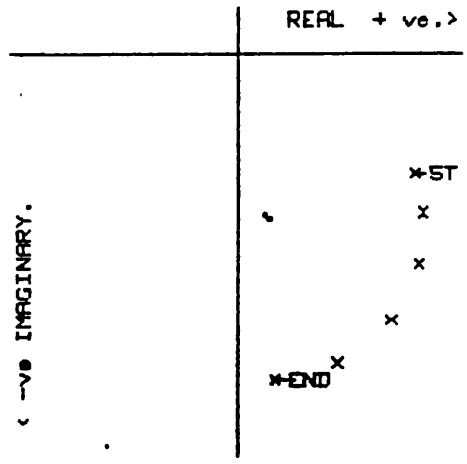

Fig. 3-7 Region of a 2 DOF system where the centers hold together (theo. data).

Unfortunately, it can fail when as little random noise as **1 %** is added, because the scatter of the circle centres can make the plot difficult to interpret (Fig. 3-8) and so, is not very useful to use when dealing with experimental data.

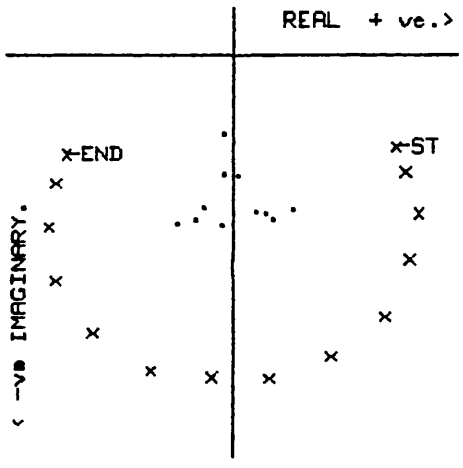

Fig. 3-8 Plot of the centres for a 2 DOF system with noise.

Although this method does not seem very useful in practical circumstances, we thought that it was worth presenting it because of its basic simplicity. It has been incorporated in a modal analysis computer program, for its academic interest.

3-2-3 The inverse of receptance

Eq. (3-3) is the receptance for a SDOF system with hysteretic damping. If the inverse of that expression is considered and writing α_r instead of $\alpha_r(j\omega)$ for simplicity, we obtain

$$\frac{1}{\alpha_r} = \frac{\omega_r^2 - \omega^2 + j\eta_r\omega_r^2}{C_r e^{j\phi_r}} \tag{3-8}$$

Real modes case

If real modes are assumed, the phase angle of the modal constants, ϕ_r, will be either 0° or 180°, and expression (3-8) will be:

$$\frac{1}{\alpha_r} = \frac{\omega_r^2 - \omega^2 + j\eta_r\omega_r^2}{C_r} \tag{3-9}$$

where C_r will be positive or negative for $\phi_r = 0^o$ or 180°, respectively. Separating into real and complex parts, we have

$$\mathrm{Re}\left(\frac{1}{\alpha_r}\right) = \frac{1}{C_r}(\omega_r^2 - \omega^2) \tag{3-10}$$

$$\mathrm{Im}\left(\frac{1}{\alpha_r}\right) = \frac{\eta_r\omega_r^2}{C_r} \tag{3-11}$$

Expression (3-10) represents a straight line in ω^2 and expression (3-11) represents a horizontal line (constant value) in ω or ω^2. Figs. 3-9 a) and b) are the graphical displays of these two expressions.

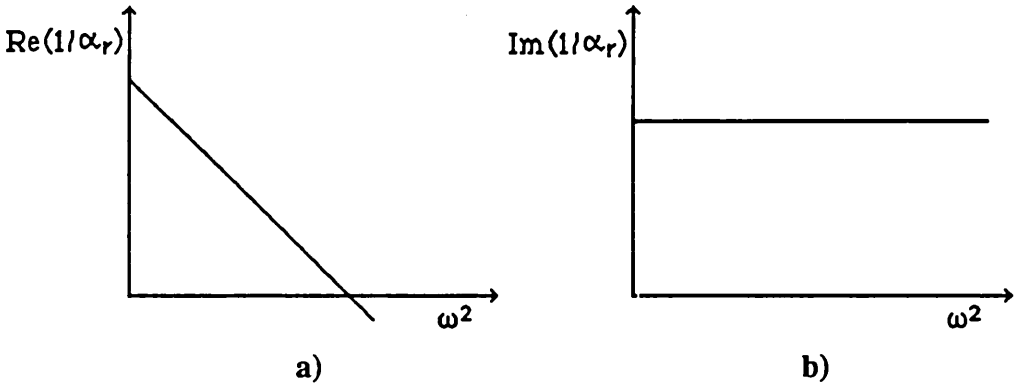

Fig. 3-9 Real and imaginary parts of the inverse of receptance, for real modes.

The case shown in Fig. 3-9 is for $\phi_r = 0°$, as the slope of $\mathbf{Re}(1/\alpha_r)$ is negative and $\mathbf{Im}(1/\alpha_r)$ is positive. For $\phi_r = 180°$, the slope of $\mathbf{Re}(1/\alpha_r)$ will be positive and $\mathbf{Im}(1/\alpha_r)$ negative. It is easy to see from Eq. (3-10) that the intercept of $\mathbf{Re}(1/\alpha_r)$ with the horizontal axis gives the value of ω_r and that the reciprocal of the slope gives the modal constant. From the imaginary part, the damping factor is obtained. One of the advantages of this representation is that there is a clear separation of the modal parameters, as the damping factor appears only in the imaginary part of the display. If a viscous damping model had been considered, instead of Eq. (3-11), we would obtain

$$\mathrm{Im}\left(\frac{1}{\alpha_r}\right) = \frac{2\,\omega\,\omega_r\,\xi_r}{C_r} \qquad (3\text{-}12)$$

A display of the imaginary part with ω would be a straight line

with slope $2\omega_r\xi_r/C_r$, and not a horizontal line as before and so it is possible to have an indication of the existing type of damping. In practice, however, this is not so clear, as the presence of neighbouring modes and non-proportional damping can cause distortions on the plots and no obvious conclusion can be drawn. Nevertheless, if the modes are well separated, and the existence of real modes is a reasonable assumption to make, this method can have some advantages over the **Circle-fitting** approach, namely (i) because it is easier to obtain the natural frequency just by fitting a staight line and calculating the intercept with the horizontal axis and (ii) because the fitting can easily be based on the points away from the immediate vicinity of the natural frequency, whenever the definition around that value is not good due to a light damping factor and/or to the existence of noise.

Complex modes case

Because in practice one has, in general, to deal with complex modes, the limitations of the previous case will be relaxed, and the expressions revised for the case of complex modes. Rewriting expression (3-8) as

$$\frac{1}{\alpha_r} = \frac{\omega_r^2 - \omega^2 + j\eta_r\,\omega_r^2}{A_r + jB_r} \tag{3-13}$$

where

$$\begin{aligned} A_r &= C_r \cos\phi_r \\ B_r &= C_r \sin\phi_r \end{aligned} \tag{3-14}$$

it follows that

$$\mathrm{Re}\left(\frac{1}{\alpha_r}\right) = \frac{(A_r + B_r\eta_r)\omega_r^2 - A_r\omega^2}{A_r^2 + B_r^2} \tag{3-15}$$

$$\mathrm{Im}\left(\frac{1}{\alpha_r}\right) = \frac{(A_r\eta_r - B_r)\omega_r^2 + B_r\omega^2}{A_r^2 + B_r^2} \tag{3-16}$$

In this case, both real and imaginary parts are straight lines in ω^2, of the form

$$\mathrm{Re}\left(\frac{1}{\alpha_r}\right) = m_R + n_R\,\omega^2 \tag{3-17}$$

$$\mathrm{Im}\left(\frac{1}{\alpha_r}\right) = m_I + n_I\,\omega^2 \tag{3-18}$$

with

$$m_R = \frac{(A_r + B_r\eta_r)\omega_r^2}{A_r^2 + B_r^2} \tag{3-19 a}$$

$$m_I = \frac{(A_r\eta_r - B_r)\omega_r^2}{A_r^2 + B_r^2} \tag{3-19 b}$$

$$n_R = -\frac{A_r}{A_r^2 + B_r^2} \tag{3-19 c}$$

$$n_I = \frac{B_r}{A_r^2 + B_r^2} \tag{3-19 d}$$

After fitting the graphs of $\mathbf{Re}(1/\alpha_r)$ and $\mathbf{Im}(1/\alpha_r)$ to straight lines, $\mathbf{m_R}$, $\mathbf{m_I}$, $\mathbf{n_R}$ and $\mathbf{n_I}$ are known and by convenient manipulation of Eqs. (3-19), we can determine the four modal parameters:

$$\omega_r = \sqrt{\frac{-m_R n_R - m_I n_I}{n_R^2 + n_I^2}} \tag{3-20 a}$$

$$\eta_r = \frac{m_R n_I - m_I n_R}{-m_R n_R - m_I n_I} \qquad (3\text{-}20\ b)$$

$$C_r = \frac{1}{\sqrt{n_R^2 + n_I^2}} \qquad (3\text{-}20\ c)$$

$$\phi_r = tg^{-1}\left(-\frac{n_I}{n_R}\right) \qquad (3\text{-}20\ d)$$

In the case of real modes, $\mathbf{n_I = 0}$ and these expressions coincide with the ones for the real modes case. Now, both slopes and intercepts of the real and imaginary parts contribute to the calculation of the modal parameters and so the imaginary part is no longer uniquely linked with the damping factor. Also, the natural frequency does not correspond any more to the intercept with the zero horizontal line.

The possibilities and usefulness of this method to identify a structure will be discussed in more detail later, as now the interest relies on its application as an indicator of the existence of close modes. Considering Eqs. (3-14) and (3-19 c) and (3-19 d), we have

$$n_R = -\frac{\cos\phi_r}{C_r} \qquad (3\text{-}21\ a)$$

$$n_I = \frac{\sin\phi_r}{C_r} \qquad (3\text{-}21\ b)$$

Depending on the value of ϕ_r, all combinations for the signs of the slopes of the real and imaginary parts of $1/\alpha_r$ against ω^2 are possible. Considering two modes with $\mathbf{0^o < \phi_1 < 90^o}$ and $\mathbf{-90^o < \phi_2 < 0^o}$, the display of the inverse FRF will be as shown in Fig. 3-10.

From the simple observation of these graphs, it seems easy to recognize the existence of two modes, even if they are very close, due to the difference in the slopes and intercepts with the vertical axis. It is known that from a Bode

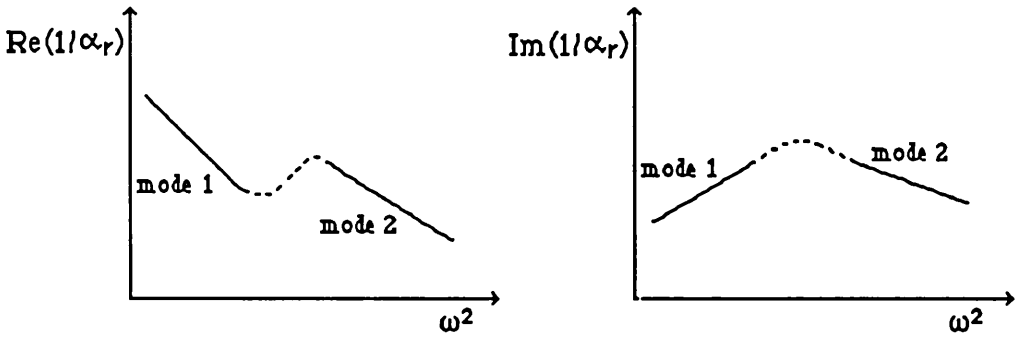

Fig. 3-10 Real and imag. parts of $1/\alpha_r$, for a 2 DOF system with complex modes.

or a Nyquist plot it may be very difficult to recognize the presence of two modes, but since we are dealing here with straight lines, it is possible that a good indicator of the existence of two close modes has been found. The most difficult situation appears to be when all the parameters of the two modes are very similar, in which case a situation like in Fig. 3-11 could arise.

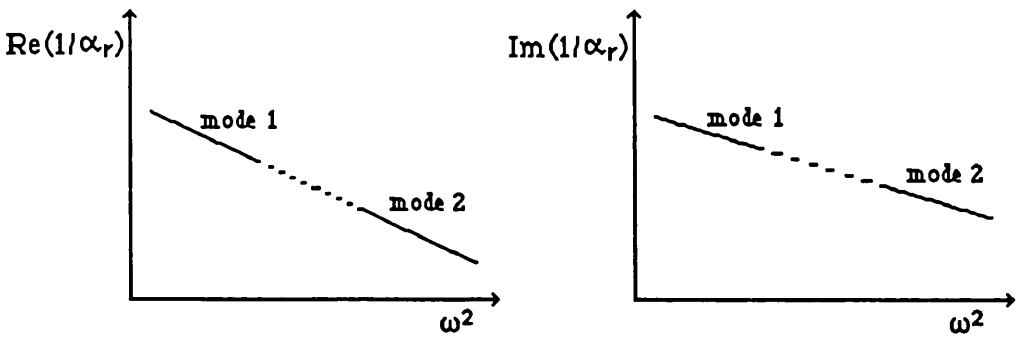

Fig. 3-11 Real and imag. parts of $1/\alpha_r$, for a 2 DOF system with complex modes and similar modal parameters.

In this case, it is possible that only one straight line is visible in each plot. The shape of the dotted line between the two modes, however, is not easy to predict theoretically, as the analytical expression for the inverse of the FRF is a complicated function of frequency. If it is not a straight line, it may still be possible to recognize the presence of two modes. For this study, theoretical data with identical modal parameters for both modes have been generated (Table 3-8). The display of the inverse FRF is shown in Fig. 3-12.

Mode	ω_r	η_r	C_r	ϕ_r
1	100	0.01	1	0
2	100	0.01	1	0

Table 3-8 Data for a 2 DOF system, with identical modal parameters.

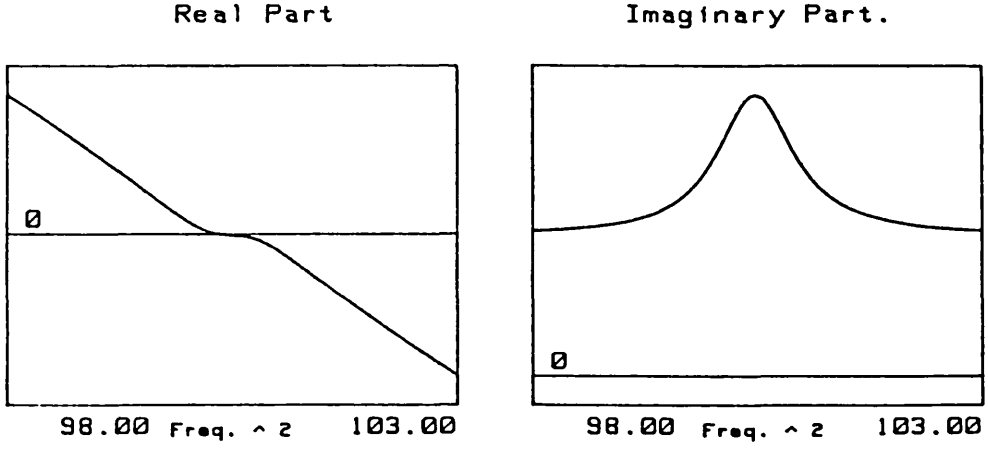

Fig. 3-12 Inverse FRF plots for the data of Table 3-8.

In Fig. 3-12 the real part shows a variation between the two modes and the imaginary part exhibits a "bump". Figs. 3-13 and 3-14 show the Bode and Nyquist plots, respectively, and one can verify that, in this example, it is easy to recognize two modes in all the different representations shown.

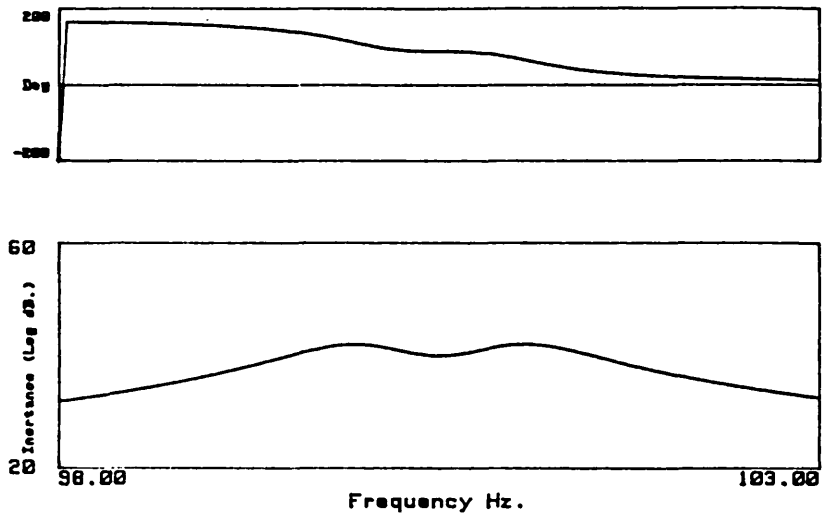

Fig. 3-13 Bode plot of Fig. 3-12.

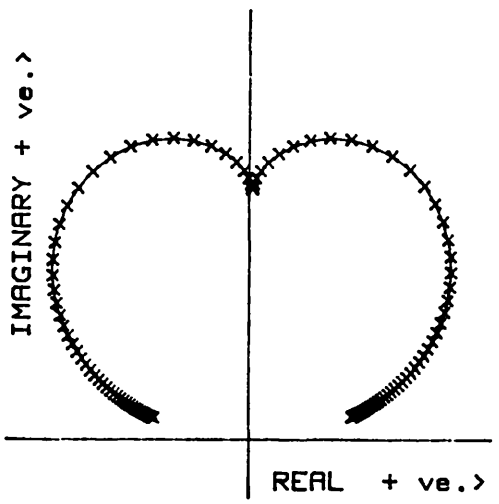

Fig. 3-14 Nyquist plot of Fig. 3-12.

If the frequency spacing between the two modes is decreased, with all the other parameters at the same values, for $\omega_1 = 100$ Hz and $\omega_2 = 100.2$ Hz the graphs presented in Figs. 3-15, 3-16 and 3-17 are obtained.

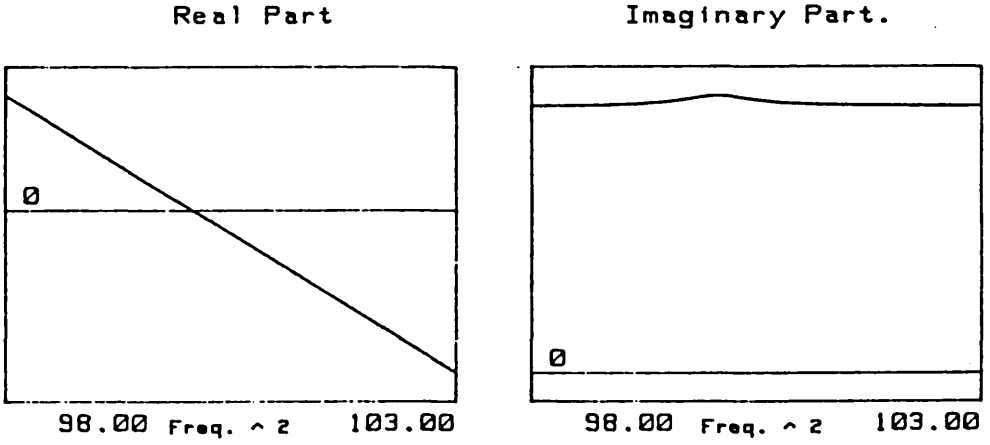

Fig. 3-15 Example of the inverse FRF of 2 very close modes.

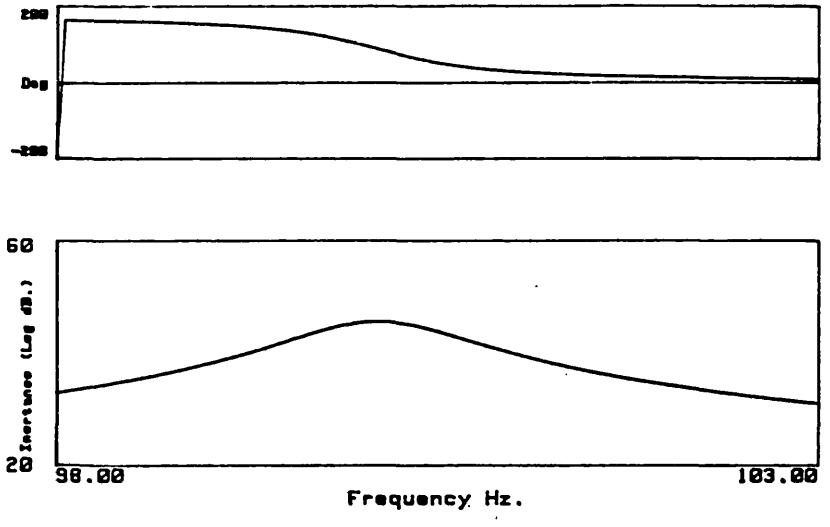

Fig 3-16 Bode plot of Fig. 3-15.

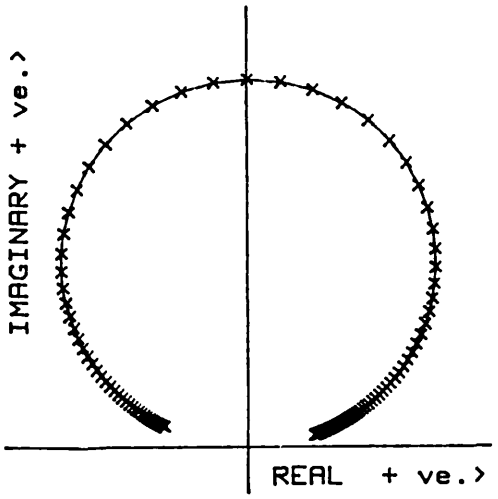

Fig 3-17 Nyquist plot of Fig. 3-15.

From Fig. 3-15, it is still possible to see a "bump" in the imaginary part of the inverse FRF, showing the presence of two modes, but not in the display of the real part. From the Bode and Nyquist graphs (Figs. 3-16 and 3-17) it is not possible to recognize the existence of these two modes. The case now presented, with $\omega_1 =$ **100 Hz** and $\omega_2 =$ **100.2 Hz** was the limiting case. With values of ω_2 below **100.2 Hz**, it was not obvious from the inverse FRF that two modes were present.

Other examples with different values for the modal parameters showed, as predicted, to be easier to interpret. For instance, with $\eta_1 =$ **0.01** and $\eta_2 =$ **0.015**, we obtain the graphs of Fig. 3-18.

If the limiting case of Fig. 3-15 is considered with a level of **3 %** of random noise added to the data, the graphs of Fig. 3-19 are obtained, and it still is possible to observe the "bump" in the display of the imaginary part.

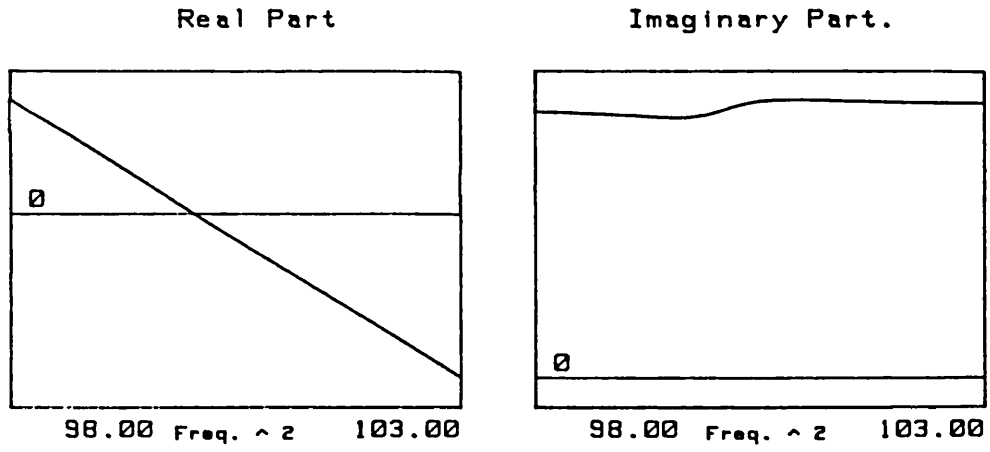

Fig. 3-18 Same case of Fig. 3-15, but with different damping factors.

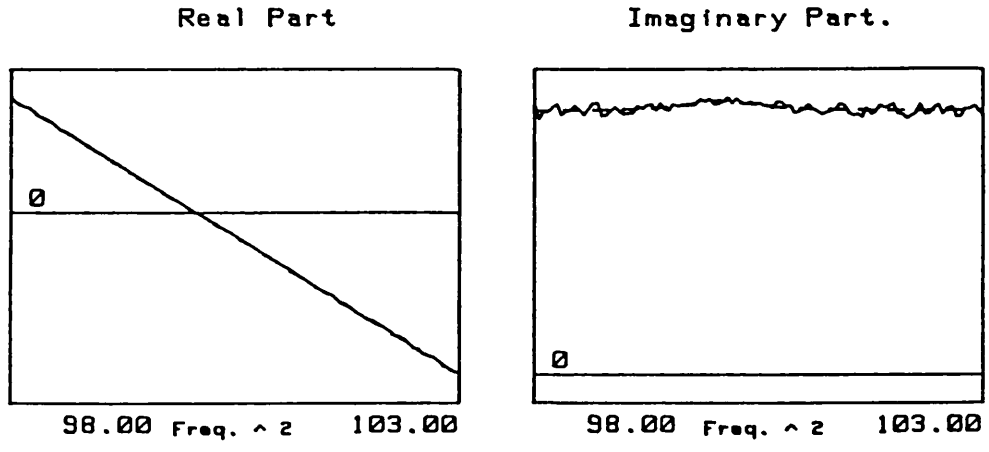

Fig. 3-19 Same case of Fig. 3-15, with 3% added noise.

Discussion

The inverse of receptance method has been generalized in order to accommodate the complex mode case, the most common encountered in practice. This development will be used in Section 3-3-1 for the purpose of identification of the modal parameters.

Simply by using the display of the real and imaginary parts of the inverse

of a FRF, we have managed to obtain a simple but reliable indicator of the existence of two close modes. If these two modes are very close indeed, and all the other modal parameters of similar value, it has been shown that the imaginary part of the display still exhibits a "bump". The limiting value for the frequency ratio was found to be **0.998** (aprox.) with a damping loss factor of **1 %**. In these cases, the usual types of display (Bode and Nyquist) appear to exhibit only one mode.

3-3 Identification in the presence of close modes

Supposing that it has been possible to establish the existence of two close modes, the problem then is how to identify them using a SDOF analysis method. It is known that the identification of a single mode in the presence of another one close to it can lead to serious errors in the estimation of the modal parameters, depending on the degree of "closeness". Usually, the least affected parameter is the natural frequency and then, by increasing order of error level, the damping factor, the modal constant and the phase angle. The question is "how to correct the estimated values?" Because the phase angle is, in general, the most affected parameter, a technique to correct the phase angles has been devised (Refs. [64], [65]), supposing that the other parameters can be considered as acceptable.

If theoretical data for two close modes are generated, assuming real modes so that the phases of the modal constants are equal to zero, it is possible from the identification using the **Circle-fitting** method to obtain satisfactory results for the natural frequencies, damping ratios and magnitude of the modal constants even thought incorrect results will be found for the phase angles (sometimes these are in error by more than 20°), thereby suggesting that the modes are complex when, in fact, they are real. Considerable care is necessary in the interpretation of the results

when there are close modes, as many times the complexity indicated is not genuine.

In general, not just the phase angles but all the modal parameters need to be corrected and a more general technique must be used. The most widely-used procedure is the one known as SIM (Ref. [69]). The idea is very simple: after a first identification of each of the modes individually, the analysis is repeated for each mode, this time subtracting from the original FRF data the contribution of the modes (besides the one under study) that have already been identified. Mathematically, this can be expressed as

$$\tilde{\alpha}_r = \tilde{\alpha} - \sum_{\substack{s=1 \\ s \neq r}}^{N} \alpha_s \qquad (3\text{-}22)$$

where $\tilde{\alpha}$ is the initially measured FRF data, $\tilde{\alpha}_r$ is the resulting FRF of the mode under consideration and α_s is the regenerated FRF contribution of each mode already analysed. This technique is very convenient for two close modes in particular and an iterative procedure can be establish between the two modes until convergence is obtained. This iterative procedure is, in the majority of cases, convergent, although it can be quite slow.

As a repetitive analysis between two modes can be very tedious by making a call to each mode at a time, an automatic SIM option (AUTO-SIM) has been implemented in a modal analysis computer program. This works as follows: after a first analysis of each mode, an indication of the existence of interference between two modes is given, based upon the amplitude criterion described in Section 3-2-1. Then, the option AUTO-SIM appears and after indicating which two modes need refinement, the program automatically iterates between those two modes until convergence is

attained. The criterion to stop this iterative procedure is that the difference in the phases of the modal constants in two consecutive iterations is less than a small quantity (0.1°, say), since, as mentioned before, the phase is the most affected parameter.

3-3-1 Circle-fitting and Inverse methods - which one to use ?

Basically, there are two methods for SDOF identification of a FRF: the **Circle-fitting** method and the **Inverse** method described in Section 3-2-3. A third method (Ref. [73]) will be discussed later. The **Circle-fitting** is, probably, the most applied technique and provided there are enough points and good quality data in the resonance area and not very low damping, it can be used without major problems. Nevertheless, it is quite sensitive with respect to the calculation of the phase of the modal constant, even for widely spaced modes. Concerning this modal parameter, the **Inverse** method may give better results but, sometimes, it does not give such accurate results for the other modal parameters, especially in the case of close modes.

If the SIM technique (progressive isolation of mode to be analysed) is to be used, then both methods show aproximately the same rate of convergence, although the initial estimation of the phase angles can sometimes be more accurate using the **Inverse** method, reducing the number of iterations needed to obtain convergence. However, application of the SIM technique has its own limitations, too. It must not be forgotten that,in order to apply SIM, it is necessary to obtain a first estimate of the modal parameters in order to carry on the iterative process. With the **Circle-fitting** method, this can be difficult to obtain, because in this method the location of the natural frequency is based on the increasing and decreasing of the angular spacing between the points around each natural frequency. If two modes

are very close in terms of natural frequency, not only do the two circles appear to be just one circle, but also the referred property of increasing and decreasing of the angular spacing may be lost, and it may become impossible to perform the **Circle-fitting** around each mode. If this is the case, the **Inverse** method may have advantages in obtaining the first estimate of the modal parameters, since with this method the angular spacing property is not used. But even if we manage to obtain the first estimate for the modal parameters, and if the modes are very close, the modal properties may come with such large errors that it is not possible to obtain a convergence with the SIM technique. The problem of obtaining the first estimate is not so acute if one mode is "stronger" than the other, i.e, if the values of δ and/or γ are different from **1**, because in this case the less affected mode can usually be identified without any problems and then, prior to analysis of the other one, the SIM technique can already be used to obtain a better result. Another peculiarity when the relative "strength" of the modes is similar is that the identified modal constants tend to be the double of their real values, which is easily understood by analysing the FRF of two close modes. In such cases, a good procedure (before starting the SIM iteration) is to consider the modal constants with half the values obtained in the first identification.

Examples

First, we shall demonstrate with a theoretical example how the **Circle-fitting** method can give wrong results for the phase angles, even for widely separated modes. Let us consider the error-free data of Table 3-9:

Mode	ω_r	η_r	C_r	ϕ_r
1	10	0.01	1	0
2	20	0.01	1	0

Table 3-9 Example data.

Using the **Circle-fitting** method, the results are (Table 3-10):

Mode	ω_r	η_r	C_r	ϕ_r
1	9.999	0.00939	0.9392	5.82
2	20.000	0.00999	0.9989	2.26

Table 3-10 Identification using the **Circle-fitting** method.

The results for ϕ_r are clearly in error. For the same case, but using the **Inverse** method, the results are (Table 3-11):

Mode	ω_r	η_r	C_r	ϕ_r
1	10.000	0.01000	0.9969	0.39
2	20.010	0.01000	0.9939	-1.55

Table 3-11 Identification using the **Inverse** method.

The results for the phase angles are better in this case. If we consider ϕ_1 as 30^0 and ϕ_2 as -30^0, the results are as shown in Table 3-12 from which it can be seen that the phase angles are again better with the **Inverse** method. Next, we shall analyse a case with heavily coupled modes (Table 3-13), with identical values for η_r and C_r, so that the mutual interference is similar.

Method	Mode	ω_r	η_r	C_r	ϕ_r
Circle-fitting	1	9.999	0.00970	0.9701	35.82
	2	20.000	0.00999	0.9985	-27.74
Inverse	1	10.000	0.01090	1.0050	30.34
	2	20.010	0.01090	1.0230	-31.06

Table 3-12 Identification using both methods, with phase angles of 30° and -30°.

Mode	ω_r	η_r	C_r	ϕ_r
1	100	0.01	1	0
2	100.4	0.01	1	0

Table 3-13 Example data of close modes.

Looking at the display of the inverse part of the FRF, there is a clear indication of the existence of two modes (Fig. 3-20).

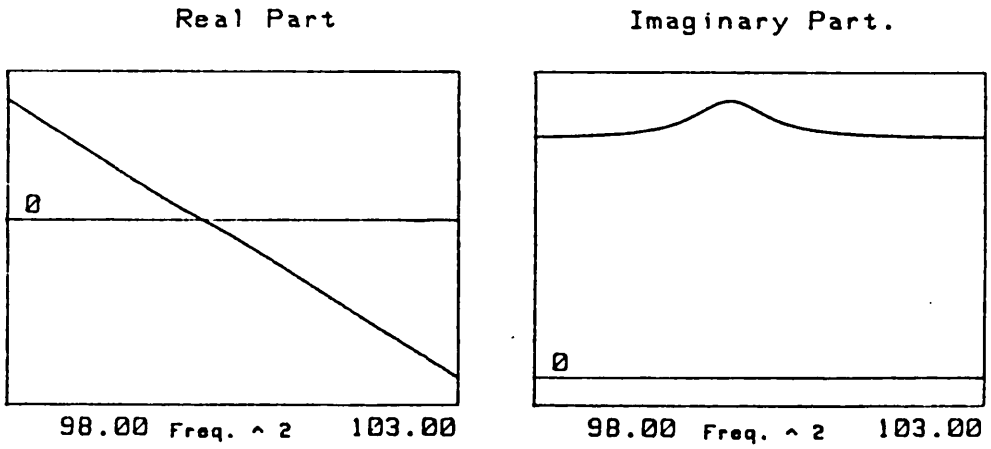

Fig. 3-20 Inverse FRF plots (example of Table 3-13).

Analysing these modes separately using the **Circle-fitting** and **Inverse** methods, we obtain (Table 3-14):

Method	Mode	ω_r	η_r	C_r	ϕ_r
Circle-fitting	1	100.025	0.01389	2.4677	24.66
	2	100.375	0.01423	2.6009	-24.61
Inverse	1	100.130	0.01210	2.0900	5.21
	2	100.280	0.01150	2.0040	-4.57

Table 3-14 Identification using both methods.

Choosing the **Circle-fitting** results as the first ones for the analysis, and taking the AUTO-SIM option, after **28** iterations the following results were obtained (Table 3-15):

No. iter.	Mode	ω_r	η_r	C_r	ϕ_r
28	1	99.998	0.01030	1.0860	5.04
28	2	100.418	0.00980	0.8883	-3.10

Table 3-15 Identification using the **Circle-fitting** method and AUTO-SIM.

Choosing the **Inverse** method results as the input results for the AUTO-SIM option, the results are (Table 3-16):

No. iter.	Mode	ω_r	η_r	C_r	ϕ_r
35	1	99.998	0.01030	1.0850	4.70
34	2	100.415	0.00980	0.8971	-2.50

Table 3-16 Identification using the **Inverse** method and AUTO-SIM.

Taking now $\phi_1 = 30^o$ and $\phi_2 = -30^o$, the first analysis gives (Table 3-17):

Method	Mode	ω_r	η_r	C_r	ϕ_r
Circle-fitting	1	100.145	0.01110	2.0865	8.65
	2	100.235	0.01130	2.1790	-4.87
Inverse	1	100.120	0.00950	1.7350	4.61
	2	100.280	0.00950	1.7390	-4.66

Table 3-17 Identification using both methods (same example, but with 30° and -30° phase angles).

The results are now in considerable error, even for the natural frequencies. Using the AUTO-SIM option with each type of results as a start, we obtain (Table 3-18):

Method	No. iter.	Mode	ω_r	η_r	C_r	ϕ_r
Circle-fitting	29	1	99.998	0.01000	0.9757	30.78
	28	2	100.398	0.01010	1.0270	-29.17
Inverse	divergence	1	–	–	–	–
		2	–	–	–	–

Table 3-18 Results after applying AUTO-SIM.

The results are very good using the initial values from the **Circle-fitting** method, but divergence was encountered when using the results from the **Inverse** method as a start. We shall try now to iterate from the results of Table 3-17, but using half the values for the modal constants as a starting point. The results are shown in Table 3-19.

Method	No. iter.	Mode	ω_r	η_r	C_r	ϕ_r
Circle-fitting	16	1	100.007	0.01040	1.1380	32.42
	16	2	100.425	0.01000	0.9296	-37.78
Inverse	10	1	100.013	0.00990	1.0050	25.42
	9	2	100.398	0.00980	0.9564	-26.14

Table 3-19 Results after applying AUTO-SIM, with 1st estimate for the modal constants as half their value.

Discussion

From the examples presented, it can be concluded that for widely spaced modes the **Inverse** method can have some advantages over the **Circle-fitting** method, namely in the calculation of the phase angles of the modal constants. When the modes are very close, both methods give a similar amount of error level for the modal parameters, although in some cases the phase angles can still be better with the **Inverse** method. The **Inverse** method is a good alternative when it is not possible to obtain an identification with the **Circle-fitting** method and the SIM technique should always be used for very close modes. In order to improve the speed of convergence, or even to avoid divergence, it may be convenient to change the values of the modal constants to half of the values obtained in the first attempt.

3-3-2 The "Bendent" method

Recently, a new SDOF method has been developed (Ref. [73]). Considering that the receptance FRF of a system is given by

$$\alpha(j\omega) = \frac{A_r + jB_r}{\omega_r^2 - \omega^2 + j\eta_r\omega_r^2} + \text{Residual term} \tag{3-23}$$

and that for a particular value $\omega = \Omega$ close to the resonance, Eq. (3-23) is given by

$$\alpha(j\Omega) = \frac{A_r + jB_r}{\omega_r^2 - \Omega^2 + j\eta_r\omega_r^2} + \text{Residual term} \tag{3-24}$$

the residual term, considered constant over the chosen frequency range, can be eliminated by subtracting each side of Eqs. (3-23) and (3-24):

$$\alpha(j\omega) - \alpha(j\Omega) =$$

$$(A_r+jB_r)\left[\frac{\omega^2 - \Omega^2}{(\omega_r^2 - \omega^2)(\omega_r^2 - \Omega^2) - \eta_r^2\omega_r^4 + j\eta_r\omega_r^2(2\omega_r^2 - \omega^2 - \Omega^2)}\right] \tag{3-25}$$

Defining a function Δ as

$$\Delta = \frac{\omega^2 - \Omega^2}{\alpha(j\omega) - \alpha(j\Omega)} =$$

$$\frac{A_r - jB_r}{A_r^2 + B_r^2}\left[(\omega_r^2 - \omega^2)(\omega_r^2 - \Omega^2) - \eta_r^2\omega_r^4 + j\eta_r\omega_r^2(2\omega_r^2 - \omega^2 - \Omega^2)\right] \tag{3-26}$$

it follows that

$$\text{Re}(\Delta) = c_R + t_R\,\omega^2 \tag{3-27 a}$$

$$\text{Im}(\Delta) = c_I + t_I\,\omega^2 \tag{3-27 b}$$

which are linear functions in ω^2, with the slopes given by

$$t_R = -\frac{1}{A_r^2 + B_r^2}\left[A_r(\omega_r^2 - \Omega^2) + B_r\eta_r\omega_r^2\right] \tag{3-28 a}$$

$$t_I = -\frac{1}{A_r^2 + B_r^2}\left[A_r\eta_r\omega_r^2 - B_r(\omega_r^2 - \Omega^2)\right] \tag{3-28 b}$$

and the intercepts given by

$$c_R = \frac{1}{A_r^2 + B_r^2} \left\{ A_r[\omega_r^2(\omega_r^2 - \Omega^2) - \eta_r^2\omega_r^4] + B_r\eta_r\omega_r^2(2\omega_r^2 - \Omega^2) \right\} \quad (3\text{-}29\ a)$$

$$c_I = \frac{1}{A_r^2 + B_r^2} \left\{ A_r\eta_r\omega_r^2(2\omega_r^2 - \Omega^2) - B_r[\omega_r^2(\omega_r^2 - \Omega^2) - \eta_r^2\omega_r^4] \right\} \quad (3\text{-}29\ b)$$

By varying Ω around ω_r, with $\Omega \neq \omega$, we obtain a family of straight lines for **Re**(Δ) and **Im**(Δ). The existence of non-linearities or the influence of neighbouring modes distort these straight lines and so we may have qualitative information about those phenomena. Due to neighbouring modes, we can usually observe curved lines instead of straight lines. This is because the assumption made that the residual term keeps constant over the frequency range around a resonance is no longer true. This effect is less noticeable when a narrow frequency range is considered, and therefore the shape of the lines can also be an useful indicator of frequency one should use for the fitting. Unfortunately, in some practical situations, these lines can appear so distorted that no easy conclusion is available. Returning to equations (3-28), we see that from these expressions it is not easy to derive the modal parameters. However, noting that Eqs. (3-28) and (3-29) represent straight lines in Ω^2, such that

$$t_R = d_R + u_R\Omega^2 \quad (3\text{-}30\ a)$$

$$t_I = d_I + u_I\Omega^2 \quad (3\text{-}30\ b)$$

and

$$c_R = s_R + v_R\Omega^2 \quad (3\text{-}31\ a)$$

$$c_I = s_I + v_I\Omega^2 \quad (3\text{-}31\ b)$$

where

$$d_R = - \frac{(A_r + B_r\eta_r)\omega_r^2}{A_r^2 + B_r^2} \qquad (3\text{-}32\ a)$$

$$d_I = - \frac{(A_r\eta_r - B_r)\omega_r^2}{A_r^2 + B_r^2} \qquad (3\text{-}32\ b)$$

$$u_R = \frac{A_r}{A_r^2 + B_r^2} \qquad (3\text{-}32\ c)$$

$$u_I = - \frac{B_r}{A_r^2 + B_r^2} \qquad (3\text{-}32\ d)$$

and

$$v_R = - \frac{(A_r + B_r\eta_r)\omega_r^2}{A_r^2 + B_r^2} \qquad (3\text{-}33\ a)$$

$$v_I = - \frac{(A_r\eta_r - B_r)\omega_r^2}{A_r^2 + B_r^2} \qquad (3\text{-}33\ b)$$

$$s_R = \frac{[A_r(1 - \eta_r^2) + 2B_r\eta_r]\omega_r^4}{A_r^2 + B_r^2} \qquad (3\text{-}33\ c)$$

$$s_I = \frac{[2A_r\eta_r - B_r(1 - \eta_r^2)]\omega_r^4}{A_r^2 + B_r^2} \qquad (3\text{-}33\ d)$$

The modal parameters can be derived by using either expressions (3-32) or (3-33) (it is curious to note that $v_R = d_R$ and $v_I = d_I$). Fig. 3-21 is a theoretical example of the type of plots we obtain in this method.

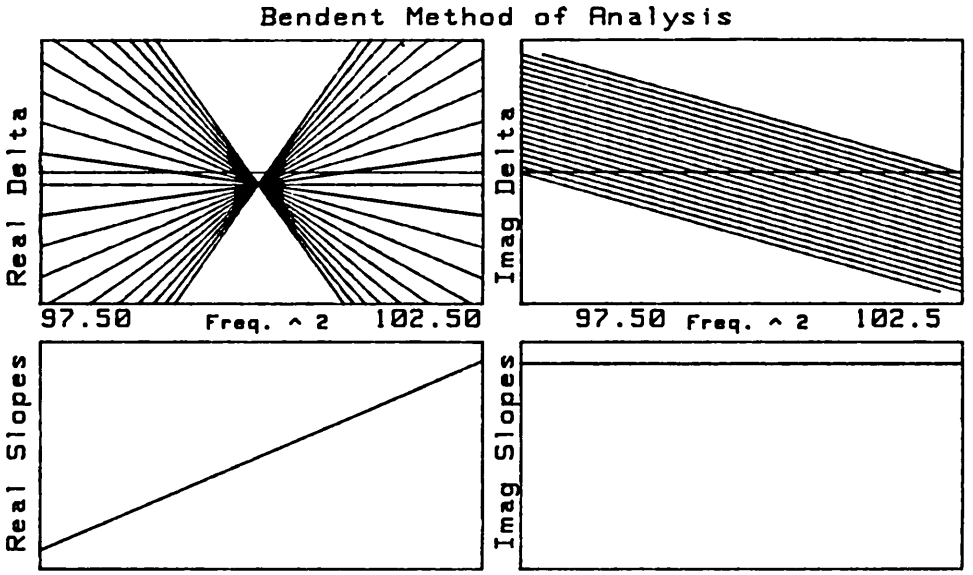

Fig. 3-21 Example of a "Bendent" analysis (theo. data).

The data used correspond to a real mode ($\phi_r = 0^o$). If the mode were complex, the graphs on the right would have a similar shape of the ones on the left.

Let us summarize the procedure: we have the display of **Re**(Δ) and **Im**(Δ) from the measurements (top graphs of Fig. 3-21), which constitute, theoretically, families of straight lines in ω^2, with slopes $\mathbf{t_R}$ and $\mathbf{t_I}$ and intercepts $\mathbf{c_R}$ and $\mathbf{c_I}$. These parameters can, therefore, be computed by fitting **Re**(Δ) and **Im**(Δ) to straight lines. $\mathbf{t_R}$, $\mathbf{t_I}$, $\mathbf{c_R}$ and $\mathbf{c_I}$ are, in theory, themselves straight lines in Ω^2 (Eqs. (3-30) and (3-31)) and by a second straight-line fitting it is possible to calculate the values on the left-hand-sides of Eqs. (3-32) and (3-33) and then, the modal parameters. But Eqs. (3-32) and (3-33) are alternative sets of expressions and so, we shall use just one of them to calculate the modal parameters. Eqs. (3-32) are chosen due to their simplicity, compared with Eqs. (3-33). Therefore,

we shall fit straight lines to $\mathbf{t_R}$ and $\mathbf{t_I}$ (bottom graphs of Fig. 3-21).

On the other hand, by comparing Eqs. (3-32) with Eqs. (3-19), it is seen that these are the same, apart from a minus sign in all of them. This also means that Eqs. (3-28) are the same as the inverse of receptance (Eqs. (3-15) and (3-16)), again apart from a minus sign and so, Eqs. (3-27) can alternatively be written as

$$\mathrm{Re}(\Delta) = c_R - \mathrm{Re}\left(\frac{1}{\alpha_r(j\Omega)}\right)\omega^2 \qquad \text{(3-34 a)}$$

$$\mathrm{Im}(\Delta) = c_I - \mathrm{Im}\left(\frac{1}{\alpha_r(j\Omega)}\right)\omega^2 \qquad \text{(3-34 b)}$$

Therefore, the modal parameters derived from "Bendent" method must be the same as the ones derived from the **Inverse** method (Eqs. (3-20)). In fact, comparing Eqs. (3-20) with Eqs. (17) to (20) of Ref. [73]†, it can be confirmed that they are identical.

However, when we compare the results of "Bendent" and **Inverse** methods, the results are slightly different. This is due to two reasons. The first is because the **Inverse** method does not take into account the effect of other modes (Eq. (3-13)), while the "Bendent" method does. The second reason (referring to Eqs. (3-28)) is because in the **Inverse** method the values of $\mathbf{Re(1/\alpha_r)}$ and $\mathbf{Im(1/\alpha_r)}$ are used directly from the measurement, while in the "Bendent" method, the parameters $\mathbf{t_R}$ and $\mathbf{t_I}$ are already the result of a straight line fitting. This is a consequence of having subtracted the effect of the residual term, which gives the possibility of having, around each frequency point, a set of values for the inverse of the

† Note: in Ref. [73] there is an error in Eq. (18). According to the notation used in that paper, it should be $\eta_r = (q - p)/(1 + pq)$.

receptance in the frequency range considered, from which average values are calculated (t_R and t_I). In the **Inverse** method, we only have one value for the inverse FRF for each frequency point, and so this method tends to be more sensitive to the presence of neighbouring modes and/or the existence of noise in the data. Briefly, the "Bendent" method considers residual effects and passes through an intermediate process of refinement that has, in general, the effect of improving the results. However, with noiseless theoretical data and for **1** single DOF, the "Bendent" method coincides with the **Inverse** method. For widely spaced modes the residual effect is not very large and the results from both methods are very similar. In any case, apart from the sign, the graphs of $\mathbf{t_R}$ and $\mathbf{t_I}$ in "Bendent" method (Fig. 3-21) are very closely related to the display of the inverse FRF (e. g., compare these graphs with Fig. 3-9, for ϕ_r =0°) and it can be said that they are displays of an averaged inverse of the FRF. Adding **2%** of noise to the data of Fig. 3-21, we obtain the plots of Fig. 3-22, where the fitting of $\mathbf{t_I}$ is quite clear. In this case, the value obtained for ϕ_r is **0.3°**, instead of **0°**.

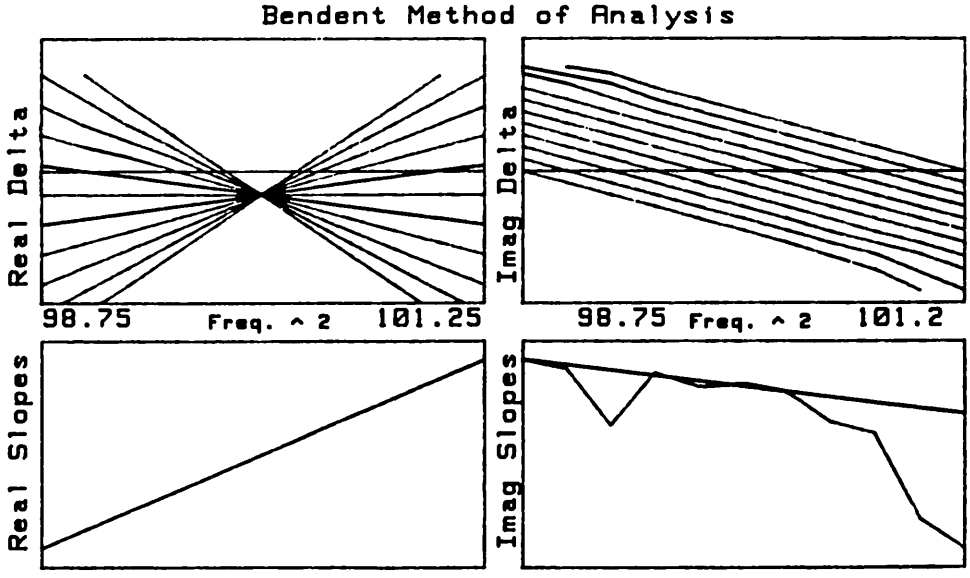

Fig. 3-22 Example of a "Bendent" analysis (theo. data + noise).

Having established this parallel between the **Inverse** and "Bendent" methods, there is now a clearer notion of what, in fact, we are analysing with this latter one, whereas before, the data analysed was somehow "disguised" and the physical interpretation had been lost in the mathematical formulation. Also, some of the disadvantages of the **Inverse** method, when compared with the **Circle-fitting** method, have now disappeared and in the great majority of cases, the "Bendent" method has proven to be the most powerful SDOF technique available at present.

3-4 Conclusions

Considering two fundamentally different alternative methods of SDOF modal analysis, the direct (Circle-fitting) and the inverse (Inverse or "Bendent" methods), it was shown that, within certain limits, it is possible to deal with the problem of close modes using either approach.

In the first place, the discussion about the interference between two modes led us to a better understanding of the parameters that govern this phenomenon and how it is possible to have the indication that a refinement of the identification was necessary.

The possibilities of having information about the existence of two modes were also discussed and it was shown that, in the majority of the cases, the observation of the graphs of the inverse FRF could be a reliable indicator.

Some examples were presented to assess the capabilities of the two basic SDOF methods in the identification of two modes, and it was concluded that for widely spaced modes, the **Inverse** method was more accurate, especially regarding the phase angles, and that for very close modes the level of errors was, in general, similar with both methods. For the most current applications, the **Inverse** method usually provides better results

for the phase angles, but less accurate results for the other modal parameters.

It was also shown that the recent "Bendent" method is a refined version of the **Inverse** method and coincides with this for the **1** DOF case with theoretically-generated data, without noise. In practical applications, the "Bendent" method gives better results than the **Inverse** method and is generally better than the **Circle-fitting** method.

CHAPTER 4

AN INVESTIGATION OF SOME *SISO* MDOF METHODS

4-1 Introduction

In this chapter, two indirect *SISO* MDOF frequency domain modal analysis methods will be investigated: the Rational Fraction Polynomial method (RFP) and a new approach for the identification of lightly damped structures. As the overall objective of this thesis is the extraction of valid modal properties from measured data, both methods will be developed keeping in mind the concern of introducing criteria and means of analysis which can allow for an identification that is able to provide indications about the quality of the results; consequently, the user will be sure that the identification obtained is the best possible one and, based upon the quality indicators, he is confident in his acceptance or rejection of the analysis.

As mentioned in Section 2-3-2, the **RFP** method was first presented in 1982 (Ref. [81]) and is, probably, the most popular and widely used MDOF frequency domain method nowadays, employed by many commercial

packages of modal analysis software. In spite of its popularity, it is believed that its theoretical background is not widely known. Concerning this method, the objectives of the present investigation are:

(i) to provide a detailed and clear explanation of the theory of the **RFP** method, so that the reader can easily make a direct use of it;

(ii) to write a computer program and implement it on a micro-computer;

(iii) to explore the capabilities of the method in the identification of close modes, a common problem which occurs, for instance, in structures that possess a degree of symmetry, like discs and cylinders;

(iv) associated with the problem of identifying a pair of close modes, there is the need for an algorithm to "recognize" whether such a pair does exist, or whether it is only one mode that for some reason (e. g., noise) appears to be a double mode. This follows the philosophy of Chapter 3, where indicators of the existence of close modes were sought, based on SDOF methods. Here, with the **RFP** method, an automatic, "intelligent" procedure for such an indication is pursued;

(v) Once the program has "decided" on the existence of one or two modes, the results for the modal parameters will be accompanied by quality indicators.

The other method that will be treated in this chapter is a new approach for the identification of lightly damped structures. It is derived from, and a particular case of, the **RFP** method. The original philosophy of the analysis of lightly damped structures is that of the **Ewins-Gleeson** method - Ref. [77] - (see Section 2-3-2) and it will be shown that the new approach now developed is an extension of that method, where the major novelty lies on the fact that the results are obtained with the minimum of intervention and experience of the user: the method is automatic and can be made "intelligent", in that it makes judgements and takes decisions.

Concerning this method, the main objectives are:

(i) to provide an exposition of the theory,which is shown to be a combination of the **Ewins-Gleeson** and **RFP** methods;

(ii) to justify more rigorously some empirical conclusions and suggestions concerning the performance of the method given in Refs. [77] and [118];

(iii) to develop an efficient computer program with the capability of "judging" which results are the best ones and their quality, the philosophy being similar to the one of the **RFP** method, i. e., based upon the repetition of the calculations;

(iv) to evaluate the method, based on theoretically generated data and also on experimental data, comparing the results with those obtained with the previous approach.

4-2 The Rational Fraction Polynomial method (RFP)

In previous work (Refs. [119], [120]) the **RFP** method has been applied using a computer program specially written to identify two close modes of vibration, including the effect of residuals outside the frequency range of interest, as this is often necessary in practical applications. The **RFP** method involves expression of the frequency response function as the ratio of two polynomials (the numerator polynomial being related to the modal constants and phase angles while the roots of the denominator polynomial - the poles - are related to the natural frequencies and damping factors) and on the minimization of an error function in order to obtain the modal parameters. This minimization leads to a system of equations that are often ill-conditioned. To overcome this problem, the polynomials are suitably replaced by orthogonal ones, with very good results in accuracy and

execution speed.

For the particular case of four modes (two modes plus two residual ones), no ill-conditioning problems were found but for the general case with a higher number of modes, or for the extension to a global analysis (as it will be discussed in Chapter 5), such problems exist and so in the theoretical development of the method the orthogonal polynomial methodology will be employed.

It was found here that this method produced very good results, even for very close complex modes. The "intelligent" procedure developed to determine whether there are two genuine modes or only one, is based on the repetition of the calculation several times, each one taking a different sub-set of the complete set of measured data points. The reason for this procedure is that - in theory - genuine modes tend to appear unchanged from every run of the program, whereas the so-called "computational" modes vary from run to run, as they are not characteristic of the system and do not have a physical meaning. Analysing the repeatability of the results (within a tolerance boundary) from the several runs, it is possible to determine the true answers. Since several runs are considered, the final answers will be average values and quality indicators may be given, based on the standard deviation of the results from the various runs. More details about the computer program will be given in Section 4-2-2.

Besides the theoretical background and the description of the algorithm, discussions and examples based on theoretical as well as experimental data are presented to illustrate the application of this method to the special case we are particularly interested in: analysis of double modes.

4-2-1 Theory

As is well known from modal analysis theory (e. g., Ref. [1]), the FRF, in

terms of receptance, for a linear system with **N** DOF and viscous damping can be given by the **partial fraction form:**

$$\alpha(j\omega) = \sum_{r=1}^{N} \frac{A_r + j\omega B_r}{\omega_r^2 - \omega^2 + j2\omega\omega_r\xi_r} \tag{4-1}$$

where $\mathbf{A_r}$ and $\mathbf{B_r}$ are constants. It is also easy to show that expression (4-1) can be written as a ratio of two polynomials in $(j\omega)$, so that

$$\alpha(j\omega) = \frac{\sum_{k=0}^{2N-1} a_k(j\omega)^k}{\sum_{k=0}^{2N} b_k(j\omega)^k} \tag{4-2}$$

in which format, the FRF is said to be in a **rational fraction form.** Defining an error function between the analytical FRF $(\alpha(j\omega))$ and the experimental values $(\tilde{\alpha}(j\omega))$ at each frequency ω_i, we have

$$e_i = \frac{\sum_{k=0}^{2N-1} a_k(j\omega_i)^k}{\sum_{k=0}^{2N} b_k(j\omega_i)^k} - \tilde{\alpha}(j\omega_i) \tag{4-3}$$

If we work with a modified error fuction $\mathbf{e_i'}$, given by

$$e_i' = e_i \sum_{k=0}^{2N} b_k(j\omega_i)^k \tag{4-4}$$

and make $\mathbf{b_{2N} = 1}$, we obtain

$$e_i' = \sum_{k=0}^{2N-1} a_k(j\omega_i)^k - \tilde{\alpha}(j\omega_i)\left[\sum_{k=0}^{2N-1} b_k(j\omega_i)^k + (j\omega_i)^{2N}\right] \tag{4-5}$$

This formulation will lead to a linear system of equations, avoiding the necessity of initial estimates for the modal parameters, as happens in the **GSH** method (see Section 2-3-2). Defining an error vector including all the measured frequencies:

$$\{E\} = \begin{Bmatrix} e_1' \\ e_2' \\ \cdot \\ \cdot \\ \cdot \\ e_L' \end{Bmatrix} \tag{4-6}$$

where **L** is the number of measured frequencies, equation (4-5) will become, in full,

$$\begin{aligned} \{E\} = & \begin{bmatrix} 1 & (j\omega_1) & (j\omega_1)^2 & \dots & (j\omega_1)^{2N-1} \\ 1 & (j\omega_2) & (j\omega_2)^2 & \dots & (j\omega_2)^{2N-1} \\ \cdot & \cdot & \cdot & & \cdot \\ \cdot & \cdot & \cdot & & \cdot \\ \cdot & \cdot & \cdot & & \cdot \\ 1 & (j\omega_L) & (j\omega_L)^2 & \dots & (j\omega_L)^{2N-1} \end{bmatrix} \begin{Bmatrix} a_0 \\ a_1 \\ \cdot \\ \cdot \\ \cdot \\ a_{2N-1} \end{Bmatrix} - \\ & \begin{bmatrix} \tilde{\alpha}(j\omega_1) & \tilde{\alpha}(j\omega_1)(j\omega_1) & \dots & \tilde{\alpha}(j\omega_1)(j\omega_1)^{2N-1} \\ \tilde{\alpha}(j\omega_2) & \tilde{\alpha}(j\omega_2)(j\omega_2) & \dots & \tilde{\alpha}(j\omega_2)(j\omega_2)^{2N-1} \\ \cdot & \cdot & & \cdot \\ \cdot & \cdot & & \cdot \\ \cdot & \cdot & & \cdot \\ \tilde{\alpha}(j\omega_L) & \tilde{\alpha}(j\omega_L)(j\omega_L) & \dots & \tilde{\alpha}(j\omega_L)(j\omega_L)^{2N-1} \end{bmatrix} \begin{Bmatrix} b_0 \\ b_1 \\ \cdot \\ \cdot \\ \cdot \\ b_{2N-1} \end{Bmatrix} - \\ & \begin{Bmatrix} \tilde{\alpha}(j\omega_1)(j\omega_1)^{2N} \\ \tilde{\alpha}(j\omega_2)(j\omega_2)^{2N} \\ \cdot \\ \cdot \\ \cdot \\ \tilde{\alpha}(j\omega_L)(j\omega_L)^{2N} \end{Bmatrix} \end{aligned} \tag{4-7}$$

or, in matrix form:

$$\underset{(Lx1)}{\{E\}} = \underset{(Lx2N)}{[P]} \underset{(2Nx1)}{\{a\}} - \underset{(Lx2N)}{[T]} \underset{(2Nx1)}{\{b\}} - \underset{(Lx1)}{\{W\}} \tag{4-8}$$

To calculate the polynomial coefficients **{a}** and **{b}** a least-squares procedure will be used, minimizing a squared error function **J**, defined as

$$J = \{E^*\}^T \{E\} \tag{4-9}$$

where * denotes complex conjugate. Substituting (4-8) in (4-9), and after some manipulations (see Appendix A), we obtain

$$\begin{aligned} J = {} & \{a\}^T \mathrm{Re}([P^*]^T [P])\, \{a\} + \{b\}^T \mathrm{Re}([T^*]^T [T])\, \{b\} + \\ & \{W^*\}^T \{W\} - 2\{a\}^T \mathrm{Re}\,([P^*]^T [T])\, \{b\} - \\ & 2\{a\}^T \mathrm{Re}([P^*]^T \{W\}) + 2\{b\}^T \mathrm{Re}([T^*]^T \{W\}) \end{aligned} \tag{4-10}$$

To minimize **J**, we shall take its derivatives with respect to **{a}** and **{b}** and set these equal to zero:

$$\begin{aligned} \frac{\partial J}{\partial \{a\}} = {} & \frac{\partial}{\partial \{a\}} \left[\{a\}^T \mathrm{Re}([P^*]^T [P])\, \{a\}\right] - \\ & 2\, \frac{\partial}{\partial \{a\}} \left[\{a\}^T \mathrm{Re}([P^*]^T [T])\, \{b\}\right] - \\ & 2\, \frac{\partial}{\partial \{a\}} \left[\{a\}^T \mathrm{Re}([P^*]^T \{W\})\right] = \{0\} \end{aligned}$$

$$\begin{aligned} \frac{\partial J}{\partial \{b\}} = {} & \frac{\partial}{\partial \{b\}} \left[\{b\}^T \mathrm{Re}([T^*]^T [T])\, \{b\}\right] - \\ & 2\, \frac{\partial}{\partial \{b\}} \left[\{a\}^T \mathrm{Re}([P^*]^T [T])\, \{b\}\right] + \\ & 2\, \frac{\partial}{\partial \{b\}} \left[\{b\}^T \mathrm{Re}([T^*]^T \{W\})\right] = \{0\} \end{aligned} \tag{4-11}$$

Solving these equations, we obtain:

$$\begin{aligned} &\mathrm{Re}([P^*]^T[P])\,\{a\} - \mathrm{Re}([P^*]^T[T])\,\{b\} - \mathrm{Re}([P^*]^T\{W\}) = \{0\} \\ &\mathrm{Re}([T^*]^T[T])\,\{b\} - \mathrm{Re}([T^*]^T[P])\,\{a\} + \mathrm{Re}([T^*]^T\{W\}) = \{0\} \end{aligned} \tag{4-12}$$

or, in matrix form:

$$\begin{bmatrix} [Y] & [X] \\ [X]^T & [Z] \end{bmatrix} \begin{Bmatrix} \{a\} \\ \{b\} \end{Bmatrix} = \begin{Bmatrix} \{G\} \\ \{F\} \end{Bmatrix} \tag{4-13}$$

where

$$\begin{aligned} [Y] &= \mathrm{Re}([P^*]^T[P]) \\ [X] &= -\mathrm{Re}([P^*]^T[T]) \\ [Z] &= \mathrm{Re}([T^*]^T[T]) \\ \{G\} &= \mathrm{Re}([P^*]^T\{W\}) \\ \{F\} &= -\mathrm{Re}([T^*]^T\{W\}) \end{aligned} \tag{4-14}$$

Eqs. (4-13) are the normal equations of the least-squares problem. It was found (Ref. [81]) that numerical problems (ill-conditioning) associated with the resolution of (4-13) could be overcome if matrices **[Y]** and **[Z]** were each an identity matrix. This means that instead of **[Y]** = **Re([P*]^T[P])** and **[Z]** = **Re([T*]^T[T])**, they will have to be the product of two orthonormal matrices. So, instead of **[P]** being given by

$$[P] = \begin{bmatrix} 1 & (j\omega_1) & (j\omega_1)^2 & \dots & (j\omega_1)^{2N-1} \\ 1 & (j\omega_2) & (j\omega_2)^2 & \dots & (j\omega_2)^{2N-1} \\ \cdot & \cdot & \cdot & & \cdot \\ \cdot & \cdot & \cdot & & \cdot \\ \cdot & \cdot & \cdot & & \cdot \\ 1 & (j\omega_L) & (j\omega_L)^2 & \dots & (j\omega_L)^{2N-1} \end{bmatrix} \tag{4-15}$$

it will be replaced by

$$[P] = \begin{bmatrix} \varphi_{1,0} & \varphi_{1,1} & \cdots \varphi_{1,2N-1} \\ \varphi_{2,0} & \varphi_{2,1} & \cdots \varphi_{2,2N-1} \\ \vdots & \vdots & \vdots \\ \varphi_{L,0} & \varphi_{L,1} & \cdots \varphi_{L,2N-1} \end{bmatrix} = [\vartheta] \tag{4-16}$$

where $\varphi_{i,j}$ means a polynomial of order **j** evaluated at frequency ω_i. Likewise, **[T]** will now be given by

$$[T] = \begin{bmatrix} \tilde{\alpha}(j\omega_1)\theta_{1,0} & \tilde{\alpha}(j\omega_1)\theta_{1,1} & \cdots & \tilde{\alpha}(j\omega_1)\theta_{1,2N-1} \\ \tilde{\alpha}(j\omega_2)\theta_{2,0} & \tilde{\alpha}(j\omega_2)\theta_{2,1} & \cdots & \tilde{\alpha}(j\omega_2)\theta_{2,2N-1} \\ \vdots & \vdots & & \vdots \\ \tilde{\alpha}(j\omega_L)\theta_{L,0} & \tilde{\alpha}(j\omega_L)\theta_{L,1} & \cdots & \tilde{\alpha}(j\omega_L)\theta_{L,2N-1} \end{bmatrix} \tag{4-17}$$

or

$$[T] = \begin{bmatrix} \tilde{\alpha}(j\omega_1) & & & 0 \\ & \tilde{\alpha}(j\omega_2) & & \\ & & \ddots & \\ 0 & & & \tilde{\alpha}(j\omega_L) \end{bmatrix} \begin{bmatrix} \theta_{1,0} & \theta_{1,1} & \cdots & \theta_{1,2N-1} \\ \theta_{2,0} & \theta_{2,1} & \cdots & \theta_{2,2N-1} \\ \vdots & \vdots & & \vdots \\ \theta_{L,0} & \theta_{L,1} & \cdots & \theta_{L,2N-1} \end{bmatrix}$$

$$= [\tilde{\alpha}][\Theta] \tag{4-18}$$

and

$$\{W\} = \begin{Bmatrix} \tilde{\alpha}(j\omega_1)\theta_{1,2N} \\ \tilde{\alpha}(j\omega_2)\theta_{2,2N} \\ \vdots \\ \tilde{\alpha}(j\omega_L)\theta_{L,2N} \end{Bmatrix} \tag{4-19}$$

So, it is necessary to find the complex functions φ and θ such that $\mathbf{Re}([\mathbf{P}^*]^T[\mathbf{P}])$ and $\mathbf{Re}([\mathbf{T}^*]^T[\mathbf{T}])$ are unit matrices. This is possible if φ

and θ are complex orthonormal polynomials (see Appendix B). The FRF will then be written in terms of these polynomials, with coefficients $\mathbf{c}_k$ and $\mathbf{d}_k$ as the unknowns, instead of $\mathbf{a}_k$ and $\mathbf{b}_k$:

$$\alpha(j\omega) = \frac{\sum_{k=0}^{2N-1} c_k \varphi_k}{\sum_{k=0}^{2N} d_k \theta_k} \tag{4-20}$$

After finding {**c**} and {**d**} (populated by coefficients c_k and d_k respectively), {**a**} and {**b**} can be recovered to calculate the modal parameters.

Calculation of orthogonal polynomials φ and θ

From what we have just seen, it will be necessary to have

$$\begin{aligned} &\mathrm{Re}([\vartheta^*]^T[\vartheta]) = [I] \\ &\mathrm{Re}([\Theta^*]^T[\tilde{\alpha}^*][\tilde{\alpha}][\Theta]) = [I] \end{aligned} \tag{4-21}$$

According to Appendix B, this means that polynomials φ will be calculated using a unit weighting function and θ will be calculated using a weighting function given by $|\tilde{\alpha}|^2$. Going back to Eq. (4-2) and developing it for a 2 DOF case (for example), it follows that

$$\alpha(j\omega) = \frac{a_0 + a_1(j\omega) + a_2(j\omega)^2 + a_3(j\omega)^3}{b_0 + b_1(j\omega) + b_2(j\omega)^2 + b_3(j\omega)^3 + b_4(j\omega)^4} \tag{4-22}$$

For this case we see that each polynomial can be regarded as a linear combination of real and imaginary orthogonal polynomials, the real ones

being even functions and the imaginary ones being odd functions, as follows (for θ the procedure is similar):

Real (even)	Imaginary (odd)
$\varphi_0 = a'_0$	$\varphi_1 = a'_1(j\omega)$
$\varphi_2 = a'_2 + a'_3(j\omega)^2$	$\varphi_3 = a'_4(j\omega) + a'_5(j\omega)^3$
$\varphi_4 = a'_6 + a'_7(j\omega)^2 + a'_8(j\omega)^4$	$\varphi_5 = a'_9(j\omega) + a'_{10}(j\omega)^3 + a'_{11}(j\omega)^5$
.	.
.	.
.	.

(4-23)

So, the numerator of (4-22) will be:

$$\begin{aligned} & a_0 + a_1(j\omega) + a_2(j\omega)^2 + a_3(j\omega)^3 \\ = \; & a'_0 + a'_1(j\omega) + a'_2 + a'_3(j\omega)^2 + a'_4(j\omega) + a'_5(j\omega)^3 \\ = \; & a'_0 + a'_2 + (a'_1 + a'_4)(j\omega) + a'_3(j\omega)^2 + a'_5(j\omega)^3 \end{aligned} \qquad (4\text{-}24)$$

This definition for the polynomials is not unique, but defining them as even and odd functions, besides being directly related to the Hermitian nature of an FRF, simplifies the calculations, as it will be shown later.

Once we are talking about even and odd functions, and if one wants somehow to take advantage of them, it is necessary to consider both positive and negative frequencies. If there are **L** points to be fitted, the orthogonal property will be:

$$\mathrm{Re}\left(\sum_{i=-L}^{L} \varphi^*_{i,k}\, \varphi_{i,j}\right) = \begin{cases} 0 & k \neq j \\ 1 & k = j \end{cases} \qquad (4\text{-}25)$$

If φ is written as $\mathbf{Re}(\varphi) + \mathbf{jIm}(\varphi)$, it follows that

$$\mathrm{Re}\left(\sum_{i=-L}^{L}\left[\mathrm{Re}(\varphi_{i,k}) - j\mathrm{Im}(\varphi_{i,k})\right]\left[\mathrm{Re}(\varphi_{i,j}) + j\mathrm{Im}(\varphi_{i,j})\right]\right) = \begin{cases} 0 & k\neq j \\ 1 & k=j \end{cases} \quad (4\text{-}26)$$

or

$$\sum_{i=-L}^{L}\left[\mathrm{Re}(\varphi_{i,k})\,\mathrm{Re}(\varphi_{i,j}) + \mathrm{Im}(\varphi_{i,k})\mathrm{Im}(\varphi_{i,j})\right] = \begin{cases} 0 & k\neq j \\ 1 & k=j \end{cases} \quad (4\text{-}27)$$

In fact, the FRF is only defined for positive frequencies and so Eq. (4-27) must be transformed so that only the positive functions for points **1** to **L** are considered. Extracting the half-functions, negative and positive, from (4-27) we obtain:

$$\sum_{i=-L}^{-1}\left[\mathrm{Re}(\varphi^{-}_{i,k})\,\mathrm{Re}(\varphi^{-}_{i,j}) + \mathrm{Im}(\varphi^{-}_{i,k})\mathrm{Im}(\varphi^{-}_{i,j})\right] +$$

$$\sum_{i=1}^{L}\left[\mathrm{Re}(\varphi^{+}_{i,k})\,\mathrm{Re}(\varphi^{+}_{i,j}) + \mathrm{Im}(\varphi^{+}_{i,k})\mathrm{Im}(\varphi^{+}_{i,j})\right] = \begin{cases} 0 & k\neq j \\ 1 & k=j \end{cases} \quad (4\text{-}28)$$

According to the definition of even and odd functions,

$$\mathrm{Re}(\varphi^{-}) = \mathrm{Re}(\varphi^{+})$$

$$\mathrm{Im}(\varphi^{-}) = -\,\mathrm{Im}(\varphi^{+})$$

Substituting in (4-28),

$$2\sum_{i=1}^{L}\left[\mathrm{Re}(\varphi^{+}_{i,k})\,\mathrm{Re}(\varphi^{+}_{i,j}) + \mathrm{Im}(\varphi^{+}_{i,k})\mathrm{Im}(\varphi^{+}_{i,j})\right] = \begin{cases} 0 & k\neq j \\ 1 & k=j \end{cases} \quad (4\text{-}29)$$

or

$$\mathrm{Re}\left(\sum_{i=1}^{L}(\varphi^{+}_{i,k})^{*}\,(\varphi^{+}_{i,j})\right) = \begin{cases} 0 & k\neq j \\ 0.5 & k=j \end{cases} \quad (4\text{-}30)$$

For polynomials θ^{+} (corresponding to polynomials θ_k in Eq. (4-20)) everything is similar but, as seen before, there will be a weighting function equal to $|\tilde{\alpha}(j\omega_i)|^2$. Hence,

$$\mathrm{Re}\left(\sum_{i=1}^{L} (\theta_{i,k}^{+})^{*}\,(\theta_{i,j}^{+})\,|\tilde{\alpha}(j\omega_i)|^2\right) = \begin{cases} 0 & k\neq j \\ 0.5 & k=j \end{cases} \tag{4-31}$$

The problem now is to generate φ^+ and θ^+ automatically so that they satisfy Eqs. (4-30) and (4-31). Out of many possible types of orthogonal polynomials (Ref. [121]), the Forsythe ones were chosen due to their computational advantages. The elementary theory of orthogonal polynomials is well known and can be found in many books (e.g., Ref. [122]). For Forsythe polynomials specifically, Refs. [123], [124] and [125] are suggested. The Forsythe recursion formulæ given in Refs. [124] and [125] can be used very conveniently as they are easy to programme. Firstly, the formulæ for the general case (not only for positive half-functions) will be presented, using a common notation of γ for either φ or θ. Let $\mathbf{q_i}$ be the weighting function and $\mathbf{m}$ the degree of the polynomial. The recursion formulæ are given by:

$$\begin{aligned}
\gamma_0(\omega) &= 1 \\
\gamma_1(\omega) &= (\omega - u_1)\gamma_0(\omega) \\
\gamma_2(\omega) &= (\omega - u_2)\gamma_1(\omega) - v_1\gamma_0(\omega) \\
&\;\;\vdots \qquad\qquad \vdots \\
\gamma_k(\omega) &= (\omega - u_k)\gamma_{k-1}(\omega) - v_{k-1}\gamma_{k-2}(\omega) \\
&\;\;\vdots \qquad\qquad \vdots \\
\gamma_m(\omega) &= (\omega - u_m)\gamma_{m-1}(\omega) - v_{m-1}\gamma_{m-2}(\omega)
\end{aligned} \tag{4-32}$$

where

$$u_k = \frac{\sum_{i=1}^{L} \omega_i[\gamma_{k-1}(\omega_i)]^2\, q_i}{D_{k-1}} \tag{4-33 a}$$

$$v_k = \frac{\sum_{i=1}^{L} \omega_i \gamma_k(\omega_i)\, \gamma_{k-1}(\omega_i)\, q_i}{D_{k-1}} \qquad (4\text{-}33\ b)$$

$$D_k = \sum_{i=1}^{L} \gamma_k(\omega_i)^2\, q_i \qquad (4\text{-}33\ c)$$

If, in Eqs. (4-33), the summation is extended from **-L** to **+L**, it is easily recognized that $\mathbf{u_k}$ is an odd function and $\mathbf{v_k}$ an even function of ω and so $\mathbf{u_k}$ will be zero and the summation in $\mathbf{v_k}$ and $\mathbf{D_k}$ will be $2\sum_{i=1}^{L}$ instead of $\sum_{i=-L}^{L}$. Then, Eqs. (4-32) become:

$$\begin{aligned}
\gamma_0^+(\omega) &= 1 \\
\gamma_1^+(\omega) &= \omega\, \gamma_0^+(\omega) \\
\gamma_2^+(\omega) &= \omega\, \gamma_1^+(\omega) - v_1^+ \gamma_0^+(\omega) \\
&\vdots \qquad\qquad \vdots \\
\gamma_k^+(\omega) &= \omega\, \gamma_{k-1}^+(\omega) - v_{k-1}^+ \gamma_{k-2}^+(\omega) \\
&\vdots \qquad\qquad \vdots \\
\gamma_m^+(\omega) &= \omega\, \gamma_{m-1}^+(\omega) - v_{m-1}^+ \gamma_{m-2}^+(\omega)
\end{aligned} \qquad (4\text{-}34)$$

with

$$v_k^+ = \frac{2\sum_{i=1}^{L} \omega_i \gamma_k^+(\omega_i)\, \gamma_{k-1}^+(\omega_i)\, q_i}{D_{k-1}^+} \qquad (4\text{-}35\ a)$$

$$D_k^+ = 2\sum_{i=1}^{L} \gamma_k^+(\omega_i)^2\, q_i \qquad (4\text{-}35\ b)$$

This represents a major simplification (given in Ref. [81]) and it is the

reason why the half-functions, defined for positive and negative frequencies, have been considered. After calculating all the polynomials γ_k^+, they must be normalized by dividing by $\sqrt{D_k^+}$, and to obtain the complex polynomials,they must be multiplied by j^k ($j = \sqrt{-1}$). To multiply in the end the resulting polynomials γ_k^+ by j^k produces the same result as calculating them for $j\omega$, instead of ω, in Eqs. (4-34) and (4-35). To avoid further numerical problems, the frequency range of interest is scaled by dividing all the frequencies by their maximum value in the considered interval, so that the maximum frequency value is **1**.

Applying Eq.(4-34), polynomials $\varphi^+(\omega_i)$ and $\theta^+(\omega_i)$ can be calculated by making $q_i=1$ or $q_i = |\tilde{\alpha}(j\omega_i)|^2$, respectively. Knowing $\varphi^+(\omega_i)$ and $\theta^+(\omega_i)$ it is possible to calculate the new **[P]** and **[T]** matrices, given by Eqs. (4-16) and (4-18), where φ and θ must be understood as φ^+ and θ^+. Now, Eqs. (4-13) will look like

$$\begin{bmatrix} \lceil 0.5 \rfloor & [X] \\ [X]^T & \lceil 0.5 \rfloor \end{bmatrix} \begin{Bmatrix} \{c\} \\ \{d\} \end{Bmatrix} = \begin{Bmatrix} \{G\} \\ \{0\} \end{Bmatrix} \tag{4-36}$$

with **[X]** and **{G}** defined as before in Eq. (4-14), but with **[P]** and **[T]** now in terms of φ^+ and θ^+. From (4-31) it is obvious that the earlier vector **{F}** = - **Re**($[T^*]^T\{W\}$) is now a zero vector. Multiplying both sides of (4-36) by **2**, we obtain

$$\begin{bmatrix} [I] & [X'] \\ [X']^T & [I] \end{bmatrix} \begin{Bmatrix} \{c\} \\ \{d\} \end{Bmatrix} = \begin{Bmatrix} \{G'\} \\ \{0\} \end{Bmatrix} \tag{4-37}$$

where

$$\begin{aligned} [X'] &= 2\,[X] \\ \{G'\} &= 2\,\{G\} \end{aligned} \tag{4-38}$$

Solving (4-37), it leads to

$$\{d\} = -([I] - [X']^T [X'])^{-1} [X']^T \{G'\} \quad (4\text{-}39\ a)$$

$$\{c\} = \{G'\} - [X']\{d\} \quad (4\text{-}39\ b)$$

Calculation of the modal parameters

We may now return to Eq. (4-20) (where φ and θ must be replaced by φ^+ and θ^+), with the FRF expressed in terms of the coefficients **{c}** and **{d}** and orthogonal polynomials φ^+ and θ^+. In order to calculate the modal parameters, Eq. (4-20) must be rewritten in terms of coefficients **{a}** and **{b}** (Eq. (4-2)). If the coefficients of polynomials φ^+ and θ^+ have been stored , it is possible to find linear transformation relationships between **{a}** and **{c}** and between **{b}** and **{d}** in the following form:

$$\underset{(2Nx1)}{\{a\}} = \underset{(2Nx2N)}{[T_{ac}]}\ \underset{(2Nx1)}{\{c\}} \quad (4\text{-}40\ a)$$

$$\underset{(2Nx1)}{\{b\}} = \underset{(2Nx2N)}{[T_{bd}]}\ \underset{(2Nx1)}{\{d\}} + \underset{(2Nx1)}{\{R\}} \quad (4\text{-}40\ b)$$

As will be seen later, this formulation shows some advantages. Knowing **{b}**, these values can be introduced into a complex polynomial solver routine to calculate the roots† (e. g., Ref. [126]), which are directly related to the resonant frequencies and damping ratios. With these results, the other modal parameters can be calculated. To understand better this procedure an example of a system with **2** DOF will be presented. For a system with viscous damping, the roots of the denominator of (4-2) (poles of the transfer function) appear in complex conjugate pairs as also

---

† This polynomial solver replaces the methods used before in Ref. [119].

do the corresponding constants in the numerator.Considering the Laplace domain (or s-domain), the root pairs are given by

$$s_{k,k^*} = -\xi_r\omega_r \pm j\omega_r\sqrt{(1-\xi_r^2)} = \sigma \pm j\,\omega_r' \tag{4-41}$$

and can be represented in the well-known s-plane (ω_r' is the damped natural frequency). As the FRF is the transfer function evaluated along the $j\omega$ axis, Eq. (4-2) can be written (for a 2 DOF system) as:

$$\alpha(s)\Big|_{s=j\omega} = \left.\frac{\sum_{i=0}^{3} a_i s^i}{\sum_{i=0}^{4} b_i s^i}\right|_{s=j\omega} = \left.\frac{a_0 + a_1 s + a_2 s^2 + a_3 s^3}{(s-s_1)(s-s_1^*)(s-s_2)(s-s_2^*)}\right|_{s=j\omega} \tag{4-42}$$

or

$$\alpha(s)\Big|_{s=j\omega} = \left.\left(\frac{A_1'}{s-s_1} + \frac{A_1'^*}{s-s_1^*} + \frac{A_2'}{s-s_2} + \frac{A_2'^*}{s-s_2^*}\right)\right|_{s=j\omega} \tag{4-43}$$

It must be emphasized that, in Eq. (4-42), the real coefficients a_0, a_1, a_2 are known, as well as the complex roots s_1, s_1^*, s_2, s_2^*. The complex constants A' must now be calculated. They are called the residues and can be evaluated using the method of partial fractions (see Appendix C). In practical terms, each coefficient A_k' is calculated by removing the factor $(s - s_k)$ from the denominator of (4-42) and evaluating this equation at $s = s_k$. For instance,

$$A_1' = \left.\frac{a_0 + a_1 s + a_2 s^2 + a_3 s^3}{(s-s_1^*)(s-s_2)(s-s_2^*)}\right|_{s=s_1} \tag{4-44}$$

or

$$A_1' = \frac{a_0 + a_1 s_1 + a_2 s_1^2 + a_3 s_1^3}{(s_1 - s_1^*)(s_1 - s_2)(s_1 - s_2^*)} \tag{4-45}$$

The same procedure is applied for all coefficients. Although in theory the roots of the denominator of (4-42) always appear as complex conjugate pairs, in practice real roots may also be obtained from an experimental FRF, corresponding either to overdamped or to computational modes. From the computer program point of view, it is generally preferable to calculate all residues **A'** from all the roots and then choose the ones that are complex conjugates, instead of deciding in the first place which roots were in pairs. Knowing the root pairs, it is easy to calculate each set of four modal parameters. From (4-41),

$$\begin{aligned} \mathrm{Re}(s_k) &= -\xi_r \omega_r \\ \mathrm{Im}(s_k) &= \omega_r \sqrt{(1 - \xi_r^2)} \end{aligned} \tag{4-46}$$

Thus,

$$\begin{aligned} \omega_r &= \sqrt{(\mathrm{Re}^2(s_k) + \mathrm{Im}^2(s_k))} \\ \xi_r &= -\mathrm{Re}(s_k) / \omega_r \end{aligned} \tag{4-47}$$

For a root s_k and from (4-1),

$$\alpha(s)\Big|_{s=j\omega} = \frac{A_r + sB_r}{s^2 + s2\omega_r\xi_r + \omega_r^2}\Bigg|_{s=j\omega} = \left(\frac{A_k'}{s - s_k} + \frac{A_k'^*}{s - s_k^*}\right)\Bigg|_{s=j\omega}$$

$$= \frac{-2[\mathrm{Re}(A_k')\,\mathrm{Re}(s_k) + \mathrm{Im}(A_k')\,\mathrm{Im}(s_k)] + s\,2\,\mathrm{Re}(A_k')}{(s - s_k)(s - s_k^*)}\Bigg|_{s=j\omega} \tag{4-48}$$

from which,

$$A_r = -2\,[\mathrm{Re}(A_k')\,\mathrm{Re}(s_k) + \mathrm{Im}(A_k')\,\mathrm{Im}(s_k)]$$
$$B_r = 2\,\mathrm{Re}(A_k') \tag{4-49}$$

From Eq. (4-1), the modal constant will be given by

$$C_r = \sqrt{A_r^2 + \omega_r^2 B_r^2} \tag{4-50}$$

and its phase by

$$\phi_r = \mathrm{tg}^{-1}\frac{\omega_r B_r}{A_r} \tag{4-51}$$

4-2-2 Computer program description

The complete flow-chart of a program to execute the above procedure is presented in Fig. 4-1 with all the options that it contains. It is appropriate to comment on a few aspects: the numerical values given are in accordance with the numerous examples tried, both theoretical and experimental. For instance, the tolerance allowed for the natural frequency when deciding on the number of modes is **0.2%**, which means that the program is able to recognize two modes with a maximum frequency resolution of **0.996**. In the experimental case presented in Section 4-2-3, the solutions have a ratio of approximately **0.995**.

A computer program was written for a **4** DOF case, being able to generate theoretical FRF data polluted with random errors or to call previously measured experimental data. In a first stage, the roots of the denominator - the poles - are calculated, using a polynomial solver routine. From these results, the natural frequency and damping ratio of each mode are obtained directly and secondly, the modal constants and phase angles are calculated.

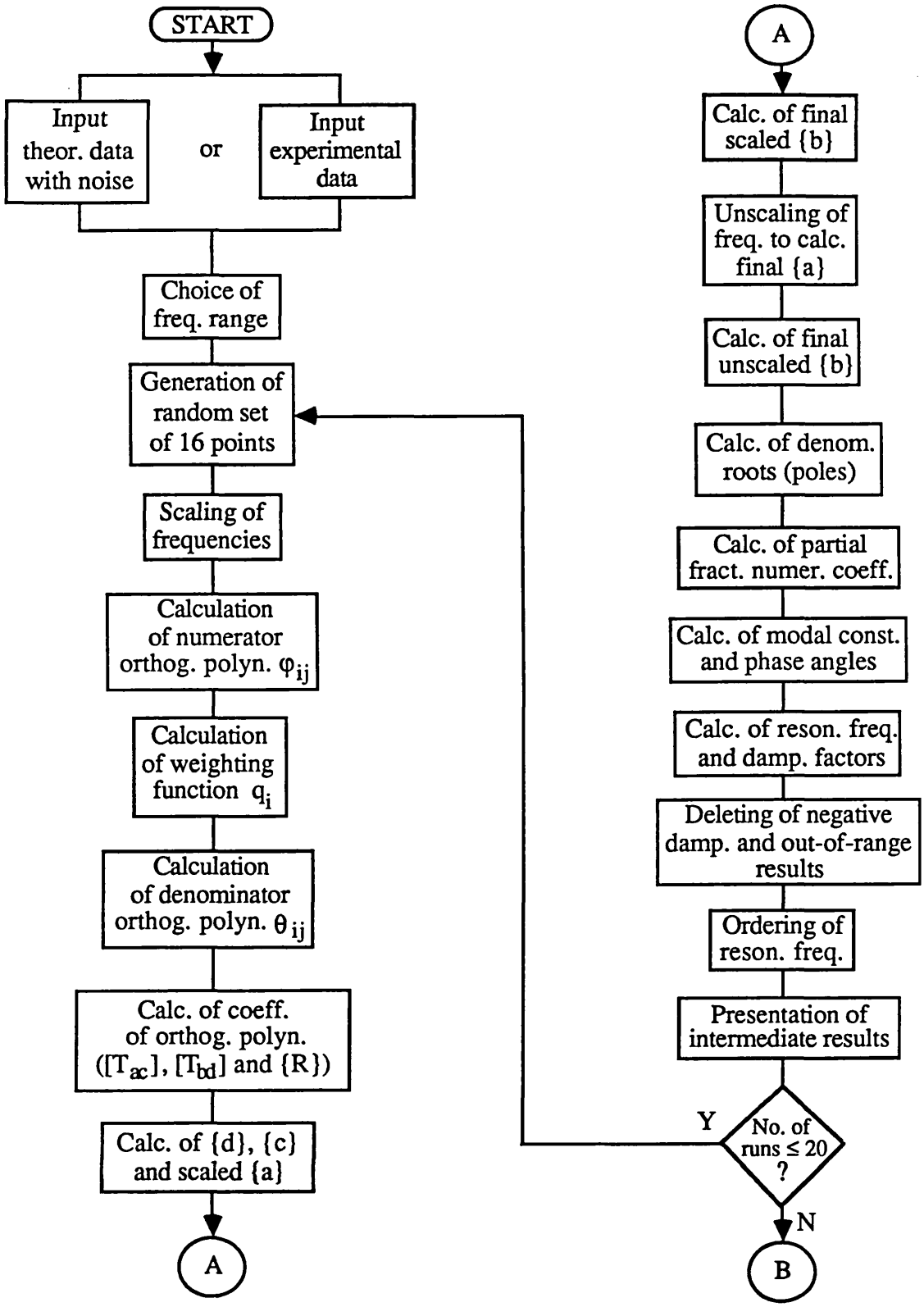

Fig. 4-1 Flow-chart of the computer program.

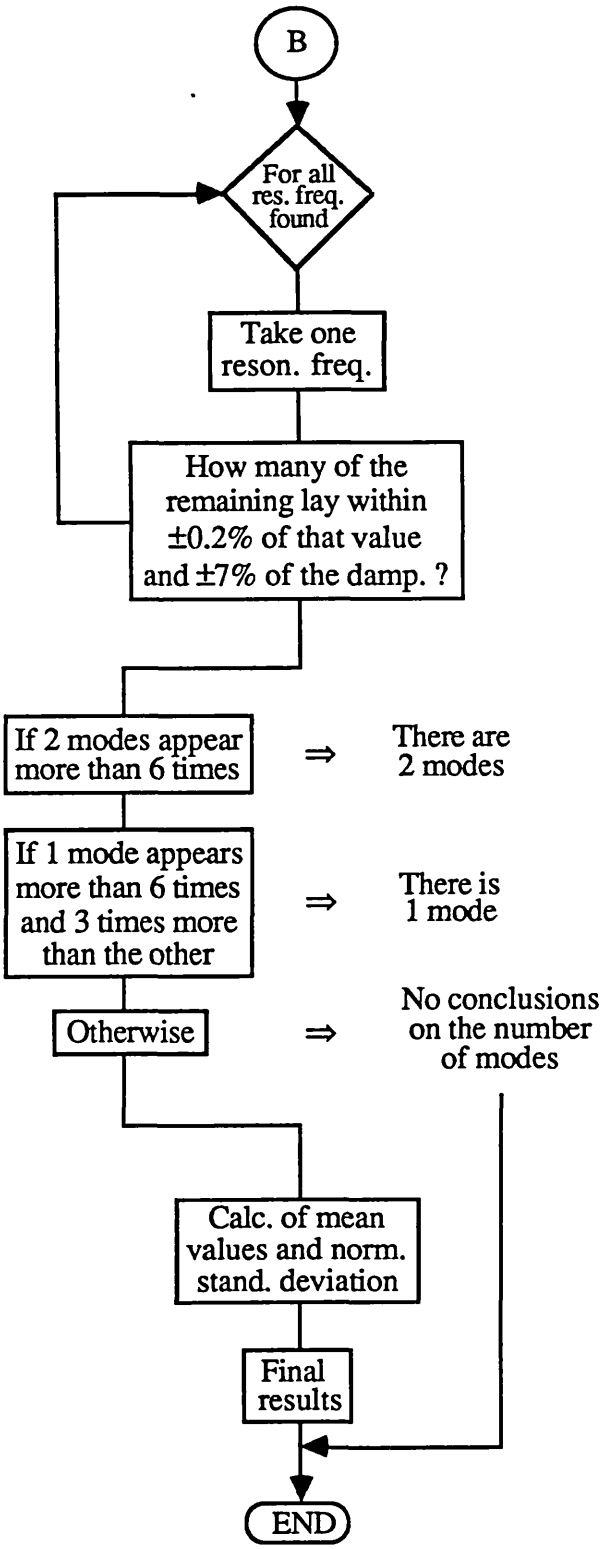

Fig. 4-1 (cont.) Flow-chart of the computer program.

When using the program with experimental data, some problems were encountered, the most important due to the fact that the use of 4 DOF leads to computational modes. As it is our aim to develop criteria which provide the answer "there is just one mode" or "there are two modes", we somehow have to identify which modes are computational ones and which are the true ones. One way of avoiding this question is to specify only two modes to the polynomial in the denominator, and then to add more terms to the numerator to take account of the residuals (Ref. [85]). However, it is found that this procedure gives rise to larger errors in the results. So, two procedures were followed: first, those results that come from the real roots are deleted, as also are those that have a negative damping or do not lie inside the specified frequency range. Secondly, the program runs several times, each time taking a different set of 16 points (the reason for this number will be explained in Section 4-2-3). The results from the various runs are examined to identify any root(s) which are found in every case: or, more precisely, to identify which roots appear repeatedly within a narrow tolerance. In addition, a maximum tolerance is given to the damping value. A decision as to whether there is one mode or two is based on examination of how many times each eigenvalue (natural frequency and damping factor) appears in the complete set of analyses. For example if, after twenty runs, one mode appears 12 times and the other one 14 times, the programme will indicate that there are two modes, as their relative incidence is similar. If, however, one mode occurs 12 times and the other once or twice, then there will almost certainly be only one true mode. After this, the program averages the results found and gives the final mean values and their normalized standard deviations.

Another problem is the choice of the 16 points with which to make the analysis, particularly if we want to go through 20 runs and in the specified range there are, for instance, a total of 40 points. A systematic change in

each set of **16** points used may then be impossible, unless the differences between sets is very small. Also, a set of points that do not embrace the two resonant frequencies will not, in general, give good results. In other words, a systematic change of the points will show poor results if concentrated at the begining and end of the frequency range. To overcome these drawbacks, the program can pick the points randomly (within the range) in each run.

4-2-3 Numerical examples

Theoretical case - evaluation of the method

No added noise

We shall begin with the data presented in Table 4-1. No noise is added to the generated FRF, in order to give an idea of the errors obtained due only to the numerical calculations.

Mode	ω_r(Hz)	ξ_r	C_r	ϕ_r
1	90	0.005	1	0
2	100	0.005	1	0
3	101	0.005	1	0
4	110	0.005	1	0

Table 4-1 Data for theo. case (0% noise).

Choosing a frequency range between **97 Hz** and **104 Hz**, the results for modes **2** and **3**, are (Table 4-2):

Mode	ω_r	ξ_r	C_r	ϕ_r
2	100.000 (0.001)	5.000×10^{-3} (0.001)	1.000 (0.001)	0.00
3	101.000 (0.001)	5.000×10^{-3} (0.001)	1.000 (0.001)	0.00

Table 4-2 Identification of modes **2** and **3**.

where the values in brackets represent the normalized standard deviation. As can be seen, the errors are negligible, but as we keep decreasing the difference between the central two natural frequencies, the errors will increase and the limiting case with admissible errors was found for ω_2 = **100 Hz** and ω_3 = **100.016 Hz**. The results of this case are:

Mode	ω_r	ξ_r	C_r	ϕ_r
2	100.000 (0.001)	5.001×10^{-3} (0.051)	9.970×10^{-1} (1.649)	0.64
3	100.016 (0.001)	5.001×10^{-3} (0.051)	1.003 (1.665)	-0.44

Table 4-3 Identification of modes **2** and **3** using the data of Table 4-1, but with ω_3 = **100.016 Hz**.

Influence of the damping factors

It is also instructive to analyse the effect of increasing the ratio between the damping factors . The data are shown in Table 4-4 and the results in Table 4-5.

Mode	ω_r(Hz)	ξ_r	C_r	ϕ_r
1	90	0.005	1	0
2	100	0.005	1	0
3	100.016	0.010	1	0
4	110	0.005	1	0

Table 4-4 Theo. data to analyse the influence of the damping factors.

Mode	ω_r	ξ_r	C_r	ϕ_r
2	100.000 (0.001)	5.001×10^{-3} (0.001)	1.000 (0.001)	0.00
3	100.016 (0.001)	1.000×10^{-2} (0.001)	1.000 (0.001)	-0.00

Table 4-5 Identification of modes **2** and **3**, using the data of Table 4-4.

Comparison between Tables 4-3 and 4-5 shows that better results are obtained in the case where different damping factors are used.

Influence of the phase angles

Let us consider $\phi_3 = \mathbf{180^o}$ (Table 4-6):

Mode	ω_r(Hz)	ξ_r	C_r	ϕ_r
1	90	0.005	1	0
2	100	0.005	1	0
3	100.016	0.005	1	180
4	110	0.005	1	0

Table 4-6 Theo. data to analyse the influence of the phase angles.

The results are presented in Table 4-7.

Mode	ω_r	ξ_r	C_r	ϕ_r
2	100.000 (0.001)	5.000×10^{-3} (0.001)	1.000 (0.001)	-0.00
3	100.016 (0.001)	5.000×10^{-3} (0.001)	1.000 (0.001)	180.00

Table 4-7 Identification of modes **2** and **3**, using the data of Table 4-6.

Comparison between Tables 4-3 and 4-7 shows that a better identification is obtained when different phase angles are used.

Added noise

As one is always faced with the presence of noise in the FRF data in practice, we shall investigate the maximum possible natural frequency resolution when **1%**, **2%** and **3%** random noise is added. For the reference values of ξ_r, C_r and ϕ_r, those of Table 4-1 will be taken. The values of the natural frequencies for which the program is still capable of producing good results are presented in Table 4-8.

Noise(%)	ω_2(Hz)	ω_3(Hz)
1	100	101
2	100	101.2
3	100	101.25

Table 4-8 Max. nat. freq. resolution with different levels of added noise (freq. range = 97 Hz to 104 Hz).

Influence of the frequency range

So far, the frequency range **97 Hz** to **104 Hz** has been considered in our analysis. However, the method is found to be sensitive to the frequency range chosen. We shall now look for the maximum natural frequency resolution as before, but taking the frequency range from **92 Hz** to **108 Hz** (with the same frequency spacing between the FRF points). The results are presented in Table 4-9.

Noise(%)	ω_2(Hz)	ω_3(Hz)
1	100	100.55
2	100	100.75
3	100	100.80

Table 4-9 Max. nat. freq. resolution with different levels of added noise (freq. range = 92 Hz to 108 Hz).

Comparison between Tables 4-8 and 4-9 shows that choosing a wider frequency range resulted in a better natural frequency resolution, i. e., the program was able to analyse correctly two closer modes.

Influence of the number of points L

From Eq.(4-20), the minimum number of points to be taken is equal to **2N+1**. As we are dealing with four modes, **L** would have to be at least **9**. Due to noise, better results were found when using **16** points and in fact this has been the number used in all the examples so far. It was also found, empirically, that there is no advantage in increasing this number beyond **16**, as the results do not improve significantly. Therefore, the fixed number of **16** points is used.

Discussion

For the theoretical noiseless case it was found that the **RFP** method works extremely well, managing to identify two very close modes. When these two modes have different values of damping and/or phase angles, the results turn out to be even better.

In the presence of noise, as in a practical situation, some difficulties are encountered, as the performance of the method shows dependence on the frequency range chosen around the two close modes. It was found empirically that considering a wider frequency range which still encompasses only the two modes under study usually gives better results than just a narrow band around those modes. This is certainly due to the fact that a wider frequency range includes points that can provide more information about the out-of-range modes, whereas a narrow range

reflects that effect to a lesser extent.

The capability of recognising two close modes decreases with an increase of the level of noise. Finally, although the influence of the number of points considered in the analysis is not easy to understand from a theoretical point of view, it was found empirically that increasing this value is not, in general, a valuable option to pursue.

Experimental case

For the experimental example, results were taken from tests made on an impeller, which is a symmetric structure and therefore bound to have repeated modes - or, in practice, very close ones. The FRF presented in Fig. 4-2 relates to the high frequency range from **3200 Hz** to **6400 Hz.**

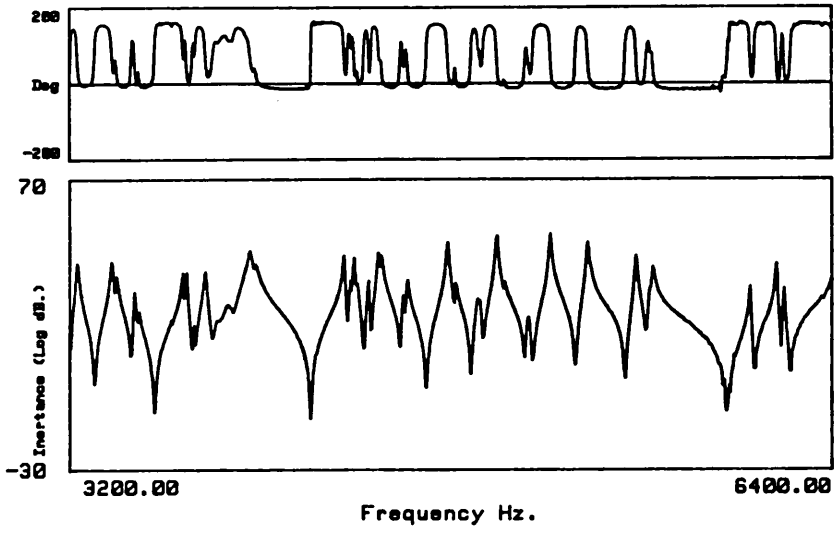

Fig. 4-2 Bode plot of an FRF taken from a real structure (impeller).

The graph of Fig. 4-2 is expanded around the second visible peak, showing in Fig. 4-3 a total of **30** points:

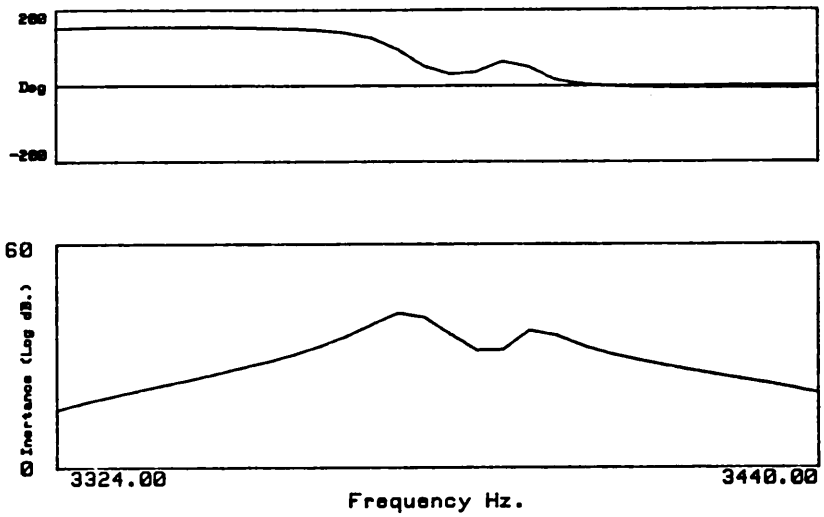

Fig. 4-3 Expanded Bode plot around the second double peak of Fig. 4-2.

Applying the program, the results are as follows (Table 4-10):

Mode	ω_r	ξ_r	C_r	ϕ_r
1	3377.223 (0.006)	$1.368\text{x}10^{-3}$ (2.113)	$3.286\text{x}10^{-1}$ (3.108)	-12.22
2	3396.003 (0.011)	$1.061\text{x}10^{-3}$ (2.244)	$1.155\text{x}10^{-1}$ (3.550)	-14.80

Table 4-10 Identification of the modes of Fig. 4-3.

where the values in brackets again represent the normalized standard deviations of the results obtained in the several runs of the program. The original and regenerated curves are shown in Fig. 4-4.

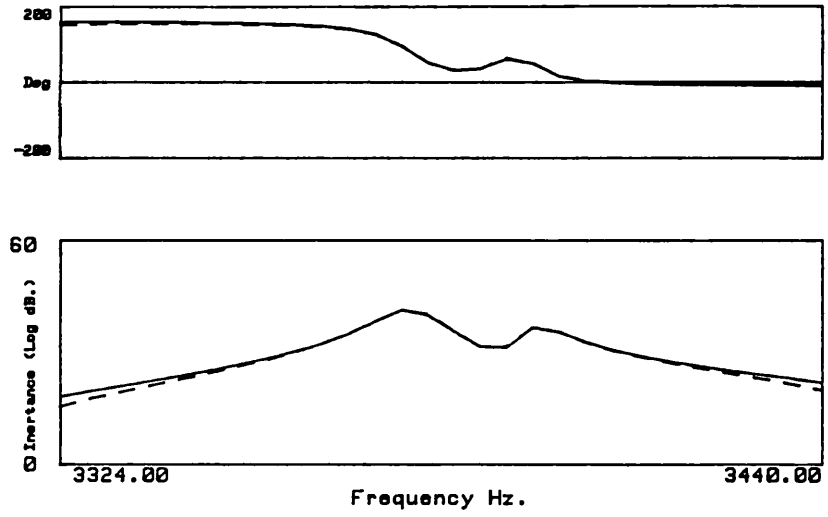

Fig. 4-4 Original (dotted line) and regenerated (solid line) FRFs.

Fig. 4-4 and Table 4-10 show that the identification obtained is a good one, not only because the regenerated FRF matches very well the original one around the two modes under study, but also because the normalized standard deviations are relatively small (for example, a value less than 5% can be considered as very good for the modal constants).

4-3 A new approach for the identification of lightly damped structures

As seen in Chapter 2, there are many methods used in modal analysis, and some of these involve highly sophisticated algorithms. There are, however, a number of applications that do not need a very complicated analysis, and for which relatively simple methods are suitable and can give quite accurate results. In this category are included the cases of structures or components which possess light damping characteristics and whose modes of vibration tend not to be very complex, i. e. whose phase angles are very

close to **0°** or **180°**. For these cases, mathematical models that assume *a priori* that the structure is "effectively undamped" and that the modes are real may be used, introducing the damping characteristics afterwards. Also, as a lightly damped stucture exhibits the resonant peaks quite clearly, the values of the natural frequencies can be established very confidently. Therefore, the main effort of the algorithm will be focussed on the calculation of the modal constants.

To address such cases, a special curve-fitting algorithm was developed some years ago for multi-degree-of-freedom modal analysis: the **Ewins-Gleeson** method presented in Section 2-3-2 (Ref. [77]). In the present work, a different approach is used for the derivation of the final expressions, and a new computer program has been written to try and avoid some drawbacks that existed in the previous method, the new one being more general, "intelligent" and automatic. Here, the FRF to be analysed is curve-fitted using a least-squares criterion to minimize a defined error function between the experimental and theoretical values, the latter being expressed in a rational fraction form rather than the more familiar, partial fraction, version. The procedure is similar to the one followed for the **RFP** method and, once more, orthogonal polynomials will be used to avoid ill-conditioning of the matrices involved. A comparison with the **Ewins-Gleeson** method is made in order to demonstrate the advantages of the new formulation and to illustrate the feasibility of incorporating an element of "intelligence" in order to achieve valid results.

4-3-1 Theory

As seen in Section 4-2-1, the receptance FRF for a linear system with **N** DOF and viscous damping, is given by the partial fraction form:

$$\alpha(j\omega) = \sum_{r=1}^{N} \frac{A_r + j\omega B_r}{\omega_r^2 - \omega^2 + j2\omega\omega_r\xi_r} \tag{4-1}$$

or by its rational fraction form:

$$\alpha(j\omega) = \frac{\sum_{k=0}^{2N-1} a_k(j\omega)^k}{\sum_{k=0}^{2N} b_k(j\omega)^k} \tag{4-2}$$

In this study we shall be concerned with lightly damped structures for which the damping factor will, in effect, be neglected in the mathematical model. This is a valid assumption because when the damping is small, it affects mostly data points which are very close to the natural frequencies, and which are not considered in the analysis. The natural frequencies will be defined in a preliminary phase since the peaks of the FRF are supposed to be well visible. In such a category of structures, e. g. beams and other structural components, it is also legitimate to assume the modes of vibration to be real (phase angles of 0° or 180°), as any non-proportionally distributed damping would be concentrated mainly at the joints. Consequently, expression (4-1) is discarded of its complexity and expressed simply as

$$\alpha(\omega) = \sum_{r=1}^{N} \frac{C_r}{\omega_r^2 - \omega^2} \tag{4-52}$$

where ω_r is known (by inspection) and C_r (modal constant, coinciding now with A_r) is the only unknown per mode. In rational fraction form, Eq. (4-52) becomes:

$$\alpha(\omega) = \frac{\sum_{k=0}^{N-1} a_k\,\omega^{2k}}{\prod_{r=1}^{N} (\omega_r^2 - \omega^2)} \tag{4-53}$$

where the denominator is known and therefore need not be expressed in a polynomial form.

Defining an error function between the real analytical FRF ($\alpha(\omega)$) and the real part of the experimental values ($Re(\tilde{\alpha}(j\omega))$) at each frequency Ω_i, we obtain:

$$e_i = \frac{\sum_{k=0}^{N-1} a_k \Omega_i^{2k}}{\prod_{r=1}^{N} (\omega_r^2 - \Omega_i^2)} - Re(\tilde{\alpha}(j\Omega_i)) \qquad (4\text{-}54)$$

Considering all the measured frequencies, an error vector is obtained:

$$\{E\} = \begin{Bmatrix} e_1 \\ e_2 \\ \cdot \\ \cdot \\ \cdot \\ e_L \end{Bmatrix} \qquad (4\text{-}55)$$

where **L** is the number of measured frequencies. Substituting (4-54) into (4-55), we obtain:

$$\{E\} = \begin{bmatrix} \frac{1}{\prod_{r=1}^{N} (\omega_r^2 - \Omega_1^2)} & \frac{\Omega_1^2}{\prod_{r=1}^{N} (\omega_r^2 - \Omega_1^2)} & \cdots & \frac{\Omega_1^{2N-2}}{\prod_{r=1}^{N} (\omega_r^2 - \Omega_1^2)} \\ \cdot & \cdot & & \cdot \\ \cdot & \cdot & & \cdot \\ \cdot & \cdot & & \cdot \\ \frac{1}{\prod_{r=1}^{N} (\omega_r^2 - \Omega_L^2)} & \frac{\Omega_L^2}{\prod_{r=1}^{N} (\omega_r^2 - \Omega_L^2)} & \cdots & \frac{\Omega_L^{2N-2}}{\prod_{r=1}^{N} (\omega_r^2 - \Omega_L^2)} \end{bmatrix} \begin{Bmatrix} a_0 \\ a_1 \\ \cdot \\ \cdot \\ \cdot \\ a_{N-1} \end{Bmatrix} - \begin{Bmatrix} Re(\tilde{\alpha}(j\Omega_1)) \\ Re(\tilde{\alpha}(j\Omega_2)) \\ \cdot \\ \cdot \\ \cdot \\ Re(\tilde{\alpha}(j\Omega_L)) \end{Bmatrix} \qquad (4\text{-}56)$$

or

$$\{E\} = \begin{bmatrix} \dfrac{1}{\prod_{r=1}^{N}(\omega_r^2 - \Omega_1^2)} & & 0 \\ & \ddots & \\ 0 & & \dfrac{1}{\prod_{r=1}^{N}(\omega_r^2 - \Omega_L^2)} \end{bmatrix} \begin{bmatrix} 1 & \Omega_1^2 & \cdots & \Omega_1^{2N-2} \\ 1 & \Omega_2^2 & \cdots & \Omega_2^{2N-2} \\ \vdots & \vdots & & \vdots \\ 1 & \Omega_L^2 & \cdots & \Omega_L^{2N-2} \end{bmatrix} \begin{Bmatrix} a_0 \\ a_1 \\ \vdots \\ a_{N-1} \end{Bmatrix} - \begin{Bmatrix} \mathrm{Re}(\tilde{\alpha}(j\Omega_1)) \\ \mathrm{Re}(\tilde{\alpha}(j\Omega_2)) \\ \vdots \\ \mathrm{Re}(\tilde{\alpha}(j\Omega_L)) \end{Bmatrix} \tag{4-57}$$

In matrix form, Eq. (4-57) can be written as

$$\underset{(Lx1)}{\{E\}} = \underset{(LxL)}{[\,1/g\,]}\ \underset{(LxN)}{[\Omega]}\ \underset{(Nx1)}{\{a\}} - \underset{(Lx1)}{\mathrm{Re}\{\tilde{\alpha}\}} \tag{4-58}$$

The least-squares method implies the definition of a squared error, **J**, given by

$$J = \{E\}^T \{E\} \tag{4-59}$$

Substituting (4-58) in (4-59), it follows that

$$J = \{a\}^T [\Omega]^T [\,1/g\,] [\,1/g\,] [\Omega] \{a\} - \mathrm{Re}\{\tilde{\alpha}\}^T [\,1/g\,] [\Omega] \{a\} -$$

$$\{a\}^T [\Omega]^T [\,1/g\,] \mathrm{Re}\{\tilde{\alpha}\} + \mathrm{Re}\{\tilde{\alpha}\}^T \mathrm{Re}\{\tilde{\alpha}\} \tag{4-60}$$

To minimize **J**, its derivative with respect to **{a}** is taken and set to zero:

$$\frac{\partial J}{\partial \{a\}} = 2\,[\Omega]^T [\,1/g\,] [\,1/g\,] [\Omega] \{a\} - 2\,[\Omega]^T [\,1/g\,] \mathrm{Re}\{\tilde{\alpha}\} = \{0\} \tag{4-61}$$

hence,

$$\{a\} = \left[[\Omega]^T [\,1/g\,] [\,1/g\,] [\Omega]\right]^{1}\ [\Omega]^T [\,1/g\,] \mathrm{Re}\{\tilde{\alpha}\} \tag{4-62}$$

Knowing {a}, it is possible to calculate the modal constants C_r using the method of partial fractions. However, some ill-conditioning problems may be encountered in the matrix inversion in Eq. (4-62).

To avoid this inversion (and the problem), an orthogonal transformation may be used, turning $[[\Omega]^T [1/g] [1/g] [\Omega]]$ into a unit matrix. As for the **RFP** method, this can be done by rewriting $[\Omega]$ in terms of real orthogonal polynomials φ and using a weighting function given by $|1/g|^2$, subjected to the orthogonality condition, a procedure which is explained in detail in Section 4-2-1:

$$\sum_{i=-L}^{L} \varphi_{i,k}\, \varphi_{i,j}\, |1/g_i|^2 = \begin{cases} 0 & k \neq j \\ 1 & k = j \end{cases} \tag{4-63}$$

In fact, we only deal with positive frequencies and so the condition will be:

$$\sum_{i=1}^{L} \varphi^{+}_{i,k}\, \varphi^{+}_{i,j}\, |1/g_i|^2 = \begin{cases} 0 & k \neq j \\ 0.5 & k = j \end{cases} \tag{4-64}$$

This expression is similar to expression (4-31), for the **RFP** method. Expression (4-53) now becomes, for each frequency Ω_i:

$$\alpha(\Omega_i) = \frac{\sum_{k=0}^{N-1} c_k\, \varphi^{+}_{i,2k}}{\prod_{r=1}^{N} (\omega_r^2 - \Omega_i^2)} \tag{4-65}$$

The error vector will consequently be given by

$$\underset{(Lx1)}{\{E\}} = \underset{(LxL)}{[1/g]}\ \underset{(LxN)}{[\vartheta^{+}]}\ \underset{(Nx1)}{\{c\}} - \underset{(Lx1)}{\mathrm{Re}\{\tilde{\alpha}\}} \tag{4-66}$$

where

$$[\vartheta^+] = \begin{bmatrix} \varphi^+_{1,0} & \varphi^+_{1,2} & \cdots & \varphi^+_{1,2N-2} \\ \varphi^+_{2,0} & \varphi^+_{2,2} & \cdots & \varphi^+_{2,2N-2} \\ \cdot & \cdot & & \cdot \\ \cdot & \cdot & & \cdot \\ \cdot & \cdot & & \cdot \\ \varphi^+_{L,0} & \varphi^+_{L,2} & \cdots & \varphi^+_{L,2N-2} \end{bmatrix} \tag{4-67}$$

Formulæ for the elements of $[\vartheta^+]$ are given in Eqs. (4-34) and (4-35) (as γ^+), where $\mathbf{q_i}$ is now $|\mathbf{1/g_i}|^2$. Following a similar procedure to that used before (starting from Eq. (4-59)), one obtains, instead of (4-62), the following expression:

$$\{c\} = 2\,[\vartheta^+]^T\,[\lceil 1/g \rfloor]\,\mathrm{Re}\{\tilde{\alpha}\} \tag{4-68}$$

where the factor **2** is due to the factor **0.5** in Eq. (4-64). The procedure for calculating **{c}** is very similar to the one that is followed in the **GRFP** method (as will be seen in Chapter 5), after having calculated the natural frequencies and damping ratios, i. e., in the second step when one wishes to calculate the modal constants and the phase angles. The present method can be considered as a particular case of that more general method.

It is not difficult to estabilish a linear relationship $[\mathbf{T_{ac}}]$ between coefficients **{c}** and **{a}**, as

$$\{a\} = [T_{ac}]\,\{c\} \tag{4-69}$$

and so, substituting (4-68) into (4-69), we obtain

$$\underset{(Nx1)}{\{a\}} = \underset{(NxN)}{2\,[T_{ac}]}\ \underset{(NxL)}{[\vartheta^+]^T}\ \underset{(LxL)}{[\lceil 1/g \rfloor]}\ \underset{(Lx1)}{\mathrm{Re}\{\tilde{\alpha}\}} \tag{4-70}$$

or

$$\underset{(Nx1)}{\{a\}} = \underset{(NxL)}{[T']}\ \underset{(Lx1)}{Re\{\tilde{\alpha}\}} \qquad (4\text{-}71)$$

where

$$[T'] = 2\ [T_{ac}]\ [\vartheta^{+}]^{T}\ [\ 1/g\ ] \qquad (4\text{-}72)$$

As mentioned before, the modal constants can be calculated from the coefficients **{a}**.

Comparing expression (4-71) with expression (2-196) (Ewins-Gleeson method), we see that they are alike, the main differences being that now one can use more data points than there are modes and that the **Ewins-Gleeson** method gives the modal constants directly. Knowing the modal constants and natural frequencies, the other modal parameters - phase angles and damping ratios - must be calculated. The phase angles are known implicitly, as the system has been assumed to have real modes and so the sign of the modal constants indicates whether the response is in- or out-of-phase. The introduction of damping into the mathematical model is also very straightforward, due to the characteristics assumed for the system. It may simply be calculated from the response at the natural frequencies, one at a time, assuming that the response at each resonance is not affected very much by the neighbouring modes. Recalling expression (4-52), and including the damping, we have:

$$\alpha(j\omega) = \sum_{r=1}^{N} \frac{C_r}{\omega_r^2 - \omega^2 + j\,2\,\omega\,\omega_r\,\xi_r} \qquad (4\text{-}73)$$

At each natural frequency, the measured response is given by

$$\tilde{\alpha}(j\omega_r) \approx \frac{C_r}{j\,2\,\omega_r^2\,\xi_r} + \sum_{\substack{s=1 \\ s\neq r}}^{N} \frac{C_s}{\omega_s^2 - \omega_r^2} \tag{4-74}$$

and so,

$$\xi_r \approx \frac{|\,C_r\,|}{2\,\omega_r^2 \left| \tilde{\alpha}(j\omega_r) - \sum_{\substack{s=1 \\ s\neq r}}^{N} \frac{C_s}{\omega_s^2 - \omega_r^2} \right|} \tag{4-75}$$

4-3-2 Considerations on the choice of data points

The method presented above has been implemented in a micro-computer and some details of the program and its performance will be discussed. Perhaps the most important aspect to be considered is the choice of points to be made from the measured FRF. Although the number of coefficients to be calculated is equal to **N**, the orthogonal polynomials φ have to be generated recursively up to order **2N-2** and therefore we shall consider the minimum number of points, **L**, as being **2N-2+1 = 2N-1**. But how should these points be chosen? Are the answers dependent on this choice? If yes, which ones might provide the best results ? Is there any advantage in choosing more points than the minimum number required ? In fact, it is known that the identification of the measured FRF depends on the location of points, as has already been pointed out in Ref. [77]. First of all, it is clear from the expressions that have been presented above that the points where the natural frequencies occur cannot be used for the analysis (see, for example, Eq. (4-54) with $\Omega_i = \omega_r$). Assuming that these frequencies are avoided, where should we locate the points?

Let us try to derive mathematically a criterion for selecting the "best"

points. Once $\{c\}$ and $\{E\}$ are defined in Eqs. (4-68) and (4-66) respectively, the squared error $J = \{E\}^T\{E\}$ can be calculated:

$$J = (\{c\}^T [\vartheta^+]^T [\lceil 1/g \rfloor] - \mathrm{Re}\{\tilde{\alpha}\}^T)([\lceil 1/g \rfloor][\vartheta^+]\{c\} - \mathrm{Re}\{\tilde{\alpha}\})$$

$$= \{c\}^T [\vartheta^+]^T [\lceil 1/g \rfloor][\lceil 1/g \rfloor][\vartheta^+]\{c\} - 2\{c\}^T [\vartheta^+]^T [\lceil 1/g \rfloor]\mathrm{Re}\{\tilde{\alpha}\} + \mathrm{Re}\{\tilde{\alpha}\}^T \mathrm{Re}\{\tilde{\alpha}\} \quad (4\text{-}76)$$

Due to orthogonality,

$$2[\vartheta^+]^T [\lceil 1/g \rfloor][\lceil 1/g \rfloor][\vartheta^+] = [I] \quad (4\text{-}77)$$

Thus,

$$J = 0.5\{c\}^T\{c\} - 2\{c\}^T [\vartheta^+]^T [\lceil 1/g \rfloor]\mathrm{Re}\{\tilde{\alpha}\} + \mathrm{Re}\{\tilde{\alpha}\}^T \mathrm{Re}\{\tilde{\alpha}\} \quad (4\text{-}78)$$

Substituting Eq. (4-68) in (4-78), we obtain:

$$J = \mathrm{Re}\{\tilde{\alpha}\}^T [[I] - 2[\lceil 1/g \rfloor][\vartheta^+][\vartheta^+]^T [\lceil 1/g \rfloor]]\mathrm{Re}\{\tilde{\alpha}\} \quad (4\text{-}79)$$

or

$$J = \mathrm{Re}\{\tilde{\alpha}\}^T [Q]\mathrm{Re}\{\tilde{\alpha}\} \quad (4\text{-}80)$$

where

$$[Q] = [I] - 2[\lceil 1/g \rfloor][\vartheta^+][\vartheta^+]^T [\lceil 1/g \rfloor] \quad (4\text{-}81)$$

From expression (4-80) it is clear that a sufficient condition for J to be zero is that the real part of the FRF ($\mathrm{Re}\{\tilde{\alpha}\}$) is zero; points at resonances and anti-resonances fulfil this condition. However, there may be other values of $\mathrm{Re}\{\tilde{\alpha}\}$ which can lead to values in $[Q]$ such that J is also zero or close to zero. Also, since in practice $\mathrm{Re}\{\tilde{\alpha}\}$ is never exactly zero, $[Q]$

could compensate and give a higher value for **J**. The matrix **[Q]** is a rather complicated function of the frequencies of the chosen points and, consequently, it is not easy to derive analytically the set of frequencies that lead to the minimum value of **J**. The behaviour of matrix **[Q]** should be checked first, as it certainly will not remain constant as different sets of points are chosen, and so a numerical study is therefore appropriate. For this task, a **2** DOF system was devised (Fig. 4-5) with the properties given in Table 4-11.

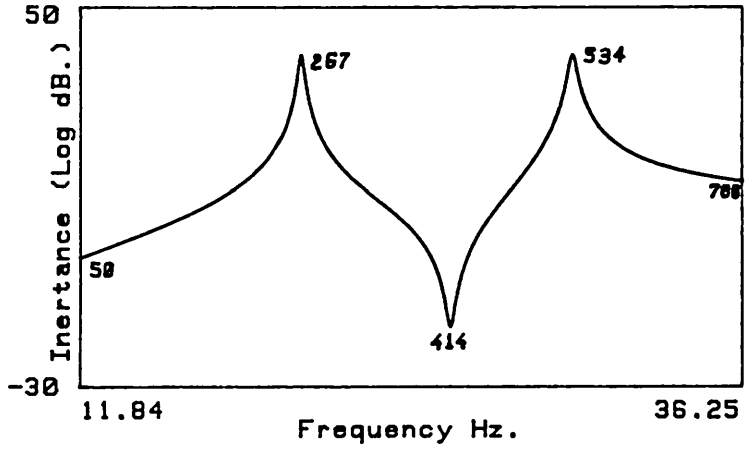

Fig. 4-5 Magnitude plot of a **2** DOF system.

Mode	ω_r(Hz)	ξ_r	C_r	ϕ_r
1	20	0.005	1	0
2	30	0.005	1	0

Table 4-11 Theo. data of the **2** DOF system of Fig. 4-5.

In this case, the default value for **L** (the number of FRF data points to be used) is **3**, and as there are several FRF data points, one can choose different sets of **3** points along the frequency range. The numbers quoted in Fig. 4-5 represent the order of some points of particular interest (extremes, resonances and anti-resonance). As the presentation of the

detailed numerical results would be quite extensive and tedious to follow, only the discussion and conclusions will be presented.

It was found that the variation of matrix **[Q]** with the different sets of points chosen depends mainly on the difference between the frequencies of these points and the resonant frequencies, i. e., on the elements of matrix [` 1/g ·]. For example, if we choose points **50, 51** and **52** and afterwards points **53, 54** and **55**, **[Q]** will exhibit only a very small change, and the same result is found if we choose points **80, 350** and **650** and points **81, 351** and **651**. In this case, points on the curve with smaller values of the real part of the response imply smaller values for **J**. But what happens if the elements of **[Q]** are small and those of **Re**$\{\tilde{\alpha}\}$ are large or, vice-versa, when **[Q]** is large and **Re**$\{\tilde{\alpha}\}$ is small ? It was found in the numerical studies that the dominant element was the FRF vector **Re**$\{\tilde{\alpha}\}$ and that the smaller (or larger) this is, the smaller (or larger) will be the value of **J**. Therefore, the requirement that the real part of the response be zero is a necessary condition for **J** to be zero. The points that best satisfy this condition are the anti-resonances and also the resonances themselves: Fig. 4-6 illustrates these points for a **2** DOF system.

In the numerical study it was found that the smallest values of **J** occurred when points near the anti-resonances and/or close to the extremes of the frequency range were chosen. However, when points around resonances were used, the results obtained were poor, in spite of the fact that some of the elements of matrix **[Q]** were quite small in these regions. In the example of Fig. 4-5, **[Q]** is a **3x3** matrix and, as it has been seen, its elements depend mainly on the differences in frequency between the FRF points used and the resonances. As a result, if we choose points **266, 535** and **650**, for example, elements **1,1** and **2,2** of **[Q]** will be very small, since the first and second points are close to resonances. How, then, can be

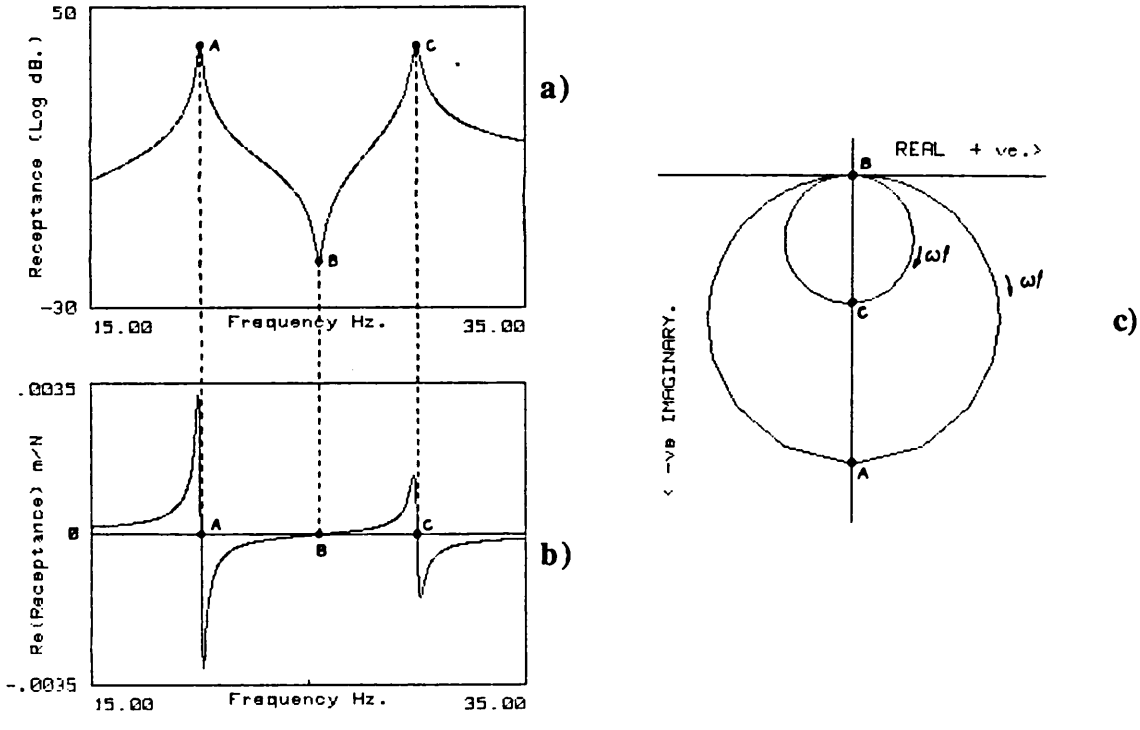

Fig. 4-6 Location of the anti-resonance and resonances on the the receptance FRF of a 2 DOF system: a) magnitude; b) real part; c) Nyquist plot.

explained that the results are poor if the first two elements of $\mathbf{Re}\{\tilde{\alpha}\}$ are also expected to be close to zero? The answer is that for lightly-damped systems the FRF phase angle changes abruptly near the natural frequency and although the neighbouring points have similar frequency values, the real part of the response may vary suddenly from near-zero (close to the natural frequency) to a large value (see Fig. 4-6 - b, c) and, as it was concluded, $\mathbf{Re}\{\tilde{\alpha}\}$ is the factor that dominates **J**, even in these cases when the elements of **[Q]** are smaller.

The data points near the resonances may, however, still be taken into consideration in some cases, especially if it exists a very good resolution of points in these regions, but no general rule can be stated.

4-3-3 Comparison with previous work

The study reported here now explains why in Ref. [77] anti-resonances are identified as "good" points for the identification process and also why in Ref. [118] it is concluded that in many cases the best choice is to take points close to the resonances. Both kinds of points are easily seen from a graph of the FRF modulus vs. frequency.

It should be noted that, as one is not always analysing point FRF measurements (excitation and response measured at the same point of the structure), we can sometimes have minima together with anti-resonances and a good choice in these curves could be to take the anti-resonance points when they exist and points close to the resonances where there are minima. This is sometimes the practice used when applying the method of Ref [77].

One might also wonder why, in the development of the expressions that led to the calculation of the modal constants in Ref [77], it was not clear that the accuracy of the answers was dependent on the values of the response. In fact, if we try to derive an expression for the error **J** in a similar way to that used in this case, we will obtain zero instead of an expression like (4-80). This is because the number of points needed to solve the equation for the modal constants in that earlier approach was exactly equal to the number of unknowns, the expression being of the type of Eq. (4-71) but with matrix **[T']** having dimensions **NxN** and vector $\mathbf{Re}\{\tilde{\alpha}\}$ being of order **N**. In that formulation, the error is exactly zero when calculated for that number of points. (This is not unlike the case of fitting a straight line to a given set of points: if only 2 points are used, the fit is perfect and the error is zero.) This does not mean that the total error using more points is zero and in fact it never is. When a "bad" set of points using the method of Ref [77] is chosen, the regenerated curve still coincides with the original one at these points, but the two curves can be quite different away from

these few frequencies. If the expressions in Ref [77] had been derived using more points than the minimum required (N), and a pseudo-inverse had been performed, an equation similar to (4-80) would have been obtained.

4-3-4 Computer program description

Criteria for the "best" modal constants

Although it has been shown that the anti-resonances are ideal points to be used in order to obtain a minimum error in the curve-fitting, it is well known that in many practical situations there is a low signal-to-noise ratio around those points. The discussion in the two previous sections served to explain more rigorously what has been found successful in practical application although, in our approach here, there is no obligation to use anti-resonance points.

In the present work, it was decided to choose arbitrarily (randomly) the sets of points - which may or may not include the anti-resonances - used to calculate the modal constants. In this process, regions around the resonances are excluded (a neighbourhood of $\pm$ 2 points). Then, the calculation is repeated several times with a different set of points each time. Having thus obtained results from several runs, it is necessary to introduce into the program some criterion so that the "best" results can be found. Perhaps the most obvious criterion one can use is to choose the run that provided the minimum error for **J**. An alternative criterion that has been devised will be explained next, using a specific example to facilitate understanding. Let us consider a system with several DOF, which has been analysed using the above method, applied **10** times. Let us suppose that we

wish to calculate the value of the modal constant of the first mode, C_1. The computer program will consider the value of C_1 from the first run, set a tolerance of $\pm\delta_0$ around that value, and look at the other values of C_1 from the remaining runs to see how many of these fall inside that tolerance. This procedure is then repeated based on the value of C_1 obtained in each of the **10** runs. In the end, the program will have "learned" that the value of C_1 in the first run was repeated, for example, **4** times; the value in the second run was repeated **3** times, etc., and it will memorize the values of C_1 that were most often repeated within that tolerance. This may have happened, for instance, in run no. **7**, where C_1 was repeated **5** times more than in runs nos. **2, 3, 6, 8** and **9**. Then, the average value of all these results is taken as the final result for C_1, together with the normalized standard deviation. For the modal constants of the other modes, the procedure is identical. This seems to be a better criterion for calculating "best" values of the modal constants than simply choosing the run that provided the least value of the error. This is because the value of **J** is calculated taking into consideration the modal constants in each run, whereas with this new criterion the best results can be obtained by averaging values coming from different runs. In the numerical examples, a comparison between these two criteria is made.

Flow-chart description

In Fig.4-7, the flow-chart of a program to perform the above analysis is presented. Following through this flow-chart: after the input of data and having chosen the part of the curve to be analysed, the resonant frequencies

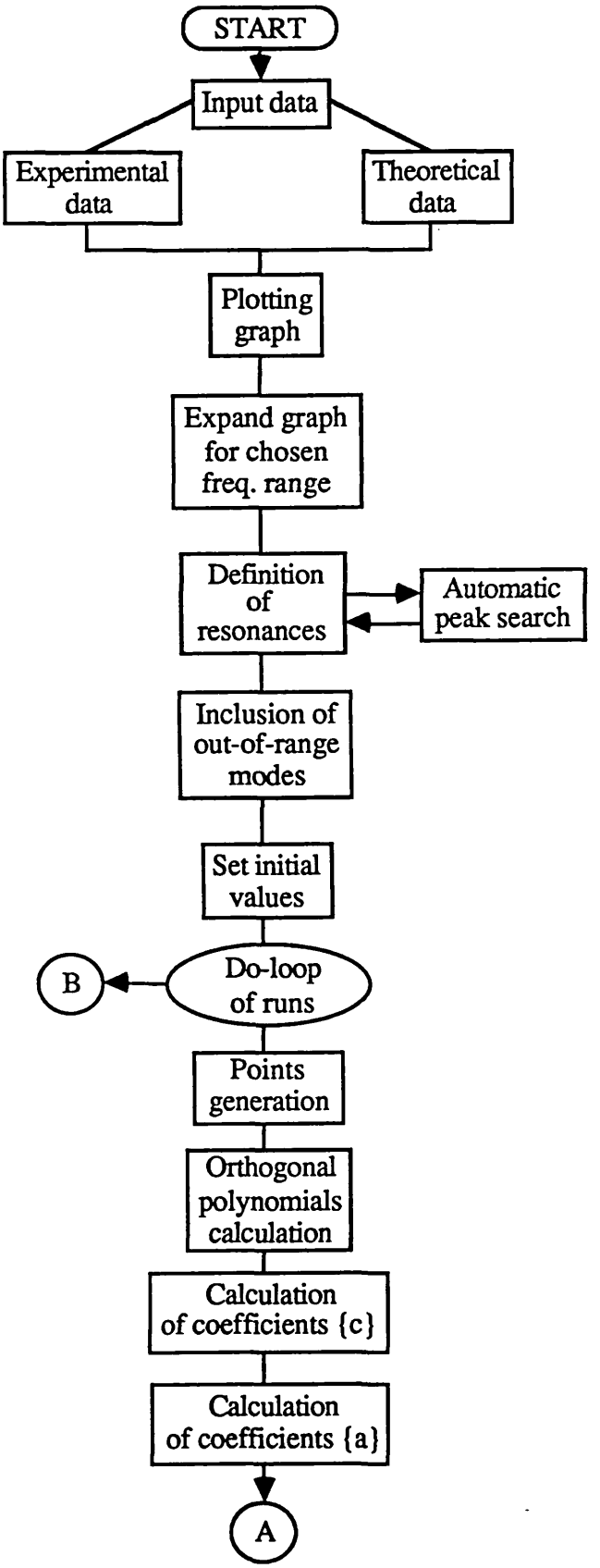

Fig. 4-7 Flow-chart of the computer program.

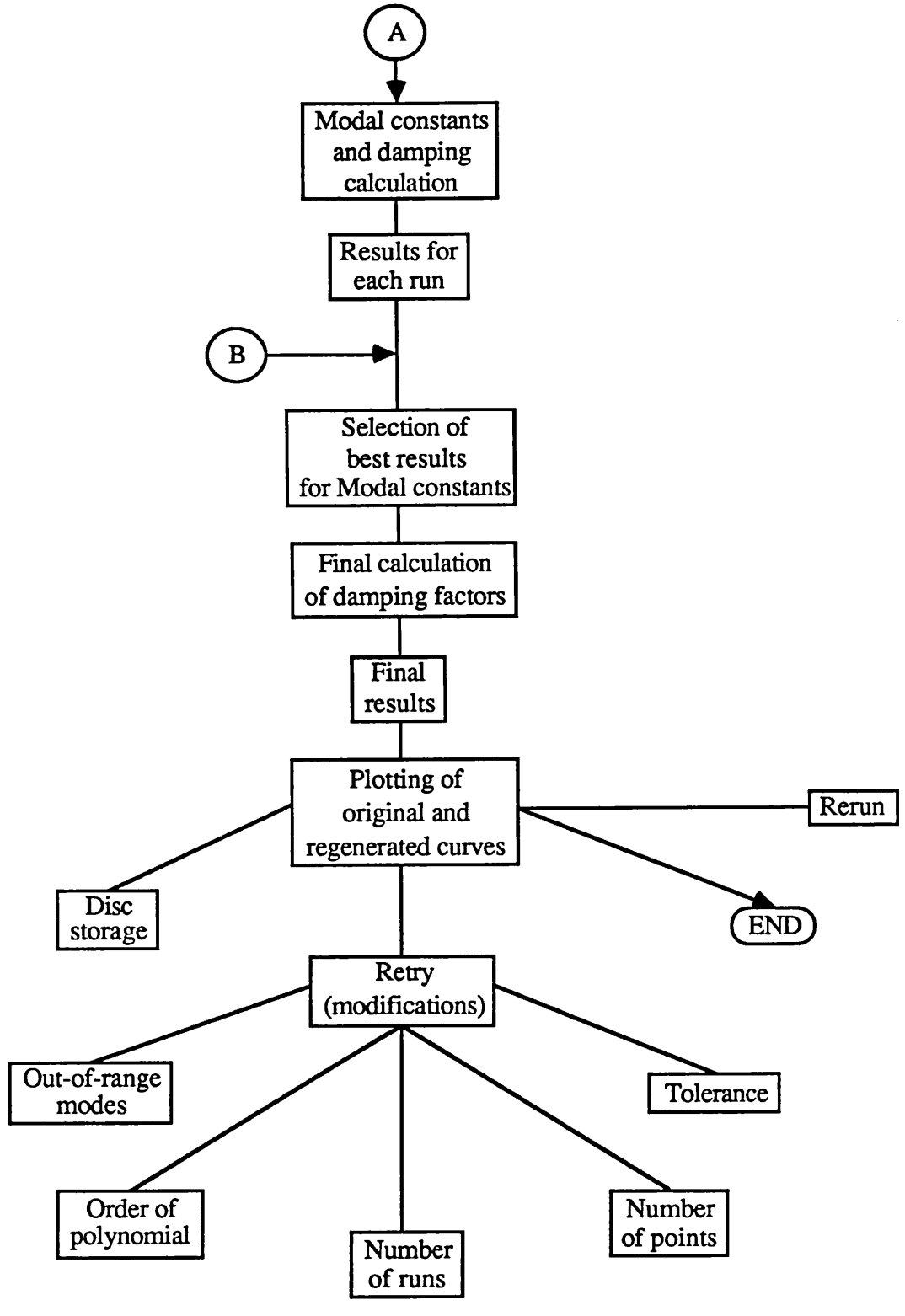

Fig. 4-7 (cont.) Flow-chart of the computer program.

must be defined. An automatic peak search routine indicates, with the cursor, each peak found and allows the user to choose whether to accept or to ignore that peak. Also, there is the possibility of deleting any peak already recorded. In this operation the user need not specify the number of modes to be analysed, as the program counts them automatically. Next, any number of out-of-range modes can be included and their frequencies specified by the user: the program will "see" which ones correspond to the low- and high-frequency ranges.

The intervention of the operator terminates here. Next, the program sets some initial default values, specifically for the order of the polynomial of expression (4-53), the number of points, the number of runs and a tolerance for the modal constants. The defaults are as follows: for the order of the polynomial and number of points, it takes their minimum values, i. e., **2N-2** and **2N-1** respectively. For the number of runs it takes **10** and for the tolerance, **10%**.

Now, the program starts calculating the modal parameters for each run, as described in the flow-chart. Eventually, the "best" values for the modal constants are determined, their mean value and normalized standard deviation being presented together with the damping factors which are calculated last. Then, a rapid regeneration of the FRF is seen on the screen, together with the initial measured one. Among the several options now offered, a useful one is the "retry" option, which permits modification of the initial default parameters mentioned above. For example, if the initial data are noisy, the number of points may be increased and if the influence of out-of-range modes is large, the order of the polynomial may be increased, too. Experience shows that increasing these values does not necessarily give better results - especially for the second one if out-of-range modes have already been specified. Nevertheless, the user is free to try any alteration he wishes.

Discussion

The advantages of this type of modal analysis procedure over previous versions are several. With this new procedure the user need not specify either the number of modes to be analysed, nor the points to be included in the calculations. Furthermore, it is not necessary to decide at the conclusion of the analysis whether to retain or reject modes which have been "found": a task often necessary in less "intelligent" procedures. Out-of-range modes may either be excluded or an arbitrary number can be given. The program now presented is quite automatic, and "intelligent" in the sense that it rejects partial results that do not agree with the general trend of the good ones. The program is not very time-consuming, compared with previous versions: the parameter that most affects the speed of running is the number of points taken into account, but usually the default value provides a good identification, and quickly.

Another advantage concerns the calculation of the modal properties associated with the specified out-of-range modes. Those values are particularly sensitive to the points that are chosen for the analysis and much more consistent results are obtained with the present approach. This is quite important when coupling sub-structures based on the identification of experimental data, because in this case the consideration of the actual values of residual modes is fundamental.

Finally, it must be noted that the expression "automatic" attributed to the present computer program is due to the fact that it requires far fewer decisions to be taken than the classical version currently available, although some intervention of the user is still needed in the first stage, specifically to define the resonance frequencies and the out-of-range modes. The automatic finding of resonant peaks may be possible but, at present, a reliable routine to perform such a task has not been found due to the existence of noise in the data.

4-3-5 Examples

Theoretical cases

Some numerical examples are presented to illustrate the effectiveness of the analysis method. A comparison with results from the standard procedure of Ref. [77] is also shown. These examples are representative of the general behaviour of the program, as experienced when analysing many different theoretical and experimental cases.

Evaluation of the method

In the first example one attempts to simulate theoretically a practical situation by generating FRF data for a **5** DOF system and then adding random noise. Attention is focussed on the middle **3** modes, so that the others act as residual modes. Also, the system parameters chosen give rise to a double anti-resonance, as this is usually a difficult case to analyse, and the values given to the modal constant phase angles differ slightly from the ideal case of **0°** or **180°**. The original modal data are presented in Table 4-12, and the generated FRF curve is shown in Fig. 4-8. Fig. 4-9 shows the expansion of Fig. 4-8 around the middle **3** modes.

Mode	ω_r(Hz)	ξ_r	C_r	ϕ_r
1	80.00	0.0025	1.5	-5.00
2	95.00	0.0050	1.0	5.00
3	120.00	0.0050	0.2	178.00
4	150.00	0.0025	1.0	6.00
5	180.00	0.0025	1.3	175.00
Added noise = 3%				

Table 4-12 Theo. data with noise.

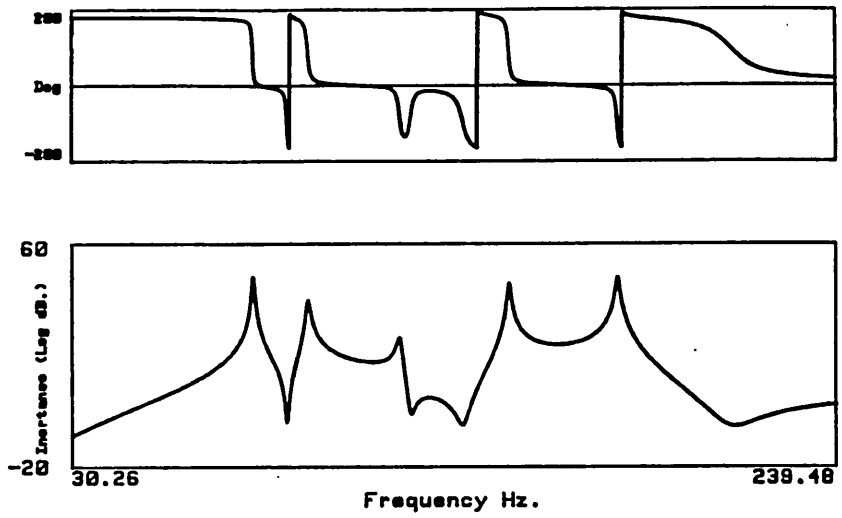

Fig. 4-8 Bode plot (inertance) of the 5 DOF system of Table (4-12).

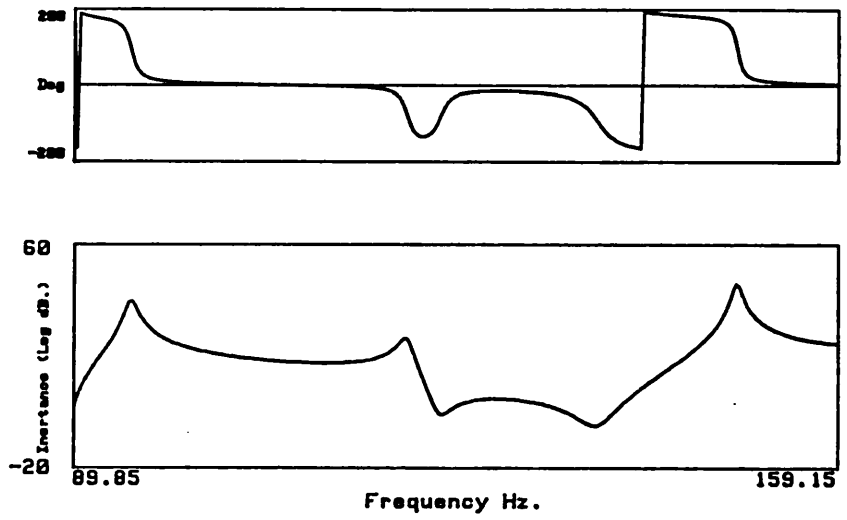

Fig. 4-9 Expanded graph of Fig. 4-8 around the 3 modes in the middle.

In order to evaluate the influence of the several parameters that might be varied in this method, each one will be modified at a time. The parameters of interest are: number and magnitude of out-of-range modes; number of points used (L); order of the polynomial (M); number of runs (NR) and tolerance for the modal constants (δ_0). For this example, the default values are:

$$L = 9$$
$$M = 8$$
$$NR = 10$$
$$\delta_0 = 10\%$$

In Table 4-13, six different cases are studied.

CASE No.	OUT-OF-RANGE MODES (Hz)		L	M	NR	δ_0(%)		MODES		
								1	2	3
1	80	180	9	8	10	10	ξ_r	4.781×10^{-3}	4.371×10^{-3}	2.624×10^{-3}
							C_r	0.944(4.6 %)	0.189 (6.7%)	0.997 (4.7%)
							ϕ_r	0	180	0
2	70	170	9	8	10	10	ξ_r	4.893×10^{-3}	4.232×10^{-3}	2.553×10^{-3}
							C_r	0.943 (5.0%)	0.178 (5.9%)	0.991 (4.5%)
							ϕ_r	0	180	0
3	80	180	11	10	10	10	ξ_r	4.986×10^{-3}	4.564×10^{-3}	2.557×10^{-3}
							C_r	0.961 (4.0%)	0.192 (4.5%)	0.992 (4.7%)
							ϕ_r	0	180	0
4	80	180	20	8	10	10	ξ_r	4.911×10^{-3}	4.573×10^{-3}	2.468×10^{-3}
							C_r	0.946 (3.0%)	0.192 (5.3%)	0.958 (4.4%)
							ϕ_r	0	180	0
5	80	180	9	8	20	10	ξ_r	4.989×10^{-3}	4.522×10^{-3}	2.521×10^{-3}
							C_r	0.961 (2.8%)	0.190 (3.7%)	0.978 (4.1%)
							ϕ_r	0	180	0
6	80	180	9	8	20	5	ξ_r	5.070×10^{-3}	4.680×10^{-3}	2.559×10^{-3}
							C_r	0.977 (3.1%)	0.197 (2.4%)	0.993 (2.7%)
							ϕ_r	0	180	0

Table 4-13 Results of the identification for six different cases.

For the first case, the default values are used and for the second the influence of varying the values of the out-of-range modes is analysed. For cases **3** to **6**, the influence of **M**, **L**, **NR** and δ_0, respectively, are analysed.The natural frequency values are not presented, as they are given in advance, while the results in brackets refer to the standard deviation. The original (dotted) and regenerated (solid) curves are shown in Figs. 4-10 to 4-15, corresponding to cases **1** to **6**.

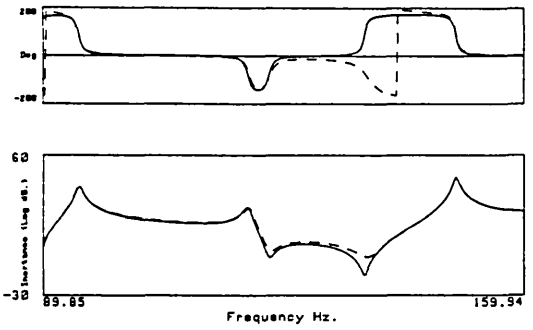

Fig. 4-10 Original (dotted) and regenerated (solid) FRFs for case **1**.

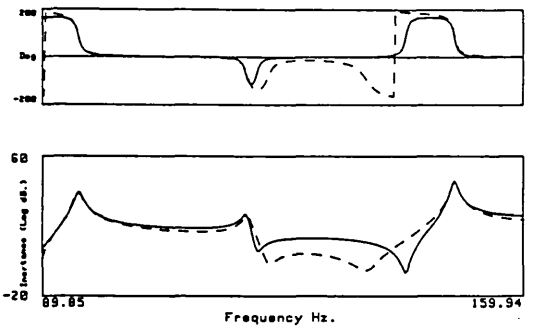

Fig. 4-11 Original (dotted) and regenerated (solid) FRFs for case **2**.

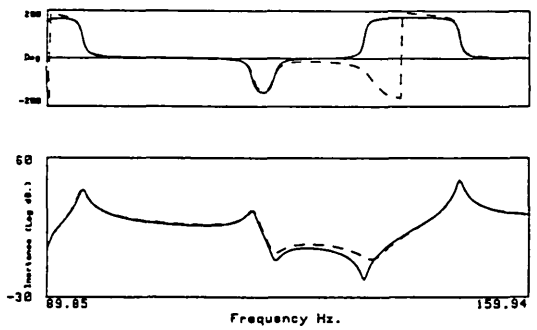

Fig. 4-12 Original (dotted) and regenerated (solid) FRFs for case **3**.

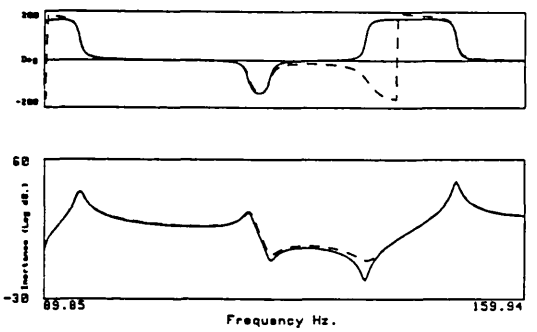

Fig. 4-13 Original (dotted) and regenerated (solid) FRFs for case **4**.

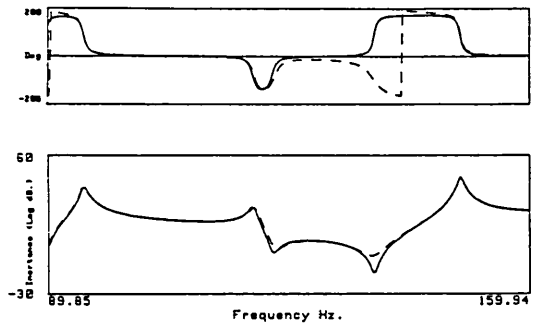

Fig. 4-14 Original (dotted) and regenerated (solid) FRFs for case **5**.

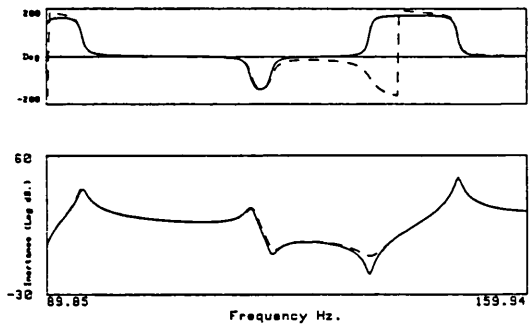

Fig. 4-15 Original (dotted) and regenerated (solid) FRFs for case **6**.

Discussion

From the cases presented, it is found that the method is sensitive to the values given for the out-of-range modes and, although not shown explicitly, two out-of-range modes are usually sufficient to represent the contribution of all the modes that are not being analysed. Increasing **M** (the polynomial order) is not, in general, a valuable measure, and may even make the results worse. In some cases, it was found that increasing **M** could give a better estimate for the modal constants up to a certain value, but beyond that value the results became worse. Increasing the value of **L** (the number of points) usually does not make things any better either, and here again the results are poorer in some cases. From the results obtained when using **20** runs (NR) instead of **10**, and with the minimum number of points, it seems that it is generally preferable to use the minimum **L** and to increase the number of runs. In this way more results are available to evaluate more reliably the modal constants. For the same reason, it is advisable to decrease the tolerance when doing so and, in fact, the last case (6) was one that gave the best estimates for the modal constants. In Fig. 4-16, a graph of the relative error in the modal constants for the several

cases studied is presented (errors in the damping are not shown, as the damping is a consequence of the calculations of the modal constants).

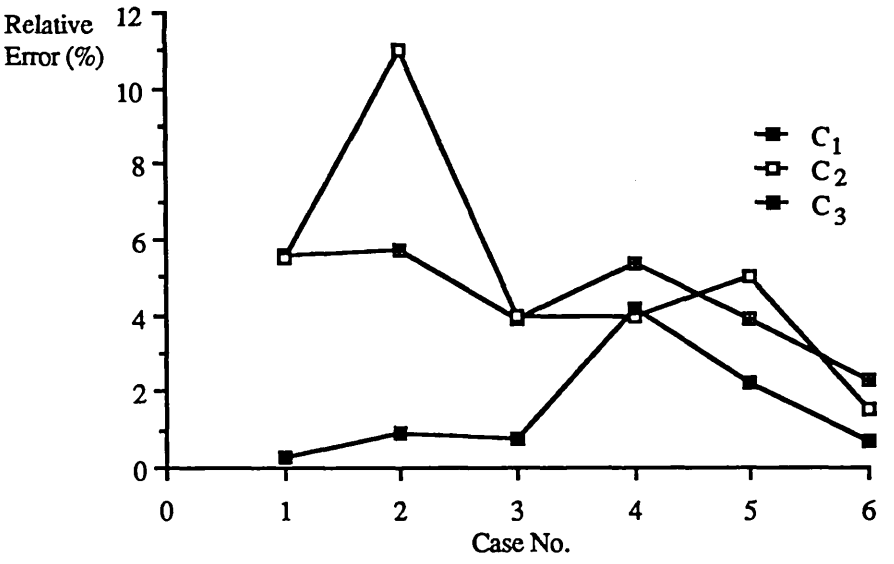

Fig. 4-16 Relative error in the identification of the modal constants, for the various cases studied.

In conclusion, it can be said that the most resonable procedure is to work with the default values and, if these do not lead to satisfactory results, to increase the number of runs and to decrease the tolerance. Also, it should not be forgotten that this method is particularly sensitive to the values attributed to the out-of-range modes, and so it is important that these be specified as precisely as possible.

Comparison of criteria

Using the criterion of minimum **J**, and the default case data (where L = 9), the same calculations were repeated **3** times. The results are presented in Table 4-14, where the values in brackets represent the standard deviations.

As can be seen, the criterion of minimum J gives very good results for the second and third tries, but not such good results for the first try where the modal constant C_1 is considerably in error. In contrast, the alternative criterion always gave quite reasonable results. It is concluded that the criterion based on the minimum error (the basic curve-fit requirement) is less reliable than the alternative. This is probably because it is based purely on mathematics, whereas the other criterion, seeking consistency in the results from several runs, has a more "physical" basis.

		J min.			Alternative criterion	
Try	Mode 1	Mode 2	Mode 3	Mode 1	Mode 2	Mode 3
1 ξ_r	7.510×10^{-3}	4.323×10^{-3}	2.841×10^{-3}	4.935×10^{-3}	4.374×10^{-3}	2.697×10^{-3}
C_r	1.477	0.180	1.075	0.971 (2.0%)	0.181 (6.4%)	1.021 (3.6%)
2 ξ_r	5.020×10^{-3}	4.739×10^{-3}	2.628×10^{-3}	5.010×10^{-3}	4.652×10^{-3}	2.543×10^{-3}
C_r	0.988	0.197	0.994	0.987 (4.5%)	0.193 (2.7%)	0.962 (5.8%)
3 ξ_r	5.260×10^{-3}	4.641×10^{-3}	2.637×10^{-3}	5.165×10^{-3}	4.419×10^{-3}	2.628×10^{-3}
C_r	1.036	0.192	0.998	1.017 (5.2%)	0.183 (5.1%)	0.994 (4.6%)

Table 4-14 Comparison of criteria for the "best" modal constants.

Experimental case

A FRF measured on a turbine blade (Fig. 4-17) was chosen to compare the results of the identification obtained using the method now proposed and those from a more conventional procedure. Using the **Ewins-Gleeson** method and choosing adequate points according to experience, a very good identification of the curve was obtained, as shown in Fig. 4-18 where the

difference between the original and the regenerated curves (plotted together) is barely visible. Using again the same method, but choosing a different set of points at random, can lead us to an answer as shown in Fig. 4-19. Using the new method, the results are shown in Fig. 4-20 (original and regenerated curves).

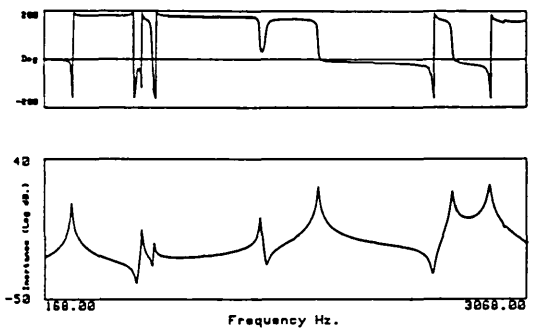

Fig. 4-17 FRF of an experimental case.

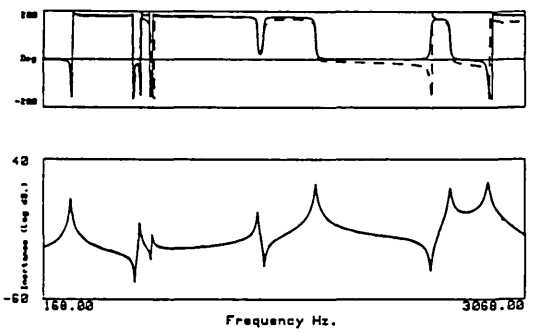

Fig. 4-18 Original (dotted) and regen. (solid) FRFs using the Ewins-Gleeson method.

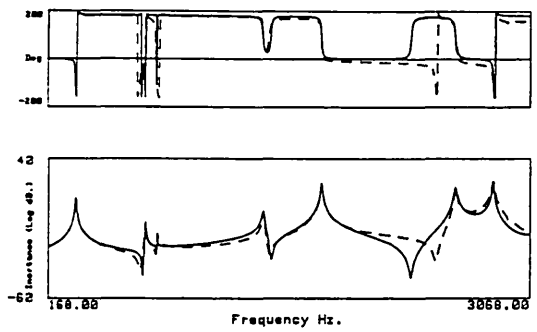

Fig. 4-19 Original (dotted) and regen. (solid) FRFs using the Ewins-Gleeson method, taking a different set of points.

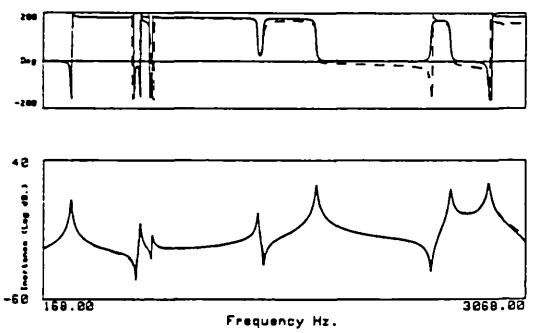

Fig. 4-20 Original (dotted) and regen. (solid) FRFs using the new proposed method.

Discussion

The comparison provided by this example is made in order to stress that an

automatic and intelligent program can overcome problems such as (in this case) a poor choice of points, and therefore can minimize the requirement for a contribution of the expertise of the user. It also provides an indication of the quality of the results, after running several times.

4-4 Conclusions

4-4-1 Conclusions on the RFP method

As reported before (Ref. [82]), the **RFP** method presents some advantages when compared with other modal parameter extraction techniques, namely when dealing with closed-spaced complex modes and in the presence of noise. Nevertheless, in some cases, it still can give either inadequate answers or results which are difficult to interpret, due to computational modes that are mixed with the true ones. To avoid this problem, several different sets of points are used, in a given frequency range, with the following advantages:

(i) - the computational modes are well identified, as they exhibit different values as different sets of data points are used;

(ii) - the correct modal parameters emerge and so one can automatically determine whether one or more close modes have been identified;

(iii) - the results of the true modes found are averaged, eliminating to some extent the errors in the estimates obtained due to noise and also, allowing for an indication of their quallity, given by the normalized standard deviation.

The method is not very sensitive to the number of data points taken into the calculations, but seems to be sensitive to the frequency range chosen.

Considering the disadvantages, it is noted that the objective of obtaining the additional reliability in the set of results is gained at the expense of speed, as the number of runs is increased.

The various parameters that have been chosen in the computer program (number of data points, number of runs, tolerances associated with the criterion to decide on the genuine number of modes) seem to be the most sensible ones, as they have permitted to obtain good results for a large number of cases studied.

4-4-2 Conclusions on the new approach for lightly damped structures

An established method for the modal identification of lightly damped structures, the **Ewins-Gleeson** method, has been re-examined. A new approach has been developed which is an extension of that original method, and is a particular case of the **RFP** method. Likewise, the **Ewins-Gleeson** method may also be seen as a particular version of the **RFP** method. The importance of these facts is that a better understanding of the inter-relationships amongst those methods is now possible. Before, the **Ewins-Gleeson** method seemed a completely separate and different modal analysis technique.

The new approach also enables the justification of some procedures that were applied in the **Ewins-Gleeson** method in the past, merely based on empirical factors, namely the choice of data points to be taken in the analysis.

The intervention of the user and the need for his experienced judgements has been reduced to a minimum, by the inclusion of a degree of "intelligence" into the algorithm used. Decisions based on physical criteria,

rather than numerical, have been used to establish "best" results for the modal parameters sought, together with indications of their quality. For this accomplishment, the experience gained with the development of the **RFP** algorithm was very helpful.

The experimental example shown illustrates the advantages of the new approach. More recent practical applications of this algorithm have demonstrated that it is very "friendly" to use and very easy and quick to rerun the program when one wishes to try a different seting for the default parameters assumed. Being fast, makes it very useful when a large quantity of FRFs need to be analysed.

CHAPTER 5

AN INVESTIGATION OF SOME *SIMO* AND *MIMO* METHODS

5-1 Introduction

With *SISO* methods, only one FRF could be analysed at a time and the best one could obtain, if a set of FRFs were to be studied, was an average of the results from the several individual analyses. As mentioned in Chapter 1, the basic philosophy of *SIMO* and *MIMO* modal analysis methods is to take advantage of all the measured FRFs of a structure, by processing them simultaneously. In this way, a unique result for the global properties of a structure (the natural frequencies and damping factors) will be obtained. With *SIMO* methods, the calculation is often divided into two stages: first, calculation of the natural frequencies and damping factors considering all the measured FRFs and, second, calculation of the modal constants and phase angles, considering each FRF at a time. With *MIMO* methods all the modal properties are usually calculated simultaneously.

Three methods will be studied in this chapter: one is the extension of the

RFP method studied in Chapter 4, the **Global RFP** (GRFP); another is simply called the **Global** method; a third is the **Spectral** method. The first two are indirect *SIMO* methods and the third one is a direct *MIMO* method.

The main objectives of the present chapter are essentially the same as those of Chapter 4 (for the RFP method), i. e., to provide a clear and detailed explanation of the theoretical background of the methods and to extend them in order to obtain more "intelligent" algorithms, able to supply the user with the best possible identification and give a clear indication of the quality of the analysis. This is accomplished by repeating the calculations with different sets of data points and analysing the consistency of the results obtained each time, keeping the ones that are mostly repeated within a given tolerance and rejecting the others. The quality indicators are based upon the standard deviation of the results accepted. We shall continue to pay special attention to the problem of the identification of double modes, which is a typical and very common situation and yet one where most of the methods often fail to give reliable answers and so, it is believed to constitute a good test for the type of algorithms which we seek to explore. Besides this, a comparison among the three methods will be carried out.

5-2 The Global Rational Fraction Polynomial method (GRFP)

In Chapter 4, the **RFP** method for identifying the modal parameters from a single FRF was explained in detail and extented to enable the valid extraction of modal parameters. If other FRFs measured on the same structure are also considered, one might expect (theoretically) exactly the same results for the resonant frequencies and damping ratios, as these are characteristic properties of the structure, although different modal constants and phase angles. The former are called "global" properties and

the latter "local" properties. Using several FRFs to calculate the global properties is to overspecify the number of equations in relation to the number of unknowns and, so, we shall make use again of a least-squares procedure. Knowing the global properties, the local ones can be calculated from each FRF. Here, the *SIMO* version of the **GRFP** method(Refs. [84] and [85]) will be explored, extending it to fulfil the desired objectives.

5-2-1 Theory

Calculation of the global properties

As seen in Chapter 4, coefficients $\mathbf{b}_k$ (Eq. (4-2)) are the ones which yield the global properties of the system. These are related to coefficients $\mathbf{d}_k$ (Eq. (4-20)) through the relationship (4-40 b), where $[\mathbf{T}_{bd}]$ and $\{\mathbf{R}\}$ are direct functions of the orthogonal polynomials coefficients.

$$\underset{(2Nx1)}{\{b\}} = \underset{(2Nx2N)}{[T_{bd}]}\ \underset{(2Nx1)}{\{d\}} + \underset{(2Nx1)}{\{R\}} \qquad (4\text{-}40\ b)$$

Rewriting (4-40 b) as

$$\{d\} = [T_{bd}]^{-1}(\{b\} - \{R\}) \qquad (5\text{-}1)$$

and (4-39 a) as

$$([I] - [X']^T[X'])\{d\} = -[X']^T\{G'\} \qquad (5\text{-}2)$$

and substituting (5-1) into (5-2), we obtain

$$([I] - [X']^T[X'])[T_{bd}]^{-1}(\{b\} - \{R\}) = -[X']^T\{G'\} \qquad (5\text{-}3)$$

or

$$[U_G]\{b\} = \{V_G\} \tag{5-4}$$

where

$$\underset{(2Nx2N)}{[U_G]} = ([I] - [X']^T[X'])\,[T_{bd}]^{-1} \tag{5-5 a}$$

$$\underset{(2Nx1)}{\{V_G\}} = [U_G]\{R\} - [X']^T\{G'\} \tag{5-5 b}$$

For each FRF we have an equation of the form of (5-4). Considering a total of **p** FRFs,

$$\underset{(2Nxp)x2N}{\begin{bmatrix} [U_G]_1 \\ [U_G]_2 \\ \vdots \\ [U_G]_p \end{bmatrix}} \underset{(2Nx1)}{\{b\}} = \underset{(2Nxp)x1}{\begin{Bmatrix} \{V_G\}_1 \\ \{V_G\}_2 \\ \vdots \\ \{V_G\}_p \end{Bmatrix}} \tag{5-6}$$

or

$$[U_T]\{b\} = \{V_T\} \tag{5-7}$$

Solving (5-7) in a least-squares sense, we obtain

$$\{b\} = ([U_T]^T[U_T])^{-1}[U_T]^T\{V_T\} \tag{5-8}$$

In the computer program, instead of building $[U_T]$ from $[U_G]_k$, $k = 1,...p$ and then computing $[U_T]^T[U_T]$, it is better to calculate each $[U_G]_k{}^T[U_G]_k$ and to make the summation for $k=1$ to p. The same applies to $[U_T]^T\{V_T\}$. So, in fact, instead of (5-8) we shall use in the program:

$$\{b\} = \left(\sum_{k=1}^{p} [U_G]_k^T [U_G]_k\right)^{-1} \left(\sum_{k=1}^{p} [U_G]_k^T \{V_G\}_k\right) \qquad (5\text{-}8\ a)$$

With **{b}**, we can use a polynomial solver to find the roots and thence to calculate the natural frequency and damping factor, as seen for the RFP method.

Calculation of the local properties

To calculate **{a}** (vector of coefficients a_k), we have two options: either to use Eq. (4-40 a) with **{c}** (vector of coefficients c_k) given by (4-39 b), using **{d}** calculated for each FRF, or, once the resonant frequencies and damping ratios have been calculated, to curve-fit <u>each</u> FRF again but now only to calculate **{a}** and then the modal constants. The second option seems to be much more rational and consistent with the global curve-fitting philosophy, and will next be explained in greater detail.

Recalling equation (4-2),

$$\alpha(j\omega) = \frac{\sum_{k=0}^{2N-1} a_k (j\omega)^k}{\sum_{k=0}^{2N} b_k (j\omega)^k} \qquad (4\text{-}2)$$

or, for each measured frequency,

$$\alpha(j\omega_i) = \sum_{k=0}^{2N-1} \left(\frac{(j\omega_i)^k}{\sum_{k=0}^{2N} b_k (j\omega_i)^k} \right) a_k \qquad (5\text{-}9)$$

or

$$\alpha(j\omega_i) = \sum_{k=0}^{2N-1} t_{ik}\, a_k \tag{5-10}$$

with

$$t_{ik} = \frac{(j\omega_i)^k}{\sum_{k=0}^{2N} b_k (j\omega_i)^k} \tag{5-11}$$

The error between the analytical and experimental values at each frequency ω_i, will be

$$e_i = \alpha(j\omega_i) - \tilde{\alpha}(j\omega_i) = \sum_{k=0}^{2N-1} t_{ik}\, a_k - \tilde{\alpha}(j\omega_i) \tag{5-12}$$

For all **L** measured frequencies, the error vector will be

$$\underset{(Lx1)}{\{E\}} = \underset{(Lx2N)}{[T_G]}\ \underset{(2Nx1)}{\{a\}} - \underset{(Lx1)}{\{\tilde{\alpha}\}} \tag{5-13}$$

where

$$[T_G] = \begin{bmatrix} t_{1,0} & t_{1,1} & \cdots & t_{1,2N-1} \\ t_{2,0} & t_{2,1} & \cdots & t_{2,2N-1} \\ \cdot & \cdot & & \cdot \\ \cdot & \cdot & & \cdot \\ \cdot & \cdot & & \cdot \\ t_{L,0} & t_{L,1} & \cdots & t_{L,2N-1} \end{bmatrix} \tag{5-14}$$

The squared error **J** will be

$$J = \{E^*\}^T \{E\} = \left\{ \{a\}^T [T_G^*]^T - \{\tilde{\alpha}^*\}^T \right\} \left\{ [T_G]\{a\} - \{\tilde{\alpha}\} \right\} \tag{5-15}$$

Developing (5-15), we have

$$J = \{a\}^T [T_G^*]^T [T_G] \{a\} - \{\tilde{\alpha}^*\}^T [T_G] \{a\}$$

$$- \{a\}^T [T_G^*]^T \{\tilde{\alpha}\} + \{\tilde{\alpha}^*\}^T \{\tilde{\alpha}\} \tag{5-16}$$

so that, following the same procedure as in Chapter 4 , we obtain

$$J = \{a\}^T \mathrm{Re}([T_G^*]^T [T_G])\,\{a\} - \mathrm{Re}(\{\tilde{\alpha}^*\}^T [T_G])\,\{a\}$$

$$- \{a\}^T \mathrm{Re}([T_G^*]^T \{\tilde{\alpha}\}) + \mathrm{Re}(\{\tilde{\alpha}^*\}^T \{\tilde{\alpha}\}) \qquad (5\text{-}17)$$

Minimizing $\mathbf{J}$ by making $\dfrac{\partial \mathbf{J}}{\partial \{a\}} = \{0\}$, we obtain

$$\mathrm{Re}([T_G^*]^T [T_G])\,\{a\} = \mathrm{Re}([T_G^*]^T \{\tilde{\alpha}\}) \qquad (5\text{-}18)$$

$$\{a\} = \mathrm{Re}([T_G^*]^T [T_G])^{-1}\, \mathrm{Re}([T_G^*]^T \{\tilde{\alpha}\}) \qquad (5\text{-}19)$$

However, once again, some numerical problems can be encountered in the inversion of $\mathbf{Re}([T_G^*]^T[T_G])$ although these can again be avoided by using orthogonal polynomials so that $\mathbf{Re}([T_G^*]^T[T_G])$ is replaced by the unit matrix. This means, following what has been done for the **RFP** method, changing (5-9) or (5-10) into:

$$\alpha(j\omega_i) = \sum_{k=0}^{2N-1} \frac{\varphi_{i,k}^+}{g_i}\, c_k = \sum_{k=0}^{2N-1} z_{i,k}\, c_k \qquad (5\text{-}20)$$

where $\mathbf{g_i}$ is the denominator of Eq. (5-9), which is known, as the coefficients $\mathbf{b_k}$ have already been calculated, and $\varphi_{i,k}^+$ is the half-positive orthogonal polynomial defined in Eqs. (4-34) and (4-35) as γ^+ and for $\mathbf{q_i} = |\mathbf{1/g_i}|^2$. For all **L** measured points, Eq. (5-20) can be written as

$$\{\alpha(j\omega)\} = [Z_G]\,\{c\} \qquad (5\text{-}21)$$

where $[\mathbf{Z_G}]$ can be expressed as $[\mathbf{1/g}]\,[\vartheta^+]$, $[\vartheta^+]$ being the matrix composed by $\varphi_{i,k}^+$. Thus, to have $\mathbf{Re}([T_G^*]^T[T_G]) = [\,\mathbf{I}\,]$ means to have

$$\mathrm{Re}([\vartheta^{+*}]^T [\Gamma (1/g)^* \lrcorner] [\Gamma 1/g \lrcorner] [\vartheta^+]) = [I] \tag{5-22}$$

Similar to what was found in (4-31), we have to generate orthogonal polynomials with respect to a weighting function $|1/g_i|^2$ and the orthogonality condition is (using the positive half-functions)

$$\mathrm{Re}\left(\sum_{i=1}^{L} (\varphi_{i,k}^+)^* (\varphi_{i,j}^+) |1/g_i|^2\right) = \begin{cases} 0 & k \neq j \\ 0.5 & k = j \end{cases} \tag{5-23}$$

Hence, Eq. (5-18) becomes

$$[\Gamma 0.5 \lrcorner] \{c\} = \mathrm{Re}([Z_G^*]^T \{\tilde{\alpha}\}) \tag{5-24}$$

So,

$$\{c\} = 2\,\mathrm{Re}([Z_G^*]^T \{\tilde{\alpha}\}) \tag{5-25}$$

The similarities between Eqs. (5-25) and (4-68) are understandable, since for the case of lightly damped structures (Section 4-3-1) we were also looking for the modal constants, the natural frequencies having already been established. **{a}** can be calculated using a transformation as in Eq. (4-40 a) and the local modal parameters can now be evaluated as previously explained for the **RFP** method.

5-2-2 Computer program description

The computer program developed is an extension of the one used for the **RFP** method (Section 4-2-2), considering now several FRFs. All the numerical parameters used before to determine the existence of one or two close modes are the same now. In Fig. 5-1 the corresponding flow-chart is presented. After calculating the "global "and "local" modal parameters, the program repeats the calculations **20** times, taking each time a randomly

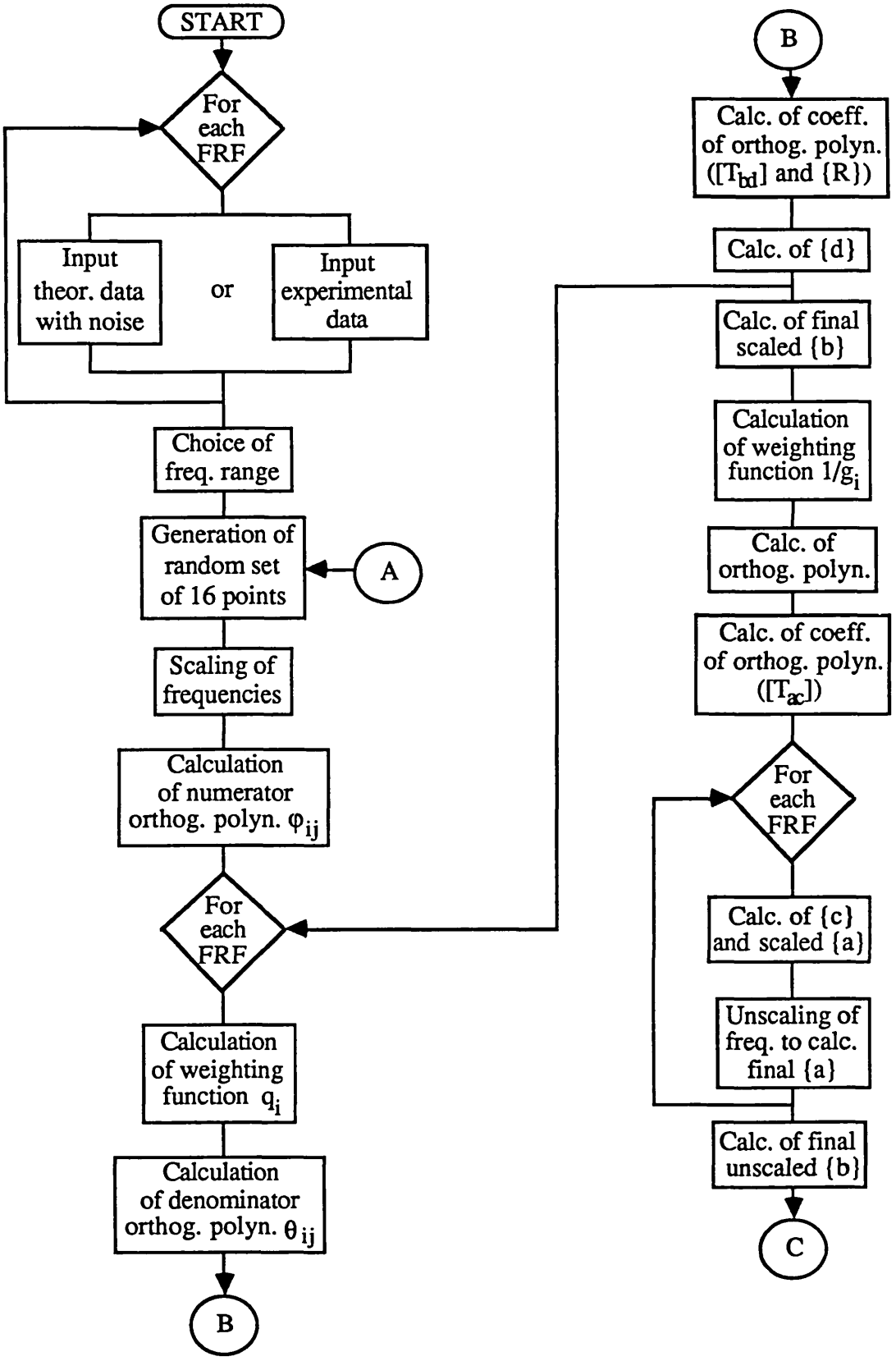

Fig. 5-1 Flow-chart of the computer program.

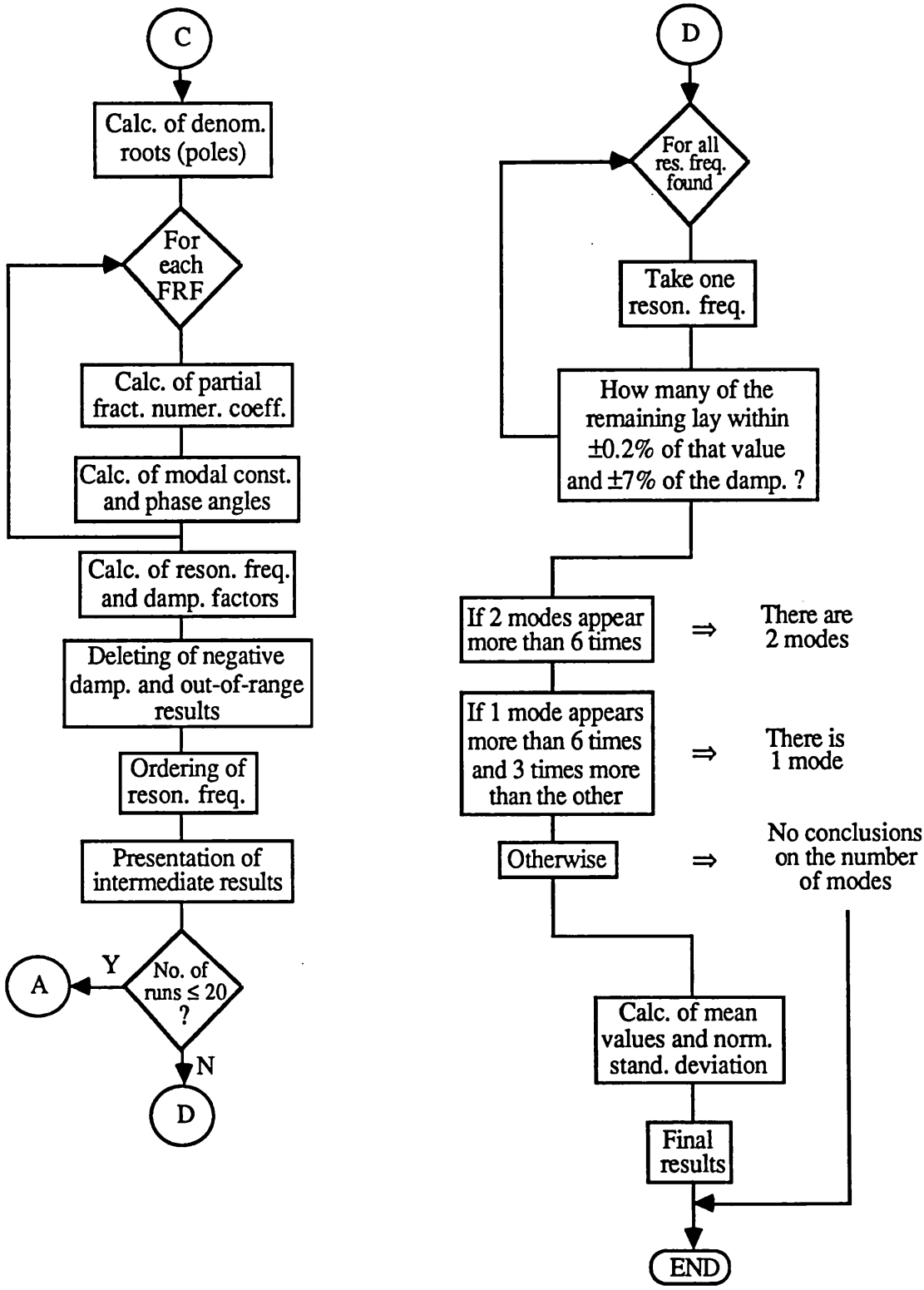

Fig. 5-1 (cont.) Flow-chart of the computer program.

chosen set of points. In a second phase, the program analyses all the calculated parameters and, based upon the criteria of acceptance or rejection presented in Fig. 5-1, "decides on the final results.

5-2-3 Numerical examples

Theoretical case - Evaluation of the method

In this case, we shall study 3 FRFs simultaneously, with the data for ω_r, ξ_r, C_r and ϕ_r given in Table 5-1.

Mode	FRF	ω_r(Hz)	ξ_r	C_r	ϕ_r
1	1	90	0.005	1	0
	2	"	"	1	0
	3	"	"	1	0
2	1	100	0.005	1	0
	2	"	"	1	0
	3	"	"	1	180
3	1	variable	0.005	1	0
	2	"	"	1	180
	3	"	"	1	180
4	1	120	0.005	1	0
	2	"	"	1	0
	3	"	"	1	0

Table 5-1 Theoretical data.

As before, we shall look for the closest value of ω_3 with respect to ω_2, still capable of being identified with good accuracy.

Influence of the frequency range

For the frequency range **97 Hz** to **104 Hz** it was not possible to obtain satisfactory results even with no added noise. For the range **92 Hz** to **108 Hz**, the results for the maximum resolution of the natural frequencies are given in Table 5-2.

Noise(%)	ω_2(Hz)	ω_3(Hz)
0	100	100.70
1	100	100.75
2	100	100.80
3	100	100.85

Table 5-2 Maximum natural frequency resolution with different levels of added noise (freq. range = 92 Hz to 108 Hz)

As for the **RFP** method, the performance of the program has a degree of dependence on the frequency range chosen (around the two modes). The choice of a wider frequency range encompassing the two modes is in general preferable, allowing for quite satisfactory results to be obtained.

Influence of the number of points used, L

The number of points taken into consideration showed the same influence on the results as in the case of the single FRF analysis: for two modes plus two residual ones the minimum number of data points is **9** and the adding of noise to the data showed that better results could be obtained if that value were increased up to **16** points, beyond which no significant improvement was found. For this reason, **16** points will be used, as for the **RFP** method.

Influence of the variation of the natural frequency from FRF to FRF

As the *raison d'être* of any global analysis is to obtain an unique set of

global properties, it is important to investigate to what extent the computer program can cope with variations in those properties (the most important being the natural frequency) from FRF to FRF. We shall analyse the behaviour of the program considering **2** FRFs, for the case where a variation on the natural frequency exists between them. The data used are presented in Table 5-3. We shall investigate the maximum variation possible in the natural frequencies for mode **2**. Modes **1** and **3** act as residual modes and a frequency range from **92 Hz** to **108 Hz** is used. The results are shown in Table 5-4.

Mode	FRF	ω_r(Hz)	ξ_r	C_r	ϕ_r
1	1	90	0.005	1	0
	2	90	0.005	1	0
2	1	100	0.005	1	0
	2	variable	0.005	1	180
3	1	110	0.005	1	0
	2	110	0.005	1	0

Table 5-3 Theoretical data to study the influence of variations of the natural frequency between FRFs.

	ω_2(Hz)	
	FRF	
Noise(%)	1	2
0	100	100.15
1	100	100.13
2	100	100.13
3	100	100.05

Table 5-4 Maximum variation allowed between the two FRFs.

Table 5-4 shows that the **GRFP** method only allows for a very small variation in the natural frequency between two FRFs, meaning that it is quite sensitive to such variations, bound to occur in experimental cases.

Experimental cases

In all the experimental data cases tried - where the FRFs were measured one at a time and not simultaneously - the program was unable to produce satisfactory results, certainly due to its sensitivity in coping with variations of the natural frequencies between the several FRFs. It must be remembered that, although the algorithm used here is already an extended "intelligent" version of the **GRFP** method, the calculation of the "global" properties is still based on the standard procedure, Eqs. (5-1) to (5-8 a). The difficulties encountered in the experimental cases led us to try an alternative to that standard procedure, which will be presented in the next Section (5-2-4).

Discussion

The version of the **GRFP** method that has been described above shows greater dependence on the frequency range chosen for the analysis (a wider one being preferable) and also a poorer capacity of identifying 2 close modes when compared with the **RFP** method. In addition, the method was found to be very sensitive to variations of the natural frequencies between different FRFs. In general it showed many difficulties, even when considering theoretical data, and could not perform effectively for experimental data. A new approach to the algorithm that will enable both theoretical and experimental data to be analysed with improved accuracy and reliability, will be presented next.

5-2-4 Improvement of the algorithm

In Section 5-2-1 we have presented an algorithm to calculate the global coefficients **{b}** of the characteristic polynomial of the system model under study. This was done by the development of Eq. (4-40 b), using Eq. (5-2), the final expression being Eq. (5-8 a). This development does not make explicit use of the intermediate calculations of coefficients **{d}**, associated with each individual FRF, as Eq. (5-1) is substituted into Eq. (5-2) to give Eq. (5-3). The mathematical derivation of the final expression (5-8 a) does not present any problems. On the other hand, for the single FRF case (RFP method), coefficients **{b}** can be calculated by direct use of Eq. (4-40 b) and, as we have shown in Chapter 4, the method works quite well in this case. Therefore, the explanation for the failure of the method when using Eq. (5-8 a) for the global coefficients **{b}** must be associated with numerical problems in the intermediate calculations. An alternative way to calculate the global coefficients **{b}** might be advantageous. But which alternative way ? One possibility will be to use Eq. (4-40 b) for each FRF. Considering **p** FRFs, we have

$$\{b\} = \begin{Bmatrix} [T_{bd}]_1 \{d\}_1 + \{R\}_1 \\ [T_{bd}]_2 \{d\}_2 + \{R\}_2 \\ \vdots \\ [T_{bd}]_p \{d\}_p + \{R\}_p \end{Bmatrix} \tag{5-26}$$

This means that we shall still have Eq. (5-8 a), but with $[U_G]_k$ and $\{V_G\}_k$ given by :

$$\begin{aligned} [U_G]_k &= [I] \\ \{V_G\}_k &= [T_{bd}]_k \{d\}_k + \{R\}_k \end{aligned} \tag{5-27}$$

Eq. (5-8 a) will then become

$$\{b\} = \left(\sum_{k=1}^{p} \{V_G\}_k\right)/p \qquad (5\text{-}28)$$

Eq. (5-28) simply represents the ordinary average of the coefficients **{b}** and it is nothing but a particular case of a least-squares procedure. Although not so elegant as the previous formulation, Eq. (5-28) proved to be much more efficient and reliable. It should also be stressed that this does not correspond to the classical method of analysing the several FRFs individually and averaging the natural frequencies and damping factors. With Eq. (5-28), what we are averaging are the coefficients of the characteristic polynomial, prior to the calculation of its roots. To calculate the roots after calculating the average values of the coefficients of the polynomials is not identical to calculate the roots of each polynomial and eventually calculating their average values; to average the coefficients **{b}** is a more rational procedure, consistent with the least-squares technique and with the philosophy of global FRF analysis.

Theoretical evaluation

The alternative way of calculating the coefficients **{b}** (Eq. (5-28)) was tried on the theoretical case study of Section 5-2-3. Previously, we could not obtain results for the frequency range **97 Hz** to **104 Hz**. Using the new procedure, we obtained the results shown in Table 5-5 which are clearly better than those of Table 5-2. Moreover, the global analysis no longer seems to be very sensitive to the frequency range any longer, as the results of Table 5-5 were not improved when the range **92 Hz** to **108 Hz** was chosen. On the other hand, the sensitivity to variations on the natural frequencies from FRF to FRF remained aproximately the same as presented in Table 5-4.

Noise(%)	ω_2(Hz)	ω_3(Hz)
0	100	100.01
1	100	100.50
2	100	100.60
3	100	100.70

Table 5-5 Maximum natural frequency resolution with different levels of added noise, using the new algorithm (freq. range = 97 Hz to 104 Hz).

Experimental cases

For all the experimental cases tried, the **GRFP** method worked quite satisfactorily, even when some of the FRFs failed to be analysed individually. The examples that will be presented below refer to some FRFs obtained from tests on an impeller, a structure that has recently been studied in our laboratory; this structure exhibits symmetrical geometry and therefore is susceptible to possessing very close modes.

Impeller -Example 1

In Section 4-2-3 we have already shown results from an analysis on a single FRF of this structure. Together with that FRF (Figs. 4-2 and 4-3), 2 more FRFs will be analysed (the three FRFs will be called FRF-1, FRF-2 and FRF-3, respectively). Fig. 5-2 shows FRF-2 and Fig. 5-3 its expansion around the modes under consideration. Figs. 5-4 and 5-5 show FRF-3 and its expansion, respectively. The results are presented in Table 5-6, with their normalized standard deviation in brackets. From Figs. 4-3, 5-3 and 5-5 one could say that no doubt would exist about the presence of two close modes, but it must be noted that the frequency resolution (4 Hz) is quite poor.

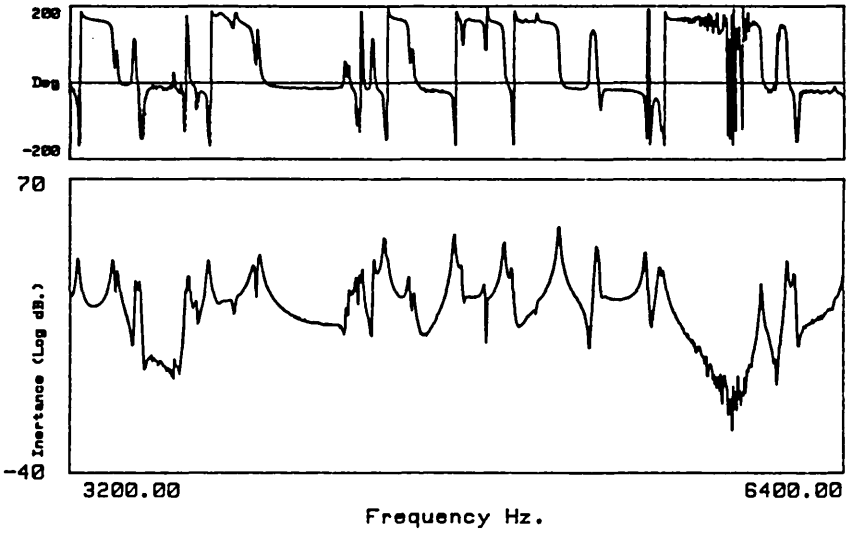

Fig. 5-2 Bode plot of FRF-2.

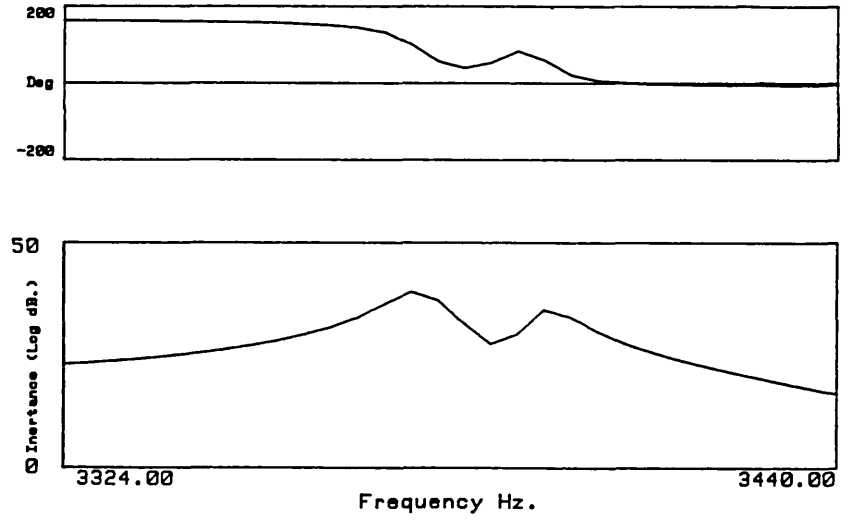

Fig. 5-3 Expanded Bode plot around the second double peak of Fig. 5-2.

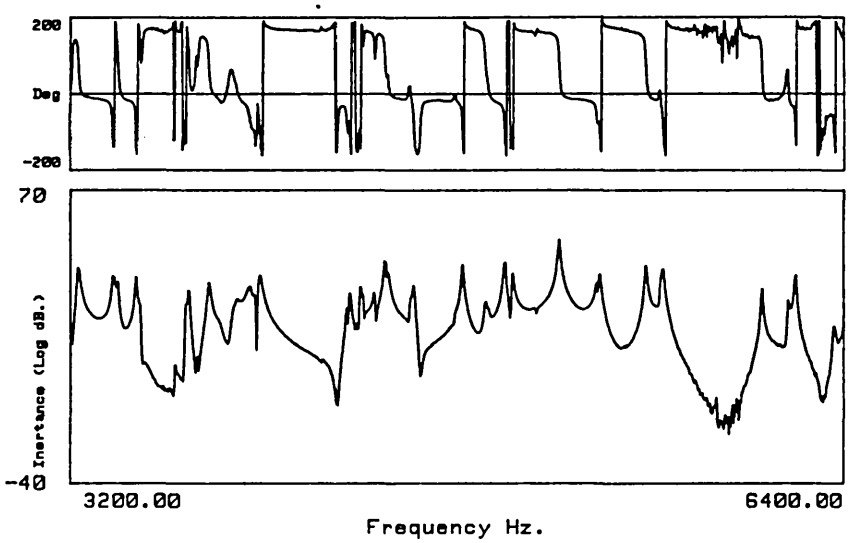

Fig. 5-4 Bode plot of FRF-3.

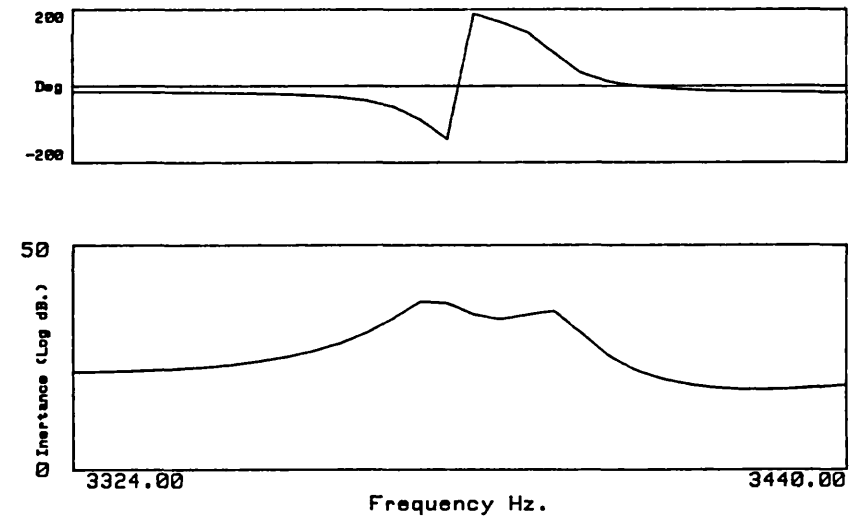

Fig. 5-5 Expanded Bode plot around the second double peak of Fig. 5-4.

Mode	FRF	ω_r	ξ_r	C_r	ϕ_r
1	1	3377.413 (0.001)	1.371×10^{-3} (1.441)	3.334×10^{-1} (1.264)	-13.87
	2	"	"	2.396×10^{-1} (1.133)	-13.61
	3	"	"	2.215×10^{-1} (0.783)	167.10
2	1	3395.897 (0.004)	1.088×10^{-3} (1.958)	1.214×10^{-1} (2.340)	-12.96
	2	"	"	1.080×10^{-1} (1.836)	-11.76
	3	"	"	1.356×10^{-1} (1.726)	-14.49

Table 5-6 Identification of the modes of the three FRFs (Figs. 4-3, 5-3 and 5-5).

The original and regenerated curves are presented in Figs. 5-6, 5-7 and 5-8, for FRFs-1, 2 and 3, respectively.

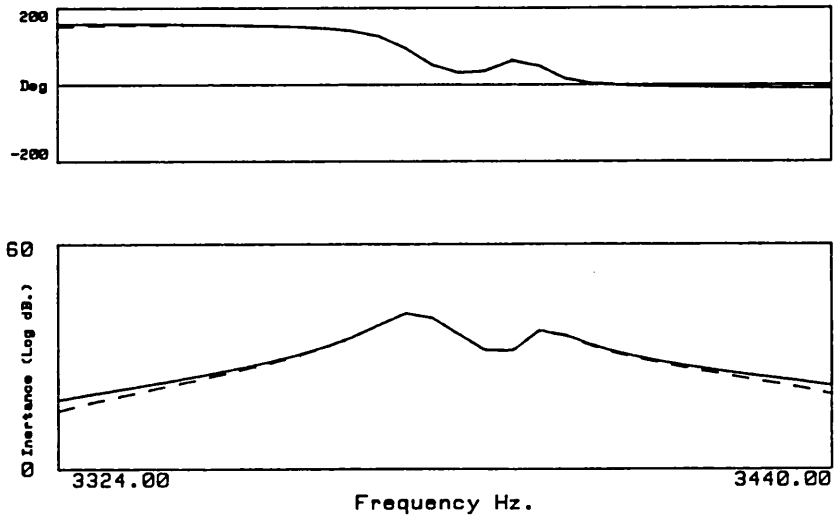

Fig. 5-6 Original (dotted line) and regenerated (solid line) FRF-1.

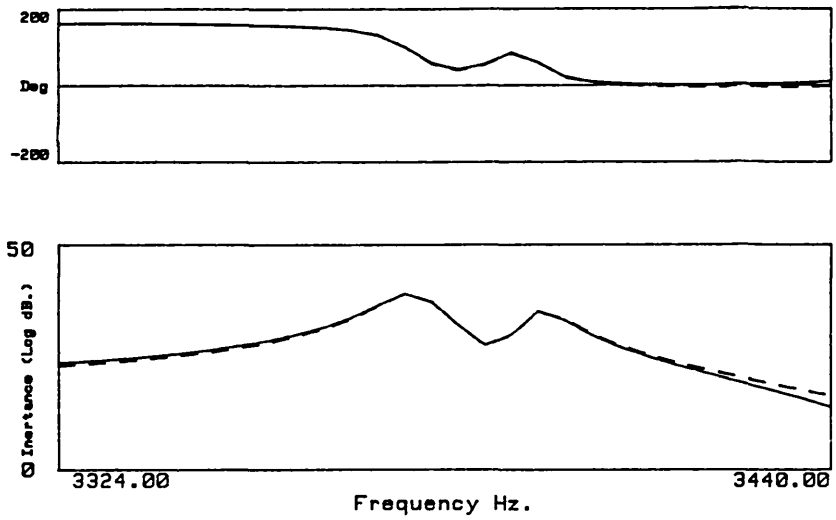

Fig. 5-7 Original (dotted line) and regenerated (solid line) FRF-2.

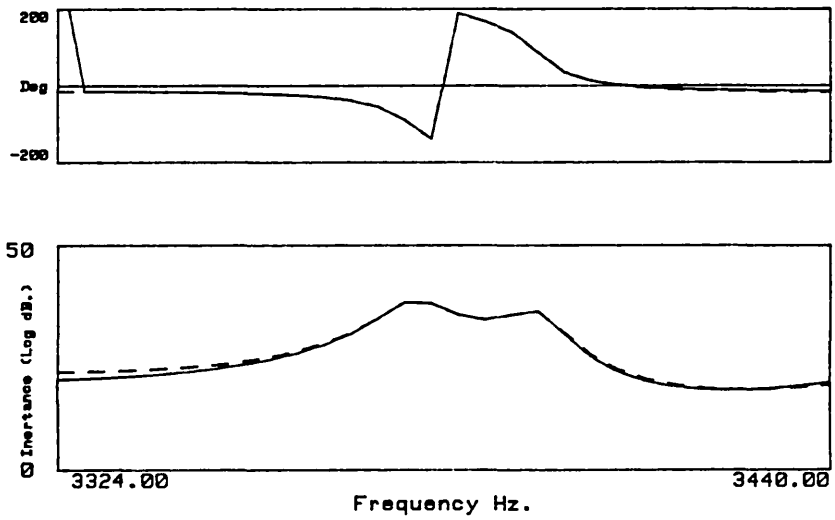

Fig. 5-8 Original (dotted line) and regenerated (solid line) FRF-3.

Comparison with the **RFP** method

In Table 5-7 the results for the three FRFs analysed individually are presented (for FRF-1, the results had already been presented in Table 4-10).

Mode	FRF	ω_r	ξ_r	C_r	ϕ_r
1	1	3377.223 (0.006)	1.368×10^{-3} (2.113)	3.286×10^{-1} (3.108)	-12.22
	2	3377.606 (0.006)	1.343×10^{-3} (2.284)	2.420×10^{-1} (3.818)	-15.06
	3	3377.355 (0.002)	1.370×10^{-3} (1.594)	2.217×10^{-1} (1.059)	168.02
2	1	3396.003 (0.011)	1.061×10^{-3} (2.244)	1.155×10^{-1} (3.550)	-14.80
	2	3395.590 (0.016)	1.082×10^{-3} (2.455)	1.096×10^{-1} (5.628)	-9.79
	3	3395.935 (0.002)	1.150×10^{-3} (1.721)	1.422×10^{-1} (1.588)	-14.52

Table 5-7 Identification of FRFs 1, 2 and 3, using the **RFP** method.

Comparing Table 5-7 with Table 5-6, we see that both results agree very well. From a conceptual point of view, we should rely more on the results from the global analysis and, in fact, the results point in that direction, as they show a smaller normalized standard deviation and also the regeneration is slightly better. However, it is not worth while to present here the regeneration for the single analysis of FRF-2 and FRF-3, as in this case the single analysis results are already quite good and from Figs. 4-4 and 5-6 we can understand that, in this case, the improvement achieved with the global analysis is not graphically perceptible.

Impeller - Example 2

When we tried to analyse, in the same frequency range, two other FRFs from the same structure (which will be called FRF-4 and FRF-5) using the **RFP** method, the program failed to identify them. We tried, then, to use the global analysis using FRFs 1, 4 and 5. The program managed to work and produced reasonable results. Figs. 5-9 and 5-10 show FRF-4 and FRF-5 and the results obtained for the global analysis of the three FRFs are presented in Table 5-8.

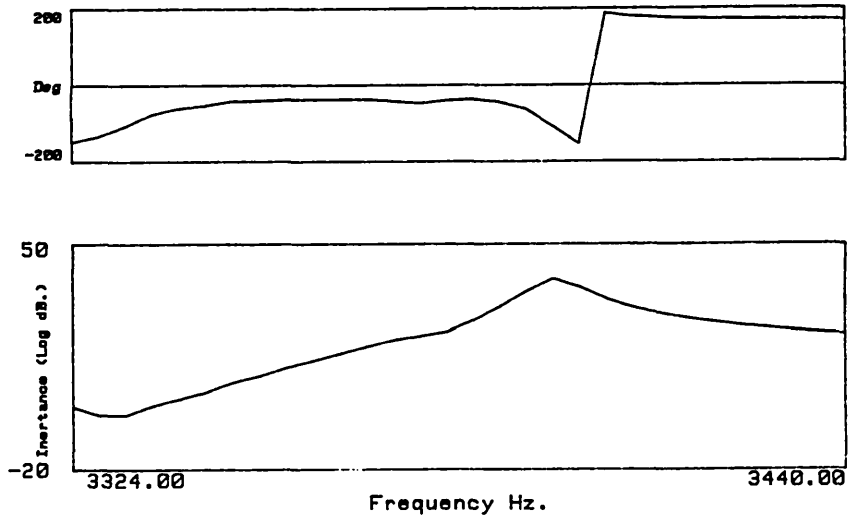

Fig. 5-9 Bode plot of FRF-4, in the same frequency range as the previous three.

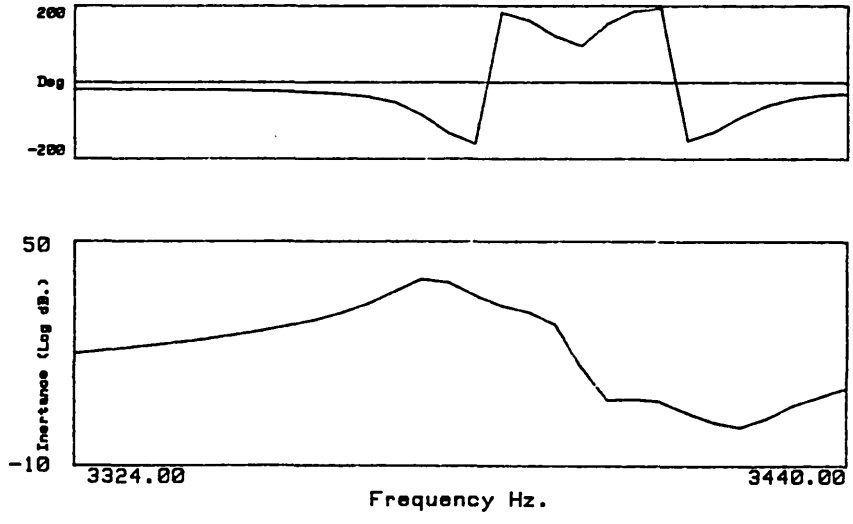

Fig. 5-10 Bode plot of FRF-5.

Mode	FRF	ω_r	ξ_r	C_r	ϕ_r
1	1	3377.153 (0.043)	9.853×10^{-4} (4.984)	2.494×10^{-1} (5.120)	-12.41
	4	"	"	9.446×10^{-3} (20.474)	134.70
	5	"	"	2.133×10^{-1} (5.275)	168.72
2	1	3396.057 (0.005)	1.058×10^{-3} (3.412)	1.279×10^{-1} (9.049)	-26.18
	4	"	"	1.999×10^{-1} (1.947)	164.69
	5	"	"	5.470×10^{-2} (22.584)	1.55

Table 5-8 Identification of FRFs 1, 4 and 5.

The original and regenerated curves are presented in Figs. 5-11, 5-12 and 5-13 for FRFs 1, 4 and 5, respectively.

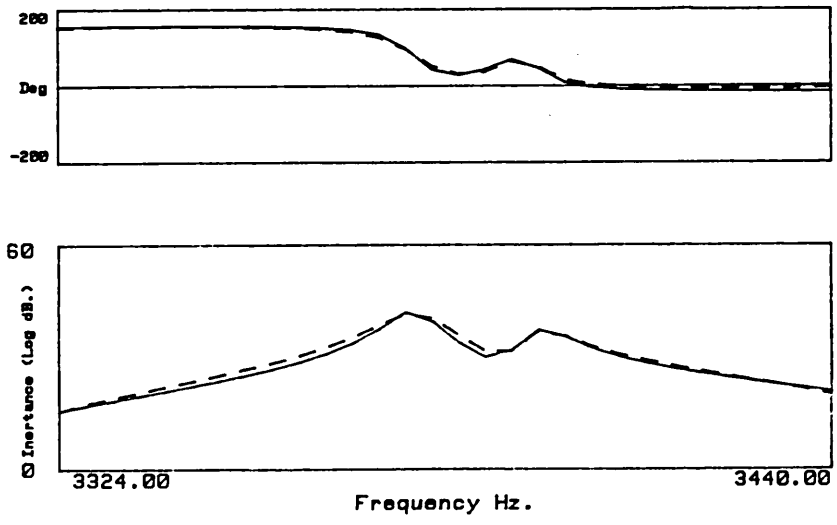

Fig. 5-11 Original (dotted line) and regenerated (solid line) FRF-1.

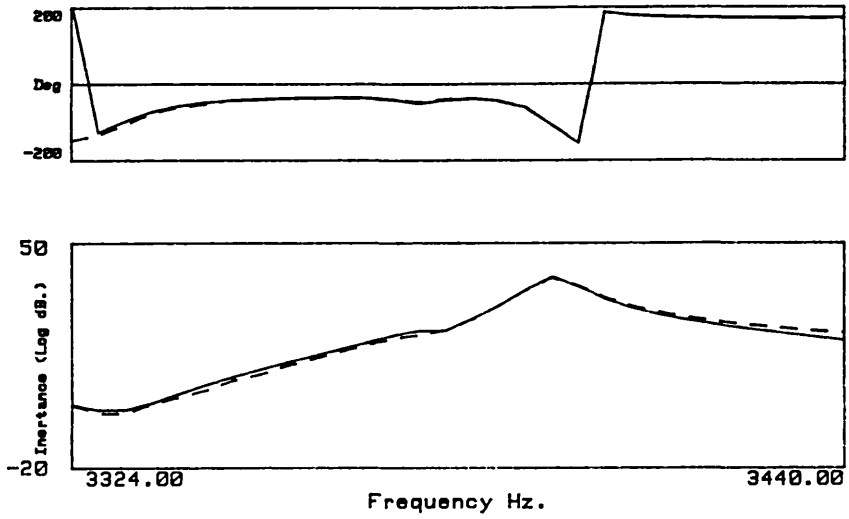

Fig. 5-12 Original (dotted line) and regenerated (solid line) FRF-4.

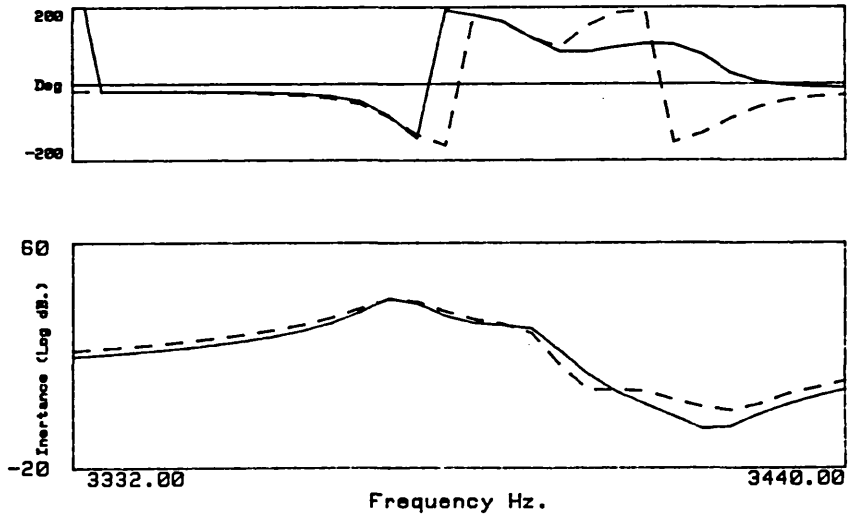

Fig. 5-13 Original (dotted line) and regenerated (solid line) FRF-5.

Comparing the global analysis of FRFs 1, 4 and 5 (Table 5-8) with the one of FRFs 1, 2 and 3 (Table 5-6) in terms of the global properties, we see that the results of Table 5-8 are worse, as the normalized standard deviation is higher. We also see that from the global analysis of FRFs 1, 4 and 5 the

regeneration for FRF-1 (Fig. 5-11) is poorer than the regeneration of FRF-1 from the global analysis of FRFs 1, 2 and 3 (Fig. 5-6), as FRF-1 has been affected by the "bad influence" of the other two problematic ones (FRFs 4 and 5). Even so, it was possible, with the **GRFP** method, to analyse these curves and the results, though not exceptional, can be considered as acceptable. It must be recalled that FRFs 4 and 5 could not be analysed by the **RFP** method.

Impeller - Example 3

In this example, we shall consider all five FRFs together. The results are presented in Table 5-9.

Mode	FRF	ω_r	ξ_r	C_r	ϕ_r
1	1	3377.231 (0.014)	1.118×10^{-3} (2.868)	2.846×10^{-1} (3.392)	-12.75
	2	"	"	2.062×10^{-1} (3.218)	-12.48
	3	"	"	1.899×10^{-1} (3.409)	168.21
	4	"	"	1.047×10^{-2} (12.716)	125.60
	5	"	"	2.447×10^{-1} (3.104)	168.59
2	1	3395.966 (0.003)	1.074×10^{-3} (2.121)	1.188×10^{-1} (8.676)	-20.88
	2	"	"	1.066×10^{-1} (6.382)	-17.99
	3	"	"	1.361×10^{-1} (4.114)	-10.54
	4	"	"	2.001×10^{-1} (1.710)	165.77
	5	"	"	5.594×10^{-2} (11.970)	-5.00

Table 5-9 Identification of FRFs 1, 2, 3, 4 and 5.

As FRFs 1, 2 and 3 could be previously analysed quite accurately, it is expected that Table 5-9 can provide evidence of better results for FRFs 4 and 5. Indeed, comparing Tables 5-9 and 5-8, we can see that the normalized standard deviation for FRFs 4 and 5 is now smaller. On the

other hand, we may also expect FRFs 4 and 5 to "pollute" the results of the other three FRFs, and this is confirmed by comparing Tables 5-9 and 5-6. In Figs. 5-14 to 5-18 the original and regenerated curves for the five FRFs are presented.

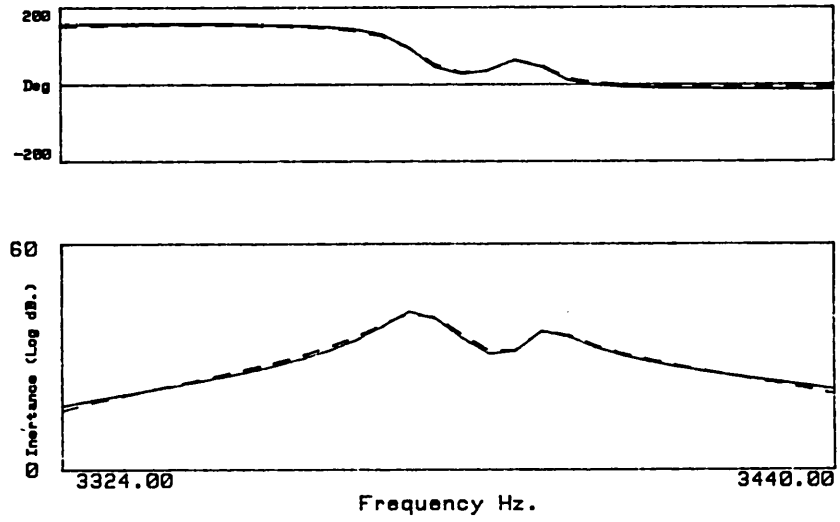

Fig. 5-14 Original (dotted line) and regenerated (solid line) FRF-1.

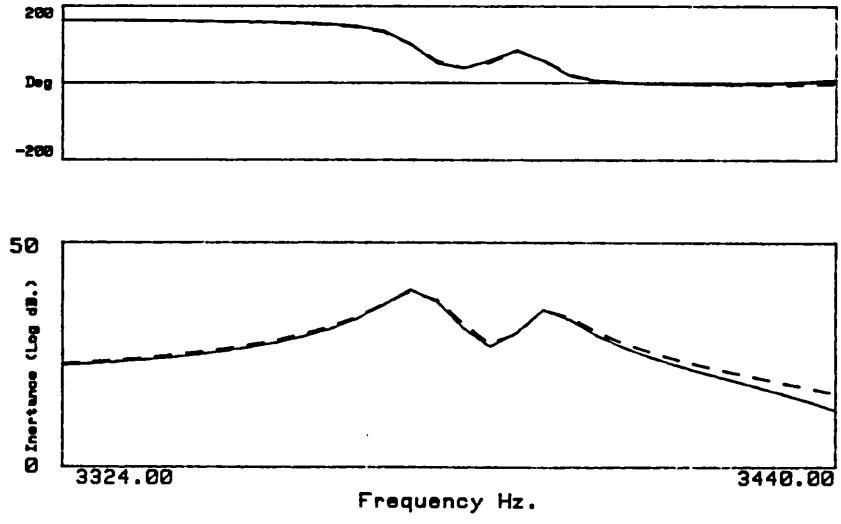

Fig. 5-15 Original (dotted line) and regenerated (solid line) FRF-2.

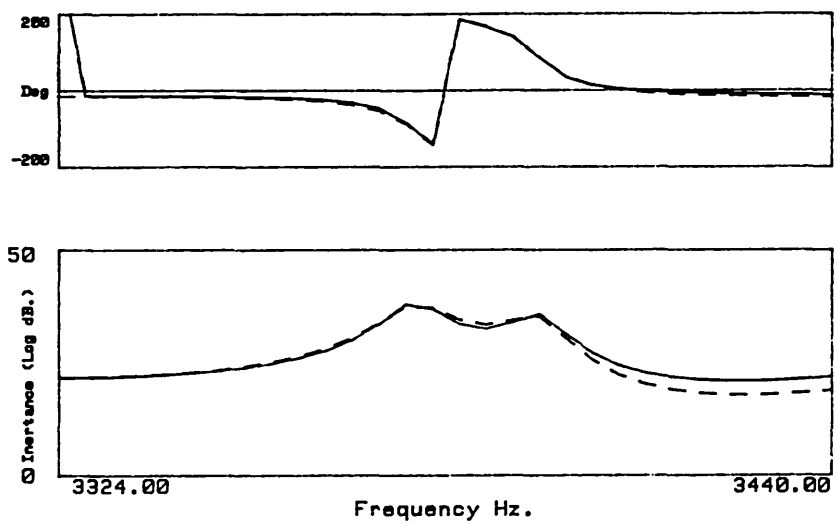

Fig. 5-16 Original (dotted line) and regenerated (solid line) FRF-3.

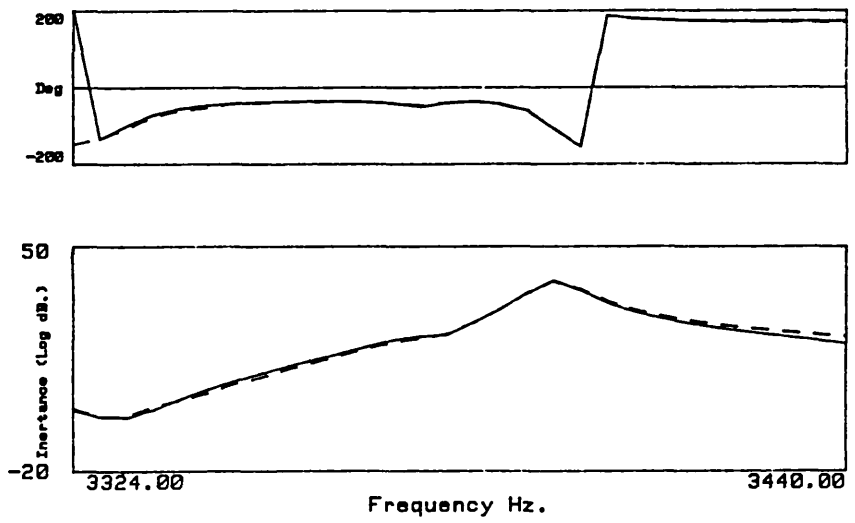

Fig. 5-17 Original (dotted line) and regenerated (solid line) FRF-4.

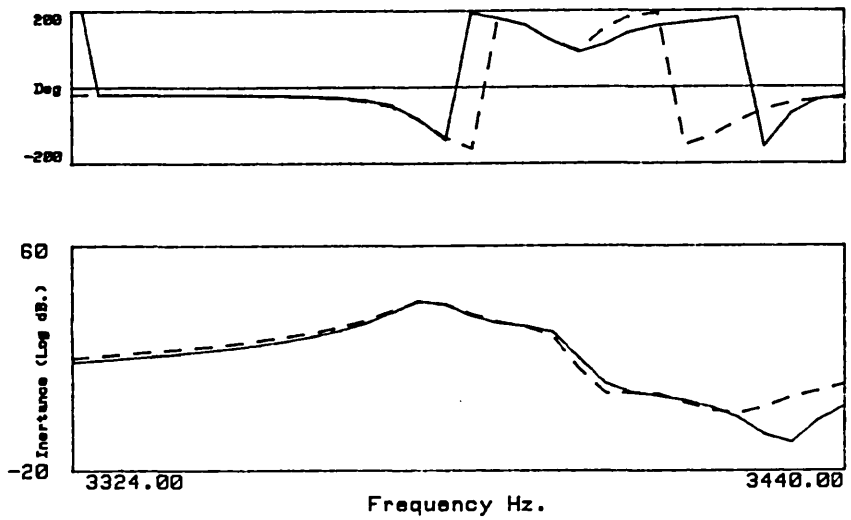

Fig. 5-18 Original (dotted line) and regenerated (solid line) FRF-5.

From these graphs, it is not easy to perceive the improvement in FRFs 4 and 5, as probably it is not easy either to verify that FRF-2 and FRF-3 are worse than before. However, by comparing Figs. 5-6, 5-11 and 5-14 (the three analyses of FRF-1), we can verify that the quality of the identification on this last graph is somewhere in between the other two.

Discussion

From the above examples we can conclude that the modification introduced in the calculation of the global parameters was a very valuable measure to take, as it enabled us to apply the method to identify real structures. However, the reason for this improvement is not clear from a theoretical point of view. It can also be concluded that to take more FRFs into the global curve-fitting has the effect of smoothing the results that may otherwise appear distorted by the presence of one or more "problematic" curves. When in doubt about the results caused by the above phenomenon, and especially if they present high normalized standard deviations, a

comparison with the single FRF analysis results may provide useful information. Finally, we can also conclude that the normalized standard deviation proved to be a very useful parameter as an indicator of the quality of the identification, not only in absolute terms but also relatively, for each mode and FRF.

5-2-5 Alternative way to calculate the global parameters

We have seen that in some cases it was not possible to obtain results for the analysis of single FRFs, but that the global analysis overcame this insurmountable stage. However, what if the opposite situation occurs, i.e., if we fail to analyse in the global sense and we only have at our disposal the individual results for each FRF ? The classical answer is simply to average the results for the global parameters. However, in this work, we have developed a useful parameter that we could make more use of: the normalized standard deviation of the modal parameters obtained in several runs of the computer program. Once it provides a reliable indication of the quality of the results, we can perform not a simple average of the results but instead a weighted average based upon it.

From the first example of the impeller, the results for the single FRF analysis were presented in Table 5-7. The weighted average of the natural frequency of mode **1** would be given by:

$$\omega_{1avg.} = \frac{3377.223/0.006 + 3377.606/0.006 + 3377.355/0.002}{1/0.006 + 1/0.006 + 1/0.002} = 3377.379 \text{ Hz}$$

For the second mode it would be:

$$\omega_{2avg.} = 3395.911 \text{ Hz}$$

Proceeding in the same way for the damping factor, we obtain the results of Table 5-10.

Mode	ω_r(Hz)	ξ_r
1	3377.379	1.362×10^{-3}
2	3395.911	1.103×10^{-3}

Table 5-10 Weighted average results based on the single FRF analysis.

By computing a simple average, the results would be (Table 5-11):

Mode	ω_r(Hz)	ξ_r
1	3377.394	1.360×10^{-3}
2	3395.843	1.098×10^{-3}

Table 5-11 Weighted average results based on the single FRF analysis.

Considering the global estimation results as exact, the relative error of each kind of average is (Table 5-12):

Average	Mode	$\varepsilon\,\omega_r$(%)	$\varepsilon\,\xi_r$(%)
Simple	1	0.0006	0.8023
	2	0.0016	0.9191
Weighted	1	0.0010	0.6565
	2	0.0004	0.0138

Table 5-12 Relative error of the single and weighted average results by comparison with the **GRFP** method.

From these results we can see that, especially for the damping factor, the

weighted average seems worth while using, as the errors are significantly smaller.

5-3 The Global method

5-3-1 Introduction

The method discussed in this section is referred to simply as "The Global method" and it is based on the works of Refs. [87] and [88]. As mentioned in Section 5-1, this is a *SIMO* method. Our objectives here are (i) to give a detailed explanation of the basic theory involved and of the specific techniques used, as such an explanation is not currently available in the literature, (ii) to extend the work already done in order to fulfil the objectives stated in Section 5-1 and (iii) to establish a comparison with the **GRFP** method. In particular, we shall be dealing once more with the problem of double modes and the introduction of criteria of decision and quality indicators that can provide us with more confidence in the results obtained.

5-3-2 Theory

Basic developments

The development presented here follows closely that given in Ref. [127], for the general case of non self-adjoint systems. The purpose is to present a rigorous development of the expressions of receptance and mobility, in terms of the modal properties. Let us consider the matrix equation of motion for a linear, viscously damped, N DOF system:

$$[M]\{\ddot{y}(t)\} + [C]\{\dot{y}(t)\} + [K]\{y(t)\} = \{F(t)\} \tag{5-29}$$

where **[M]**, **[C]** and **[K]** are **NxN** real symmetric matrices of mass, viscous damping and stiffness, respectively, **{F(t)}** is an **Nx1** complex vector of applied forces and **{y(t)}**, **{$\dot{y}$(t)}** and **{$\ddot{y}$(t)}** are **Nx1** complex vectors of displacement, velocity and acceleration, respectively. It is well known that in order to solve this **2nd** order linear differential equation it is convenient to define a **2Nx1** complex state vector **{u(t)}** as:

$$\{u(t)\} = \begin{Bmatrix} \{y(t)\} \\ \{\dot{y}(t)\} \end{Bmatrix} \tag{5-30}$$

In terms of this new variable, it is also well known that the equations of motion can be written as follows:

$$\begin{bmatrix} [C] & [M] \\ [M] & [0] \end{bmatrix} \{\dot{u}(t)\} + \begin{bmatrix} [K] & [0] \\ [0] & -[M] \end{bmatrix} \{u(t)\} = \begin{Bmatrix} \{F(t)\} \\ \{0\} \end{Bmatrix} \tag{5-31}$$

or, more simply,

$$[A]\{\dot{u}(t)\} + [B]\{u(t)\} = \{F'(t)\} \tag{5-32}$$

This formulation is often called as "state space analysis", by contrast with the usual "vector space analysis". **[A]** and **[B]** are **2Nx2N** real symmetric matrices and **{F'(t)}** is a **2Nx1** complex vector. Let us consider the homogeneous solution of (5-32), i. e., the free vibration solution with the right-hand-side of (5-32) set to zero:

$$[A]\{\dot{u}(t)\} + [B]\{u(t)\} = \{0\} \tag{5-33}$$

In the vector space, we look for a solution of (5-33) in the form

$$\{y(t)\} = \{\bar{y}\}\, e^{st} \tag{5-34}$$

where $\{\bar{y}\}$ is a **Nx1** complex vector representing the complex amplitude of the response and **s** is a complex quantity. The derivatives with respect to time will be

$$\{\dot{y}(t)\} = s\{\bar{y}\}\, e^{st} = s\{y(t)\} \tag{5-35}$$

$$\{\ddot{y}(t)\} = s^2\{\bar{y}\}\, e^{st} = s^2\{y(t)\} \tag{5-36}$$

Hence, the state vectors will be

$$\{u(t)\} = \begin{Bmatrix} \{\bar{y}\} \\ s\{\bar{y}\} \end{Bmatrix} e^{st} = \{\bar{u}\}\, e^{st} \tag{5-37}$$

$$\{\dot{u}(t)\} = \begin{Bmatrix} s\{\bar{y}\} \\ s^2\{\bar{y}\} \end{Bmatrix} e^{st} = s\{\bar{u}\}\, e^{st} \tag{5-38}$$

Therefore, a solution for (5-33) will have the form given in Eq. (5-37). Substituting (5-37) and (5-38) in (5-33), we obtain for all time **t**,

$$[s[A] + [B]]\{\bar{u}\} = \{0\} \tag{5-39}$$

Eq. (5-39) represents a generalized eigenproblem whose solution comprises a set of eigenvalues and eigenvectors. Because **[A]** and **[B]** are **2Nx2N** real matrices, the **2N** eigenvalues and eigenvectors will be real, or will exist in complex conjugate pairs. For the case in which we are interested, i. e., sub-critical damping, the values will always appear in complex conjugate pairs. The eigenvalues will be designated by s_r and s_r^* and the eigenvectors by $\{\psi_r'\}$ and $\{\psi_r'^*\}$, where * denotes complex conjugate. For the state space formulation, the eigenvectors will be

$$\{\psi_r'\} = \begin{Bmatrix} \{\psi_r\} \\ \{\psi_r\}\, s_r \end{Bmatrix} \tag{5-40}$$

$$\{\psi_r'^*\} = \begin{Bmatrix} \{\psi_r^*\} \\ \{\psi_r^*\}\, s_r^* \end{Bmatrix} \tag{5-41}$$

where $\{\psi_r\}$ and $\{\psi_r^*\}$ are the **Nx1** complex eigenvectors corresponding to the vector space coordinates **{y}**.

Assuming that it is possible to express the response of the **2Nx2N** state space system as a superposition of the responses of **2N** SDOF systems, for which the coordinates are designated by **p**, we have

$$\{u(t)\} = \sum_{r=1}^{2N} \{\psi_r'\}\, p_r(t) \tag{5-42}$$

The superposition of responses $\mathbf{p_r(t)}$ is weighted by the corresponding modal vector. In matrix form, (5-42) will become

$$\{u(t)\} = [\Psi']\,\{p(t)\} \tag{5-43}$$

where $[\Psi']$ is a **2Nx2N** complex matrix, which can be called as the state space modal matrix. Coordinates **{p}** are called the principal coordinates. For $\{\dot{u}(t)\}$, it will be:

$$\{\dot{u}(t)\} = [\Psi']\,\{\dot{p}(t)\} \tag{5-44}$$

Substituting (5-43) and (5-44) into (5-33) and pre-multiplying by $[\Psi']^T$, we obtain

$$[\Psi']^T [A]\,[\Psi']\,\{\dot{p}(t)\} + [\Psi']^T [B]\,[\Psi']\,\{p(t)\} = \{0\} \tag{5-45}$$

Due to the well known orthogonality properties, $[\Psi']^T$ **[A]** $[\Psi']$ and $[\Psi']^T$ **[B]** $[\Psi']$ are diagonal matrices, and so:

$$[\,a_r\,]\,\{\dot{p}(t)\} + [\,b_r\,]\{p(t)\} = \{0\} \tag{5-46}$$

Eqs. (5-46) are uncoupled and each of the **2N** solutions for **p(t)** is the solution for a **1** DOF system. Considering each solution to take the form

$$p_r(t) = \bar{p}_r\, e^{s_r t} \tag{5-47}$$

where $\bar{p}_r$ depends on the initial conditions, we have

$$(a_r s_r + b_r)\, \bar{p}_r e^{s_r t} = 0 \tag{5-48}$$

and so,

$$s_r = -\frac{b_r}{a_r} \tag{5-49}$$

Substituting (5-47) in (5-42), we obtain the free vibration response in terms of the state space coordinates:

$$\{u(t)\} = \sum_{r=1}^{2N} \{\psi_r'\}\, \bar{p}_r\, e^{s_r t} \tag{5-50}$$

$\bar{p}_r$ is a weighting factor associated with each mode $\{\psi_r'\}$, representing the contribution from each mode to the total response at each point. It is often described as a "modal participation factor".

Returning to the general equation of motion for forced vibration (5-32), and substituting Eqs. (5-43) and (5-44) into it, it follows that

$$[A]\,[\Psi']\,\{\dot{p}(t)\} + [B]\,[\Psi']\,\{p(t)\} = \{F'(t)\} \tag{5-51}$$

Pre-multiplying this equation by $[\Psi']^T$ and considering the orthogonality properties, we obtain

$$[\,a_r\,]\,\{\dot{p}(t)\} + [\,b_r\,]\{p(t)\} = [\Psi']^T\,\{F'(t)\} \tag{5-52}$$

As discussed above, expression (5-52) represents a set of **2N** uncoupled

equations. Considering Eq. (5-49), each of those **2N** equations can be written as

$$\dot{p}_r(t) - s_r p_r(t) = \frac{1}{a_r} \{\psi_r'\}^T \begin{Bmatrix} \{F(t)\} \\ \{0\} \end{Bmatrix} \tag{5-53}$$

For a harmonic excitation force vector of the form $\{\mathbf{F(t)}\} = \{\bar{F}\}e^{j\omega t}$, the response will be of the form $\{\mathbf{p(t)}\} = \{\bar{p}\}\, e^{j\omega t}$. Thus, Eq. (5-53) will become

$$(j\omega - s_r)\, \bar{p}_r = \frac{1}{a_r} \{\psi_r'\}^T \begin{Bmatrix} \{\bar{F}\} \\ \{0\} \end{Bmatrix} \tag{5-54}$$

and so,

$$\bar{p}_r = \left(\frac{1}{j\omega - s_r}\right) \frac{1}{a_r} \{\psi_r'\}^T \begin{Bmatrix} \{\bar{F}\} \\ \{0\} \end{Bmatrix} \tag{5-55}$$

Substituting (5-55) in (5-42) and considering harmonic excitation, we will obtain the forced response of the system:

$$\{u(t)\} = \sum_{r=1}^{2N} \{\psi_r'\} \left(\frac{1}{j\omega - s_r}\right) \frac{1}{a_r} \{\psi_r'\}^T \begin{Bmatrix} \{\bar{F}\} \\ \{0\} \end{Bmatrix} e^{j\omega t} \tag{5-56}$$

Normalizing the eigenvectors with respect to $\mathbf{a_r}$, we obtain

$$\{\phi_r'\} = \frac{1}{\sqrt{a_r}} \{\psi_r'\} \tag{5-57}$$

and Eq (5-56) becomes

$$\{u(t)\} = \sum_{r=1}^{2N} \{\phi_r'\} \left(\frac{1}{j\omega - s_r}\right) \{\phi_r'\}^T \begin{Bmatrix} \{\bar{F}\} \\ \{0\} \end{Bmatrix} e^{j\omega t} \tag{5-58}$$

where $\{\phi_r'\}$ is a **2Nx1** eigenvector of the form

$$\{\phi_r'\} = \begin{Bmatrix} \{\phi_r\} \\ \{\phi_r\}\, s_r \end{Bmatrix} \tag{5-59}$$

Considering Eq. (5-37) for harmonic response, i. e., for $s = j\omega$, and substituting (5-59) in (5-58), we obtain the expression for the amplitude of the response:

$$\begin{Bmatrix} \{\bar{y}\} \\ j\omega\{\bar{y}\} \end{Bmatrix} = \sum_{r=1}^{2N} \begin{Bmatrix} \{\phi_r\} \\ \{\phi_r\}\, s_r \end{Bmatrix} \left(\frac{1}{j\omega - s_r}\right) \begin{Bmatrix} \{\phi_r\} \\ \{\phi_r\}\, s_r \end{Bmatrix}^T \begin{Bmatrix} \{\bar{F}\} \\ \{0\} \end{Bmatrix} \tag{5-60}$$

or

$$\begin{Bmatrix} \{\bar{y}\} \\ j\omega\{\bar{y}\} \end{Bmatrix} = \sum_{r=1}^{2N} \begin{Bmatrix} \{\phi_r\} \\ \{\phi_r\}\, s_r \end{Bmatrix} \left(\frac{1}{j\omega - s_r}\right) \{\phi_r\}^T \{\bar{F}\} \tag{5-61}$$

We are now close to achieving our aim, i. e., to obtain expressions for the receptance and mobility in terms of the modal properties. Returning to the vector space coordinates and extracting the values of their amplitude responses, it follows that:

$$\{\bar{y}\} = \sum_{r=1}^{2N} \{\phi_r\} \left(\frac{1}{j\omega - s_r}\right) \{\phi_r\}^T \{\bar{F}\} \tag{5-62}$$

Likewise,

$$j\omega\{\bar{y}\} = \sum_{r=1}^{2N} \{\phi_r\}\, s_r \left(\frac{1}{j\omega - s_r}\right) \{\phi_r\}^T \{\bar{F}\} \tag{5-63}$$

The modal participation factors for Eqs. (5-62) and (5-63) correspond now to the product $\{\phi_r\}^T \{\bar{F}\}$. The receptance α_{ik} is defined as the

displacement at a point **i** due to a force at a point **k**, all other forces being zero ($\{\bar{F}\} = \{0\ 0 \ldots \bar{F}_k \ldots 0\ 0\}^T$). Thus, considering the response displacement $\bar{y}_i$, we have

$$\alpha_{ik}(j\omega) = \frac{\bar{y}_i}{\bar{F}_k} = \sum_{r=1}^{2N} {}_r\phi_i \left(\frac{1}{j\omega - s_r}\right) {}_r\phi_k \tag{5-64}$$

Eq. (5-63) becomes:

$$j\omega\alpha_{ik}(j\omega) = \sum_{r=1}^{2N} {}_r\phi_i\, s_r \left(\frac{1}{j\omega - s_r}\right) {}_r\phi_k \tag{5-65}$$

But $j\omega\, \alpha_{ik}(j\omega)$ is the mobility ($= \dot{\alpha}_{ik}(j\omega)$) and so,

$$\dot{\alpha}_{ik}(j\omega) = \sum_{r=1}^{2N} {}_r\phi_i\, s_r \left(\frac{1}{j\omega - s_r}\right) {}_r\phi_k \tag{5-66}$$

Because the eigenvalues and eigenvectors appear in complex conjugate pairs, we can write Eqs. (5-64) and (5-66) as

$$\alpha_{ik}(j\omega) = \sum_{r=1}^{N} \left[{}_r\phi_i\, (j\omega - s_r)^{-1}\, {}_r\phi_k + {}_r\phi_i^*\, (j\omega - s_r^*)^{-1}\, {}_r\phi_k^*\right] \tag{5-67}$$

$$\dot{\alpha}_{ik}(j\omega) = \sum_{r=1}^{N} \left[{}_r\phi_i\, s_r\, (j\omega - s_r)^{-1}\, {}_r\phi_k + {}_r\phi_i^*\, s_r^*\, (j\omega - s_r^*)^{-1}\, {}_r\phi_k^*\right] \tag{5-68}$$

From now on we shall make the approximation that the first term of the summations in Eqs. (5-67) and (5-68) are the ones that effectively contribute to the response of the system and that the second terms (complex conjugates) plus the modes that lie outside the frequency range of interest act as residuals. In these terms, Eqs. (5-67) and (5-68) will become

$$\alpha_{ik}(j\omega) = \sum_{r=1}^{N} {}_r\phi_i\, (j\omega - s_r)^{-1}\, {}_r\phi_k + R_1(j\omega) \tag{5-69}$$

$$\dot{\alpha}_{ik}(j\omega) = \sum_{r=1}^{N} {}_r\phi_i \, s_r \, (j\omega - s_r)^{-1} \, {}_r\phi_k + R_2(j\omega) \tag{5-70}$$

In matrix notation, we obtain:

$$\alpha_{ik}(j\omega) = \{{}_1\phi_i \, {}_2\phi_i \cdots {}_N\phi_i\} \begin{bmatrix} (j\omega - s_1) & & 0 \\ & (j\omega - s_2) & \\ 0 & & \ddots \\ & & & (j\omega - s_N) \end{bmatrix}^{-1} \begin{Bmatrix} {}_1\phi_k \\ {}_2\phi_k \\ \vdots \\ {}_N\phi_k \end{Bmatrix} + R_1(j\omega) \tag{5-71}$$

$$\dot{\alpha}_{ik}(j\omega) = \{{}_1\phi_i \, {}_2\phi_i \cdots {}_N\phi_i\} \begin{bmatrix} s_1 & & 0 \\ & s_2 & \\ 0 & & \ddots \\ & & & s_N \end{bmatrix} \begin{bmatrix} (j\omega - s_1) & & 0 \\ & (j\omega - s_2) & \\ 0 & & \ddots \\ & & & (j\omega - s_N) \end{bmatrix}^{-1} \begin{Bmatrix} {}_1\phi_k \\ {}_2\phi_k \\ \vdots \\ {}_N\phi_k \end{Bmatrix}$$

$$+ R_2(j\omega) \tag{5-72}$$

Specific developments concerning the Global method

As mentioned in the introduction, this method considers the excitation force at one point and the responses taken at several locations. As a consequence, we shall have several FRFs as defined in (5-71) where **i** varies and **k** remains the same. Considering **p** locations (i. e., p FRFs), it follows that

$$\begin{Bmatrix} \alpha_{1k}(j\omega) \\ \alpha_{2k}(j\omega) \\ \vdots \\ \alpha_{pk}(j\omega) \end{Bmatrix} = \begin{bmatrix} {}_1\phi_1 & {}_2\phi_1 & \cdots & {}_N\phi_1 \\ {}_1\phi_2 & {}_2\phi_2 & \cdots & {}_N\phi_2 \\ \vdots & \vdots & & \vdots \\ {}_1\phi_p & {}_2\phi_p & \cdots & {}_N\phi_p \end{bmatrix} \begin{bmatrix} (j\omega - s_1) & & 0 \\ & (j\omega - s_2) & \\ & & \ddots \\ 0 & & & (j\omega - s_N) \end{bmatrix}^{-1} \begin{Bmatrix} {}_1\phi_k \\ {}_2\phi_k \\ \vdots \\ {}_N\phi_k \end{Bmatrix} + \begin{Bmatrix} R_{11}(j\omega) \\ R_{12}(j\omega) \\ \vdots \\ R_{1p}(j\omega) \end{Bmatrix}$$

(5-73)

or,

$$\underset{(px1)}{\{\alpha_k(j\omega)\}} = \underset{(pxN)}{[\Phi]}\,\underset{(NxN)}{[\,(j\omega - s_r)\,]^{-1}}\,\underset{(Nx1)}{\{\phi_k\}^T} + \underset{(px1)}{\{R_1(j\omega)\}} \tag{5-74}$$

Similarly, from Eq. (5-72), we obtain

$$\underset{(px1)}{\{\dot{\alpha}_k(j\omega)\}} = \underset{(pxN)}{[\Phi]}\,\underset{(NxN)}{[\,s_r\,]}\,\underset{(NxN)}{[\,(j\omega - s_r)\,]^{-1}}\,\underset{(Nx1)}{\{\phi_k\}^T} + \underset{(px1)}{\{R_2(j\omega)\}} \tag{5-75}$$

The subscript **k** in Eqs. (5-73) to (5-75) means that the force is applied at a location **k**. If we define a vector **{g(jω)}** as

$$\underset{(Nx1)}{\{g(j\omega)\}} = \underset{(NxN)}{[\,(j\omega - s_r)\,]^{-1}}\,\underset{(Nx1)}{\{\phi_k\}^T} \tag{5-76}$$

and, dropping the subscript **k** for simplicity, we obtain

$$\{\alpha(j\omega)\} = [\Phi]\,\{g(j\omega)\} + \{R_1(j\omega)\} \tag{5-77}$$

$$\{\dot{\alpha}(j\omega)\} = [\Phi]\,[\,s_r\,]\,\{g(j\omega)\} + \{R_2(j\omega)\} \tag{5-78}$$

Considering the receptance at two nearby frequencies ω_i and ω_{i+c}, we obtain

$$\{\alpha(j\omega_i)\} = [\Phi]\,\{g(j\omega_i)\} + \{R_1(j\omega_i)\} \tag{5-79}$$

$$\{\alpha(j\omega_{i+c})\} = [\Phi]\,\{g(j\omega_{i+c})\} + \{R_1(j\omega_{i+c})\} \tag{5-80}$$

Subtracting Eq. (5-80) from Eqs. (5-79) , we obtain

$$\{\alpha(j\omega_i)\} - \{\alpha(j\omega_{i+c})\} = [\Phi]\{\{g(j\omega_i)\} - \{g(j\omega_{i+c})\}\} + \{R_1(j\omega_i)\} - \{R_1(j\omega_{i+c})\} \tag{5-81}$$

Now, we shall make the assumption that the effect of the out-of-range modes is a complex constant over the frequency range in which we are interested. This is the same principle as adopted by the "Bendent" method (Section 3-3-2). Accordingly, Eq. (5-81) becomes

$$\{\alpha(j\omega_i)\} - \{\alpha(j\omega_{i+c})\} = [\Phi]\{\{g(j\omega_i)\} - \{g(j\omega_{i+c})\}\} \quad (5\text{-}82)$$

or

$$\{\Delta\alpha(j\omega_i)\} = [\Phi]\{\Delta g(j\omega_i)\} \quad (5\text{-}83)$$

For the above assumption to be reasonable, ω_{i+c} must be close to ω_i but not so close that it might cause numerical problems later on. A reasonable value for **c** must be established when we undertake the computer implementation.

Using the same principle, we obtain for the mobility:

$$\{\Delta\dot{\alpha}(j\omega_i)\} = [\Phi]\,[\,s_r\,]\,\{\Delta g(j\omega_i)\} \quad (5\text{-}84)$$

Considering **L** measured points in the frequency range of interest (that will have at least **L+c** points for the differences to be calculated), Eqs. (5-83) and (5-84) become

$$[\{\Delta\alpha(j\omega_1)\}\ \{\Delta\alpha(j\omega_2)\}\ \ldots\ \{\Delta\alpha(j\omega_L)\}] = [\Phi]\,[\{\Delta g(j\omega_1)\}\ \{\Delta g(j\omega_2)\}\ \ldots\{\Delta g(j\omega_L)\}] \quad (5\text{-}85)$$

$$[\{\Delta\dot{\alpha}(j\omega_1)\}\ \{\Delta\dot{\alpha}(j\omega_2)\}\ \ldots\ \{\Delta\dot{\alpha}(j\omega_L)\}] = [\Phi]\,[\,s_r\,]\,[\{\Delta g(j\omega_1)\}\ \{\Delta g(j\omega_2)\}\ \ldots\{\Delta g(j\omega_L)\}] \quad (5\text{-}86)$$

or

$$[\Delta\alpha] = [\Phi]\,[\Delta g] \qquad (5\text{-}87)$$
(pxL) (pxN) (NxL)

$$[\dot{\Delta\alpha}] = [\Phi]\,[\,s_r\,]\,[\Delta g] \qquad (5\text{-}88)$$
(pxL) (pxN) (NxN) (NxL)

It will be assumed that

$$L \geq p \geq N \qquad (5\text{-}89)$$

which means the availability of more FRFs than the number of modes and more frequency data points than the number of FRFs. Now, we shall eliminate [Δg] between Eqs. (5-87) and (5-88).

$$[\Delta g] = [\Phi]^{+}\,[\Delta\alpha] \qquad (5\text{-}90)$$
(NxL) (Nxp) (pxL)

where $[\Phi]^{+}$ is the pseudo-inverse of [Φ], given by

$$[\Phi]^{+} = ([\Phi^{*}]^{T}\,[\Phi])^{-1}\,[\Phi^{*}]^{T} \qquad (5\text{-}91)$$
(Nxp) (NxN) (Nxp)

and from Eq. (5-88),

$$[\Delta g] = [\,s_r\,]^{-1}\,[\Phi]^{+}\,[\dot{\Delta\alpha}] \qquad (5\text{-}92)$$
(NxL) (NxN) (Nxp) (pxL)

Combining Eqs. (5-90) and (5-92),

$$[\Phi]^{+}\,[\Delta\alpha] = [\,s_r\,]^{-1}\,[\Phi]^{+}\,[\dot{\Delta\alpha}] \qquad (5\text{-}93)$$

or

$$[\Delta\alpha]^{T}\,[\Phi]^{+T}\,[\,s_r\,] = [\dot{\Delta\alpha}]^{T}\,[\Phi]^{+T} \qquad (5\text{-}94)$$
(Lxp) (pxN) (NxN) (Lxp) (pxN)

Making a change of variable as

$$[z] = [\Phi]^{+T} \tag{5-95}$$

we obtain the following generalized eigenproblem

$$[[\Delta\dot{\alpha}]^T - s_r [\Delta\alpha]^T]\{z_r\} = \{0\} \tag{5-96}$$

As we shall be dealing with experimentally acquired data, $\Delta\alpha$ and $\Delta\dot{\alpha}$ will be denoted, respectively, as $\Delta\tilde{\alpha}$ and $\Delta\dot{\tilde{\alpha}}$ from now on. Thus, Eq. (5-96) will be written as:

$$[[\Delta\dot{\tilde{\alpha}}]^T - s_r [\Delta\tilde{\alpha}]^T]\{z_r\} = \{0\} \tag{5-96 a}$$

This equation enables the calculation of the eigenvalues s_r and, consequently, the global parameters (natural frequencies and damping factors). Later on, we shall see how to calculate the local parameters (modal constants and phase angles). Before that, we shall make some remarks about Eq. (5-96 a). Matrix $[\Delta\tilde{\alpha}]^T$ is calculated directly from the measured receptance FRFs. The calculation of matrix $[\Delta\dot{\tilde{\alpha}}]^T$ is easy, as there is a simple relationship between receptance and mobility:

$$\dot{\alpha}(j\omega) = j\omega\, \alpha(j\omega) \tag{5-97}$$

Hence, for each element of matrix $[\Delta\tilde{\alpha}]^T$, given by

$$\tilde{\alpha}(j\omega_i) - \tilde{\alpha}(j\omega_{i+c}) \tag{5-98}$$

we shall have a corresponding element of matrix $[\Delta\dot{\tilde{\alpha}}]^T$, given by

$$j\omega_i\, \tilde{\alpha}(j\omega_i) - j\omega_{i+c}\, \tilde{\alpha}(j\omega_{i+c}) \tag{5-99}$$

So, matrices $[\Delta\tilde{\alpha}]^T$ and $[\Delta\dot{\tilde{\alpha}}]^T$ are easy to obtain. However, we may experience some difficulty in solving Eq. (5-96 a) due to the fact that the matrices involved will be, in general, rank deficient, since we usually have more FRFs than modes. This could be solved in a least-squares sense, pre-multiplying Eq. (5-96 a) by the hermitian transpose of $[\Delta\tilde{\alpha}]^T$. But the resulting matrices would still be of order **p** and we are looking for **N** eigenvalues (p>N), so the matrices would still be rank deficient (their ranks are exactly equal to N).

A good eigensolution routine (Ref.[128]) could solve the problem, and from the **p** eigenvalues we could extract the significant **N** values for our solution. It must be remembered that in practical situations, with noisy data, we may not be sure of the number of genuine existing modes and so **N** is not a known quantity. To determine **N** (and therefore the rank of the matrices) we shall make use of the Singular Value Decomposition (Ref. [129]) , a technique that has many applications (Ref. [130]) and is the best known way of computing the rank of a matrix. In Appendix D, an explanation of this technique is given, together with references to the most significant articles published on the subject.

Use of the Singular Value Decomposition

The Singular Value Decompositon (SVD) of a **Lxp** complex matrix **[A]** ($L \geq p$) is given by

$$[A] = [U]\,[\Sigma]\,[V]^H \tag{5-100}$$

where the superscript ^{H} denotes hermitian transpose and **[U]** and **[V]** are unitary complex matrices of order **LxL** and **pxp**, respectively. **[Σ]** is an

Lxp real matrix, with elements $\sigma_{ij} = 0$ if $i \neq j$ and $\sigma_{ii} = \sigma_i \geq 0$. The quantities σ_i are the singular values of [A]. Matrix [Σ] is of the form

$$[\Sigma] = \underbrace{\begin{bmatrix} \sigma_1 & & 0 \\ & \sigma_2 & \\ & \ddots & \\ 0 & & \sigma_p \\ \hline & 0 & \end{bmatrix}}_{p} \begin{matrix} \} p \\ \} L\text{-}p \end{matrix} \qquad (5\text{-}101)$$

We shall assume that $\sigma_1 > \sigma_2 > \ldots > \sigma_p$ (most of the SVD routines give the results in this form). In matrix [Σ] there will be **N** high values of σ_i and **p-N** small values. The comparison between the magnitude of these values enables us to determine the rank of the matrix and, therefore, the number of genuine modes, **N**. We must establish, then, a criterion that can recognize the relative magnitudes of the singular values. In Ref. [88] it is suggested the graphical representation of the sucessive ratios of the singular values, i. e., σ_1/σ_2 , σ_2/σ_3 , etc. As the rank is equal to **N**, σ_{N+1} will be much smaller than σ_N and therefore the ratio σ_N/σ_{N+1} will have a very high value, and a peak will be clearly visible on the graph. We have decided here to consider the rank as the value corresponding to the maximum result of the several ratios, because in this way there is no need to make a judgement based on the referred graph.

The SVD technique will be applied to $[\Delta\tilde{\alpha}]^T$ and $[\dot{\Delta\tilde{\alpha}}]^T$, and it is noted that both these matrices should obviously have the same rank, **N**. Their decomposition is given by

$$\underset{(Lxp)}{[\Delta\tilde{\alpha}]^T} = \underset{(LxL)}{[U]_\alpha} \underset{(Lxp)}{[\Sigma]_\alpha} \underset{(pxp)}{[V]_\alpha^H} \qquad (5\text{-}102)$$

$$\underset{(Lxp)}{[\Delta\tilde{\alpha}]^T} = \underset{(LxL)}{[U]_{\dot{\alpha}}}\ \underset{(Lxp)}{[\Sigma]_{\dot{\alpha}}}\ \underset{(pxp)}{[V]_{\dot{\alpha}}^H} \qquad (5\text{-}103)$$

As the rank of $[\Delta\dot{\tilde{\alpha}}]^T$ is the same for $[\Delta\tilde{\alpha}]^T$ it would seem pointless to decompose $[\Delta\dot{\tilde{\alpha}}]^T$. However, there is an advantage in doing so, as we shall see next. Having calculated the rank, we will have **p-N** small values of σ_i, but not exactly zero as they should be if the data were noiseless. This means that $[\Delta\tilde{\alpha}]^T$ and $[\Delta\dot{\tilde{\alpha}}]^T$ can be "improved" if we recalculate them after setting to zero the small **p-N** singular values in matrices $[\Sigma]_\alpha$ and $[\Sigma]_{\dot{\alpha}}$. The new matrix $[\Sigma]_\alpha'$ will be of the form

$$[\Sigma]_\alpha' = \begin{bmatrix} \sigma_1 & & & & \\ & \sigma_2 & & 0 & \\ & & \ddots & & \\ & 0 & & \sigma_N & \\ \hline & & & & \\ & 0 & & 0 & \\ & & & & \\ \hline & & 0 & & \end{bmatrix} \begin{matrix} \left.\vphantom{\begin{matrix}a\\b\\c\end{matrix}}\right\} N \\ \left.\vphantom{\begin{matrix}a\\b\\c\end{matrix}}\right\} p \\ \left.\vphantom{\begin{matrix}a\\b\end{matrix}}\right\} L\text{-}p \end{matrix} \qquad (5\text{-}104)$$

$$\underbrace{\qquad\qquad}_{p}$$

The "improved" matrices $[\Delta\tilde{\alpha}]^{T'}$ and $[\Delta\dot{\tilde{\alpha}}]^{T'}$ will be given by

$$[\Delta\tilde{\alpha}]^{T'} = [U]_\alpha\ [\Sigma]_\alpha'\ [V]_\alpha^H \qquad (5\text{-}105)$$

$$[\Delta\dot{\tilde{\alpha}}]^{T'} = [U]_{\dot{\alpha}}\ [\Sigma]_{\dot{\alpha}}'\ [V]_{\dot{\alpha}}^H \qquad (5\text{-}106)$$

where only the first **N** columns of **[U]** and the first **N** rows of $[V]^H$ will contribute to the product, because only the first **N** singular values of $[\Sigma]_\alpha'$ and $[\Sigma]_{\dot{\alpha}}'$ are non-zero, i. e.,

$$[\Delta\tilde{\alpha}]^{T'} = [U]_{\alpha}\,[\Sigma]_{\alpha}'\,[V]_{\alpha}^{H} \qquad (5\text{-}107)$$
(Lxp) (LxN) (NxN) (Nxp)

$$\dot{[\Delta\tilde{\alpha}]}^{T'} = [U]_{\dot{\alpha}}\,[\Sigma]_{\dot{\alpha}}'\,[V]_{\dot{\alpha}}^{H} \qquad (5\text{-}108)$$
(Lxp) (LxN) (NxN) (Nxp)

Considering the new matrices $[\Delta\tilde{\alpha}]^{T'}$ and $\dot{[\Delta\tilde{\alpha}]}^{T'}$, relations (5-87) and (5-88) still hold, becoming

$$[\Delta\tilde{\alpha}]' = [\Phi]\,[\Delta g] \qquad (5\text{-}109)$$

$$\dot{[\Delta\tilde{\alpha}]}' = [\Phi]\,[\dot{s}_r]\,[\Delta g] \qquad (5\text{-}110)$$

Using a similar route to that which led to Eq. (5-96 a), we obtain

$$\left[\dot{[\Delta\tilde{\alpha}]}^{T'} - s_r\,[\Delta\tilde{\alpha}]^{T'}\right]\{z_r\} = \{0\} \qquad (5\text{-}111)$$

We can solve Eq. (5-111) by pre-multiplying it by the pseudo-inverse of $[\Delta\tilde{\alpha}]^{T'}$:

$$\Big[\underbrace{([\Delta\tilde{\alpha}]^{T'})^{+}\,\dot{[\Delta\tilde{\alpha}]}^{T'}}_{(pxp)} - s_r\,[\,I\,]\Big]\{z_r\} = \{0\} \qquad (5\text{-}112)$$
(pxp)

which is a problem of eigenvalues and eigenvectors of a complex matrix. To calculate the pseudo-inverse of $[\Delta\tilde{\alpha}]^{T'}$, we can make use of its singular value decomposition. Considering Eq. (5-107), but before having taken away the **p-N** zero singular values, we have

$$[\Delta\tilde{\alpha}]^{T'} = [U]_{\alpha}\,[\Sigma]_{\alpha}'\,[V]_{\alpha}^{H} \qquad (5\text{-}113)$$
(Lxp) (LxL) (Lxp) (pxp)

Thus,

$$([\Delta\tilde{\alpha}]^{T'})^{+} = ([V]_{\alpha}^{H})^{+}\,([\Sigma]_{\alpha}')^{+}\,([U]_{\alpha})^{+} \qquad (5\text{-}114)$$
(pxL) (pxp) (pxL) (LxL)

But the pseudo-inverse of a square matrix coincides with its simple inverse, and so,

$$\underset{(pxL)}{([\Delta\tilde{\alpha}]^{T'})^{+}} = \underset{(pxp)}{([V]_{\alpha}^{H})^{-1}} \underset{(pxL)}{([\Sigma]_{\alpha}')^{+}} \underset{(LxL)}{([U]_{\alpha})^{-1}} \tag{5-115}$$

Remembering that $[V]_{\alpha}$ and $[U]_{\alpha}$ are unitary matrices, for which the hermitian transpose equals the inverse, we obtain:

$$\underset{(pxL)}{([\Delta\tilde{\alpha}]^{T'})^{+}} = \underset{(pxp)}{[V]_{\alpha}} \underset{(pxL)}{([\Sigma]_{\alpha}')^{+}} \underset{(LxL)}{[U]_{\alpha}^{H}} \tag{5-116}$$

The pseudo-inverse of a rectangular diagonal matrix like $[\Sigma]_{\alpha}'$ given by Eq. (5-104) is defined in the following form:

$$([\Sigma]_{\alpha}')^{+} = \left[\begin{array}{ccc|c|c} 1/\sigma_1 & & & & \\ & 1/\sigma_2 & 0 & & \\ & \ddots & & 0 & 0 \\ 0 & & 1/\sigma_N & & \\ \hline & 0 & & 0 & \\ & & & \ddots & \\ & & & & 0 \end{array}\right] \begin{array}{l} \Big\} \text{p} \end{array} \tag{5-117}$$

$$\underbrace{\qquad\qquad}_{N} \qquad \underbrace{\qquad\qquad\qquad}_{p} \; \underbrace{\quad}_{L-p}$$

such that

$$\underset{(pxL)}{([\Sigma]_{\alpha}')^{+}} \underset{(Lxp)}{([\Sigma]_{\alpha}')} = \underset{(pxp)}{[\,I\,]'} \tag{5-118}$$

where $[\,I\,]'$ is a diagonal matrix with **N** unit values and **p-N** zeros. Now, only the first **N** columns of $[V]_{\alpha}$ and the first **N** rows of $[U]_{\alpha}^{H}$ will

contribute to the product, and we will have

$$\underset{(pxL)}{([\Delta\tilde{\alpha}]^{T'})^{+}} = \underset{(pxN)}{[V]_{\alpha}} \underset{(NxN)}{([\Sigma]_{\alpha}')^{-1}} \underset{(NxL)}{[U]_{\alpha}^{H}} \tag{5-119}$$

As we already know $[V]_{\alpha}$ and $[U]_{\alpha}^{H}$, we only have to calculate the inverses of the **N** singular values in order to evaluate the pseudo-inverse. Substituting Eq. (5-119) in (5-112), we obtain

$$[[A_S] - s_r [I]] \{z_r\} = \{0\} \tag{5-120}$$

where $[A_S]$ is a **pxp** complex matrix which is called the system matrix, given by

$$[A_S] = [V]_{\alpha} ([\Sigma]_{\alpha}')^{-1} [U]_{\alpha}^{H} [\Delta\tilde{\alpha}]^{T'} \tag{5-121}$$

This eigenvalue problem will produce **N** non-zero eigenvalues and **p-N** zero eigenvalues.

Note on the use of differences of forced response

We have made use of the differences of forced responses to obtain the final eigenproblem of Eq. (5-120). The advantage of doing so is that the residual influence of extra modes is taken directly into consideration. But is it really necessary to use those differences, or could we just take the responses as measured and incorporate the residuals later ? We shall discuss this point based on the response of a SDOF system. For this case, and according to inequality (5-89), one FRF and one data point should be enough to calculate the eigenvalue. Let us consider Eq. (5-96 a), with the responses instead of their differences. For a single degree-of-freedom, Eq. (5-96 a) would give

$$(\tilde{\alpha} - s_r \tilde{\alpha})\, z_r = 0 \tag{5-122}$$

Considering the response at a frequency ω_0, $\dot{\tilde{\alpha}} = j\,\omega_0\,\tilde{\alpha}$, and

$$(j\omega_0\tilde{\alpha} - s_r \tilde{\alpha})\, z_r = 0 \tag{5-123}$$

Hence,

$$s_r = j\omega_0 \tag{5-124}$$

This simple example is enough to prove that the method does not work when only the responses are used, as we would obtain only pure imaginary results, i. e., the damping values would be zero. Let us consider now, for the same case, the difference of responses between two data points, **1** and **2**. Here,

$$\Delta\dot{\tilde{\alpha}} = \dot{\tilde{\alpha}}_2 - \dot{\tilde{\alpha}}_1 = j(\omega_2\tilde{\alpha}_2 - \omega_1\tilde{\alpha}_1) \tag{5-125}$$

and so, Eq. (5-96 a) would be

$$[j(\omega_2\tilde{\alpha}_2 - \omega_1\tilde{\alpha}_1) - s_r(\tilde{\alpha}_2 - \tilde{\alpha}_1)]\, z_r = 0 \tag{5-126}$$

and

$$s_r = j\frac{\omega_2\tilde{\alpha}_2 - \omega_1\tilde{\alpha}_1}{\tilde{\alpha}_2 - \tilde{\alpha}_1} \tag{5-127}$$

But $\tilde{\alpha}_1$ and $\tilde{\alpha}_2$ are given by

$$\tilde{\alpha}_1 = \frac{A + jB}{j\omega_1 - s_r} \tag{5-128}$$

$$\tilde{\alpha}_2 = \frac{A + jB}{j\omega_2 - s_r} \tag{5-129}$$

Substituting (5-128) and (5-129) in (5-127), we obtain

$$s_r = j\frac{\dfrac{\omega_2}{j\omega_2 - s_r} - \dfrac{\omega_1}{j\omega_1 - s_r}}{\dfrac{1}{j\omega_2 - s_r} - \dfrac{1}{j\omega_1 - s_r}} \tag{5-130}$$

or

$$s_r = j\frac{j\omega_1\omega_2 - s_r\omega_2 - j\omega_1\omega_2 + \omega_1 s_r}{j\omega_1 - s_r - j\omega_2 + s_r} \tag{5-131}$$

Hence,

$$s_r = \frac{js_r(\omega_1 - \omega_2)}{j(\omega_1 - \omega_2)} \tag{5-132}$$

from which,

$$s_r = s_r \tag{5-133}$$

The identity (5-133) proves that by taking the differences of response, the eigenvalue could be recovered.

Calculation of the eigenvectors

Having calculated the eigenvalues using Eq. (5-120), we know the global parameters of the system, i. e., the natural frequencies and damping ratios. Now, we can go back to each FRF to calculate the local parameters, i. e., modal constants and phase angles. Eq. (5-69) will be rewritten as

$$\tilde{\alpha}_{ik}(j\omega) = \sum_{r=1}^{N} \frac{{}_rA_{ik}}{j\omega - s_r} + R_1(j\omega) \tag{5-134}$$

where

$${}_rA_{ik} = {}_r\phi_i \, {}_r\phi_k \tag{5-135}$$

is the residue of mode **r**. Considering the residual term $\mathbf{R_1}(j\omega)$ of the form†

$$R_1(j\omega) = R_K + \frac{R_M}{\omega^2} \tag{5-136}$$

and for all the **L** data points, we have:

$$\begin{aligned}
\tilde{\alpha}_{ik}(j\omega_1) &= \sum_{r=1}^{N} \frac{{}_rA_{ik}}{j\omega_1 - s_r} + R_K + \frac{R_M}{\omega_1{}^2} \\
\tilde{\alpha}_{ik}(j\omega_2) &= \sum_{r=1}^{N} \frac{{}_rA_{ik}}{j\omega_2 - s_r} + R_K + \frac{R_M}{\omega_2{}^2} \\
&\vdots \qquad\qquad\qquad\qquad \vdots \\
\tilde{\alpha}_{ik}(j\omega_L) &= \sum_{r=1}^{N} \frac{{}_rA_{ik}}{j\omega_L - s_r} + R_K + \frac{R_M}{\omega_L{}^2}
\end{aligned} \tag{5-137}$$

In matrix form, this will be:

---

† The form of Eq. (5-134) suggests the residual term to be given by

$$R_1(j\omega) = R_K + \frac{R_M}{j\omega} \tag{5-136 a}$$

but this would mean an additional and unnecessary restriction, as the contribution of the complex conjugate part of the residual would not be contemplated.

$$\begin{bmatrix} 1 & \frac{1}{\omega_1^2} & \frac{1}{j\omega_1 - s_1} & \cdots & \frac{1}{j\omega_1 - s_N} \\ 1 & \frac{1}{\omega_2^2} & \frac{1}{j\omega_2 - s_1} & \cdots & \frac{1}{j\omega_2 - s_N} \\ \vdots & \vdots & \vdots & & \vdots \\ 1 & \frac{1}{\omega_L^2} & \frac{1}{j\omega_L - s_1} & \cdots & \frac{1}{j\omega_L - s_N} \end{bmatrix} \begin{Bmatrix} R_K \\ R_M \\ {}_1A_{ik} \\ \vdots \\ {}_NA_{ik} \end{Bmatrix} = \begin{Bmatrix} \tilde{\alpha}_{ik}(j\omega_1) \\ \tilde{\alpha}_{ik}(j\omega_2) \\ \vdots \\ \tilde{\alpha}_{ik}(j\omega_L) \end{Bmatrix} \quad (5\text{-}138)$$

(Lx(N+2)) ((N+2)x1) (Lx1)

or

$$[T_S]\,\{A\} = \{\tilde{\alpha}\} \quad (5\text{-}139)$$

{A} can be obtained by calculating the pseudo-inverse of $[T_S]$.

$$\{A\} = [T_S]^+\,\{\tilde{\alpha}\} \quad (5\text{-}140)$$

with

$$[T_S]^+ = ([T_S^*]^T\,[T_S])^{-1}\,[T_S^*]^T \quad (5\text{-}141)$$

Expression (5-140) is not exactly the same as Eq. (5-19) because here the vector {A} is complex. The pseudo-inverse in (5-140) can be evaluated more efficiently by means of another SVD calculation. The use of orthogonal polynomials does not seem to be easily applicable in this case, as the form of Eq. (5-134) does not lead to a polynomial expansion in (jω) in the numerator. {A} contains the values for the residuals and the values of ${}_rA_{ik}$ (residues) from which the modal constants and phase angles can be derived, by a similar process to that presented in Section 4-2-1 (Eqs. (4-48) to (4-51)). Comparison of each identified FRF with the corresponding measured one can be made by regenerating the former using Eq. (5-134) and superimposing both graphs.

5-3-3 Computer program description

A new computer program for the **Global** method has been developed and implemented in a micro-computer. In addition to the main program to read in the data files and to establish the equations, routines for the singular value decomposition and eigenvalue problem have been incorporated.

New developments to the Global method

Inequality (5-89) shows that for **p** data files only **L=p** data points are necessary. Usually, there are many more points available in the frequency range considered and we can take advantage of this fact to proceed as we did before, i. e., instead of running once, the program may run several times, taking a different set of randomly chosen data points each time. With theoretical data, the results are not improved by increasing the number of points, but because experimental data always contain some noise, it is advisable to use more points than the minimum required. We have chosen the same fixed number of points as used in the **GRFP** method, i. e., **16** points. Further discussion of this subject is made later on.

Before, in the **GRFP** method, the use of several runs had the objective of determining the number of genuine modes and also the calculation of mean values and standard deviations for the modal parameters. Now, due to the use of the SVD technique, we already have a good means of obtaining the effective number of modes present in a given frequency range. Even so, and particularly for very noisy data, the program may yield different results for the number of modes when different sets of data points are used. Eventually, the program will give the number of genuine modes found (= rank of $[\Delta\tilde{\alpha}]$) and a confidence factor that tells us how many times the most repeated number of modes was found in a given number of runs. For

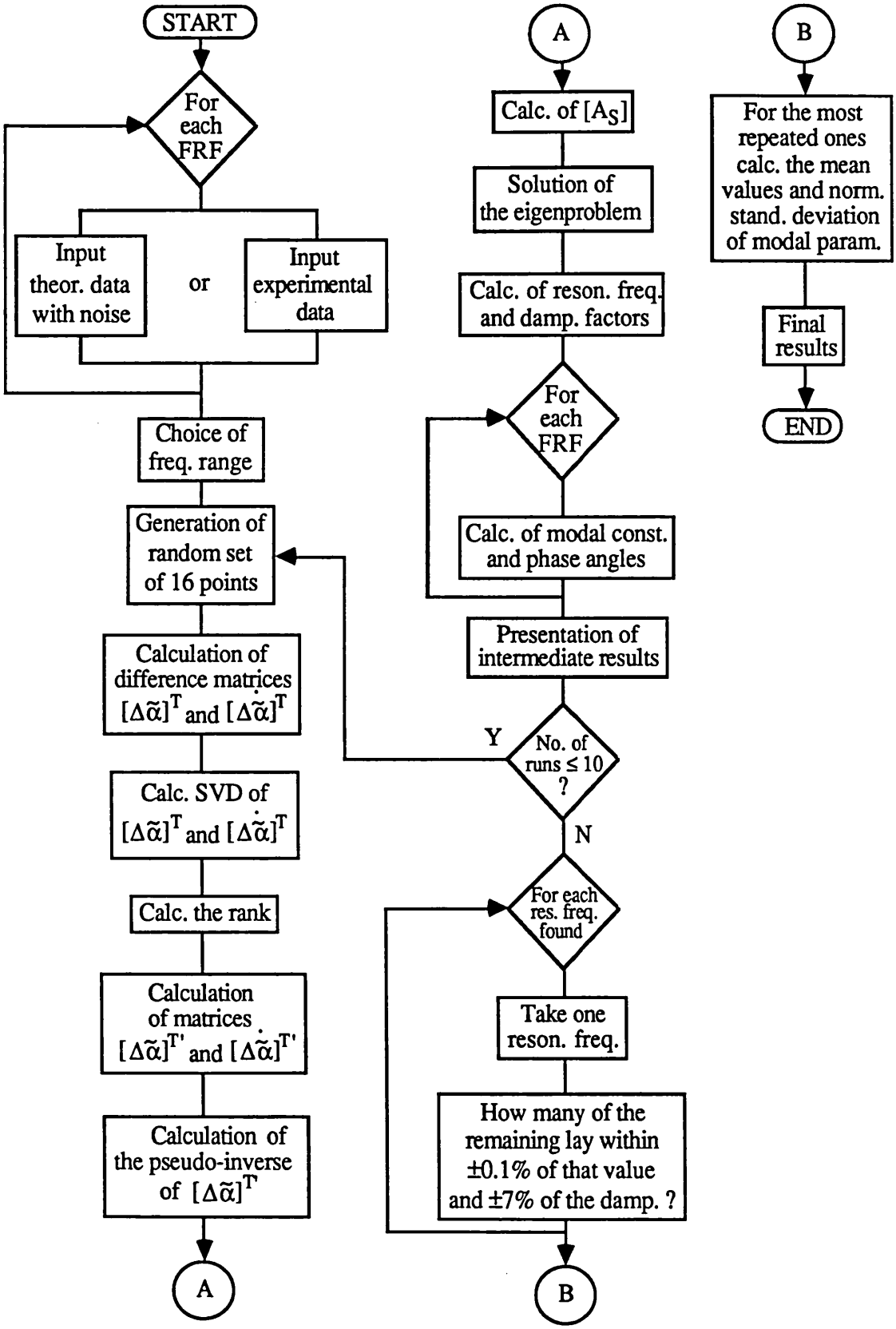

Fig. 5-19 Flow-chart of the computer program.

instance, if the program finds there to be **3** modes in **7** out of **10** runs, the answer will be **3** with a confidence factor of **70%**. In addition, the program will give the mean values for the modal parameters and their standard deviations, after looking for those results that were most often repeated, taking in consideration a narrow tolerance around the values of the natural frequency and damping factors. In this way, the user will have the answers he is looking for and, most importantly, an indication of their quality. In Fig. 5-19 the flow-chart of the computer program is presented.

5-3-4 Examples

Examples based on theoretical data will be presented first to investigate the performance of the method. The same experimental cases used to test the **GRFP** method will then be used to evaluate the behaviour of the **Global** method in practical situations. Special attention will be given to the case of two close modes,as before, but the program is not restricted to this case.

Theoretical case - evaluation of the method for two close modes

The data chosen for this example are the same as previously given in Table 5-1 (Section 5-2-3). We shall look for the values of ω_3 which are the closest possible to ω_2 that the program is capable of identifying. Modes **1** and **4** act as residual ones. Noise levels from **0** to **3%** are added to the data. The results are shown in Table 5-13.

Noise(%)	ω_2(Hz)	ω_3(Hz)
0	100	100.2
1	100	100.3
2	100	100.4
3	100	100.5

Table 5-13 Maximum natural frequency resolution with different levels of added noise.

Influence of the frequency range and the number of data points

It was found that the frequency range and the number of data points taken into the analysis were two inter-related factors in the **Global** method. For a given number of data points, as the frequency range used is larger, the results are poorer. This is due to the fact that the data points will be spread over the frequency range and it was found here that this method works better if the data points are close to the natural frequencies. This results from the fact that the method works with the differences of the forced responses and the assumption made that the effect of neighbouring modes is constant is more correct for points in the region of each resonance peak.

Our special interest is to obtain a good identification for close modes. For this case, the frequency range is chosen to encompass these modes and the data points will be always near the natural frequencies. If we are interested in identifying a wide frequency range with several modes that can be quite separate from each other, then it will be better either to have a means of choosing regions around the peaks where the data points should lie or (which is obviously equivalent) to neglect regions with no peaks. A wide frequency range could also lead to numerical difficulties and in this case weighting factors associated with the frequency values could be used to

overcome the problem. For the study of close modes we will not have this sort of problem.

Influence of the variation of the natural frequencies from FRF to FRF

In a practical situation where we have a set of FRFs, small variations in the resonant frequencies are expected to be found between one FRF and the next. That is why a global analysis is so important, as we wish to find a consistent and unique set of global parameters. However, if those variations are significant, the method used for the analysis may fail to produce the right answers, especially concerning the number of modes. Several theoretical examples using the **Global** method, where the values of the natural frequencies and damping ratios were modified from FRF to FRF, showed that within the specified frequency range the program always gave the correct value for the number of modes. With added noise, it failed sometimes in only one or two runs (out of the 10 used in the program), but it can be said that this method is almost insensitive to this problem.

Discussion and comparison with the **GRFP** method

Based on the results from the theoretical cases, the **Global** method seems to offer a very powerful means of analysing a set of FRFs. Referring to close modes, it was able to detect them to a very good limit of frequency spacing (Table 5-13). This result is, in general, better than the ones obtained with the **GRFP** method (Tables 5-2 and 5-5). The influence of the frequency range is not an important factor for a region encompassing several close modes and it is not a limiting factor as for the **GRFP** method (Section 5-2-3). A great advantage of this method is its ability to handle sets of data that have variations of the global parameters (natural frequencies

and damping ratios) amongst the several FRFs. This was a very limiting aspect in the **GRFP** method, as the variations tolerated were very small (Table 5-4).

Moreover, a more reliable calculation of the number of genuine modes is now possible, based on the calculation of the rank of the matrices of response data. Examples based on experimentally obtained data are presented next.

Experimental cases

The same examples as given in Section 5-2-4 for the **GRFP** method are now tested with the **Global** method.

Impeller - Example 1

The results are given in Table 5-14. Two modes were found with a confidence factor of **100%**.

Mode	FRF	ω_r	ξ_r	C_r	ϕ_r
1	1	3377.431 (0.004)	1.371×10^{-3} (3.511)	3.277×10^{-1} (3.109)	-14.93
	2	"	"	2.342×10^{-1} (2.852)	-14.96
	3	"	"	2.176×10^{-1} (3.894)	167.32
2	1	3396.050 (0.007)	1.193×10^{-3} (2.979)	1.316×10^{-1} (2.235)	-16.53
	2	"	"	1.171×10^{-1} (2.157)	-14.76
	3	"	"	1.474×10^{-1} (3.021)	-14.85

Table 5-14 Identification of FRFs 1, 2 and 3.

The original (dotted line) and regenerated (solid line) curves are presented in Figs. 5-20, 5-21 and 5-22, for FRFs **1**, **2** and **3**, respectively.

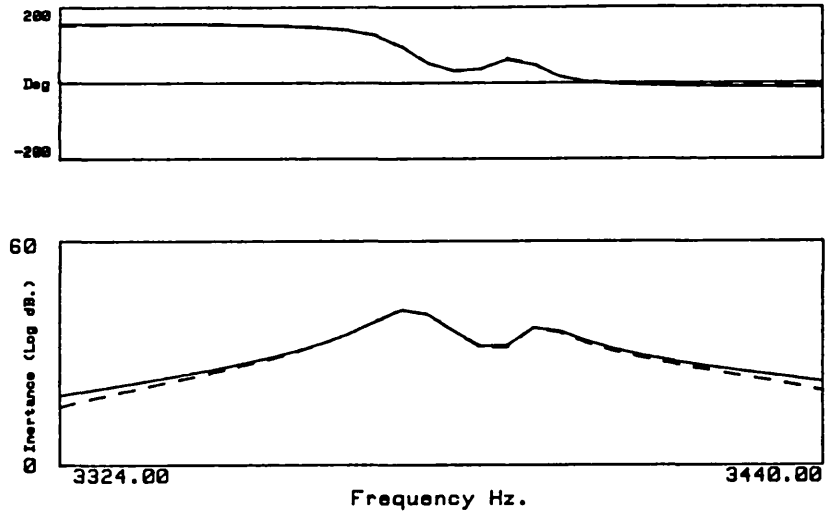

Fig. 5-20 Original (dotted line) and regenerated (solid line) FRF-1.

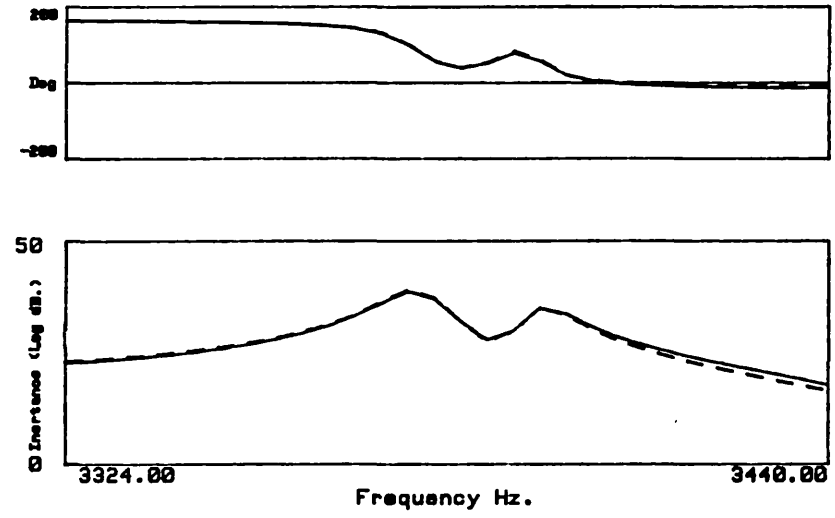

Fig. 5-21 Original (dotted line) and regenerated (solid line) FRF-2.

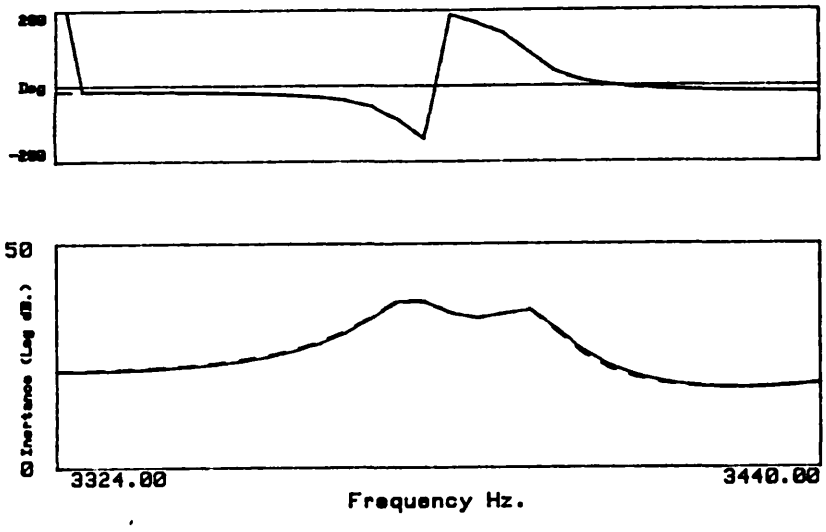

Fig. 5-22 Original (dotted line) and regenerated (solid line) FRF-3.

Impeller - Example 2

For this example, **2** modes were found, again with a confidence factor of **100%**. The results are shown in Table 5-15.

Mode	FRF	ω_r	ξ_r	C_r	ϕ_r
1	1	3377.367 (0.004)	1.296×10^{-3} (2.971)	3.166×10^{-1} (1.897)	-13.78
	4	"	"	9.787×10^{-3} (30.947)	114.12
	5	"	"	2.745×10^{-1} (2.674)	167.39
2	1	3396.138 (0.006)	1.183×10^{-3} (3.293)	1.293×10^{-1} (2.860)	-18.99
	4	"	"	2.149×10^{-1} (2.996)	164.230
	5	"	"	5.680×10^{-2} (3.318)	-14.51

Table 5-15 Identification of FRFs 1, 4 and 5.

The original (dotted line) and regenerated (solid line) curves are presented in Figs. 5-23, 5-24 and 5-25, for each FRF.

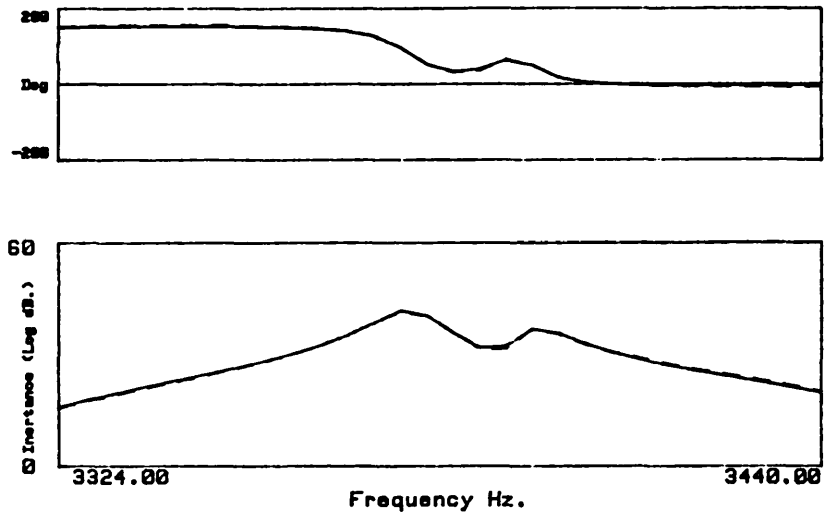

Fig. 5-23 Original (dotted line) and regenerated (solid line) FRF-1.

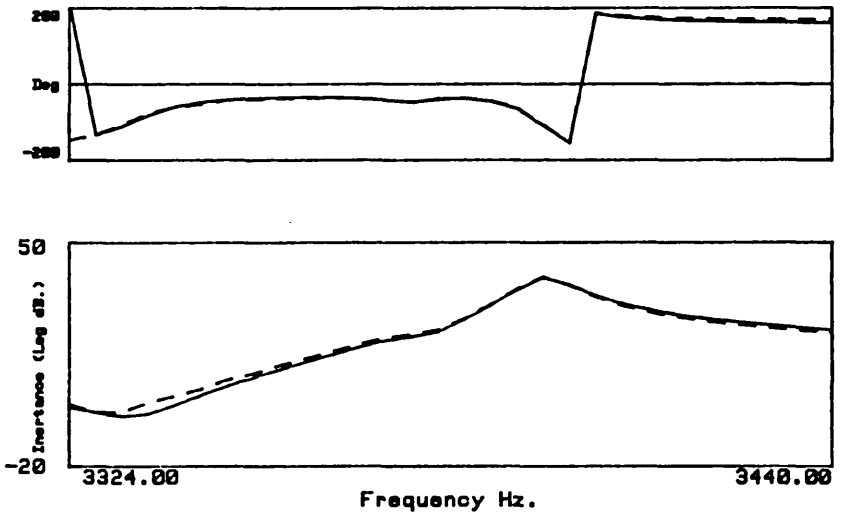

Fig. 5-24 Original (dotted line) and regenerated (solid line) FRF-4.

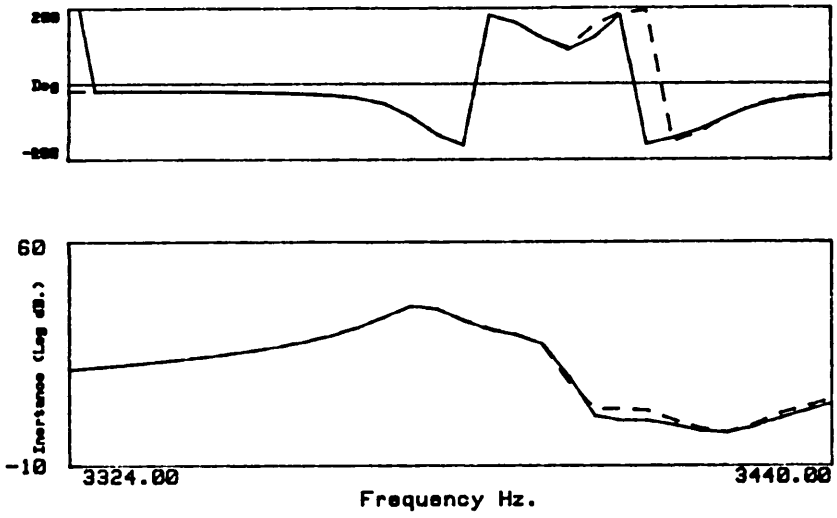

Fig. 5-25 Original (dotted line) and regenerated (solid line) FRF-5.

Impeller - Example 3

For this case, the results are given in Table 5-16. Two modes were found, again with a confidence of **100%**.

Mode	FRF	ω_r	ξ_r	C_r	ϕ_r
	1	3377.311 (0.004)	1.320×10^{-3} (2.993)	3.200×10^{-1} (2.522)	-13.48
	2	"	"	2.292×10^{-1} (2.113)	-13.06
1	3	"	"	2.158×10^{-1} (2.565)	167.73
	4	"	"	8.282×10^{-3} (42.875)	110.01
	5	"	"	2.784×10^{-1} (2.532)	167.84
	1	3396.358 (0.003)	1.131×10^{-3} (1.068)	1.239×10^{-1} (1.892)	-20.23
	2	"	"	1.102×10^{-1} (1.963)	-17.95
2	3	"	"	1.453×10^{-1} (1.886)	-18.13
	4	"	"	2.089×10^{-1} (1.336)	161.78
	5	"	"	5.784×10^{-2} (2.774)	-18.89

Table 5-16 Identification of FRFs 1, 2, 3, 4 and 5.

Figs. 5-26 to 5-30 show the original (dotted line) and regenerated (solid line) curves for each FRF.

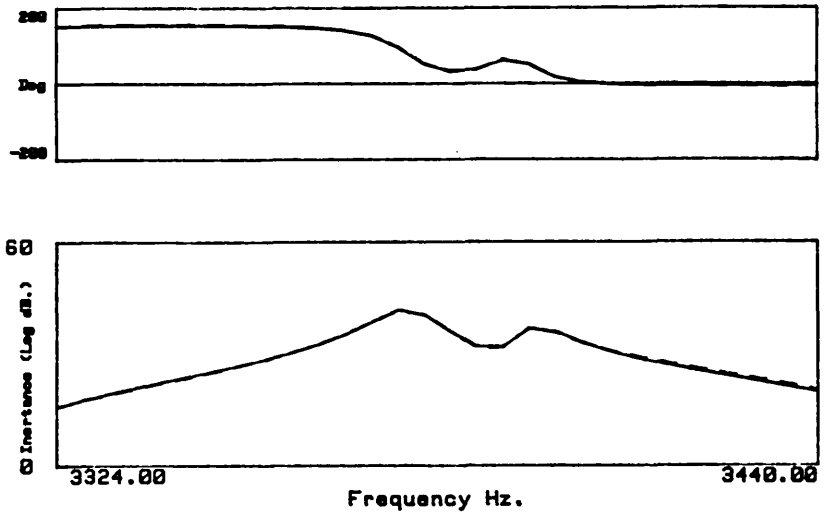

Fig. 5-26 Original (dotted line) and regenerated (solid line) FRF-1.

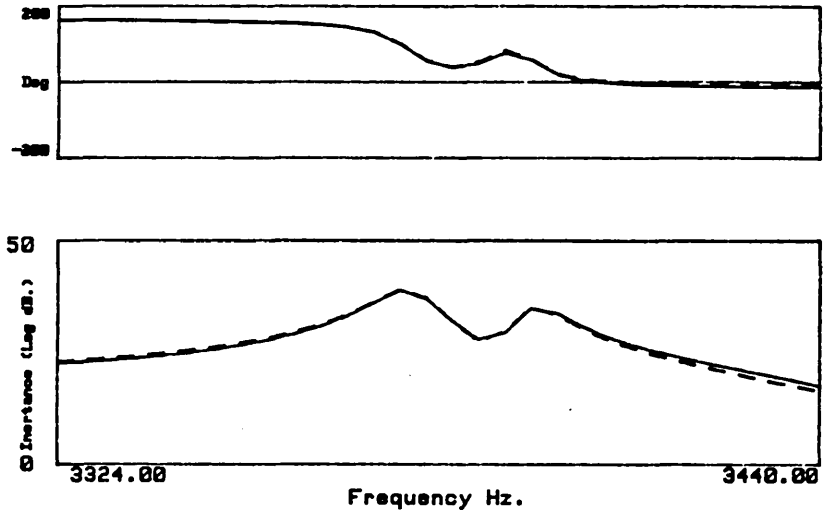

Fig. 5-27 Original (dotted line) and regenerated (solid line) FRF-2.

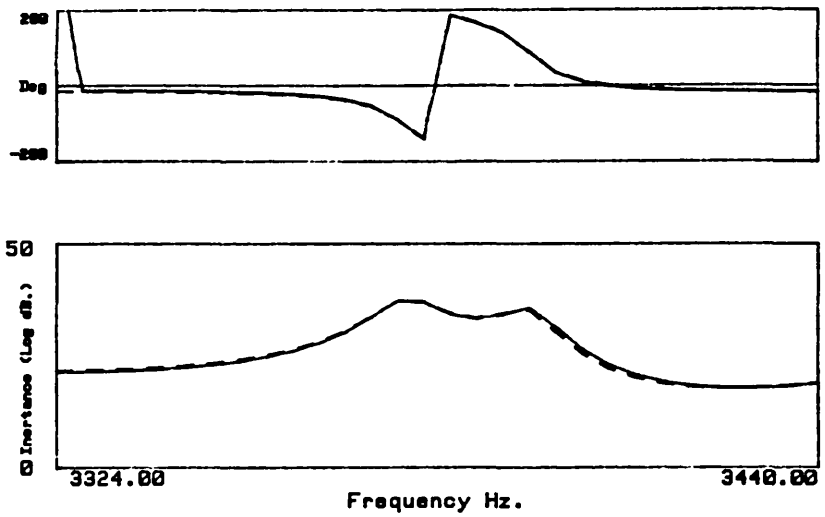

Fig. 5-28 Original (dotted line) and regenerated (solid line) FRF-3.

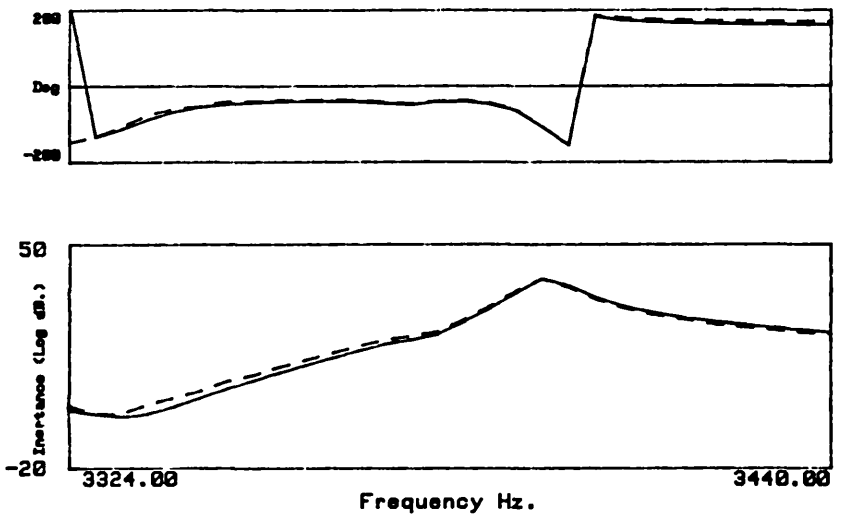

Fig. 5-29 Original (dotted line) and regenerated (solid line) FRF-4.

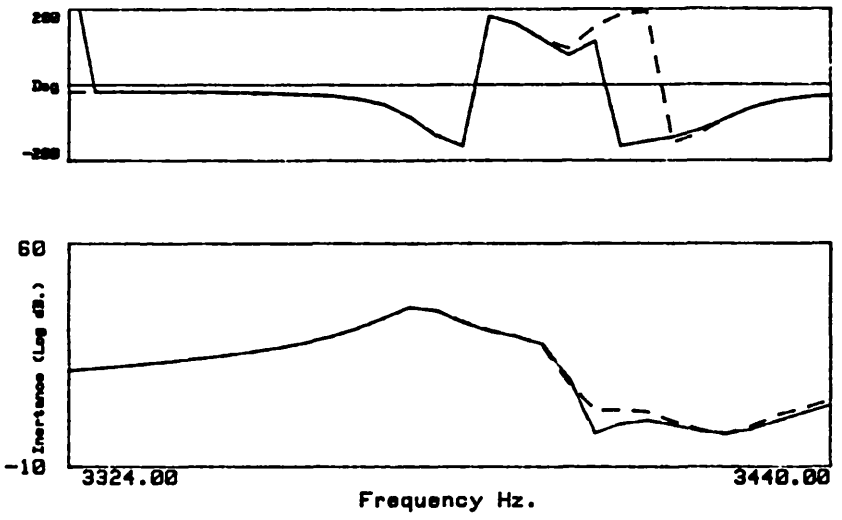

Fig. 5-30 Original (dotted line) and regenerated (solid line) FRF-5.

Discussion and comparison with the **GRFP** method

Comparing the results given in Tables 5-14 to 5-16 with the corresponding results given for the **GRFP** method (Tables 5-6, 5-8 and 5-9) and comparing the corresponding graphs of the original and regenerated data, we can see that the answers are very similar. However, the **Global** method is preferable, as it does not suffer from so many restrictions, namely in terms of frequency range and variations of the global parameters from FRF to FRF. In addition to these aspects, it is also less time-consuming.

5-4 The Spectral method

5-4-1 Introduction

The **Spectral** method was first presented by Klosterman (Ref. [16]) as being suitable for dealing with systems with nearly coincident natural

frequencies, and therefore it seems appropriate to include it in this survey. Because it works with data obtained from several input reference locations, it falls into the category of *MIMO* methods (see Section 1-3) and because it deals directly with the matrix equation of dynamic equilibrium, it can be classified as a direct method. Nevertheless, its approach is much simpler than other modern direct methods, like the **SFD** or the **Multi-matrix** (Section 2-3-3). Here, the basic theory will be presented and some variations discussed. A computer program was written for this purpose. Evaluation of the method is made through several examples.

5-4-2 Theory

The damping model assumed by this method is the hysteretic one, although a viscous damping model version could also be developed. The equation of motion for an **N** DOF system is given by

$$[[K] + j[H] - \omega^2[M]]\ \{\bar{y}\} = \{\bar{F}\} \tag{5-142}$$

where **[K]**, **[H]** and **[M]** are **NxN** real matrices of stiffness, hysteretic damping and mass, respectively. $\{\bar{y}\}$ and $\{\bar{F}\}$ are **Nx1** complex vectors of the amplitudes of response and force, respectively. The receptance matrix $[\alpha]$ will be given by:

$$[\alpha] = [[K] + j[H] - \omega^2[M]]^{-1} \tag{5-143}$$

and hence,

$$[\alpha]^{-1} = [[K] + j[H] - \omega^2[M]] \tag{5-144}$$

Grouping **[K]** and **j[H]** in a single matrix, it gives

$$[\alpha]^{-1} = [[K'] - \omega^2[M]] \tag{5-145}$$

with

$$[K'] = [[K] + j[H]] \tag{5-146}$$

Let us suppose that the receptance matrix $[\alpha]$ is known from a set of measurements over the chosen frequency range. In practice, it is not possible to have a complete **NxN** matrix, and this problem will be discussed in Section 5-4-4. What is sought with this method is to calculate from $[\alpha]$ the matrices of the system, **[K']** and **[M]**, in order to calculate the eigenvalues and eigenvectors and, eventually, the modal parameters. Eq. (5-145) has two unknowns, **[K']** and **[M]**. Therefore, all that has to be done is to establish two equations, each one for a different frequency (ω_1 and ω_2, say). Thus,

$$[\alpha]^{-1}_{\omega_1} = [[K'] - \omega_1^2[M]] \tag{5-147}$$

$$[\alpha]^{-1}_{\omega_2} = [[K'] - \omega_2^2[M]] \tag{5-148}$$

By subtracting Eq. (5-148) from (5-147), **[K']** is eliminated:

$$[\alpha]^{-1}_{\omega_1} - [\alpha]^{-1}_{\omega_2} = (\omega_2^2 - \omega_1^2)[M] \tag{5-149}$$

from which one can determine the mass matrix:

$$[M] = \frac{1}{\omega_2^2 - \omega_1^2}[[\alpha]^{-1}_{\omega_1} - [\alpha]^{-1}_{\omega_2}] \tag{5-150}$$

Multiplying Eq. (5-147) by ω_2^2 and Eq. (5-148) by ω_1^2 and subtracting, enables the calculation of matrix **[K']**:

$$\omega_2^2 [\alpha]_{\omega_1}^{-1} - \omega_1^2 [\alpha]_{\omega_2}^{-1} = (\omega_2^2 - \omega_1^2) [K'] \tag{5-151}$$

Hence,

$$[K'] = \frac{1}{\omega_2^2 - \omega_1^2} [\omega_2^2 [\alpha]_{\omega_1}^{-1} - \omega_1^2 [\alpha]_{\omega_2}^{-1}] \tag{5-152}$$

from which the stiffness and damping matrices can be calculated:

$$[K] = \text{Re}\,[K'] \tag{5-153}$$

$$[H] = \text{Im}\,[K'] \tag{5-154}$$

Knowing **[K']** and **[M]**, the following generalized complex eigenproblem can be solved, whose eigenvalues and eigenvectors correspond to the ones of the homogeneous solution of Eq. (5-142):

$$[[K'] - \lambda_r [M]] \{\psi_r\} = \{0\} \tag{5-155}$$

Klosterman's approach

Klosterman suggests a solution of the eigenproblem of Eq. (5-155) by expressing **[K']** and **[M]** in terms of the receptance matrices, in the following way: substituting Eqs. (5-150) and (5-152) in Eq. (5-155), it follows that

$$\left[\frac{1}{\omega_2^2 - \omega_1^2} [\omega_2^2 [\alpha]_{\omega_1}^{-1} - \omega_1^2 [\alpha]_{\omega_2}^{-1}] - \lambda_r \frac{1}{\omega_2^2 - \omega_1^2} [[\alpha]_{\omega_1}^{-1} - [\alpha]_{\omega_2}^{-1}]\right] \{\psi_r\} = \{0\} \tag{5-156}$$

or

$$\left[\frac{\omega_2^2 - \lambda_r}{\omega_2^2 - \omega_1^2}[\alpha]_{\omega_1}^{-1} - \frac{\omega_1^2 - \lambda_r}{\omega_2^2 - \omega_1^2}[\alpha]_{\omega_2}^{-1}\right]\{\psi_r\} = \{0\} \tag{5-157}$$

As it is always possible to choose $\omega_1 \neq \omega_2$, Eq. (5-157) can be further simplified to

$$[[\alpha]_{\omega_1}[\alpha]_{\omega_2}^{-1} - \gamma_r[I]]\{\psi_r\} = \{0\} \tag{5-158}$$

where

$$\gamma_r = \frac{\omega_2^2 - \lambda_r}{\omega_1^2 - \lambda_r} \tag{5-159}$$

Once the γ_r are known, λ_r can be easily recovered by

$$\lambda_r = \frac{\gamma_r \omega_1^2 - \omega_2^2}{\gamma_r - 1} \tag{5-160}$$

For practical application, it is undoubtedly convenient to consider more than 2 frequency points in the calculations, as noise is always present. Taking **p'** pairs of points, one can write **p'** equations like (5-158), where there will be an error on the right side, instead of zero:

$$\begin{aligned}
[([\alpha]_{\omega_1}[\alpha]_{\omega_2}^{-1})_1 - \gamma_1[I]]\{\psi_r\} &= \{E\}_1 \\
[([\alpha]_{\omega_1}[\alpha]_{\omega_2}^{-1})_2 - \gamma_2[I]]\{\psi_r\} &= \{E\}_2 \\
\vdots \qquad\qquad & \qquad \vdots \\
[([\alpha]_{\omega_1}[\alpha]_{\omega_2}^{-1})_{p'} - \gamma_{p'}[I]]\{\psi_r\} &= \{E\}_{p'}
\end{aligned} \tag{5-161}$$

Setting the summation of the error vector to zero, it gives

$$\left[\sum_{i=1}^{p'} ([\alpha]_{\omega_1} [\alpha]_{\omega_2}^{-1})_i - (\sum_{i=1}^{p'} \gamma_i) [I] \right] \{\psi_r\} = \{0\} \tag{5-162}$$

or

$$[[\alpha_T] - \gamma_T [I]] \{\psi_r\} = \{0\} \tag{5-163}$$

where

$$[\alpha_T] = \sum_{i=1}^{p'} ([\alpha]_{\omega_1} [\alpha]_{\omega_2}^{-1})_i \tag{5-164}$$

$$\gamma_T = \sum_{i=1}^{p'} \gamma_i \tag{5-165}$$

In order to establish a modal representation for each **FRF**, of the form

$$\alpha_{ij} = \sum_{r=1}^{N} \frac{{}_r\psi_i \, {}_r\psi_j}{k_r' - \omega^2 m_r} \tag{5-166}$$

it is now necessary to calculate the modal masses and stiffnesses, $\mathbf{m_r}$ and $\mathbf{k_r'}$. From the orthogonal properties of eigenvectors, it is known that

$$\{\psi_r\}^T [K'] \{\psi_r\} = k_r' \tag{5-167}$$

$$\{\psi_r\}^T [M] \{\psi_r\} = m_r \tag{5-168}$$

Taking into consideration Eq. (5-145), it follows that

$$\{\psi_r\}^T [\alpha]^{-1} \{\psi_r\} = k_r' - \omega^2 m_r \tag{5-169}$$

The separation of Eq. (5-169) into its real and imaginary parts leads to

$$\begin{aligned} \mathrm{Re}(\{\psi_r\}^T [\alpha]^{-1} \{\psi_r\}) &= \mathrm{Re}(k_r') - \omega^2 \mathrm{Re}(m_r) \\ \mathrm{Im}(\{\psi_r\}^T [\alpha]^{-1} \{\psi_r\}) &= \mathrm{Im}(k_r') - \omega^2 \mathrm{Im}(m_r) \end{aligned} \tag{5-170}$$

or

$$\begin{aligned} \mathrm{Re}(q_\alpha) &= \mathrm{Re}(k_r') - \omega^2\,\mathrm{Re}(m_r) \\ \mathrm{Im}(q_\alpha) &= \mathrm{Im}(k_r') - \omega^2\,\mathrm{Im}(m_r) \end{aligned} \tag{5-171}$$

with

$$q_\alpha = \{\psi_r\}^T [\alpha]^{-1} \{\psi_r\} \tag{5-172}$$

Considering **L** frequency values (which can be the same p' pairs of points taken before to solve the eigenproblem of Eq. (5-162)), one has for the real part:

$$\begin{aligned} \mathrm{Re}(q_\alpha)_1 &= \mathrm{Re}(k_r') - \omega_1^2\,\mathrm{Re}(m_r) \\ \mathrm{Re}(q_\alpha)_2 &= \mathrm{Re}(k_r') - \omega_2^2\,\mathrm{Re}(m_r) \\ \vdots & \qquad\qquad \vdots \\ \mathrm{Re}(q_\alpha)_L &= \mathrm{Re}(k_r') - \omega_L^2\,\mathrm{Re}(m_r) \end{aligned} \tag{5-173}$$

An equivalent expression can be written for the imaginary part. In a least-squares sense, the error, defined by

$$J = \sum_{i=1}^{L} [\,\mathrm{Re}(q_\alpha)_i - \mathrm{Re}(k_r') + \omega_i^2\,\mathrm{Re}(m_r)]^2 \tag{5-174}$$

will be minimized, by partial differentiation of Eq. (5-174) with respect to $\mathbf{Re}(k_r')$ and $\mathbf{Re}(m_r)$ and equating the result to zero:

$$\begin{aligned} &-2\sum_{i=1}^{L} [\,\mathrm{Re}(q_\alpha)_i - \mathrm{Re}(k_r') + \omega_i^2\,\mathrm{Re}(m_r)] = 0 \\ &+2\sum_{i=1}^{L} [(\mathrm{Re}(q_\alpha)_i - \mathrm{Re}(k_r') + \omega_i^2\,\mathrm{Re}(m_r))\,\omega_i^2] = 0 \end{aligned} \tag{5-175}$$

from which the normal equations are obtained:

$$\sum_{i=1}^{L} \mathrm{Re}(q_\alpha)_i - L\,\mathrm{Re}(k_r') + \mathrm{Re}(m_r) \sum_{i=1}^{L} \omega_i^2 = 0$$

$$\sum_{i=1}^{L} \mathrm{Re}(q_\alpha)_i\,\omega_i^2 - \mathrm{Re}(k_r') \sum_{i=1}^{L} \omega_i^2 + \mathrm{Re}(m_r) \sum_{i=1}^{L} \omega_i^4 = 0 \qquad (5\text{-}176)$$

or

$$\begin{Bmatrix} \mathrm{Re}(k_r') \\ \mathrm{Re}(m_r) \end{Bmatrix} = \begin{bmatrix} -L & \sum_{i=1}^{L} \omega_i^2 \\ -\sum_{i=1}^{L} \omega_i^2 & \sum_{i=1}^{L} \omega_i^4 \end{bmatrix}^{-1} \begin{Bmatrix} \sum_{i=1}^{L} \mathrm{Re}(q_\alpha)_i \\ \sum_{i=1}^{L} \mathrm{Re}(q_\alpha)_i\,\omega_i^2 \end{Bmatrix} \qquad (5\text{-}177)$$

Likewise, for the imaginary part, it follows that

$$\begin{Bmatrix} \mathrm{Im}(k_r') \\ \mathrm{Im}(m_r) \end{Bmatrix} = \begin{bmatrix} -L & \sum_{i=1}^{L} \omega_i^2 \\ -\sum_{i=1}^{L} \omega_i^2 & \sum_{i=1}^{L} \omega_i^4 \end{bmatrix}^{-1} \begin{Bmatrix} \sum_{i=1}^{L} \mathrm{Im}(q)_i \\ \sum_{i=1}^{L} \mathrm{Im}(q)_i\,\omega_i^2 \end{Bmatrix} \qquad (5\text{-}178)$$

Eqs. (5-177) and (5-178) will be solved **N** times to calculate all the values of $\mathbf{k_r'}$ and $\mathbf{m_r}$.

All the parameters needed to construct the theoretical model are now available, using Eq. (5-166). Because it is usually convenient to determine the mass-normalized mode-shapes and the natural frequencies and damping factors, and because it is difficult to recover the values γ_i from Eq. (5-165), those modal parameters can be calculated based upon the results of $\mathbf{k_r'}$ and $\mathbf{m_r}$. In this way, the mass-normalized mode-shapes $\{\phi_r\}$ will be calculated by dividing $\{\psi_r\}$ by $\sqrt{m_r}$. The natural frequencies and

hysteretic damping factors will be given, respectively, by:

$$\omega_r = \mathrm{Re}(k_r'/m_r) \tag{5-179}$$

$$\eta_r = \mathrm{Im}(k_r'/m_r)\,/\mathrm{Re}(k_r'/m_r) \tag{5-180}$$

Alternative approach

The theoretical formulation developed so far suggests that matrices **[K']** and **[M]** may be calculated alternatively, based on the **p'** pairs of frequency points and not by a simple average, as done before. This alternative approach will be tried next, with the objective of comparing the results with Klosterman's approach, in order to determine which one leads to more accurate results. Knowing **[K']** and **[M]**, Eq. (5-155) can be solved for the eigenvalues and eigenvectors. Let Eq. (5-149) be written for the **p'** pairs of points:

$$\begin{aligned}
(\omega_2^2 - \omega_1^2)_1\,[M] &= \left([\alpha]_{\omega_1}^{-1} - [\alpha]_{\omega_2}^{-1}\right)_1 \\
(\omega_2^2 - \omega_1^2)_2\,[M] &= \left([\alpha]_{\omega_1}^{-1} - [\alpha]_{\omega_2}^{-1}\right)_2 \\
&\;\;\vdots \qquad\qquad\quad \vdots \\
(\omega_2^2 - \omega_1^2)_{p'}\,[M] &= \left([\alpha]_{\omega_1}^{-1} - [\alpha]_{\omega_2}^{-1}\right)_{p'}
\end{aligned} \tag{5-181}$$

or, in matrix form,

$$\underset{(p'NxN)}{[\Omega_T]}\;\underset{(NxN)}{[M]} = \underset{(p'NxN)}{[\alpha_T]'} \tag{5-182}$$

where

$$[\Omega_T] = \begin{bmatrix} (\omega_2^2 - \omega_1^2)_1 [I] \\ (\omega_2^2 - \omega_1^2)_2 [I] \\ \vdots \\ (\omega_2^2 - \omega_1^2)_{p'} [I] \end{bmatrix} \tag{5-183}$$

$$[\alpha_T]' = \begin{bmatrix} ([\alpha]_{\omega_1}^{-1} - [\alpha]_{\omega_2}^{-1})_1 \\ ([\alpha]_{\omega_1}^{-1} - [\alpha]_{\omega_2}^{-1})_2 \\ \vdots \\ ([\alpha]_{\omega_1}^{-1} - [\alpha]_{\omega_2}^{-1})_{p'} \end{bmatrix} \tag{5-184}$$

The least-squares solution of Eq. (5-182) is given by

$$[M] = ([\Omega_T]^T [\Omega_T])^{-1} [\Omega_T]^T [\alpha_T]' \tag{5-185}$$

In this case, it is simple to obtain an explicit version of Eq. (5-185) as

$$[M] = \frac{\sum_{i=1}^{p'} \{ (\omega_2^2 - \omega_1^2)_i [[\alpha]_{\omega_1}^{-1} - [\alpha]_{\omega_2}^{-1}]_i \}}{\sum_{i=1}^{p'} \{ (\omega_2^2 - \omega_1^2)^2 \}} \tag{5-186}$$

Proceeding in a similar way for matrix **[K']**, leads to:

$$[K'] = \frac{\sum_{i=1}^{p'} \{ (\omega_2^2 - \omega_1^2)_i [\omega_2^2 [\alpha]_{\omega_1}^{-1} - \omega_1^2 [\alpha]_{\omega_2}^{-1}]_i \}}{\sum_{i=1}^{p'} \{ (\omega_2^2 - \omega_1^2)^2 \}} \tag{5-187}$$

Knowing **[K']** and **[M]**, the eigenproblem of Eq. (5-155) can be solved,

allowing the natural frequencies, damping ratios and mass-normalized mode-shapes to be calculated. The advantages of knowing the system matrices are enormous, especially for the post-processing stage of analysis, already referred in Section 1-1.

5-4-3 Computer program description

A computer program for this modal identification method has been developed and implemented in a micro-computer. Several sets of pairs of frequency points are specified and picked up randomly from the given FRFs, and the modal parameters are calculated using both approaches cited above. In Fig. 5-31 the flow-chart of the program is presented.

5-4-4 Examples

Theoretical cases

The program must be supplied with the "measured" receptance matrix $[\alpha]$, each individual FRF containing all the measured frequency points. The order of this matrix is **N**, the number of degrees-of-freedom of the system. For self-adjoint systems, as is usually the case, this implies the provision of $(N^2+N)/2$ FRFs. For instance, for a **4** DOF system, it would be necessary to measure **10** FRFs. If the system is complete, and noiseless theoretical data are used, there is no doubt that both approaches to the present method give exact results and the calculated matrices are also exact. The important question is to know how well the method behaves when the system is incomplete and/or the data are noisy. For this purpose, noiseless theoretical data were generated first, assuming that the complete system has **4** modes but that the hypothetical measured data available correspond

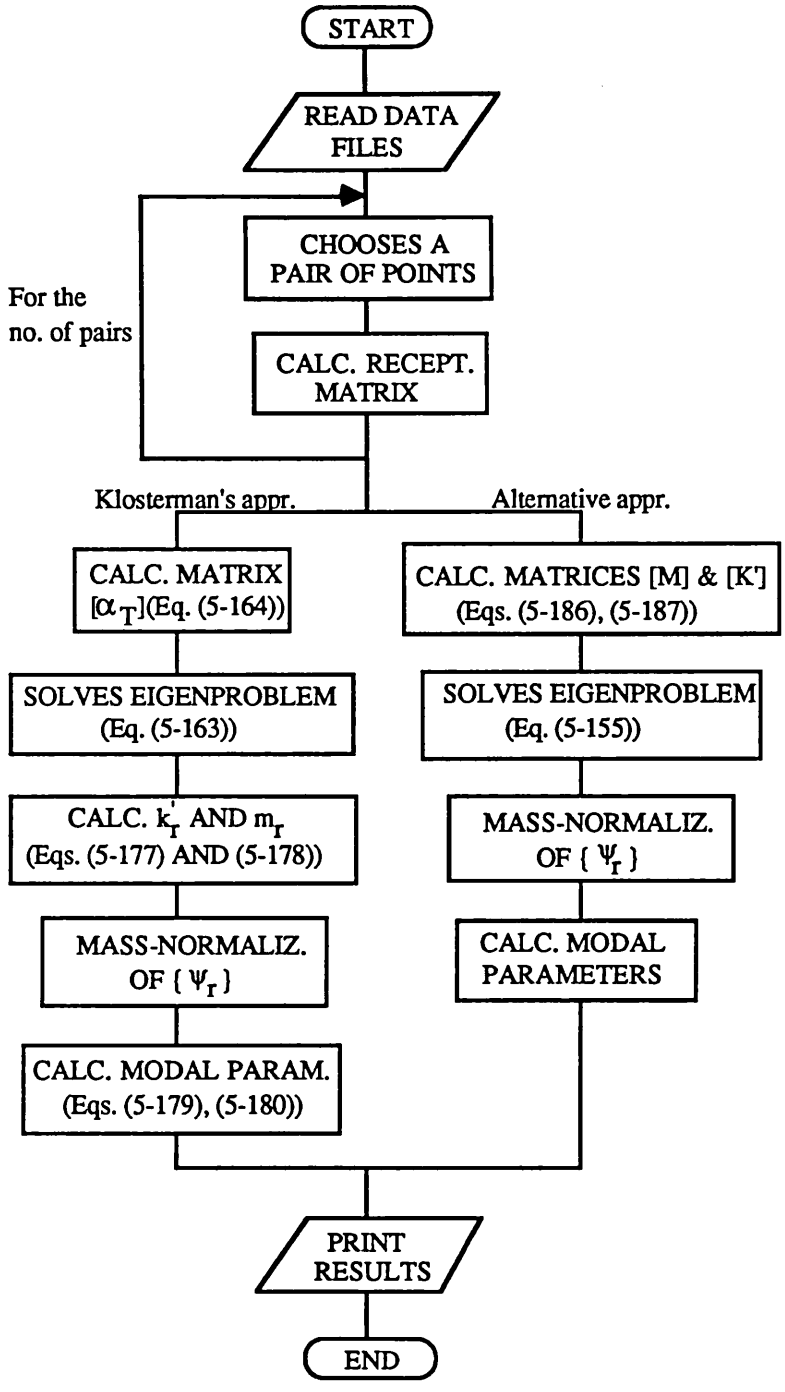

Fig. 5-31 Flow-chart of the computer program.

to a 2 DOF system, i. e., there will be only 2 visible resonances in the frequency range of interest. To analyse the corresponding 2 modes, only 3 FRFs - α_{11}, α_{12} and α_{22} - will be generated (considering 4 modes). The frequency range chosen for this analysis will encompass the two central modes. It will be investigated how well the program is able to identify those two middle modes, the other two acting as residuals.. The data are given in Table 5-17.

Mode	FRF	ω_r(Hz)	η_r	C_r	ϕ_r
	α_{11}	90	0.01	1	0
1	α_{12}	"	"	0.7	0
	α_{22}	"	"	0.49	0
	α_{11}	100	0.01	0.8	0
2	α_{12}	"	"	0.7	0
	α_{22}	"	"	0.6125	0
	α_{11}	101	0.01	0.8	0
3	α_{12}	"	"	0.5	180
	α_{22}	"	"	0.3125	0
	α_{11}	110	0.01	1	0
4	α_{12}	"	"	1	0
	α_{22}	"	"	1	0

Table 5-17 Theoretical data .

A set of 10 pairs of points is used. In this case, the results for modes 2 and 3 are given in Table 5-18. Considering again the case defined in Table 5-17, but choosing a narrower frequency range around modes 2 and 3, the results obtained are shown in Table 5-19.

Approach	Mode	FRF	ω_r(Hz)	η_r	C_r	ϕ_r
Klosterman	2	α_{11}	99.9058	0.0099	0.6796	1.039
		α_{12}	"	"	0.6283	4.539
	3	α_{11}	101.0023	0.0100	0.8661	-0.639
		α_{12}	"	"	0.4880	179.929
Alternative	2	α_{11}	99.9251	0.0092	0.6675	4.520
		α_{12}	"	"	0.6086	6.063
	3	α_{11}	101.0017	0.0100	0.8466	-1.221
		α_{12}	"	"	0.4922	-179.845

Table 5-18 Identification of the theoretically generated data using both approaches.

Approach	Mode	FRF	ω_r(Hz)	η_r	C_r	ϕ_r
Klosterman	2	α_{11}	99.9636	0.0096	0.7415	2.395
		α_{12}	"	"	0.6637	4.082
	3	α_{11}	101.0001	0.0100	0.8183	-1.667
		α_{12}	"	"	0.4968	-179.754
Alternative	2	α_{11}	99.9576	0.0097	0.7422	3.138
		α_{12}	"	"	0.6647	4.170
	3	α_{11}	101.0001	0.0100	0.8156	-1.633
		α_{12}	"	"	0.4972	-179.764

Table 5-19 Identification of the theoretically generated data considering a narrow frequency range around modes **2** and **3**.

Comparing Tables 5-18 and 5-19, it is observed that the results of the latter are more accurate. It seems preferable, then, to use a narrower frequency

range encompassing the modes that are to be analysed. This is not surprising, as the narrower the range around a natural frequency is, the less important is the effect of neighbouring modes.

For the same case, but if **3%** of random noise is added, the results obtained are shown in Table 5-20, and can be seen not to differ significantly from the previous case (Table 5-19).

Approach	Mode	FRF	ω_r(Hz)	η_r	C_r	ϕ_r
Klosterman	2	α_{11}	99.9602	0.0094	0.7430	2.930
		α_{12}	"	"	0.6527	4.386
	3	α_{11}	101.0013	0.0101	0.8051	-1.632
		α_{12}	"	"	0.5003	-179.940
Alternative	2	α_{11}	99.9725	0.0091	0.7369	4.301
		α_{12}	"	"	0.6484	5.094
	3	α_{11}	101.0113	0.0102	0.8155	-1.578
		α_{12}	"	"	0.5056	179.567

Table 5-20 Identification of the theoretically generated data considering a narrow frequency range around modes **2** and **3**, and with 3% added noise.

As the results are satisfactory and of similar accuracy using both approaches, the next stage will be to investigate the limits of the method, i. e., how close two modes can be, with the method still producing accurate results. As before, this problem will be studied in terms of the frequency closeness, and for several levels of added noise. The results are presented in Table 5-21.

Noise (%)	ω_2 (Hz)	ω_3(Hz)
0	100	100.25
1	100	100.30
2	100	100.35
3	100	100.45

Table 5-21 Maximum natural frequency resolution with different levels of added noise.

From the analysis of Tables 5-18 to 5-20, it is observed that although both approaches provide similar results, Klosterman's approach is slightly better (the corresponding values are closer to the theoretical data given in Table 5-17) and, thus, it is not worthwhile using the alternative approach as suggested. From now on, the results will only refer to Klosterman's approach. The results of Table 5-21 have a similar order of magnitude when compared to the ones obtained with the **GRFP** and **Global** methods.

Because the results improve when a narrower frequency range around a resonance is taken, the simultaneous analysis of several modes will be better if those modes are reasonably close together, or, conversely, if the neighbouring modes are sufficiently distant from the region of interest. Moreover, it was found that the accuracy of the results will generally improve by considering more pairs of data points.

Experimental cases

In order to evaluate the method in a real case, a disc made asymmetric by the adding of a small eccentric mass was tested, using an impact hammer and a small accelerometer. The characteristics of such a disc imply the existence of several sets of double modes. The disc was sucessively hit at three different points, and responses were captured at those three points, in order to acquire a data-base for our work. Figs. 5-32 (a) to (f) show the

curves obtained. Considering the first double peak (near 1850 Hz), a narrow band around it was chosen (1828 - 1874 Hz), and just **3** FRFs taken for the analysis (α_{11}, α_{12} and α_{22}).

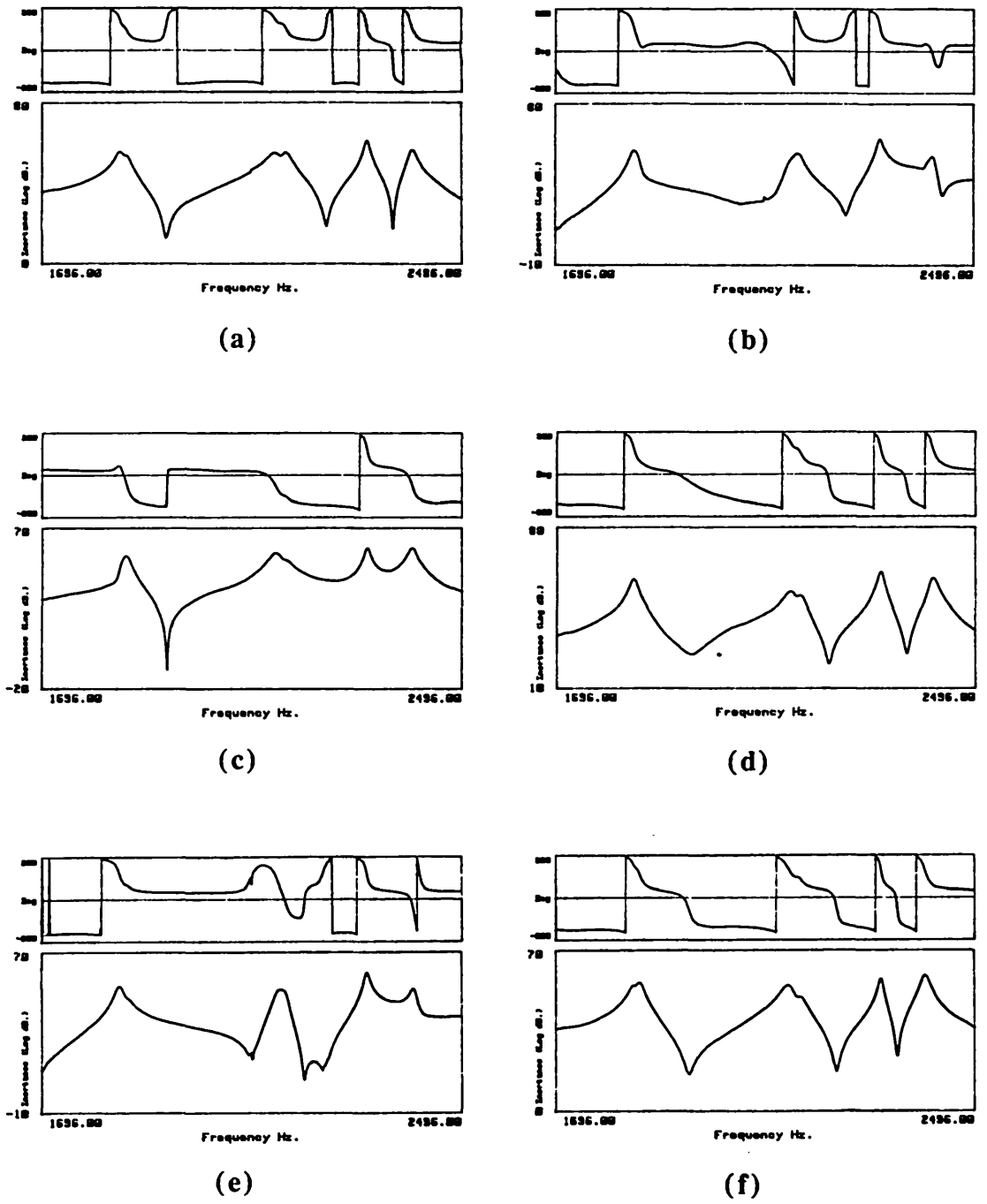

Fig. 5-32 Bode plots of an experimental case: (a) α_{11}; (b) α_{12}; (c) α_{13}; (d) α_{22}; (e) α_{23}; (f) α_{33}.

The results are presented in Table 5-22. The original (dotted line) and regenerated (solid line) curves for α_{11} and α_{12} around those close modes are shown in Figs. 5-33 and 5-34, respectively, after having introduced the residual effect of the neighbouring modes. Visual inspection of Figs. 5-33 and 5-34 indicates that the identification is not a particularly good one, especially for the second FRF. The **GRFP** and **Global** methods will be tried, in order to compare results.

Mode	FRF	ω_r(Hz)	η_r	C_r	ϕ_r
1	α_{11}	1843.987	5.947×10^{-3}	2.852	22.232
	α_{12}	"	"	3.725	23.653
2	α_{11}	1853.133	1.160×10^{-2}	4.574	42.453
	α_{12}	"	"	0.928	-143.731

Table 5-22 Identification of the first double peak of Fig. 5-32 using α_{11}, α_{12} and α_{22}.

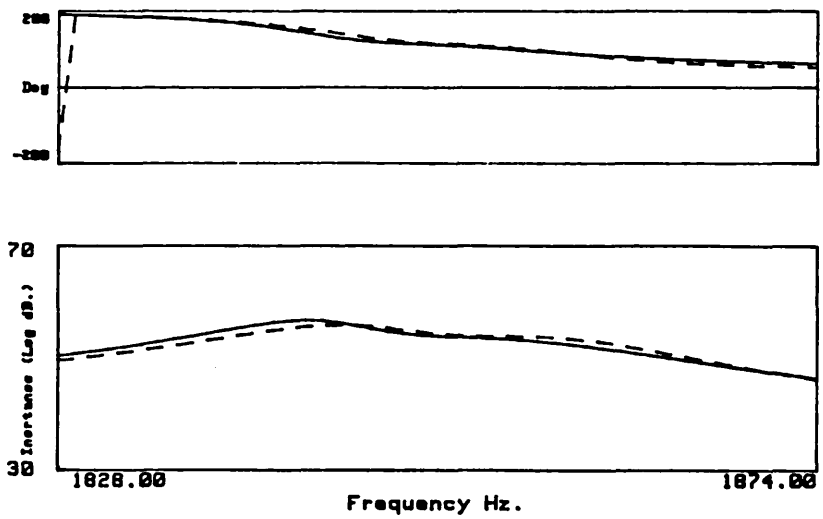

Fig. 5-33 Original (dotted line) and regenerated (solid line) α_{11} using the **Spectral** method.

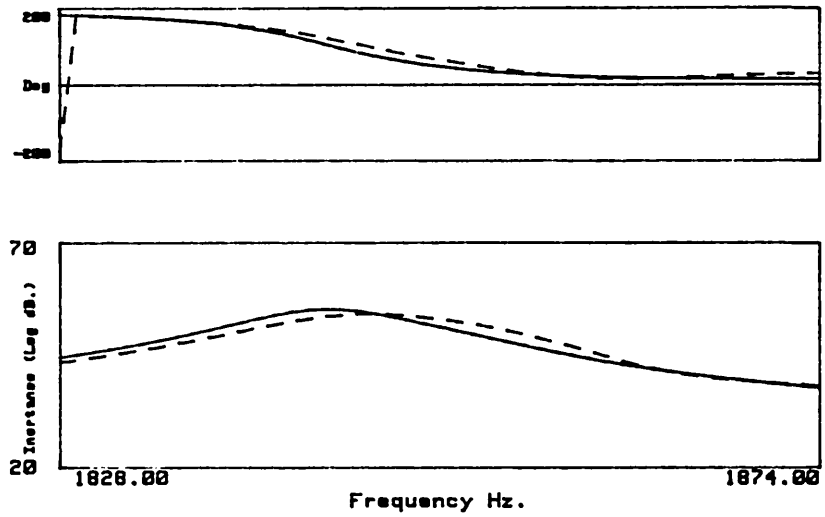

Fig. 5-34 Original (dotted line) and regenerated (solid line) α_{12} using the **Spectral** method.

Comparison with the GRFP and Global methods

Curves α_{11}, α_{12} and α_{13} were analysed using the **GRFP** and **Global** methods. The results, in terms of modal parameters, were obtained for the referred modes and for curves α_{11} and α_{12}. Table 5-23 shows the comparison of results obtained by all three methods. The numbers in brackets refer to the normalized standard deviation obtained with the **GRFP** and **Global** methods (results of viscous damping have been converted to hysteretic damping). Both these methods gave indications of the existence of 2 modes.

Mode	Method	FRF	ω_r	η_r	C_r	ϕ_r
	Spectral	α_{11}	1843.987	5.947×10^{-3}	2.852	22.232
		α_{12}	"	"	3.725	23.653
1	GRFP	α_{11}	1846.138 (0.013)	8.010×10^{-3} (3.457)	4.409 (7.033)	29.690
		α_{12}	"	"	4.367 (5.327)	27.340
	Global	α_{11}	1845.636 (0.003)	7.860×10^{-3} (1.093)	3.966 (1.695)	32.050
		α_{12}	"	"	4.301 (2.030)	32.470
	Spectral	α_{11}	1853.133	1.160×10^{-2}	4.574	42.453
		α_{12}	"	"	0.928	-143.731
2	GRFP	α_{11}	1857.704 (0.050)	7.712×10^{-3} (3.592)	2.048 (19.311)	29.000
		α_{12}	"	"	1.322 (18.963)	-154.000
	Global	α_{11}	1856.945 (0.011)	8.154×10^{-3} (3.708)	2.476 (5.822)	31.060
		α_{12}	"	"	1.476 (7.071)	-143.010

Table 5-23 Comparison of the identification using the **Spectral**, **GRFP** and **Global** methods.

Using the same information concerning the residual effect of the out-of-range modes, the original (dotted line) and regenerated (solid line) curves are presented in Figs. 5-35 (α_{11}) and 5-36 (α_{12}) for the **GRFP** method and in Figs. 5-37 (α_{11}) and 5-38 (α_{12}) for the **Global** method.

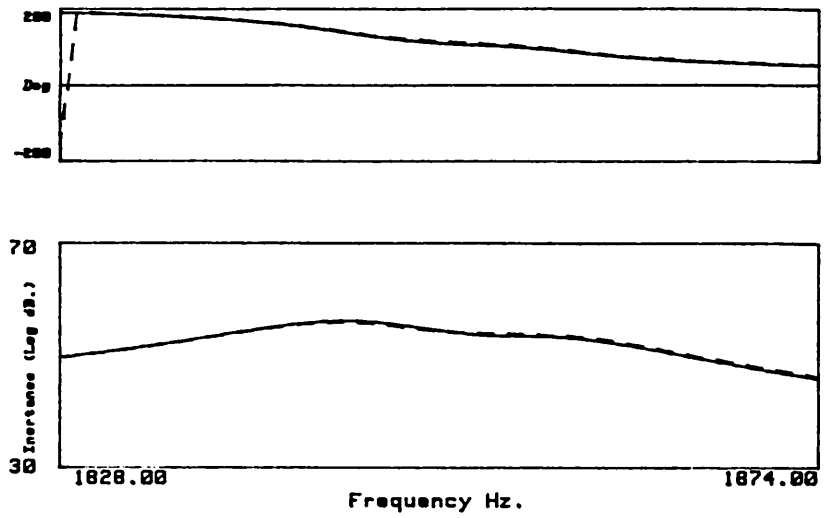

Fig. 5-35 Original (dotted line) and regenerated (solid line) α_{11} using the GRFP method.

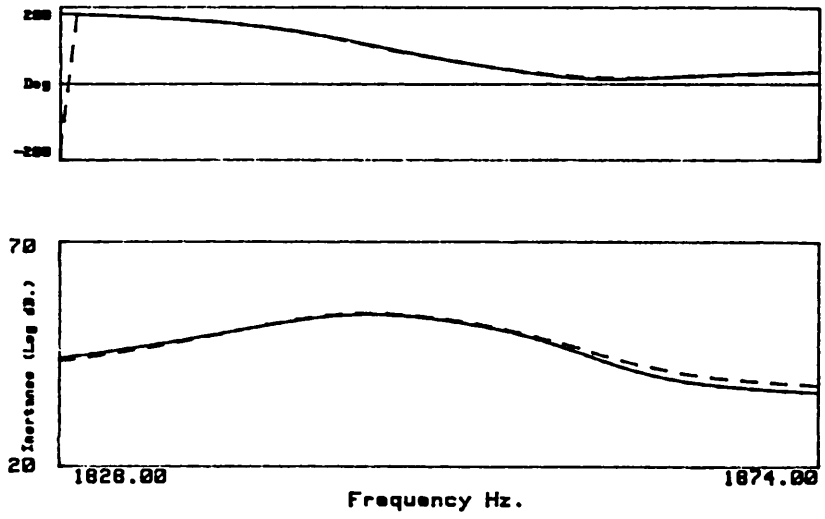

Fig. 5-36 Original (dotted line) and regenerated (solid line) α_{12} using the GRFP method.

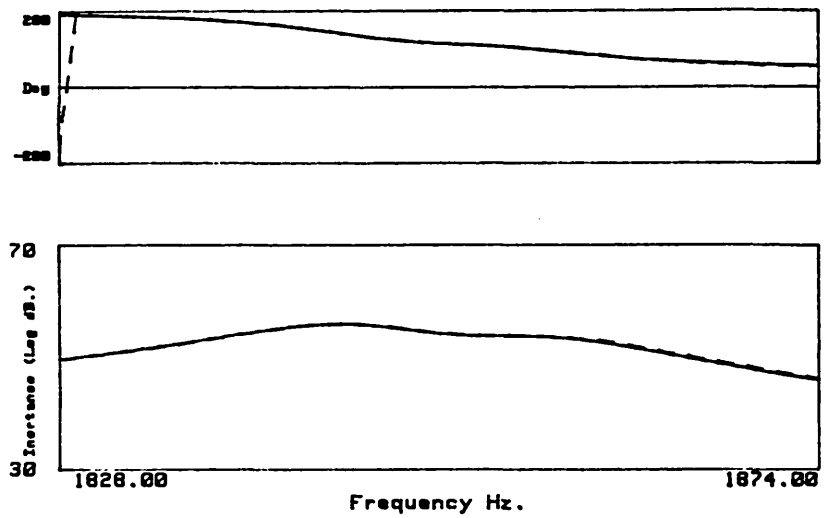

Fig. 5-37 Original (dotted line) and regenerated (solid line) α_{11} using the **Global** method.

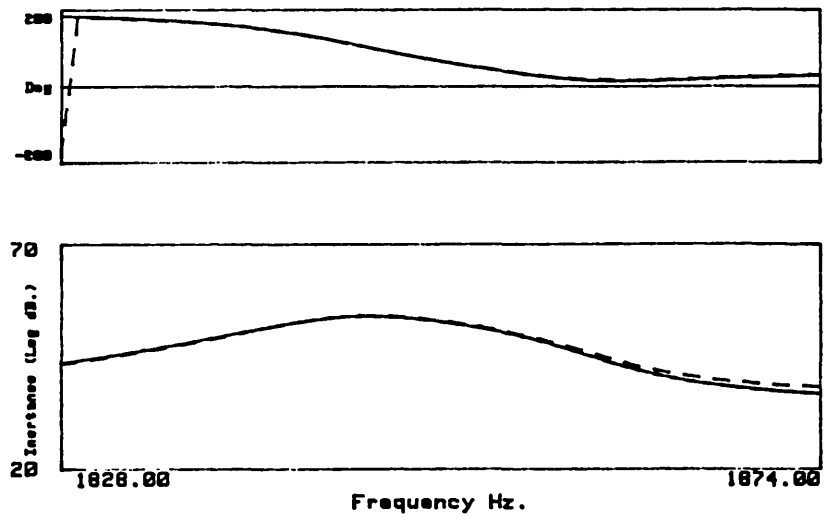

Fig. 5-38 Original (dotted line) and regenerated (solid line) α_{12} using the **Global** method.

5-4-5 Discussion

Analysing the results of Table 5-23, it can be seen that the **GRFP** and **Global** methods agree very well, and that the best curves are those of Figs. 5-37 and 5-38, corresponding to the **Global** method. Considering the results from the **Global** method as the most reliable ones, a comparison of the results from the **Spectral** with respect to the **Global** method give the following relative errors (Table 5-24):

Mode	FRF	$\varepsilon\,\omega_r(\%)$	$\varepsilon\,\eta_r(\%)$	$\varepsilon\,C_r(\%)$	$\lvert\Delta\phi_r\rvert$(deg.)
1	α_{11}	0.09	24.34	28.09	9.82
	α_{12}	"	"	13.39	8.82
2	α_{11}	0.21	42.26	84.73	11.39
	α_{12}	"	"	37.13	0.72

Table 5-24 Relative errors of the identification of the **Spectral** method with respect to the **Global** method.

The errors in the natural frequency and even in the phase angles are acceptable, but the errors in the damping ratios and modal constants are very high. The regeneration of the experimental curves using the **Spectral** method, is not completely disastrous only because the errors in the damping ratios and modal constants tend to compensate each other, which proves once more that a reasonable regeneration does not necessarily mean a valid identification.

It is important now to establish how the accuracy of the Spectral method could be assessed without having to compare it with other methods. One possible solution is to let the computer program run several times, as for the **GRFP** or **Global** methods, and to obtain quality indicators for each of the modal parameters. A variation of the program presented here was

written for this purpose with the result that the program was unable to provide an answer, i. e., the scatter of results from run to run was such that no consistent modal parameters could be found within an allowed tolerance. This proved that the method was not suitable for analysing this practical problem as it could not cope with the influence of the out-of-range modes. This kind of answer (i. e., "No consistent results were found") is, in our opinion, more informative and preferable than to have unreliable results, such as those in Table 5-22, where it is not clear to what extent the analysis is good or bad. The result now obtained, although a "negative" one, shows the importance of developing techniques in such a way that numerical results obtained by modal analysis algorithms are given together with indications of their quality. If the quality of those results is not good, another method must be tried. Inconclusive or poor results obtained for other experimental cases using the **Spectral** method showed that it does not seem to be appropriate to analyse accurately real structures.

5-5 Conclusions

5-5-1 Conclusions on the GRFP method

The conclusions drawn in Chapter 4 for the **RFP** method also apply to the **GRFP** method, except in respect of the frequency range chosen for the analysis: the **GRFP** method does not seem to be so much afflicted by that parameter. In addition to those conclusions, some more may be added now:

(i) the conventional formulation of the **GRFP** method was found here to have some difficulties, especially for the analysis of experimental data. An alternative formulation proposed in Section 5-2-4 proved to be much more reliable;

(ii) some problems may be encountered when using the **GRFP** method due to its sensitivity to variations of the global modal parameters from FRF to FRF. A failure of this method could well mean that systematic variations of the global parameters exist among the various FRFs used, due to incorrect measurement procedures or to genuine non-linearities of the system. This may be checked by analysing each FRF individually or by analysing globally two or three FRFs at a time;

(iii) the normalized standard deviation percentage proved to be a reliable indicator of the quality of the results and its direct use can serve to estimate the global modal parameters from a single FRF analysis, if for any reason the global analysis fails to work;

(iv) the results obtained confirm that the **GRFP** method gives more reliable values than the **RFP** method, as it can be checked by comparing the quality of both kind of results.

5-5-2 Conclusions on the Global method

The present investigation into the Global method led to the following conclusions:

(i) the algorithm of the method, considering differences of responses to take account of neighbouring modes (a philosophy similar to the "Bendent" method - Section 3-3-2), proved very reliable, even for very close modes;

(ii) the SVD technique has shown to be effective in obtaining accurate results and in giving a reliable indication of the number of genuine modes existing in the frequency range of interest;

(iii) when the data are considerably noisy, however, even the SVD may fail to give the right answers for the genuine number of modes. In that case, the calculations can be repeated several times, each taking a different set of points, in a similar way as in the **GRFP** method. The repeatability of the number of genuine modes obtained in each run of the program is analysed and a final answer is given (the most frequently repeated one), with an indication of the number of times it has occurred. Average values and standard deviations of the corresponding modal properties are also given;

(iv) the implicit assumption that the contribution of neighbouring modes is a constant around each mode under consideration means that the data points taken into the analysis should be concentrated around the resonant peaks of the FRFs. This is directly related to the frequency range chosen: in the case of two close modes, a narrow frequency range must be taken around them and, for widely spaced modes, sets of narrow frequency ranges around the several peaks must be specified. Moreover, the differences of response to be calculated must be taken between close data points, although a compromise should be established: differences between data points too close may lead to numerical problems;

(v) in contrast to the **GRFP** method, the **Global** method proved to be practically invulnerable to variations of the global properties from FRF to FRF;

(vi) finally, the theoretical and experimental examples showed the **Global** method to be a very powerful technique for analysing a set of FRFs and to be more accurate and reliable than the **GRFP** method, as well as being less time-consuming.

5-5-3 Conclusions on the Spectral method

With respect to this method, the conclusions are:

(i) the method works reasonably well for theoretical data, to analyse close modes. The frequency range taken into the analysis must be as narrow as possible, in order to avoid the influence of neighbouring modes;

(ii) an alternative approach for this method was tried, but no improvements were achieved, when tested with theoretical examples;

(iii) a comparison with the **GRFP** and **Global** methods showed that, for experimental data, the results obtained with the **Spectral** method were very poor. A modification of the algorithm to include analyses from several runs with different sets of data points each time (as done for the previous methods) was tried but the conclusion drawn was that reliable answers could not be obtained. The final conclusion is that this method is not appropriate to analyse practical cases.

CHAPTER 6

REAL MODES vs. COMPLEX MODES

6-1 Introduction

The major objective of the previous chapters of this work has been the extraction of valid modal properties from measured data. According to Section 1-1, one has been dealing with the second stage of experimental modal analysis, the identification process. In a large number of practical applications, we are content with such a study, as it provides the mathematical model sought for the structure under consideration. There are, however, other cases where further study is desired, and it is necessary to go into the post-processing stage of EMA. A typical application is the calculation of real modes from a set of complex modes.

The identification process usually supplies the user with a set of complex mode-shapes, but in some cases it is important to determine the corresponding real mode-shapes, i. e., the mode-shapes of the associated conservative structure, in the pursuit of valid modal models. It seems

appropriate, therefore, to include in our work a discussion on this subject.

The evaluation of the real modes of a structure plays a particularly important role in the area of comparison/validation/up-dating of theoretical models and has been a matter of great interest for some time. In practice, we are often confronted by two kinds of results: a set of complex modes, after applying methods of curve- fitting and modal analysis to the experimental response functions, and a set of real modes, resulting from the theoretical modelling of a structure, usually using FEM models. If the experimental procedure and modal analysis have been carefully applied, we have, in principle, a more precise set of results in the complex modes, with the actual distribution of damping taken into consideration. If we have at our disposal a reliable method for extracting the real modes, then these can be compared with the theoretical results and thus validate and/or up-date the theoretical predictions.

Several different methods have been proposed on this subject (Refs. [131] to [138]). The objective of this chapter is to highlight, discuss and compare two very simple techniques that can be used for this purpose. An evaluation of the two methods is made using theoretical data and each of them is compared against the "exact" results using the well-known Modal Assurance Criterion (MAC), in order to assess which one is more reliable in obtaining a valid set of real mode-shapes.

6-2 Theory

6-2-1 Niedbal's method

This method (Ref. [139]) is based on the simple assumption that the real modes must be related to the complex modes through a linear transformation $[T_1]$ (complex, in general):

$$[\Phi_u] = [\Phi]\,[T_1] \tag{6-1}$$

Separation of Eq. (6-1) into its real and imaginary parts, leads to:

$$[\Phi_u] = \mathrm{Re}[\Phi]\,\mathrm{Re}[T_1] - \mathrm{Im}[\Phi]\,\mathrm{Im}[T_1] \tag{6-2}$$

$$[\,0\,] = \mathrm{Im}[\Phi]\,\mathrm{Re}[T_1] + \mathrm{Re}[\Phi]\,\mathrm{Im}[T_1] \tag{6-3}$$

From (6-3), it follows that

$$\mathrm{Re}[\Phi]\,\mathrm{Im}[T_1] = -\,\mathrm{Im}[\Phi]\,\mathrm{Re}[T_1] \tag{6-4}$$

In general, we only have an incomplete mass-normalized modal matrix $\mathbf{pxN_0}$ available (with $\mathbf{p \geq N_0}$) from a **NxN** system; pre-multiplying (6-4) by $\mathbf{Re[\Phi]^T}$, an $\mathbf{N_0xN_0}$ matrix equation is obtained:

$$\mathrm{Re}[\Phi]^T\,\mathrm{Re}[\Phi]\,\mathrm{Im}[T_1] = -\,\mathrm{Re}[\Phi]^T\,\mathrm{Im}[\Phi]\,\mathrm{Re}[T_1] \tag{6-5}$$

from which,

$$\mathrm{Im}[T_1] = -\,[\mathrm{Re}[\Phi]^T\,\mathrm{Re}[\Phi]]^{-1}\,\mathrm{Re}[\Phi]^T\,\mathrm{Im}[\Phi]\,\mathrm{Re}[T_1] \tag{6-6}$$

Substituting in (6-2), we obtain

$$[\Phi_u] = \left[\mathrm{Re}[\Phi] + \mathrm{Im}[\Phi]\,[\mathrm{Re}[\Phi]^T\,\mathrm{Re}[\Phi]]^{-1}\,\mathrm{Re}[\Phi]^T\,\mathrm{Im}[\Phi]\right]\mathrm{Re}[T_1] \tag{6-7}$$

From the above equations, it can be observed that the transformation stated in (6-1) is not unique and so it is necessary to use another condition in order to make it so. If the theoretical (and unknown) matrices of the system are **[M]** and **[K']**, then one can write :

$$\begin{aligned} [\,m\,] &= [\Phi]^T\,[M]\,[\Phi] = [\,I\,] \\ [\,k'\,] &= [\Phi]^T\,[K']\,[\Phi] = [\,\lambda'\,] \end{aligned} \tag{6-8}$$

and substituting (6-1) in (6-8),

$$\begin{aligned} [\,m\,] &= [T_1]^{-T}\,[\Phi_u]^T\,[M]\,[\Phi_u]\,[T_1]^{-1} = [\,I\,] \\ [\,k'\,] &= [T_1]^{-T}\,[\Phi_u]^T\,[K']\,[\Phi_u]\,[T_1]^{-1} = [\,\lambda'\,] \end{aligned} \tag{6-9}$$

or

$$\begin{aligned} [\,m\,] &= [T_1]^{-T}\,[\bar{M}]\,[T_1]^{-1} = [\,I\,] \\ [\,k'\,] &= [T_1]^{-T}\,[\bar{K}']\,[T_1]^{-1} = [\,\lambda'\,] \end{aligned} \tag{6-10}$$

from which

$$\begin{aligned} [\bar{M}] &= [T_1]^T\,[T_1] \\ [\bar{K}'] &= [T_1]^T\,[\,\lambda'\,]\,[T_1] \end{aligned} \tag{6-11}$$

If $[\bar{K}]$ is the real part of $[\bar{K}']$, $[\bar{M}]$ and $[\bar{K}]$ must satisfy

$$[[\bar{K}] - \lambda_u\,[\bar{M}]]\,\{q_u\} = \{0\} \tag{6-12}$$

In order to make $[\bar{M}]$ and $[\bar{K}]$ diagonal, we have to solve this eigenproblem and find the transformation $[T_2]$ to yield the principal coordinates $\{p_u\}$:

$$\{q_u\} = [T_2]\,\{p_u\} \tag{6-13}$$

and so,

$$\begin{aligned} [\,\bar{m}\,] &= [T_2]^T\,[\bar{M}]\,[T_2] = [\,I\,] \\ [\,\bar{k}\,] &= [T_2]^T\,[\bar{K}]\,[T_2] = [\,\lambda_u\,] \end{aligned} \tag{6-14}$$

Substituting (6-11) in (6-14),

$$[\bar{m}] = [T_2]^T [T_1]^T [T_1] [T_2] = [I]$$
$$[\bar{k}] = [T_2]^T \mathrm{Re}[[T_1]^T [\lambda'] [T_1]] [T_2] = [\lambda_u] \tag{6-15}$$

From equations (6-11) and (6-15) we see that should the matrix $\mathbf{Re}[\mathbf{T_1}]$ be well chosen, matrix $[\mathbf{T_2}]$ would be the identity matrix. In general, $\mathbf{Re}[\mathbf{T_1}]$ can be given any value and the transformation from the complex modes to the mass-normalized real modes will be

$$[\Phi_u] = [\Phi] [T_1] [T_2] \tag{6-16}$$

For simplicity, we will take $\mathbf{Re}[\mathbf{T_1}]$ to be the identity matrix.

Next, a summary of this method is presented; in practice, since $[\Phi]$ and $[\lambda']$ are known values, we must go through the following steps :

1 - Assume $\mathbf{Re}[\mathbf{T_1}]$ to be the identity matrix and calculate $\mathbf{Im}[\mathbf{T_1}]$, applying Eq. (6-6);

2 - Calculate $[\bar{\mathbf{M}}]$ and $[\bar{\mathbf{K}}]$ using Eq. (6-11);

3 - Solve the eigenproblem of Eq. (6-12) to calculate $[\lambda_u]$ and $[\mathbf{T_2}]$;

4 - Calculate the real mass-normalized modes, using Eq. (6-16).

6-2-2 Asher's method

This method, already mentioned in Section 2-4, uses the fact that the application of several shakers that are suitably tuned can excite individual undamped (real) modes of vibration of a structure.

Usually, application of the method gives values for the undamped natural

frequencies and the relative forces the shakers must apply. As also mentioned in Section 2-4, an alternative approach is to simulate numerically the application of those forces, instead of actually applying them to the structure. For the basic theory of this method, we can follow, for example, Ref. [116].

The matrix equilibrium equation of a system can be expressed as

$$[M]\{\ddot{y}(t)\} + [C]\{\dot{y}(t)\} + [K]\{y(t)\} = \{f(t)\} \tag{6-17}$$

If $\{f(t)\} = \{\bar{F}\}\sin\omega t$, the response will be $\{y(t)\} = \{\bar{Y}\}\sin(\omega t - \theta)$. Hence,

$$[[K] - \omega^2[M]]\{\bar{Y}\}\sin(\omega t - \theta) + [C]\,\omega\cos(\omega t - \theta)\{\bar{Y}\} = \{\bar{F}\}\sin\omega t \tag{6-18}$$

For all time **t**, we have

$$\begin{aligned} &\cos\theta\,[[K] - \omega^2[M]]\{\bar{Y}\} + \omega\sin\theta\,[C]\{\bar{Y}\} = \{\bar{F}\} \\ &-\sin\theta\,[[K] - \omega^2[M]]\{\bar{Y}\} + \omega\cos\theta\,[C]\{\bar{Y}\} = \{0\} \end{aligned} \tag{6-19}$$

for $\theta = 90^\circ$, the displacements will be in quadrature with the excitation forces and we obtain

$$\omega[C]\{\bar{Y}\} = \{\bar{F}\} \tag{6-20 a}$$

$$[[K] - \omega^2[M]]\{\bar{Y}\} = \{0\} \tag{6-20 b}$$

We can see from (6-20 b) that the condition $\theta = 90^\circ$ corresponds to the undamped solution of the system and the force distribution is given by $\{\bar{F}\}$. This means that if we were to excite the system with the force distribution $\{\bar{F}\}$ we would obtain the real modes of vibration. Writing the amplitude response of the system in terms of the complex frequency response function $[\alpha(j\omega)]$, we have

$$\{\bar{Y}\} = [[K] - \omega^2 [M] + j\omega [C]]^{-1} \{\bar{F}\}$$

$$= [Re[\alpha(j\omega)] + jIm[\alpha(j\omega)]] \{\bar{F}\} \quad (6\text{-}21)$$

The condition of the displacements being in quadrature with the forces means that

$$Re[\alpha(j\omega)] \{\bar{F}\} = \{0\} \quad (6\text{-}22)$$

Solving

$$\det [Re[\alpha(j\omega)]] = 0 \quad (6\text{-}23)$$

enables us to determine the undamped natural frequencies which, when substituted in (6-22), give us the force distribution $\{\bar{F}\}$. Moreover, from (6-21), we can find the real modes of vibration, which will be given by

$$\{\phi_u\} = Im[\alpha(j\omega)] \{\bar{F}\} \quad (6\text{-}24)$$

Reviewing this method, we identify the following steps:

1 - From the complex identified modes and frequencies, $[\Phi]$ and $[\lambda']$, calculate $[\alpha(j\omega)]$ (given by $[\Phi] [\lambda' - \omega^2]^{-1} [\Phi]^T$);

2 - The undamped natural frequencies are calculated from (6-23);

3 - The force distribution is calculated from (6-22);

4 - The real modes are calculated using (6-24).

6-3 Numerical examples

Complex modes of vibration exist whenever we have a non-proportional distribution of damping around a structure. In practice, this is always the

case to a degree but usually the complexity is very weak and the modes can be considered as real. Apart from the non-proportional distribution of damping, the amount of damping itself and the closeness of modes in terms of natural frequencies are the factors that influence the degree of complexity of a structure. To generate complex modes theoretically in order to test the methods above mentioned, we will choose a system with a high degree of non-proportionality and very close modes in terms of natural frequency spacing.

6-3-1 Example 1

It is well known that systems with circular symmetry like discs, for example, have very close natural frequencies, even repeated ones in theory. We will consider the system of Fig. 6-1, with **10** degrees-of-freedom, having all the masses, springs and dampers identical, apart from one mistuned spring and damper (element 10).

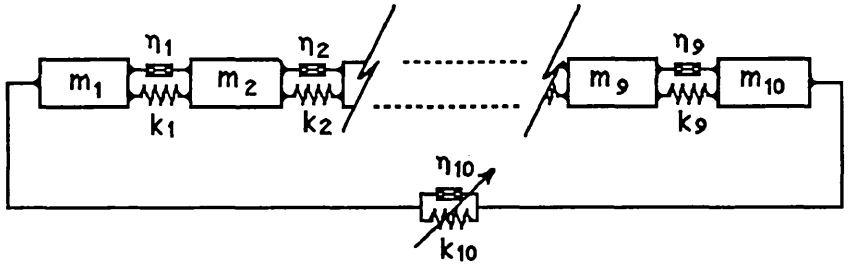

Fig. 6-1 - 10 DOF System.

The system has a rigid body mode and should all the elements be equal, the system would possess several repeated roots. The mistuning elements will provide separation in the natural frequencies, depending on the degree of asymmetry. To generate very close modes, the relation between the mistuned spring and all the others will be set at **1.01** while for the damper we will have a ratio of **20**. All the masses will have the numerical value of

Eigenvalues		Eigenvectors																	
		1		2		3		4		5		6		7		8		9		10	
Sq. Freq.	Damp.	Mod.	Phase	Mod.	Phase	Mod.	Phase	Mod.	Phase	Mod.	Phase	Mod.	Phase	Mod.	Phase	Mod.	Phase	Mod.	Phase	Mod.	Phase
0.000	0.000	0.316	0.000	0.425	0.000	0.135	-9.163	0.362	0.000	0.259	-9.105	0.263	0.000	0.366	171.205	0.138	0.000	0.487	177.152	0.326	29.345
0.382	0.010	0.316	0.000	0.263	0.000	0.361	-1.187	0.138	180.000	0.432	2.430	0.425	180.000	0.175	207.769	0.362	180.000	0.320	-23.624	0.325	190.932
0.385	0.046	0.316	0.000	0.000	166.037	0.448	0.567	0.447	180.000	0.031	77.960	0.000	-69.918	0.453	1.456	0.447	0.000	0.142	95.137	0.339	-2.795
1.382	0.010	0.316	0.000	0.263	180.000	0.364	1.314	0.138	180.000	0.426	180.046	0.425	0.000	0.137	167.446	0.362	180.000	0.270	202.056	0.356	168.572
1.393	0.047	0.316	0.000	0.425	180.000	0.139	1.621	0.362	0.000	0.265	181.865	0.263	180.000	0.365	182.724	0.138	0.000	0.413	8.747	0.367	-15.523
2.618	0.010	0.316	0.000	0.425	180.000	0.139	181.621	0.362	0.000	0.265	1.865	0.263	180.000	0.365	2.724	0.138	0.000	0.413	188.747	0.367	164.477
2.638	0.047	0.316	0.000	0.263	180.000	0.364	181.314	0.138	180.000	0.426	0.046	0.425	0.000	0.137	-12.554	0.362	180.000	0.270	22.056	0.356	-11.428
3.618	0.010	0.316	0.000	0.000	93.077	0.448	180.567	0.447	180.000	0.031	257.960	0.000	121.282	0.453	181.456	0.447	0.000	0.142	-84.863	0.339	177.205
3.636	0.051	0.316	0.000	0.263	0.000	0.361	178.813	0.138	180.000	0.432	182.430	0.425	180.000	0.175	27.769	0.362	180.000	0.320	156.376	0.325	10.932
3.968	0.027	0.316	0.000	0.425	0.000	0.135	170.837	0.362	0.000	0.259	170.895	0.263	0.000	0.366	-8.795	0.138	0.000	0.487	-2.848	0.326	209.345

Table 6-1 Damped eigensolution for system of Fig. 6-1.

Eigenvalues	Eigenvectors									
Sq. Freq.	1	2	3	4	5	6	7	8	9	10
0.000	0.316	- 0.425	- 0.137	- 0.362	0.261	- 0.263	- 0.359	- 0.138	0.424	0.324
0.382	0.316	- 0.263	- 0.361	0.138	0.426	0.425	- 0.142	0.362	- 0.256	- 0.319
0.383	0.316	0.000	- 0.447	0.447	0.002	0.000	0.448	- 0.447	- 0.007	0.315
1.382	0.316	0.263	- 0.362	0.138	- 0.425	- 0.425	- 0.137	0.362	0.268	- 0.312
1.385	0.316	0.425	- 0.138	- 0.362	- 0.263	0.263	- 0.363	- 0.138	- 0.428	0.311
2.618	0.316	0.425	0.138	- 0.362	0.263	0.263	0.363	- 0.138	0.428	- 0.311
2.623	0.316	0.263	0.362	0.138	0.425	- 0.425	0.137	0.362	- 0.268	0.312
3.618	0.316	- 0.000	0.447	0.447	- 0.002	- 0.000	- 0.448	- 0.447	0.007	- 0.315
3.625	0.316	- 0.263	0.361	0.138	- 0.426	0.425	0.142	0.362	0.256	0.319
4.004	0.316	- 0.425	0.137	- 0.362	- 0.261	- 0.263	0.359	- 0.138	- 0.424	- 0.324

Table 6-2 Undamped eigensolution for system of Fig. 6-1.

1, as will the springs (except the mistuned one). All the dampers will be equal to **0.01** (again, except the mistuned one). Due to the geometry, there will always be some real modes. The damped eigensolution is presented in Table 6-1 and the undamped eigensolution is presented in Table 6-2.

Incompletness of the model was simulated by using only **9x9**, **8x8**, **7x7**, **6x6** and **5x5** sub-matrices from the initial **10x10** one. For the **5x5** case, the results are presented in Tables 6-3 and 6-4 using both **Niedbal** and **Asher** methods, respectively.

Eigenvalues	Eigenvectors				
(squared freq.)	**1**	**2**	**3**	**4**	**5**
0.000	0.316	0.429	-0.123	0.371	0.243
0.382	0.316	0.272	-0.355	-0.123	0.442
0.387	0.316	0.011	-0.449	-0.447	0.025
1.382	0.316	-0.254	-0.371	-0.153	-0.424
1.410	0.316	-0.422	-0.150	0.352	-0.280

Table 6-3 - **Niedbal**'s method (5x5)

Eigenvalues	Eigenvectors				
(squared freq.)	**1**	**2**	**3**	**4**	**5**
0.000	1.000	0.425	0.134	0.362	0.256
0.382	1.420	0.270	0.388	-0.120	0.466
0.386	0.561	0.012	0.493	-0.436	0.027
1.382	-0.522	-0.251	0.408	-0.150	-0.447
1.410	-0.443	-0.418	0.165	0.344	-0.295

Table 6-4 - **Asher**'s method (5x5)

The Modal Assurance Criterion - MAC - (Ref. [140]) was applied to the **5x5** case, and the exact undamped modes were compared with the real

modes obtained from both methods (Tables 6-5 and 6-6).

	1	2	3	4	5 (predicted)
1	**1.000**	0.000	0.834	0.000	0.000
2	0.000	**0.999**	0.001	0.001	0.789
3	0.837	0.001	**0.999**	0.161	0.001
4	0.000	0.000	0.163	**0.999**	0.003
5	0.000	0.798	0.001	0.001	**0.997**
(exact)					

Table 6-5 - MAC values for **Niedbal**'s method

	1	2	3	4	5 (predicted)
1	**0.214**	0.001	0.833	0.000	0.000
2	0.665	**0.999**	0.001	0.001	0.789
3	0.223	0.001	**0.999**	0.161	0.001
4	0.016	0.000	0.163	**0.999**	0.003
5	0.765	0.798	0.001	0.001	**0.997**
(exact)					

Table 6-6 - MAC values for **Asher**'s method

Discussion

Both methods are very simple in theory. However, in practice, some problems may occur and the programs written to apply them show that in particular **Asher**'s method has more problems when we are using incomplete models, which is always the practical situation. Sometimes it is not possible to find the correct result for the undamped natural frequencies or even any result at all, obliging us to use as an approximation the damped natural frequency. A major disadvantage is the difficulty of dealing with incomplete systems when we have the

information of the complex modes with more coordinate responses than modes, i. e., when the modal matrix is not square, as in that case the matrix $[\alpha(j\omega)]$ is rank deficient and we would have to use a partition, so that the number of forces (corresponding to the number of shakers) would be equal to the number of modes. As seen in Section 2-4, extensions of **Asher**'s method can accomodate that case, but here only the basic technique has been tried.

Numerical problems may also be found when dealing with rigid body modes, giving rise to errors in the real mode shape although this is not a very serious problem, as we already know which those modes are. **Niedbal**'s method was very easy to programme, found to work very well - even for highly incomplete models - and was able to use more coordinates than modes. The results are given in terms of mass-normalized real modes and the only problem found was that sometimes the incompletness of the model makes the mass matrix non-positive definite and equation (6-12) gives an incorrect result for $[T_2]$. When this happens, a message is given and what we must try is to give one or more coordinates of the identified complex modes. For instance, if we had given a **7x7** modal matrix, we could try and give a **8x7** or **9x7**, thus requiring one or more frequency response functions to be analysed.

The results of Table 6-5 show that the correlation between the exact modes and the predicted ones is good, except for the second method in the term **1,1** which corresponds to the rigid body mode. Some off diagonal elements are very large, where they were expected to be close to zero. By just looking at these values, it is not clear why this happens, but if we plot some graphs (Fig. 6-2 - Niedbal's method, Fig. 6-3 - Asher's method), where good results should align along a **45°** slope straight line, we can understand what is going on. For instance, from Table 6-5 (Niedbal's method), we see that the correlation between the exact mode **5** and the

predicted mode 2 is quite high, but if we look at the corresponding graph in Fig. 6-2, we note that there is a great deal of scatter in the results.

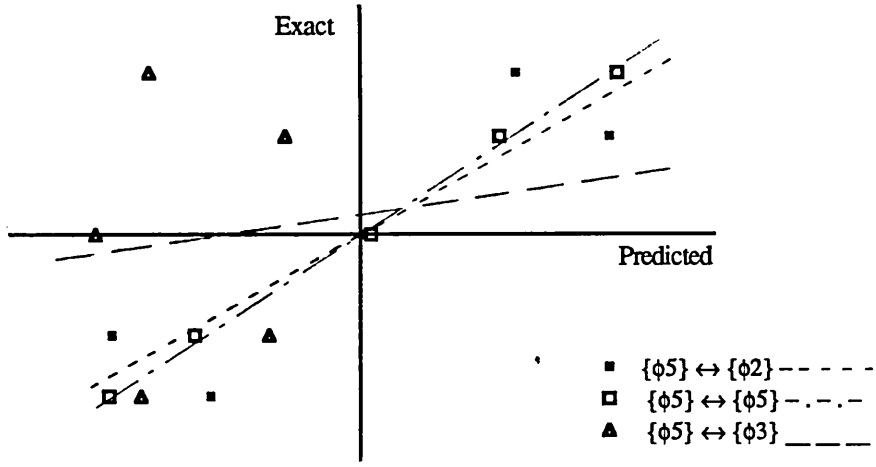

Fig. 6-2 - Some exact against predicted modes (Niedbal's method).

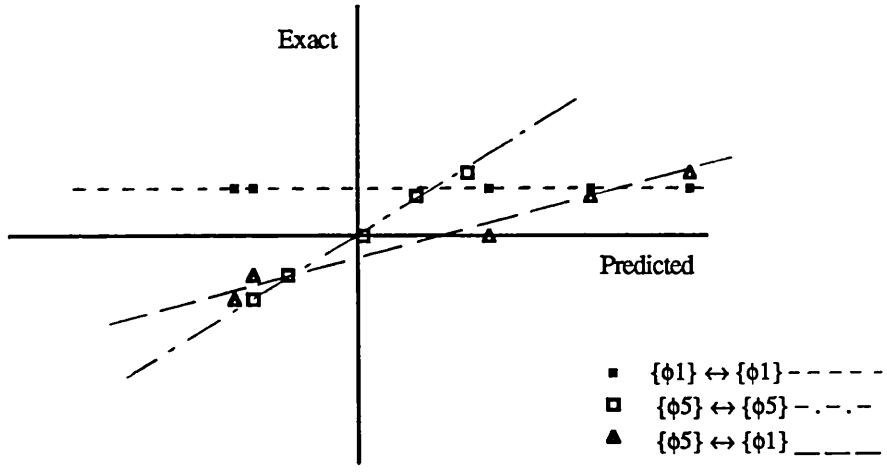

Fig. 6-3 - Some exact against predicted modes (Asher's method).

A good correlation is, for instance, the one between predicted and exact mode **5**. An example of a poor result is the correlation between exact mode **5** and predicted mode **3**. For **Asher**'s method, the MAC value between exact and predicted mode **1**, is very low. From Fig. 6-3 we see that this corresponds to a horizontal line, which indicates the existence of a rigid body mode. Fig. 6-3 also shows that the high MAC value between exact mode **5** and predicted mode **1** corresponds, in fact, to a staight line with a small slope, which indicates a poor correlation. The correlation between exact and predicted mode **5** is again very good, as confirmed by that graph. The results from the other cases of model incompleteness presented a similar trend.

6-3-2 Example 2

It can be argued that the previous example is not a very difficult one, as the modes, although quite close, are not very complex. In this second example the complexity of the modes will be increased by mistuning spring elements **1** and **10** by a factor of **1.005** and the damper elements **1** and **9** by a ratio of **20**. The damped solution is shown in Table 6-7. Because now, instead of one mistuned stifness element with the value **1.01**, we have two mistuned elements of **1.005** each, and because the numbers are quite small, the undamped solution is virtually the same as before and at least to the third decimal place, there is no difference. However, the damped solution provides modes with a considerable amount of complexity.

Asher's method showed many difficulties in dealing with this example and no reliable answers could be obtained. **Niedbal**'s method, on the contrary, worked reasonably well and some results will be presented, namely for the **10x5**, **8x5** and **5x5** cases of incompletness. The undamped eigensolutions for these cases are presented in Tables 6-8, 6-9 and 6-10, and the MAC values are shown in Tables 6-11, 6-12 and 6-13, respectively.

Eigenvalues		Eigenvectors															
		1		2		3		4		5		6		7		8		9		10	
Sq. Freq.	Damp.	Mod.	Phase	Mod.	Phase	Mod.	Phase	Mod.	Phase	Mod.	Phase	Mod.	Phase	Mod.	Phase	Mod.	Phase	Mod.	Phase	Mod.	Phase
0.000	0.000	0.316	180.000	0.381	180.003	0.228	- 15.237	0.394	174.513	0.227	178.781	0.398	5.104	0.128	- 82.421	0.570	180.062	0.233	15.199	0.090	64.120
0.385	0.024	0.316	180.000	0.166	177.636	0.414	- 0.980	0.328	186.972	0.320	5.706	0.318	172.670	0.457	5.990	0.287	- 52.094	0.415	181.046	0.215	191.466
0.401	0.161	0.316	180.000	0.113	6.062	0.442	3.051	0.194	- 1.484	0.412	- 0.818	0.198	182.178	0.382	177.844	0.136	77.007	0.440	- 3.103	0.353	0.944
1.411	0.132	0.316	180.000	0.348	1.954	0.294	3.505	0.439	0.453	0.101	216.833	0.434	- 0.419	0.139	178.935	0.065	190.667	0.293	176.225	0.450	177.393
1.422	0.053	0.316	180.000	0.449	0.689	0.031	- 23.949	0.094	- 46.970	0.463	182.974	0.092	223.226	0.496	0.707	0.064	- 36.839	0.031	19.849	0.488	- 3.470
2.606	0.074	0.316	180.000	0.378	- 0.832	0.252	189.093	0.417	187.527	0.202	158.319	0.408	172.605	0.281	198.316	0.061	171.782	0.249	- 8.789	0.462	177.644
2.818	0.068	0.316	180.000	0.162	- 5.753	0.430	184.801	0.333	161.207	0.367	12.361	0.336	17.008	0.312	159.426	0.111	62.402	0.427	175.230	0.377	1.355
3.506	0.352	0.316	180.000	0.120	190.393	0.439	178.924	0.300	34.907	0.403	- 7.300	0.280	- 36.283	0.525	5.007	0.241	- 65.351	0.438	0.879	0.247	191.167
3.603	0.027	0.316	180.000	0.352	182.934	0.282	164.442	0.492	- 5.702	0.186	225.314	0.487	184.144	0.266	240.770	0.480	166.281	0.286	194.705	0.116	49.841
3.869	0.018	0.316	180.000	0.434	176.662	0.032	108.672	0.105	- 82.513	0.409	168.131	0.104	27.138	0.358	141.815	0.764	10.793	0.033	16.114	0.109	- 72.137

Table 6-7 Damped eigensolution for system of Fig. 6-1 with two mistuned springs and dampers.

Eigenvalues	Eigenvectors				
(squared freq.)	**1**	**2**	**3**	**4**	**5**
0.000	0.316	- 0.432	- 0.118	- 0.442	- 0.105
0.384	0.316	- 0.273	- 0.349	0.003	- 0.459
0.391	0.316	- 0.012	- 0.449	0.436	- 0.158
1.404	0.316	0.254	- 0.377	0.254	0.366
1.441	0.316	0.423	- 0.152	- 0.278	0.369
	0.316	0.431	0.133	- 0.419	- 0.157
	0.316	0.271	0.361	0.022	- 0.464
	0.316	0.008	0.448	0.433	- 0.102
	0.316	- 0.256	0.367	0.245	0.417
	0.316	- 0.413	0.135	- 0.254	0.295

Table 6-8 - **Niedbal**'s method (10x5).

Eigenvalues	Eigenvectors				
(squared freq.)	**1**	**2**	**3**	**4**	**5**
0.000	0.316	0.417	0.146	- 0.369	0.263
0.384	0.316	0.239	0.369	0.168	0.471
0.400	0.316	- 0.031	0.455	0.460	0.012
1.421	0.316	- 0.289	0.359	0.099	- 0.446
1.600	0.316	- 0.437	0.112	- 0.396	- 0.248
	0.316	- 0.416	- 0.180	- 0.330	0.319
	0.316	- 0.235	- 0.393	0.198	0.427
	0.316	0.036	- 0.448	0.447	- 0.108

Table 6-9 - **Niedbal**'s method (8x5).

Eigenvalues	Eigenvectors				
(squared freq.)	**1**	**2**	**3**	**4**	**5**
0.000	0.316	0.395	0.176	0.099	0.507
0.385	0.316	0.193	0.410	- 0.419	0.303
0.426	0.316	- 0.084	0.476	- 0.327	- 0.285
1.495	0.316	- 0.330	0.334	0.241	- 0.393
1.815	0.316	- 0.447	0.048	0.467	0.121

Table 6-10 - **Niedbal**'s method (5x5).

	1	**2**	**3**	**4**	**5**	(predicted)
1	**1.000**	0.000	0.000	0.000	0.000	
2	0.000	**0.999**	0.001	0.000	0.000	
3	0.000	0.001	**0.999**	0.000	0.001	
4	0.000	0.000	0.000	**0.917**	0.077	
5	0.000	0.000	0.000	0.082	**0.914**	
(exact)						

Table 6-11 - MAC values for **Niedbal**'s method (10x5).

	1	**2**	**3**	**4**	**5**	(predicted)
1	**1.000**	0.087	0.025	0.011	0.070	
2	0.079	**0.994**	0.058	0.021	0.070	
3	0.037	0.013	**0.997**	0.010	0.025	
4	0.007	0.023	0.001	**0.991**	0.014	
5	0.079	0.103	0.060	0.002	**0.982**	
(exact)						

Table 6-12 - MAC values for **Niedbal**'s method (8x5).

	1	2	3	4	5 (predicted)
1	**1.000**	0.029	0.773	0.010	0.021
2	0.000	**0.965**	0.021	0.384	0.403
3	0.837	0.035	**0.975**	0.062	0.018
4	0.000	0.006	0.204	**0.496**	0.449
5	0.000	0.772	0.017	0.505	**0.524**
(exact)					

Table 6-13 - MAC values for **Niedbal**'s method (5x5).

Discussion

The results presented in Tables 6-8, 6-9 and 6-10 show that as we go from the **10x10** to the **5x5** case, the results from **Niedbal**'s method become poorer, as reflected in the corresponding MAC values. It is clear that this method is more sensitive to incompletness in terms of number of coordinates than in terms of number of modes: the MAC values for the **10x5** and **8x5** cases (Tables 6-11 and 6-12) are very good, while for the **5x5** case (Table 6-13), only the first **3** modes can be considered as well identified.

6-4 Conclusions

Two different methods of calculating the real modes of vibration for a structure from knowledge of the identified complex modes - **Niedbal**'s and **Asher**'s methods - have been programmed and the results compared against theoretical values using the Modal Assurance Criterion. Although both methods are very simple in theory, some numerical problems arose and **Niedbal**'s method proved to be more reliable and easy to implement than **Asher**'s method, giving very accurate results, even for incomplete sets of close complex modes.

CHAPTER 7

CONCLUSIONS

7-1 General conclusions

In each of the previous chapters of this work, discussions and conclusions have already been included: in this section a general summary of those conclusions is presented.

Many modal analysis identification methods are available nowadays. Normally, the most sophisticated ones are also the most automatic ones and they tend to be used as "black boxes", with little or no intervention by the user. This can be "dangerous", in the sense that a solution is always provided but it may be difficult to assess how good that solution is. The alternative simple methods are easy to manipulate and to control by an experienced user, but the analysis may become very time-consuming and costly. Nevertheless, these simple methods are the ones that can provide more insight into the way a structure behaves. The choice of the method to use is very important and depends on many factors, such as the kind of

software and hardware available, the objectives sought, the type of structure to be analysed, the time and money available, the experience of the user, etc.

When large amounts of data are to be analysed, the current tendency is to go for completely automatic methods (provided the means exist), where all the data are analysed simultaneously. Because of the drawbacks that such an analysis may embody (as mentioned above), the ideal solution should be to introduce into the software the capacity of judgement so as to obtain a final answer that would contain information about the quality of the analysis. The necessity of having "intelligent" computer programs of analysis is, naturally, more important whenever the data obtained from the measurements are difficult to handle, as in the case when noise is present and/or close vibration modes exist; in such a situation, it can be difficult to know whether the results are a consequence of noise or the true properties of the structure.

Throughout this thesis, several modal analysis methods have been described and their performance assessed, based upon data that contained close modes and a certain amount of noise. The theoretical background of those methods has been explained in detail and improvements and new developments introduced in order to provide a degree of "intelligence" into the analysis. This has been done in MDOF methods, considering one or more data curves in the analysis, but a study of SDOF methods has also been made. One may question whether it is appropriate to bother nowadays with SDOF methods, often considered as being rather simple or, at least, out-of-fashion. Our belief is that a good understanding of the physical implications of the behaviour of a structure possessing, for example, close vibration modes, has necessarily to begin by studying few modes and using simple methods of analysis, like the SDOF ones. Here, a study of the interference between two close modes has shown that some SDOF methods can still cope with that situation, within certain limits or, at least, provide

useful indications about the true existence of one or two modes. Therefore, to a certain extent, SDOF methods can also be made more automatic and "intelligent".

As a general conclusion, we can say that a full expert system, capable of taking decisions is yet far from achievement, but it is believed that in this work some steps towards such a goal have been taken. An expert system would ideally be able of eliminating the intervention of the user, which may comprise (i) decison on the method to be utilized, (ii) a first estimation of the number of modes existing in a particular frequency range, (iii) sorting out of the results obtained, (iv) estimation of the number of genuine existing modes, (v) assessment of the identification by comparing the original and regenerated FRF(s), (vi) cross-checking of the results obtained with different locations of the input force(s), (vii) confirmation of the linear behaviour assumption, etc. These several aspects may be more expanded in the future, by developing reliable numerical techniques and introducing criteria of decision into the algorithms. It is desired that the various points to be developed individually can be brought together to build up more powerful and "intelligent" algorithms. In addition, some of the items mentioned above could be optional (e. g., (vi) and (vii)).

7-2 New contributions of the present research

Specific contributions of this research are listed next, chapter by chapter, so that it becomes clear to the reader which parts of the work constitute new developments or attempts to new developments. The itemized description given below is justified by the fact that the new contributions are spread throughout the thesis, rather than being concentrated in any particular part of it.

In Chapter 2, the contribution given is a comprehensive classification and

detailed description of the great majority of current modal analysis methods, which helps not only the understanding of the theoretical background, but also the relationship between the several methods. Other works on this matter cover only some methods and/or give a short and even inadequate explanation of the theory involved.

In Chapter 3, the major contributions are as follows:

i) critical discussion on the degree of interference between two close modes and the implications for their identification;

ii) derivation and implementation in a modal analysis computer program of an indicator of close modes, based on the plotting of the centers of the consecutive circles for each set of four points around the frequency range of interest;

iii) establishment of the inspection of inverse of receptance plots as a means of recognizing the existence of two close modes;

iv) derivation and implementation in the modal analysis computer program of the **Inverse** method (for complex modes) as an alternative SDOF method to estimate the modal parameters of a structure;

v) implementation of one of the interference criteria in the cited program, to give an indication whether or not the SIM technique should be used and also the implementation in the same program of the option AUTO-SIM to iterate automatically and to refine the identification of two close modes;

vi) establishment of a parallel between the **Inverse** and "Bendent" methods, so that this last one can be more easily interpreted from a physical point of view.

The contributions concerning Chapter 4 are the following:

(i) a detailed explanation of the **RFP** method, very popular nowadays although the theory is, in general, not well presented;

(ii) exploitation of the capabilities of identification of close modes and the programming of an "intelligent" algorithm that can recognize the existence of one or two close modes and give quality indicators of the results;

(iii) the development of a new approach for the identification of lightly damped structures, and the establishment of a parallel with another already existing method, also dedicated to the analysis of that kind of structures, justifying more rigorously some empirical guide-lines suggested in previous works related to that other method;

(iv) the development and discussion of a fast, automatic and "intelligent" algorithm for that new approach, to obtain results with quality indicators.

In Chapter 5, the new developments are as follows:

(i) the reformulation of the **GRFP** method to deal better with experimentally obtained data, while the capabilities of taking decisions concerning two close modes remain as for the **RFP** method;

(ii) the presentation of an alternative way of calculating the global properties of a structure, based upon the identification of single FRFs and taking advantage of the knowledge of the quality indicators, and a comparison between the **GRFP** and **RFP** methods;

(iii) a detailed explanation of the theoretical background of the **Global** method, not currently available in the literature, that intends to attract the attention for this powerful method;

(iv) exploitation of the **Global** method capacities in identifying close modes and the extension of this method to include also the possibilities of obtaining more informative answers, in terms of quality;

(v) an attempt to improve the **Spectral** method, although not successful, and a comparison between the **GRFP**, **Global** and **Spectral** methods.

With respect to Chapter 6, the contribution given is a critical comparison between two known methods of calculating real modes from identified complex modes and the illustration, through some examples, of the good performance of **Niedbal**'s method.

7-3 Suggestions for future work

Some topics for further investigation on the matter of extraction of valid modal properties are indicated next. Two categories of developments are considered: short term and long term ones. The former refer to direct extensions of the work presented in this thesis while the latter constitute larger research projects on their own.

Considering the short term developments, we may identify the following ideas:

(i) extension of the algorithm that subtracts already identified modes from an FRF, based on SDOF methods, to make it totally automatic for the analysis of all the modes in the frequency range of interest;

(ii) development of an algorithm to locate reliably the resonance frequencies in FRFs taken from lightly damped structures;

(iii) improvement of the **RFP** method, substituting the polynomial solver by an eigensolver and to extend the "intelligent" procedure to the

analysis of a general number of modes;

(iv) to develop the **GRFP** "intelligent" algorithm to analyse also a general number of modes and to analyse automatically systematic deviations of the global properties of a structure, among the several FRFs;

(v) to develop the **SFD** method including "intelligent" capabilities, as this seems to be a very promising method.

Two long term projects that we envisage, are:

(i) an investigation on the various sources that may contribute to the existence of noise in the measured data, in order to assess the quality of the measured data prior to the analysis, by establishing, for example, boundaries of expected noise around particular frequency ranges;

(ii) the development of an "intelligent" algorithm based on several methods that would applied each method at a time and could decide on the best identification. It could, possibly, "decide" that the best identification was obtained using one particular method over one given frequency range and another method for another frequency range. One could start by studying only one single FRF using two different methods and then proceed for more complicated cases.

APPENDIX A

Derivation of Eq. (4-10)

Developing (4-9),

$$J = \{\{a^*\}^T[P^*]^T - \{b^*\}^T[T^*]^T - \{W^*\}^T\}\{[P]\{a\} - [T]\{b\} - \{W\}\}$$

$$= \{a^*\}^T[P^*]^T[P]\{a\} - \{a^*\}^T[P^*]^T[T]\{b\} - \{a^*\}^T[P^*]^T\{W\}$$

$$- \{b^*\}^T[T^*]^T[P]\{a\} + \{b^*\}^T[T^*]^T[T]\{b\} + \{b^*\}^T[T^*]^T\{W\}$$

$$- \{W^*\}^T[P]\{a\} + \{W^*\}^T[T]\{b\} + \{W^*\}^T\{W\} \qquad (4\text{-}9\ a)$$

But, as defined, **{a}** and **{b}** are real vectors, so **{a*}** = **{a}** and **{b*}** = **{b}**. Also, each term of (4-10) is a scalar, so identic to its transpose. We can write then,

$$J = \frac{1}{2}(\{a\}^T[P^*]^T[P]\{a\} + \{a\}^T[P]^T[P^*]\{a\}) - \{a\}^T[P^*]^T[T]\{b\}$$

$$- \{a\}^T[P^*]^T\{W\} - \{a\}^T[P]^T[T^*]\{b\} + \frac{1}{2}(\{b\}^T[T^*]^T[T]\{b\}$$

$$+ \{b\}^T[T]^T[T^*]\{b\}) + \{b\}^T[T^*]^T\{W\} - \{a\}^T[P]^T\{W^*\}$$

$$+ \{b\}^T[T]^T\{W^*\} + \{W^*\}^T\{W\} \qquad (4\text{-}9\ b)$$

or, rearranging,

$$J = \frac{1}{2}\{a\}^T([P^*]^T[P] + [P]^T[P^*])\{a\}$$

$$+ \frac{1}{2}\{b\}^T([T^*]^T[T] + [T]^T[T^*])\{b\}$$

$$- \{a\}^T([P^*]^T[T] + [P]^T[T^*])\{b\} - \{a\}^T([P^*]^T\{W\} + [P]^T\{W^*\})$$

$$+ \{b\}^T([T^*]^T\{W\} + [T]^T\{W^*\}) + \{W^*\}^T\{W\} \qquad (4\text{-}9\ c)$$

It is easy to see that

$$[P^*]^T[P] + [P]^T[P^*] = 2\,\mathrm{Re}([P^*]^T[P])$$

$$[P^*]^T[T] + [P]^T[T^*] = 2\,\mathrm{Re}([P^*]^T[T])$$

$$[T^*]^T[T] + [T]^T[T^*] = 2\,\mathrm{Re}([T^*]^T[T]) \qquad \text{(4-9 d)}$$

$$[P^*]^T\{W\} + [P]^T\{W^*\} = 2\,\mathrm{Re}([P^*]^T\{W\})$$

$$[T^*]^T\{W\} + [T]^T\{W^*\} = 2\,\mathrm{Re}([T^*]^T\{W\})$$

as the second term of the summation is the complex conjugate of the first. Therefore,

$$J = \{a\}^T\mathrm{Re}([P^*]^T[P])\{a\} + \{b\}^T\mathrm{Re}([T^*]^T[T])\{b\} + \{W^*\}^T\{W\}$$
$$- 2\{a\}^T\mathrm{Re}([P^*]^T[T])\{b\} - 2\{a\}^T\mathrm{Re}([P^*]^T\{W\})$$
$$+ 2\{b\}^T\mathrm{Re}([T^*]^T\{W\}) \qquad \text{(4-10)}$$

APPENDIX B

Orthogonal Functions

A set of functions $\mathbf{f_1(x)}$, $\mathbf{f_2(x)}$, ... $\mathbf{f_n(x)}$, is said to be mutually orthogonal over an interval $\mathbf{a \le x \le b}$ if

$$\int_a^b f_i(x)\, f_j(x)\, dx = 0 \qquad i \neq j$$

$$\int_a^b f_i^2(x)\, dx = Q_i > 0 \qquad i = j \tag{B-1}$$

and if $\mathbf{f_i(x)}$ are real, continuous and not identically zero.

We can normalize $\mathbf{f_i(x)}$ by defining

$$g_i(x) = f_i(x) / \sqrt{Q_i} \tag{B-2}$$

so that

$$\int_a^b g_i(x)\, g_j(x)\, dx = \begin{cases} 0 & i \neq j \\ 1 & i = j \end{cases} \tag{B-3}$$

when the data that we have to curve-fit is not of equal reliability, we can introduce a measure of the relative precision of the value to be assigned to $\mathbf{g_i(x)}$ by means of a weighting function $\mathbf{q(x) \ge 0}$. The functions are then said to be orthonormal relatively to to the weighting function $\mathbf{q(x)}$, over **[a, b]**:

$$\int_a^b q(x)\, g_i(x)\, g_j(x)\, dx = \begin{cases} 0 & i \neq j \\ 1 & i = j \end{cases} \tag{B-4}$$

If the functions $g_i(x)$ are to be calculated at **L** discrete points, the integral will be replaced by a summation over that number of points:

$$\sum_{k=1}^{L} q(x_k)\, g_i(x_k)\, g_j(x_k) = \begin{cases} 0 & i \neq j \\ 1 & i=j \end{cases} \qquad \text{(B-5)}$$

Usually, $g_i(x_k)$ will be polynomials. As in our case we are using complex polynomials, (B-5) becomes

$$\mathrm{Re}\left\{\sum_{k=1}^{L} q(x_k)\, g_i^*(x_k)\, g_j(x_k)\right\} = \begin{cases} 0 & i \neq j \\ 1 & i=j \end{cases} \qquad \text{(B-6)}$$

where * denotes complex conjugate.

APPENDIX C

Method of partial fractions

Let **N(s)/D(s)** denote the ratio of two polynomials, with no common factors, such that the degree **n** of **D(s)** is greater than that of **N(s)**, and suppose that **D(s)** has **n** distinct zeros $s_1, s_2, \ldots s_n$. Then, the coefficients in the partial fraction expansion

$$\frac{N(s)}{D(s)} = \frac{A_1}{s - s_1} + \frac{A_2}{s - s_2} + \ldots + \frac{A_n}{s - s_n} = \sum_{k=1}^{n} \frac{A_k}{s - s_k} \qquad \text{(C-1)}$$

are determined by the equation

$$A_k = \lim_{s \to s_k} (s - s_k) \frac{N(s)}{D(s)} \qquad \text{(C-2)}$$

or

$$A_k = \frac{N(s_k)}{D'(s_k)} \qquad \text{(C-3)}$$

where $D'(s_k)$ is the first derivative of **D(s)** for $s = s_k$.

Proof :

Multiplying Eq. (C-1) by $(s - s_k)$,

$$(s - s_k)\frac{N(s)}{D(s)} = (s - s_k)\frac{A_1}{s - s_1} + \ldots + (s - s_k)\frac{A_k}{s - s_k} + \ldots + (s - s_k)\frac{A_n}{s - s_n}$$

$$= (s - s_k)\frac{A_1}{s - s_1} + \ldots + A_k + \ldots + (s - s_k)\frac{A_n}{s - s_n} \qquad \text{(C-4)}$$

Taking the limit when $s \to s_k$, all terms on the right-hand-side of (C-4) vanish, except A_k:

$$A_k = \lim_{s \to s_k} (s - s_k) \frac{N(s)}{D(s)} \tag{C-5}$$

If we write (C.5) in the form

$$A_k = \frac{\lim_{s \to s_k} N(s)}{\lim_{s \to s_k} \frac{D(s)}{s - s_k}} \tag{C-6}$$

we obtain

$$A_k = \frac{N(s)}{0/0} \tag{C-7}$$

which is an indetermination. Applying L'Hôpital rule to the denominator of (C.6), we have

$$\lim_{s \to s_k} \frac{D(s)}{s - s_k} = \lim_{s \to s_k} \frac{D'(s)}{(s - s_k)'} = D'(s_k) \tag{C-8}$$

Hence,

$$A_k = \frac{N(s_k)}{D'(s_k)} \tag{C-9}$$

■

If in (C.6) we divide **D(s)** by $s - s_k$ or, equivalently, remove the factor $s - s_k$ from **D(s)**, and call it **Q(s)**, we obtain a more practical expression for A_k :

$$A_k = \frac{N(s_k)}{Q(s_k)} \tag{C-10}$$

APPENDIX D

The Singular Value Decomposition technique (SVD)

D-1 Introduction

The purpose of this Appendix is to give a simple introduction to the Singular Value Decomposition technique (SVD). This introduction follows closely the one given in Ref. [141]. It is not our intention to present a detailed explanation with a full and rigorous mathematical description, but instead a simple approach that enhances the main characteristics of this technique and highlights some common applications, providing the reader a first contact with this powerful numerical method before attacking a more profound text.

D-2 The rank of a matrix

The concept of rank of a matrix is directly related to the linear dependency of the rows (or columns) of that matrix. For example, an **NxN** matrix whose rows are linearly independent will have rank = **N** (full rank). If one of the rows is a linear combination of the others, then the rank will be **N-1**. In other words, the rank of a matrix equals its number of linearly independent rows. An **MxN** matrix with $M \geq N$ is said to be of 'full rank' if its rank = **N**, or 'rank-deficient' if its rank < **N**. For a square matrix, rank deficiency implies that the matrix is singular, i. e., the determinant equals zero.

The classical way of calculating the rank of a matrix is by means of Gauss elimination. An **NxN** matrix with rank = **r** < **N** will have **N-r** zero rows after a Gauss elimination. If we think of the rows of a matrix as being

vectors, two linearly dependent rows means two parallel vectors. Thus, the most linearly independent case for two rows is when the corresponding vectors are perpendicular, or in general, orthogonal. In practice, we can have anything in between these two extremes. If two vectors are almost but not exactly parallel, then the two corresponding rows of the matrix will not be linearly dependent ,but almost so and, in general, we will not have exact zero rows after a Gauss elimination, but a set of relatively small elements. These rows of small elements must be compared with the other rows of the matrix in order to assess the rank of the matrix. To compare rows, or vectors, may not be an easy task, especially for large matrices. The problem is even more complicated if the elements of the rows are complex quantities. It would be preferable to have a means of comparison in terms of scalars. The SVD of a matrix allows this comparison.

D-3 The Singular Value Decomposition

The **SVD** of an **MxN** real matrix [A] is given by:

$$\underset{(MxN)}{[A]} = \underset{(MxM)}{[U]} \; \underset{(MxN)}{[\Sigma]} \; \underset{(NxN)}{[V]^T} \tag{D-1}$$

where **[U]** and **[V]** are orthogonal matrices , i.e.,

$$[U]^T [U] = [U] [U]^T = [V]^T [V] = [V] [V]^T = [I] \tag{D-2}$$

and

$$[U]^T = [U]^{-1} \quad \text{and} \quad [V]^T = [V]^{-1} \tag{D-3}$$

[Σ] is a real matrix with elements $\sigma_{ij} = \sigma_i$ for **i=j** and $\sigma_{ij} = 0$ for **i≠j.** The values σ_i are called the singular values of matrix [A]. Without loss of

generality we shall assume them to be in decreasing order ($\sigma_1 > \sigma_2 > \ldots > \sigma_N$).

$$[\Sigma] = \underbrace{\begin{bmatrix} \sigma_1 & & & \\ & \sigma_2 & 0 & \\ & & \ddots & \\ 0 & & & \sigma_N \\ \hline & & 0 & \end{bmatrix}}_{N} \begin{matrix} \left.\vphantom{\begin{matrix}a\\b\\c\\d\end{matrix}}\right\} N \\ \left.\vphantom{\begin{matrix}a\\b\end{matrix}}\right\} M-N \end{matrix} \qquad \text{(D-4)}$$

The relationship between this decomposition and the rank of the matrix **[A]** is that the value of the rank is equal to the number of non-zero singular values (the multiplication by orthogonal matrices does not alter the value of the rank). For a **3x3** matrix with one linearly-dependent row, σ_3 would be zero. The advantage of the SVD to calculate the rank is that if the considered row is not totally linearly dependent, we would obtain a small value for σ_3 , instead of zero, but now we only have to compare this small value with the other singular values. Having established a criterion for the rejection or acceptance of small singular values, we would have an answer concerning the value of the rank. This criterion may depend on the accuracy of the expected results. If **[A]** is a complex matrix, then Eq. (D-1) becomes

$$\underset{(MxN)}{[A]} = \underset{(MxM)}{[U]} \quad \underset{(MxN)}{[\Sigma]} \quad \underset{(NxN)}{[V]^H} \qquad \text{(D-5)}$$

where the superscript **H** denotes complex conjugate (hermitian) transpose. **[U]** and **[V]** are unitary† matrices, i. e.,

$$[U]^H [U] = [U] [U]^H = [V]^H [V] = [V] [V]^H = [I] \qquad \text{(D-6)}$$

---

† This designation replaces the term "orthogonal" when the matrices are complex.

and

$$[U]^H = [U]^{-1} \quad \text{and} \quad [V]^H = [V]^{-1} \tag{D-7}$$

The singular values σ_i are the non-negative square-roots of the eigenvalues of the matrix $[A]^T [A]$, if [A] is real, and of $[A]^H [A]$, if [A] is complex. Because $[A]^T [A]$ is symmetric and $[A]^H [A]$ is hermitian, their eigenvalues are always real and therefore both Eqs. (D-1) and (D-5) provide real singular values.

We shall consider the case where $M \geq N$ (without loss of generality), because it is the most common case in engineering applications. If $M \leq N$, then we could decompose $[A]^T$ instead. For simplicity, we shall assume [A] to be real from now on. Because there is a close relationship between the singular values of [A] and the eigenvalues of $[A]^T [A]$ (the same as the eigenvalues of $[A] [A]^T$), the columns of [U] and [V] are particular choices of, respectively, the eigenvectors of $[A] [A]^T$ and $[A]^T [A]$, and are called the left and right singular vectors. For this reason, the algorithms to compute the SVD are very similar to the ones used to compute eigenvalues and eigenvectors. It is possible to use the SVD as an eigensolver, but for this application the SVD is not advantageous, as current eigensolvers are very well developed and are quite reliable. Usually, the SVD computation is performed in two stages: first, a reduction of [A] to a bidiagonal form using Householder transformations and second a reduction of the superdiagonal elements to a negligible size, using the QR algorithm. These numerical methods can be studied in Ref. [142]. Detailed application to the SVD can be found in Ref. [129]. Improved algorithms can be found in Refs. [143] to [145]. In Ref. [129], an Algol program is given and in Ref. [141] a Fortran subroutine is presented. In Ref. [146], a subroutine for the case when [A] is complex can be found. Ref. [147] is another relevant article with details about the algorithms used. In Ref. [143], a list

of references is given for the use of the SVD to several applications. The book by Golub (Ref. [130]) is also an excellent reference.

D-4 Applications of the SVD

D-4-1 Recalculation of [A]

Besides the calculation of the rank of a matrix, many other applications exist for the SVD. The first one is the recalculation of matrix [A] after having removed small non-zero singular values and calculated the rank. For instance, if [A] is a **5x3** matrix, [U] will be **5x5**, [Σ] **5x3** and $[V]^T$ **3x3**. If the rank is **2**, then only the first two columns of [U] and [V] are effectively operational, and [A] (5x3) can be recomputed with [U] as **5x2**, [Σ] **2x2** and $[V]^T$ **2x3**. This procedure is quite convenient in the majority of cases, as it leads to an improved [A] matrix.

D-4-2 Condition number

Another simple application is the calculation of the condition number of a matrix. After performing the decomposition, the condition number can be expressed as the ratio $\sigma_{max} / \sigma_{min}$ where σ_{min} is the smallest non-zero singular value. This calculation can serve as an indicator of potential problems, as a high value reflects an ill-conditioned matrix.

D-4-3 Linear system of equations

The SVD can be very useful in solving over-determined linear systems of equations of the form

$$[A]\ \{x\} = \{b\} \tag{D-8}$$

(MxN) (Nx1) (Mx1)

where **M>N**. Applying the SVD on **[A]**, we obtain

$$[U]\ [\Sigma]\ [V]^T\ \{x\} = \{b\} \tag{D-9}$$

(MxM) (MxN) (NxN) (Nx1) (Mx1)

or

$$[\Sigma]\ [V]^T\ \{x\} = [U]^T\ \{b\} \tag{D-10}$$

(MxN) (NxN) (Nx1) (MxM) (Mx1)

or

$$[\Sigma]\ \{z\} = \{d\} \tag{D-11}$$

(MxN) (Nx1) (Mx1)

with

$$\{z\} = [V]^T\ \{x\} \tag{D-12}$$

$$\{d\} = [U]^T\ \{b\} \tag{D-13}$$

Eq. (D-11) represents a set of uncoupled **M** equations with **N** unknowns. From (D-11), we have

$$\sigma_j\ z_j = d_j \qquad \text{for } j \le N \text{ and } \sigma_j \neq 0 \tag{D-14 a}$$

$$0 \cdot z_j = d_j \qquad \text{for } j \le N \text{ and } \sigma_j = 0 \tag{D-14 b}$$

$$0 = d_j \qquad \text{for } j > N \tag{D-14 c}$$

Eqs.(D-14 b) and (D-14 c) will only be consistent if $\mathbf{d_j = 0}$ for $\sigma_j = 0$ or **j > N**. The range of **[A]**, i. e., the set of **{b}** for which **[A] {x} = {b}** has a solution **{x}**, implies that $\mathbf{d_j}$ has to be zero for $\sigma_j = 0$ if $\mathbf{j \le N}$ or for **j > N**. If this does not happen, then **{b}** does not belong to the range of **[A]** and Eq. (D-8) has no exact solutions. In this case, $\mathbf{z_j}$ cannot be determined from (D-14 b), although approximate solutions can be obtained

by setting z_j to zero whenever $\sigma_j = 0$. This corresponds to the shortest solution (minimization of $\|[A]\{x\} - \{b\}\|^2$) in a least-squares sense. Having calculated {z}, the vector {x} can be recovered from (D-12), by doing

$$\{x\} = [V]\{z\} \tag{D-15}$$

D-4-4 Pseudo-inverse

The NxM matrix $[A]^+$ is called the Moore-Penrose pseudo-inverse of [A] if the following conditions are satisfied:

$$\begin{aligned} &\text{i)} && [A][A]^+[A] = [A] \\ &\text{ii)} && [A]^+[A][A]^+ = [A]^+ \\ &\text{iii)} && [A][A]^+ \text{ is symmetric} \\ &\text{iv)} && [A]^+[A] \text{ is symmetric} \end{aligned} \tag{D-16}$$

$[A]^+$ always exists and it is unique. If [A] is square and non-singular, then $[A]^+ = [A]^{-1}$ and if [A] is rectangular and of full rank, then $[A]^+ = ([A]^T [A])^{-1} [A]^T$. In this last case, if [A] is complex, then $[A]^+ = ([A]^H [A])^{-1} [A]^H$. If [A] is not of full rank, the best way to calculate the pseudo-inverse is via the SVD. The pseudo-inverse is related to the least-squares problem, as the value of {x} that minimizes $\| [A]\{x\} - \{b\} \|^2$ can be given by $\{x\} = [A]^+ \{b\}$. Considering Eq. (D-1) and calculating the pseudo-inverse, we obtain:

$$\underset{(NxM)}{[A]^+} = \underset{(NxN)}{([V]^T)^+} \underset{(NxM)}{[\Sigma]^+} \underset{(MxM)}{[U]^+} \tag{D-17}$$

Because [U] and [V] are orthogonal and full rank matrices, the pseudo-inverse coincides with the classical inverse and Eq. (D-3) holds. Therefore,

$$\underset{(NxM)}{[A]^+} = \underset{(NxN)}{[V]} \; \underset{(NxM)}{[\Sigma]^+} \; \underset{(MxM)}{[U]^T} \tag{D-18}$$

$[\Sigma]^+$ is an **NxM** real diagonal matrix, constituted by the inverse values of the non-zero singular values σ_i. Each element of $[A]^+$ can be computed more efficiently by

$$a_{ij}^+ = \sum_{\sigma_k \neq 0} \frac{v_{ik}\, u_{jk}}{\sigma_k} \tag{D-19}$$

where v_{ik} and u_{jk} are the corresponding elements of $[V]$ and $[U]^T$. The summation excludes the values of σ_k that are zero. In practical terms, considering only the singular values that are bigger than a critical value τ, we have

$$a_{ij}^+ = \sum_{\sigma_k > \tau} \frac{v_{ik}\, u_{jk}}{\sigma_k} \tag{D-20}$$

This practical condition of acceptance for the singular values σ_k implies that the first condition of Eq. (D-16) is no longer true† and in this case it should be replaced by the condition:

$$\| [A]\,[A]^+\,[A] - [A] \| < \tau \tag{D-21}$$

The other three conditions of (D-16) remain valid. Since one of the four conditions of (D-16) is not fulfilled, the pseudo-inverse will not be unique, but amongst the possible answers, condition (D-21) is the one that minimizes $\| [A]^+ \|$, providing the minimum error for the least-squares problem.

---

† As a consequence, $[A]^+\,[A]$ will not equal the unit matrix.

D-4-5 Determinants

In some problems, we want to evaluate the values of **z** that make **[A(z)]** singular, i. e., the values of **z** such that the determinant of **[A(z)]** is zero. Using the SVD, we have:

$$\det [A] = \det [U] \det [\Sigma] \det [V]^T \tag{D-22}$$

Because **[U]** and **[V]** are orthogonal matrices, their determinants are ± 1, and so,

$$\det [A] = \pm \prod_{i=1}^{N} \sigma_i \tag{D-23}$$

It is possible to determine exactly the value of **det [A]**. But if we only want to know when its value is zero, one does not even have to calculate the product of the singular values, but only to investigate the variation of σ_N (the smallest singular value) and evaluate the value of **z** that makes σ_N a minimum.

D-5 Example

We shall present here an example that uses the same matrix as in Ref. [141]. The problem is to solve **[A] {x} = {b}**, such that:

$$\begin{bmatrix} 1 & 6 & 11 \\ 2 & 7 & 12 \\ 3 & 8 & 13 \\ 4 & 9 & 14 \\ 5 & 10 & 15 \end{bmatrix} \begin{Bmatrix} x_1 \\ x_2 \\ x_3 \end{Bmatrix} = \begin{Bmatrix} 5 \\ 5 \\ 5 \\ 5 \\ 5 \end{Bmatrix}$$

Note that **[A]** is rank deficient, as the middle column is the mean value of the other two. Solving in the classical way,

$$\{x\} = ([A]^T [A])^{-1} [A]^T \{b\} = \begin{Bmatrix} -0.4688 \\ 0.3125 \\ 0.3125 \end{Bmatrix}$$

If we calculate **[A] {x}**, we obtain

$$\{b\} = \begin{Bmatrix} 4.844 \\ 5.000 \\ 5.156 \\ 5.313 \\ 5.469 \end{Bmatrix}$$

which is clearly in error. Applying the **SVD** on **[A]**, we obtain

$$\underset{(5x3)}{[A]} = \underset{(5x5)}{[U]} \; \underset{(5x3)}{[\Sigma]} \; \underset{(3x3)}{[V]^T}$$

According to (D-4), the last two rows of [Σ] are zero and therefore the last two columns of **[U]** do not contribute to the product. Thus, we shall work with a **5x3** [U] matrix and a **3x3** [Σ] matrix. Computer programs usually provide only this reduced version of the decomposition, which is effectively what is strictly necessary. Hence, matrices [U], [Σ] and [V] are:

$$[U] = \begin{bmatrix} -0.3546 & -0.6887 & 0.5623 \\ -0.3987 & -0.3756 & -0.6404 \\ -0.4428 & -0.0624 & 0.0000 \\ -0.4870 & 0.2507 & -0.3290 \\ -0.5311 & 0.5638 & 0.4067 \end{bmatrix}$$

$$[\Sigma] = \begin{bmatrix} 35.1300 & 0. & 0. \\ 0. & 2.4650 & 0. \\ 0. & 0. & 2.840 \times 10^{-15} \end{bmatrix}$$

$$[V] = \begin{bmatrix} -0.2017 & 0.8903 & 0.4082 \\ -0.5168 & 0.2573 & -0.8165 \\ -0.8320 & -0.3757 & 0.4082 \end{bmatrix}$$

From matrix [Σ] we see clearly that the matrix has rank = 2 and we can put the third singular value to zero. As a consequence, we can also work only with the two first columns of [U] and [V] and calculate the pseudo-inverse as:

$$[A]^{+} = \begin{bmatrix} -0.2017 & 0.8903 \\ -0.5168 & 0.2573 \\ -0.8320 & -0.3757 \end{bmatrix} \begin{bmatrix} 1/35.130 & 0. \\ 0. & 1/2.465 \end{bmatrix}$$

$$\times \begin{bmatrix} -0.3546 & -0.3987 & -0.4428 & -0.4870 & -0.5311 \\ -0.6887 & -0.3756 & -0.0624 & 0.2507 & 0.5638 \end{bmatrix}$$

The solution is now

$$\{x\} = \begin{Bmatrix} -0.5000 \\ -0.0000 \\ 0.5000 \end{Bmatrix}$$

If we calculate now **[A] {x}**, we obtain exactly the initial vector **{b}**. Also, the answer is the shortest possible one.

REFERENCES

[1] - **Ewins, D. J.**
"Modal Testing: Theory and Practice"
Research Studies Press Ltd., England, 1984.

[2] - **Wellstead, P. E.**
"Methods And Applications Of Digital Spectral Techniques"
Solartron Technical Report No. 008/83.

[3] - **Hewlett Packard**
"The Fundamentals Of Modal Testing"
Application Note 243-3, 1986.

[4] - **Broch, J. T.**
"Mechanical Vibration And Shock Measurements"
Brüel & Kjær, 1980.

[5] - **Brüel & Kjær**
"Digital Signal Analysis Using Digital Filters And FFT Techniques"
Selected Reprints from Technical Review, Jan. 1985.

[6] - **Serridge, M., Licht, T. R.**
"Piezoelectric Accelerometer And Vibration Preamplifier Handbook"
Brüel & Kjær, Oct. 1986.

[7] - **Bendat, J. S., Piersol, A. G.**
"Random Data - Analysis And Measurement Procedures"
John Wiley & Sons, 2nd Ed., 1986.

[8] - **Newland, D. E.**
"An Introduction To Random Vibrations And Spectral Analysis"
Longman, 2nd Ed., 1984.

[9] - **Cooley, J. W., Tukey, J. W.**
"An Algorithm For The Machine Calculation Of Complex Fourier Series"
Mathematics of Computation, Vol. 19, Apr. 1965, pp. 297-301.

[10] - **Bishop, R. E. D., Gladwell, G. M. L.**
"An Investigation Into The Theory Of Resonace Testing"
Philosophical Trans. of the Royal Society of London, Vol. 255 A 1055, 1963, pp. 241-280.

[11] - **Pendered, J. W., Bishop, R. E. D.**
"The Determination Of Modal Shapes In Resonance Testing"
Journal Mech. Eng. Science, Vol. 5, No. 4, 1963, pp. 379-385.

[12] - **Kennedy, C. C., Pancu, C. D. P.**
"Use Of Vectors In Vibration Measurement And Analysis"
Journal of the Aeronautical Sciences, Vol. 14, No. 11, Nov. 1947, pp. 603-625.

[13] - **Walker, P. B., Clegg, A. W.**
"The Technique Of Wing Resonance Tests"
Report No. A. D. 3105/M. T. 11767, Royal Aircraft Establ.,
South Farnborough, England, Feb. 1939.

[14] - **Leuridan, J.**
"Some Direct Parameter Model Identification Methods Applicable For Multiple Modal Analysis"
PhD. Diss., Dept. Mech. and Ind. Eng., Univ. of Cincinnati, 1984.

[15] - **Vold, H., Leuridan, J.**
"A Generalized Frequency Domain Matrix Estimation Method For Structural Parameter Identification"
7th Int. Seminar on Modal Analysis, K. U. Leuven, Belgium, Sept. 1982.

[16] - **Klosterman, A.**
"On the Experimental Determination And Use Of Modal Representation Of Dynamic Characteristics"
PhD. Thesis, University of Cincinnati, 1971.

[17] - **Mitchell, L. D.**
"A Perspective View Of Modal Analysis"
Keynote Address, Proc. of IMAC VI, Kissimmee, Florida, 1988,
pp. xvii-xxi.

[18] - **Snoeys, R., Sas, P.**
"Reflections On Modal Analysis And Its Applications"
Keynote Address, Proc. of IMAC V, London, U. K., 1987, pp. xviii-xxii.

[19] - **Stroud, R. C.**
"Excitation, Measurement And Analysis Methods For Modal Testing"
Combined Experimental Analytical Modeling Of Dynamic Structural Systems, AMD - Vol. 67, presented at The Joint ASCE/ASME Mechanics Conference, Albuquerque, New Mexico, June 24-26, 1985, pp. 49-78.

[20] - **Rades, M.**
"Frequency Domain Experimental Modal Analysis Techniques"
The Shock and Vibration Digest, Vol. 17, No. 6, June 1985, pp. 3-15.

[21] - **Füllekrug, U.**
"Survey Of Parameter Estimation Methods In Experimental Modal Analysis"
Proc. of IMAC V, London, U. K., 1987, pp. 460-467.

[22] - **Allemang, R. J.**
"Experimental Modal Analysis"
The Winter Annual Meeting of the American Society of Mechanical Engineers, Boston, Massachusetts, Nov. 13-18, 1983, pp. 1-29.

[23] - **Snoeys, R., Sas, P., Heylen, W., Van Der Auweraer, H.**
"Trends In Experimental Modal Analysis"
Proc. of the 10th Int. Seminar on Modal Analysis, Part III, K. U. Leuven, Belgium, 1985.

[24] - **Zhang, L., Yao, Y.**
"Advances In Modal Identification - From SISO, SIMO To MIMO Methods"
Proc. of IMAC V, London, U. K., 1987, pp. 1003-1007.

[25] - **Ibrahim, S. R.**
"Modal Identification Techniques Assessment And Comparison"
Proc. of the 10th Int. Seminar on Modal Analysis, Part III, K. U. Leuven, Belgium, 1985.

[26] - **Mergeay, M.**
"General Review Of Parameter Estimation Methods By Modal Analysis"
7th Int. Seminar on Modal Analysis, K. U. Leuven, Belgium, Sept. 15-17, 1982.

[27] - **Brown, D. L., Allemang, R. J., Zimmerman, R., Mergeay, M.**
"Parameter Estimation Techniques For Modal Analysis"
SAE Technical Paper Series, No. 790221, 1979.

[28] - **Allemang, R. J.**
"Experimental Modal Analysis Bibliography"
Proc. of IMAC II, Orlando, Florida, Feb. 1984, pp. 1085-1097.

[29] - **Mitchell, L. D., Mitchell, L. D.**
"Modal Analysis Bibliography - An Update - 1980-1983"
Proc. of IMAC II, Orlando, Florida, 1984, pp. 1098-1114.

[30] - **Spitznogle, F. R., Quazi, A. H.**
"Representation And Analysis Of Time-Limited Signals Using A Complex Exponential Algorithm"
The Journal of The Acoustical Society of America, Vol. 47, No. 5 (Part 1), 1970, pp. 1150-1155.

[31] - **Spitznogle, F. R., *et al.***
"Representation And Analysis Of Sonar Signals, Volume 1: Improvements In The Complex Exponential Signal Analysis Computational Algorithm"
Texas Instruments, Inc., Report No. U1-829401-5 Office of Naval Research-Contract No. N00014-69-C0315, 1971, 37 pp.

[32] - **Prony, R.**
"Essai Expérimental Et Analitique Sur Les Lois De La Dilatabilité Des Fluides Élastiques Et Sur Celles De La Force Expansive De La Vapeur De L'Eau Et De La Vapeur De L'Alkool, À Différentes Températures"
Journal de L'École Polytechnique (Paris), Vol. 1, Cahier 2, Floréal et Prairial, An. III, 1795, pp. 24-76.

[33] - **Vold, H., Kundrat, J., Rocklin, G. T., Russel, R.**
"A Multi-Input Modal Estimation Algorithm For Mini-Computers"
SAE Technical Paper Series, No. 820194, 1982.

[34] - **Vold, H., Rocklin, G. T.**
"The Numerical Implementation Of A Multi-Input Modal Estimation Method For Mini-Computers"
Proc. of IMAC I, Orlando, Florida, Nov. 8-10, 1982, pp. 542-548.

[35] - **Deblauwe, F., Allemang, R. J.**
"The Polyreference Time-Domain Technique"
Proc. of the 10th Int. Seminar on Modal Analysis, Part IV, K. U. Leuven, Belgium, 1985.

[36] - **Brillhart, R. D., Hunt, D. L., Crowley, S. M.**
"Comparison Of Modal Parameter Estimation Methods For Highly Damped Structures"
Proc. of IMAC VI, Kissimmee, Florida, 1988, pp. 705-711.

[37] - **Ibrahim, S. R., Mikulcik, E. C.**
"A Time Domain Modal Vibration Test Technique"
The Shock & Vibration Bulletin, Vol. 43 (4), 1973, pp. 21-37.

[38] - **Ibrahim, S. R., Mikulcik, E. C.**
"The Experimental Determination Of Vibration Parameters From Time Responses"
The Shock & Vibration Bulletin, Vol. 46 (5), 1976, pp. 187-196.

[39] - **Ibrahim, S. R., Mikulcik, E. C.**
"A Method For The Direct Identification Of Vibration Parameters From The Free Response"
The Shock & Vibration Bulletin, Vol. 47 (4), 1977, pp. 183-198.

[40] - **Ibrahim, S. R.**
"A Modal Identification Algorithm For Higher Accuracy Requirements"
AIAA Paper No. 84-0928, Proc. of the 25th Structures, Structural Dynamics and Materials Conference, Palm Springs, California, May 1984, pp. 117-122.

[41] - **Ibrahim, S. R.**
"Modal Confidence Factor In Vibration Testing"
The Shock & Vibration Bulletin, Vol. 48 (1), 1978, pp. 65-75.

[42] - **Pappa, R.S., Ibrahim, S.R.**
"A Parametric Study Of The Ibrahim Time Domain Identification Algorithm"
The Shock & Vibration Bulletin, Vol. 51 (3), 1981, pp. 43-72.

[43] - **Ibrahim, S. R.**
"An Upper Hessenberg Sparse Matrix Algorithm For Modal Identification of Mini-computers"
Proc. of the 10th Int. Seminar on Modal Analysis, Part III, K. U. Leuven, Belgium, 1985.

[44] - **Zaghlool, S. A.**
"Single-Station Time-Domain (SSTD) Vibration Testing Technique: Theory And Application"
Journal of Sound & Vibration, 72 (2), 1980, pp. 205-234.

[45] - **Juang, J.-N., Pappa, R. S.**
"An Eigensystem Realization Algorithm For Modal Parameter Identification And Model Reduction"
Journal of Guidance, Control, and Dynamics, Vol. 8, No.5, Sept.-Oct. 1985, pp. 620-627.

[46] - **Juang, J.-N.**
"Mathematical Correlation Of Modal-Parameter-Identification Methods Via System Realization Theory"
The Int. Journal of Analytical and Experimental Modal Analysis, Vol. 2, No. 1, Jan. 1987.

[47] - **Juang, J.-N., Pappa, R. S.**
"Effects Of Noise On Modal Parameters Identified By The Eigensystem Realization Algorithm"
Journal of Guidance, Control, and Dynamics, Vol. 9, No.3, May-June 1986, pp. 294-303.

[48] - **Gersch, W.**
"Estimation Of The Autoregressive Parameters Of A Mixed Autoregressive Moving-Average Time Series"
IEEE Trans. on Automatic Control, Vol. AC-15, Oct. 1970, pp. 583-588.

[49] - **Gersch, W., Luo, S.**
"Discrete Time Series Synthesis Of Randomly Excited Structural System Response"
The Journal of the Acoustical Society of America, Vol. 51, No. 1 (Part 2), 1972, pp. 402-408.

[50] - **Gersch, W., Sharpe, D. R.**
"Estimation Of Power Spectra With Finite-Order Autoregressive Models"
IEEE Trans. on Automatic Control, Vol. AC-18, 1973, pp. 367-369.

[51] - **Gersch, W., Nielsen, N. N., Akaike, H.**
"Maximum Likelihood Estimation Of Structural Parameters From Random Vibration Data"
Journal of Sound & Vibration, 31 (3), 1973, pp. 295-308.

[52] - **Gersch, W.**
"On The Achievable Accuracy Of Structural System Parameter Estimates"
Journal of Sound & Vibration , 34 (1), 1974, pp. 63-79.

[53] - **Gersch, W., Foutch, D. A.**
"Least Squares Estimates Of Structural System Parameters Using Covariance Function Data"
IEEE Trans. on Automatic Control, Vol. AC-19, Dec. 1974, pp. 898-903.

[54] - **Gersch, W.**
"Parameter Identification: Stochastic Process Techniques"
The Shock and Vibration Digest, Vol. 7, No. 11, Nov. 1975, pp. 71-86.

[55] - **Gersch, W., Liu, R. S.-Z.**
"Time Series Methods For The Synthesis Of Random Vibration Systems"
Trans. of the ASME, Journal of Appl. Mech., Vol. 43/1, Mar. 1976, pp. 159-165.

[56] - **Gersch, W., Martinelli, F.**
"Estimation Of Structural System Parameters From Stationary And Non-Stationary Ambient Vibrations: An Exploratory-Confirmatory Analysis"
Journal of Sound & Vibration, 65 (3), 1979, pp. 303-318.

[57] - **Gersch, W., Brotherton, T.**
"Estimation Of Stationary Structural System Parameters From Non-Stationary Random Vibration Data: A Locally Stationary Model Method"
Journal of Sound & Vibration, 81 (2), 1982, pp. 215-227.

[58] - **Leuridan, J., Vold, H.**
"A Time Domain Linear Model Estimation Technique For Multiple Input Modal Analysis"
The Winter Annual Meeting of the American Society of Mechanical Engineers, Boston, Massachusetts, Nov. 13-18, 1983, pp. 51-62.

[59] - **Pendered, J. W., Bishop, R. E. D.**
"A Critical Introduction To Some Industrial Resonance Testing Techniques"
Journal Mech. Eng. Science, Vol. 5, No. 4, 1963, pp. 345-367.

[60] - **Pendered, J. W.**
"Theoretical Investigation Into The Effects Of Close Natural Frequencies In Resonance Testing"
Journal of Mechanical Engineering Science, Vol. 7, No. 4, 1965, pp. 372-379.

[61] - **Woodcock, D. L.**
"On The Interpretation Of The Vector Plots Of Forced Vibrations Of A Linear System With Viscous Damping"
The Aeronautical Quaterly, Feb. 1963, pp. 45-62.

[62] - **Marples, V.**
"The Derivation Of Modal Damping Ratios From Complex-Plane Response Plots"
Journal of Sound & Vibration, 31(1), 1973, pp. 105 - 117.

[63] - **Ewins, D. J., Sidhu, J.**
"Modal Testing And The Linearity Of Structures"
Mécanique, Matériaux, Électricité, No. 389-390-391, 1982.

[64] - **Maia, N. M. M.**
"Interference Criteria In Modal Identification"
M. Sc. Thesis, Technical University of Lisbon, 1985 (in Portuguese).

[65] - **Silva, J. M. M., Maia, N. M. M.**
"Single Mode Identification Techniques For Use With Small Micro Computers"
Journal of Sound & Vibration, 124 (1), July 1988, pp. 13-26.

[66] - **Silva, J. M. M.**
"Measurements And Applications Of Structural Mobility Data For The Vibration Analysis Of Complex Structures"
PhD. Thesis, Imperial College of Science & Technology, London, U. K., Mar. 1978.

[67] - **Robb, D. A., Ewins, D. J., Maia, N. M. M.**
"Modal Tests On The End Windings Of An Electric Motor"
Report No. 531/1, Modal Testing Unit, Dept. of Mech. Eng., Imperial College of Science & Technology, London, U. K., Oct. 1985.

[68] - **Robb, D. A., Ewins, D. J., Maia, N. M. M.**
"Modal Tests On The End Windings Of An Electric Motor - Results Of Further Tests On A Single Straight Section Of Winding Material And On A Single Coil"
Report No. 531/2, Modal Testing Unit, Dept. of Mech. Eng., Imperial College of Science & Technology, London, U. K., Apr. 1986.

[69] - **Robb, D. A.**
"User's Guide To Program MODENT"
Dynamics Section, Dept. of Mech. Eng., Imperial College of Science & Technology, London, U. K.

[70] - **Talapatra, D. C., Haughton, J. M.**
"Modal Testing Of A Large Test Facility For Space Shuttle Payloads"
Proc. of IMAC II, Orlando, Florida, Feb. 1984, pp. 1-7.

[71] - **Kirshenboim, J., Ewins, D. J.**
"A Method For The Derivation Of Optimal Modal Parameters From Several Single-Point Excitation Tests"
Proc. of IMAC II, Orlando, Florida, Feb. 1984, pp. 991-997.

[72] - **Dobson, B. J.**
"Modal Analysis Using Dynamic Stiffness Data"
Royal Naval Engineering College (RNEC), TR-84015, June 1984.

[73] - **Dobson, B. J.**
"A Straight-Line Technique For Extracting Modal Properties From Frequency Response Data"
Mechanical Systems and Signal Processing, Vol. 1, No. 1, Jan. 1987.

[74] - **Goyder, H. G. D.**
"Methods And Applications Of Structural Modelling From Measured Structural Frequency Response Data"
Journal of Sound & Vibration , 68 (2), 1980, pp. 209-230.

[75] - **Petrick, L.**
"Obtaining Global Frequency And Damping Estimates Using Single Degree-Of-Freedom Real Mode Methods"
Proc. of IMAC II, Orlando, Florida, Feb. 1984, pp. 425-431.

[76] - **Gaukroger, D. R., Skingle, C. W., Heron, K. H.**
"Numerical Analysis Of Vector Response Loci"
Journal of Sound & Vibration , 29 (3), 1973, pp. 341-353.

[77] - **Ewins, D. J., Gleeson, P. T.**
" A Method For Modal Identification Of Lightly Damped Structures"
Journal of Sound & Vibration (1982), 84(1), pp. 57-79.

[78] **Brittingham, J. N., Miller, E. K., Willows, J. L.**
"Pole Extraction From Real-Frequency Information"
Proc. of IEEE, Vol. 68, No. 2, Feb. 1980, pp. 263-273.

[79] - **Schmerr, L. W.**
"A New Complex Exponential Frequency Domain Technique For Analysing Dynamic Response Data"
Proc. of IMAC I, Orlando, Florida, Nov. 8-10, 1982.

[80] - **Juang, J.-N., Suzuki, H.**
"An Eigensystem Realization Algorithm In Frequency Domain For Modal Parameter Identification"
Trans. of the ASME (J. of Vib., Acoust., Stress, and Reliab. in Design), Vol. 110, Jan. 1988, pp. 24-29.

[81] - **Richardson, M. H., Formenti, D. L.**
"Parameter Estimation From Frequency Response Measurements Using Rational Fraction Polynomials"
Proc. of IMAC I, Orlando, Florida, Nov. 8-10, 1982.

[82] - **Smiley, R. G., Wey, Y. S., Hogg, K. D.**
"A Simplified Frequency Domain MDOF Curve-Fitting Process"
Proc. of IMAC II, Vol. I, Orlando, Florida, Feb. 1984.

[83] - **Adcock, J., Potter, R.**
"A Frequency Domain Curve Fitting Algorithm With Improved Accuracy"
Proc. of IMAC III, Orlando, Florida, Jan. 28-31, 1985.

[84] - **Richardson, M. H., Formenti, D. L.**
"Global Curve-Fitting Of Frequency Response Measurements Using The Rational Fraction Polynomial Method"
Proc. of IMAC III, Orlando, Florida, Jan. 28-31, 1985.

[85] - **Richardson, M. H.**
"Global Frequency & Damping Estimates From Frequency Response Measurements"
Proc. of IMAC IV, Los Angeles, California, Feb. 3-6, 1986.

[86] - **Van Der Auweraer, H., Leuridan,J.**
"Multiple Input Orthogonal Polynomial Parameter Estimation"
Mechanical Systems And Signal Processing, 1 (3), 1987, pp. 259-272.

[87] - **Fillod, R., Lallement, G., Piranda, J., Raynaud, J. L.**
"Méthode Globale D'Identification Modale"
Mécanique, Matériaux, Électricité, Mar.-Apr. 1984.

[88] - **Fillod, R., Lallement, G., Piranda, J., Raynaud, J. L.**
"Global Method Of Modal Identification"
Proc. of IMAC III, Vol. II, Orlando, Florida, 1985, pp. 1145-1151.

[89] - **Fillod, R., Lallement, G., Piranda, J., Raynaud, J. L.**
"Identification À Partir D'Une Excitation Multipoints À Phase Variable"
GAMI, Colloque Vib. Chocs, Lyon ECL, France, June 10-12, 1986.

[90] - **Zhang,L., Kanda, H.**
"The Algorithm And Application Of A New Multi-Input-Multi-Output Modal Parameter Identification Method"
The 56th Shock & Vibration Symposium, Oct. 1985.

[91] - **Zhang,L., Kanda, H., Brown, D., Allemang, R.**
"A Polyreference Frequency Domain Method For Modal Parameter Identification"
ASME Paper 85-DET-106, 1985, pp. 1-6.

[92] - **Zhang,L., Kanda, H., Lembregts, F.**
"Some Applications Of Frequency Domain Polyreference Modal Parameter Identification Method"
Proc. of IMAC IV, Vol. II, Los Angeles, California, Feb. 3-6, 1986, pp. 1237-1245.

[93] - **Lembregts, F., Leuridan, J., Zhang,L., Kanda, H.**
"Multiple Input Modal Analysis Of Frequency Response Functions Based On Direct Parameter Identification"
Proc. of IMAC IV, Vol. I, Los Angeles, California, Feb. 3-6, 1986, pp. 589-598.

[94] - **Giménez, J. G., Carrascosa, L. I.**
"On The Use Of Constraint Equations In The Global Fitting Algorithms Of Transfer Functions"
Proc. of IMAC II, Orlando, Florida, Feb. 1984, pp. 998-1003.

[95] - **Wu, W.-Z., Lwo, T.-W.**
"Global Modal Parameter Estimation Combined With A Statistical Criterion"
Proc. of IMAC VI, Kissimmee, Florida, 1988, pp. 121-128.

[96] - **Shih, C. Y., Tsuei, Y. G., Allemang, R. J., Brown, D. L.**
"A Frequency Domain Global Parameter Estimation Model For Multiple Reference Frequency Response Measurements"
Proc. of IMAC VI, Kissimmee, Florida, 1988, pp. 389-396.

[97] - **Coppolino, R. N.**
"A Simultaneous Frequency Domain Technique For Estimation Of Modal Parameters From Measured Data"
SAE Tech. Paper Series No. 811046, 1981.

[98] - **Coppolino, R. N., Stroud, R. C.**
"A Global Technique For Estimation Of Modal Parameters From Measured Data"
Proc. of IMAC IV, Los Angeles, California, Feb. 3-6, 1986, pp. 674-681.

[99] - **Craig Jr., R. R., Blair, M. A.**
"A Generalized Multiple-Input, Multiple-Output Modal Parameter Estimation Algorithm"
AIAA Journal, Vol. 23, No. 6, June 1985, pp. 931-937.

[100] - **Link, M., Vollan, A.**
"Identification Of Structural System Parameters From Dynamic Response Data"
Z. Flugwiss. Weltraumforsch, 2 (3), 1978, pp. 165-174.

[101] - **Link, M.**
"Identification Of Physical System Matrices Using Incomplete Vibration Test Data"
Proc. of IMAC IV, Los Angeles, California, Feb. 3-6, 1986.

[102] - **Leuridan, J. M., Kundrat, J. A.**
"Advanced Matrix Methods For Experimental Modal Analysis - A Multi-Matrix Method For Direct Parameter Excitation"
Proc. of IMAC I, Orlando, Florida, Nov. 8-10, 1982, pp. 192-200.

[103] - **Lewis, R. C., Wrisley, D. L.**
"A System For The Excitation Of Pure Natural Modes Of Complex Structures"
Journal of the Aeronautical Sciences, Vol. 17, No. 11, 1950, pp. 705-722.

[104] - **Asher, G. W.**
"A Method Of Normal Mode Excitation Utilizing Admittance Measurements"
Proc. National Specialists' Meeting in Dynamics and Aeroelasticity, Institute of the Aeronautical Sciences, 1958, pp. 69-76.

[105] - **Trail-Nash, R. W.**
"On The Excitation Of Pure Natural Modes In Aircraft Resonance Testing"
Journal of Aerospace Sciences, Vol. 25, Dec. 1958, pp. 775-778.

[106] - **Craig Jr., R. R., Su, Y.-W. T.**
"On Multiple-Shaker Resonance Testing"
AIAA Journal, Vol. 12, No. 7, July 1974, pp. 924-931.

[107] - **Smith, S., Stroud, R. C., Hanema, G. A., Hallauer, W.L., Yee, R. C.**
"MODALAB - A Computarized Data Acquisition And Analysis System For Structural Dynamic Testing"
ISA - ASI 75230, 1975, pp. 183-189.

[108] - **Ibáñez, P.**
"Force Appropriation By Extended Asher's Method"
SAE Paper No. 760873, 1976.

[109] - **Hallauer Jr., W. L., Stafford, J. F.**
"On The Distribution Of Shaker Forces In Multiple-Shaker Modal Testing"
The Shock & Vibration Bulletin, Sept. 1978.

[110] - **Gold, R. R., Hallauer, W. L. Jr.**
"Modal Testing With Asher's Method Using A Fourier Analyser And Curve Fitting"
Instrum. Aerospace Indust., 25, Adv. Test Measure., 16, Part I, Proc. 25th Int. Symp., Anaheimn, CA, May 1979, pp.185-192.

[111] - **Ensminger, R., Turner, M. J.**
"Structural Parameter Identification From Measured Vibration Data"
AIAA/ASME/ASCE/AHS 20th Structural Dynamics Materials Conference, St. Louis, AIAA Paper 79-0829, 1979, pp. 410-416.

[112] - **Craig Jr., R. R., Chung, Y. T.**
"Modal Analysis Using A Fourier Analyser, Curve-Fitting, and Modal Tuning"
Report No. NASA-CR-161886, CAR-81-1, Oct. 1981.

[113] - **Rades, M.**
"Identification Of Resonance Frequencies By A Singular Value Approach"
Buletinul Instit. Politehnic Bucaresti, Seria Transport. Aeronave, Vol. 45, 1983, pp. 33-40.

[114] - **Ibáñez, P., Blakely, K. D.**
"Automatic Force Appropriation - A Review And Suggested Improvements"
Proc. of IMAC II, Orlando, Florida, Feb. 1984, pp. 903-907.

[115] - **Hunt, D. L., Peterson, E. L., Vold, H., Williams, R.**
"Optimal Selection Of Excitation Methods For Enhanced Modal Testing"
AIAA Paper No. 84-1068, presented at the AIAA Dynamics Conference, Palm Springs, CA, 18th May 1984, pp. 549-553.

[116] - **Zaveri, K.**
"Modal Analysis Of Large Structures - Multiple Exciter Systems"
Brüel &Kjær publications, Nov. 1984.

[117] - **Traill-Nash, R. W., Long, G., Bailey, C. M.**
"Experimental Determination Of The Complete Dynamical Properties Of A Two-Degree-Of-Freedom Model Having Nearly Coincident Natural Frequencies"
Journal of Mechanical Engineering Science, Vol. 9, No. 5, 1967, pp. 402-413.

[118] - **Dobson, B. J.**
"Experimental Modal Analysis Using An Undamped Mathematical Model"
Royal Naval Engineering College, Report RNEC-TR-84012, Jun. 1984.

[119] - **Maia, N. M. M.**
"Modal Analysis Of Double Modes"
Internal Report No. 86006, Dynamics Section, Dept. of Mech. Eng., Imperial College of Science & Technology, London, U. K., Aug. 1986.

[120] - **Maia, N. M. M., Ewins, D. J.**
"Modal Analysis Of Double Modes: A First Approach To Intelligent Curve-Fitting"
Proc. of IMAC V, Vol. II, London, U. K., 1987, pp. 1302-1308.

[121] - **National Bureau of Standards**
"Handbook Of Mathematical Functions - Chapter 22 - Orthogonal Polynomials"
1964.

[122] - **Chihara, T. S.**
"An Introduction To Orthogonal Polynomials"
Gordon and Breach Science Publishers, London, 1978.

[123] - **Ascher, M., Forsythe, G. E.**
"SWAC Experiments On The Use Of Orthogonal Polynomials For Data Fitting"
J. Assoc. Comput. Mach., Vol. 5, Jan. 1958.

[124] - **Forsythe, G. E.**
"Generation And Use Of Orthogonal Polynomials For Data-Fitting With A Digital Computer"
Journal of the Society for Industrial and Applied Mathematics, Vol. 5, 1957.

[125] - **Kelly, L. G.**
"Handbook Of Numerical Methods And Applications - Chapter 5 - Curve Fitting And Data Smoothing"
Addison-Wesley Pub. Co. Inc., 1967.

[126] - **Rao, S. S.**
"Mechanical Vibrations"
Addison-Wesley Pub. Co. Inc., 1986.

[127] - **Rogers, P. J.**
"Modal Analysis Theory For Systems With General (Symmetric Or Asymmetric) System Matrices"
Report No. 8714, Dynamics Section, Dept. of Mech. Eng., Imperial College of Science & Technology, London, U. K., Aug. 1987.

[128] - **Kaufman, L.**
"The LZ Algorithm To Solve The Generalized Eigenvalue Problem For Complex Matrices [F2]"
ACM Trans. On Math. Software, Vol. 1, No. 3, Sept. 1975, pp. 271-281.

[129] - **Golub, G. H., Reinch, C.**
"Singular Value Decomposition And Least Squares Solutions"
Numerische Mathematik, Vol. 14, 1970, pp. 403-420.

[130] - **Golub, G. H., Van Loan, C. F.**
"Matrix Computations"
North Oxford Academic, 1983.

[131] - **Gaukroger, D. R., Copley, J. C.**
"Methods Of Determining Undamped Normal Modes And Transfer Functions From Receptance Measurements"
Royal Aircraft Establishment, Technical report 79071, 1979.

[132] - **Ibrahim, S. R.**
"Dynamic Modeling Of Structures From Measured Complex Modes"
AIAA Journal, Vol. 21, No. 6, June 1983, pp. 898-901.

[133] - **Zhang, Q., Lallement, G.**
"New Method Of Determining The Eigensolutions Of The Associated Conservative Structure From The Identified Eigensolutions"
Proc. of IMAC III, Orlando, Florida, Jan. 28-31, 1985, pp. 322-328.

[134] - **Lin, C., Ibrahim, S. R.**
"The Use Of Complex Versus Normal Modes In Structural Model Improvement"
Proc. of IMAC II, Orlando, Florida, Feb. 1984, pp. 415-424.

[135] - **Good, M., Macioce, D.**
"Using Modal Analysis To Improve Confidence In Finite Element Analysis"
Sound and Vibration, Jan. 1984, pp. 18-22.

[136] - **Natke, H. G., Rotert, D.**
"Determination Of Normal Modes From Identified Complex Modes"
Z. Flugwiss. Weltraumforsch, 9 (2), 1985, pp. 82-88.

[137] - **Ibrahim, S. R.**
"Computation Of Normal Modes From Identified Complex Modes"
AIAA Journal, Vol. 21, No. 3, Mar. 1983, pp. 446-451.

[138] - **Zhang, Q., Lallement, G.**
"Comparison Of Normal Eigenmodes Calculation Methods Based On Identified Complex Eigenmodes"
Proc. of the 10th Int. Seminar on Modal Analysis, Part III, K. U. Leuven, Belgium, 1985.

[139] - **Niedbal, N.**
"Analytical Determination Of Real Normal Modes From Measured Complex Responses"
25th Structures, Structural Dynamics and Materials Conference, Palm Springs, California, May 14-16, 1984 and AIAA Dynamics Specialists Conference, Part 2, California, May 17-18, 1984, pp. 292-295.

[140] - **Allemang, R. J., Brown, D. L.**
"A Correlation Coefficient For Modal Vector Analysis"
Proc. of IMAC I, Orlando, Florida, Nov. 8-10, 1982.

[141] - **Forsythe, G. E., Malcolm, M. A., Moler, C. B.**
"Computer Methods For Mathematical Computations"
Prentice-Hall, 1977.

[142] - **Wilkinson, J. H.**
"The Algebraic Eigenvalue Problem"
Oxford Univ. Press, 1965.

[143] - **Chan, T. F.**
"An Improved Algorithm For Computing The Singular Value Decomposition"
ACM Trans. On Math. Software, Vol. 8, No. 1, Mar. 1982, pp. 72-83.

[144] - **Chan, T. F.**
"Algorithm 581 - An Improved Algorithm For Computing The Singular Value Decomposition [F1]"
ACM Trans. On Math. Software, Vol. 8, No. 1, Mar. 1982, pp. 84-88.

[145] - **Paige, C. C., Saunders, M. A.**
"Towards A Generalized Singular Value Decomposition"
SIAM J. Numer. Anal., Vol. 18, No. 3, June 1981, pp. 398-405.

[146] - **Businger, P. A., Golub, G. H.**
"Algorithm 358 - Singular Value Decomposition Of A Complex Matrix [F1, 4, 5]"
Comm. of the ACM, Vol. 12, No. 10, Oct. 1969, pp. 564-565.

[147] - **Golub, G. H., Kahan, W.**
"Calculating The Singular Values And Pseudo-Inverse Of A Matrix"
SIAM J. Numer. Anal., Ser. B, Vol. 2, No. 2, 1965.